THE TRANSFER OF CADMIUM FROM ROCK TO SOIL AND THE ASSOCIATED VEGETATION COVER UNDER NATURAL CONDITIONS AT THE SWISS JURA MOUNTAINS

Thesis presented by

Raul P. Quezada Hinojosa

in October 2010 for a

Doctorate in Science

at the University of Neuchâtel, Switzerland

Jury Commitee:

Prof. Karl Föllmi (Lausanne)	Director
Dr. Virginie Matera (INRS Lorraine)	Supervisor
Prof. Thierry Adatte (Lausanne)	Examiner
Prof. Eric Verrecchia (Lausanne)	Examiner
Dr. Denis Baize (INRA Orléans)	Examiner

Université de Neuchâtel

FACULTE DES SCIENCES
Secrétariat-Décanat de la faculté
Rue Emile-Argand 11
CH-2000 Neuchâtel

IMPRIMATUR POUR LA THESE

The transfer of Cadmium from rock to soil and the associated vegetation cover under natural conditions at the Swiss Jura Moutains

Raul Percy QUEZADA HINOJOSA

UNIVERSITE DE NEUCHATEL

FACULTE DES SCIENCES

La Faculté des sciences de l'Université de Neuchâtel,
sur le rapport des membres du jury

Mme V. Matera (Nancy F), MM. K. Föllmi (directeur de thèse),
E. Verrecchia, T. Adatte et D. Baize (Orléans F)

autorise l'impression de la présente thèse.

Neuchâtel, le 14 décembre 2010

Le doyen :
P. Kropf

THE TRANSFER OF CADMIUM FROM ROCK TO SOIL AND THE ASSOCIATED VEGETATION COVER UNDER NATURAL CONDITIONS AT THE SWISS JURA MOUNTAINS

Thesis presented by

Raul P. Quezada Hinojosa

in October 2010 for a
Doctorate in Science
at the University of Neuchâtel, Switzerland

Jury Commitee :

Prof. Karl Föllmi (Lausanne)	Director
Dr. Virginie Matera (INRS Lorraine)	Supervisor
Prof. Thierry Adatte (Lausanne)	Examiner
Prof. Eric Verrecchia (Lausanne)	Examiner
Dr. Denis Baize (INRA Orléans)	Examiner

CONTENTS

CHAPTER 1

GENERAL INTRODUCTION

CHAPTER 2

CADMIUM, SOILS & ENVIRONMENT

CHAPTER 3

CADMIUM DISTRIBUTION IN SOILS COVERING JURASSIC OOLITIC LIMESTONE WITH HIGH Cd CONTENTS IN THE SWISS JURA

CHAPTER 4

CADMIUM DISTRIBUTION IN A NATURALLY CONTAMINATED SITE OF THE SWISS JURA USING SEQUENTIAL EXTRACTIONS AND MULTIVARIABLE ANALYSES OF THE MAIN PHYSICOCHEMICAL SOIL PROPERTIES

CHAPTER 5

CADMIUM ACCUMULATION IN SIX COMMON PLANT SPECIES ASSOCIATED WITH SOILS CONTAINING HIGH Cd CONCENTRATIONS OF GEOGENIC ORIGIN

CHAPTER 6

CONCLUSIONS

APPENDIX

ABSTRACT

As a result of soil-surveying studies conducted in the Swiss and French Jura Mountains during the early 1990's, anomalous cadmium (Cd) concentrations were identified in soils developed mostly on Bajocian and Oxfordian limestone. Measured Cd concentrations exceed in most of the cases the Swiss official tolerance guideline concentration for non-polluted soils established at 0.8 mg·kg^{-1}. Several research works have confirmed the geogenic origin of Cd in soils derived mainly from the weathering of a Cd-rich carbonate substrata.

Cd is a highly toxic trace element and the pedogenic / physicochemical conditions leading to its transfer from rocks to soils and its potential bioavailability to plants are in need of a detailed geochemical assessment. The aim of the present work is to complete the geochemical database by studying rock-soil-plant interactions with regard to this element under natural conditions in two specific sites.

A first study of rock-soil interaction was carried out determining Cd-bearing phases in a soil developed on top of a road-cut section outcropping at the SW-facing slope of the Schleifenberg hill (canton Basel-Land, Switzerland). This section consisting of an oblique succession of Bajocian oolitic carbonate includes several horizons which are anomalously enriched in Cd (0.03–4.90 mg·kg^{-1}). Cd contents in this soil are in the 0.3–2.0 mg·kg^{-1} range. Vertical pedogenetic processes (weathering of underlying bedrock) as well as lateral colluvial limestone (weathering of uphill carbonates) are responsible for the origin of Cd in the soil. Half of the Cd still resides in the carbonate fraction, while the Cd released from the weathered carbonates is associated either with organic matter (over 10%) or with Fe and Mn-oxyhydroxides (approximately 30%). Adsorption of a low percentage of Cd on clays is of less importance since Pb, Zn, Cu and Cr ions will compete with Cd to gain adsorbed sites on clays. No exchangeable Cd phase was found and this, together with the buffer capacity of this calcareous soil, suggests that the amount of mobile Cd is quite negligible, which also greatly reduce the amount of bioavailable Cd. Where developed on steep slopes, the soil will hardly accumulate and colluviums will constantly renew it.

A second study regarding the transfer and distribution of geogenic Cd in the soil was conducted on six closely spaced soil profiles at the site called Le Gurnigel (canton Neuchâtel, Switzerland). The soils consist mainly of cambisols and cambic-neoluvisols showing an important allochthonous, aeolian fraction. Cd concentrations generally increase down the soil profiles, showing maxima (up to 16.3 mg·kg^{-1}) near the soil-bedrock interface. Most Cd resides in the carbonate and organic fractions in topsoils, whereas the amorphous oxyhydroxides fraction becomes the most important Cd-bearing phase in the middle and in subsoils. Cd, Zn and Cr are positively correlated with comparable distributions in the soil profiles suggesting a common bearing phase such as Fe oxyhydroxides for these three elements. A complex transfer pattern of Cd starts with the release of Cd from the underlying bedrock, and then transferred into oxide, hydroxide, carbonate and organic phases. Additionally, the lateral advection of Cd-rich soils formed on steep slopes acts as a local allochthonous input of Cd to these soils, which in turn is transferred from the topsoil towards the deeper horizons by biological and pedogenic processes. The amount of readily exchangeable and therefore potentially bioavailable Cd is low in these soils (on average 0.2 mg·kg^{-1}) provided that the pH remains above 5. Under stronger acidic and oxidizing conditions, Cd bound to organic matter may be mobilised and the bioavailability of Cd would range between 3.3–5.4 mg·kg^{-1} in cambisols and reach up to 1.7 mg·kg^{-1} in deeper cambic-neoluvisols.

Soil-plant interactions were studied at the Le Gurnigel analyzing six local plants chosen for their ubiquity in the studied soil profiles. Cadmium accumulation was separately determined in roots and shoots. Three herbs, two graminoids and a tree were used for this purpose. They showed that the accumulation of Cd varies from one species to another and even between plants from the same family. Global levels of Cd in the selected vegetation are in the 2–6 mg·kg^{-1} range, thus exceeding the official limit value of Cd concentration tolerated in vegetal food for animals established at 1 mg·kg^{-1}. The different behaviours were compared as a function of the variability of Cd in soils. A rise in the concentration of Cd in the soil progressively reduces the transport of Cd toward the shoots reducing also the yield production and increasing the accumulation of Cd in roots. Transfer coefficients from soil / rhizosphere to plant are inversely proportional to the total Cd concentration in soils and do not depend on species identity but instead on soil type. Sequential chemical extractions revealed that variations of Cd distribution between distant soil and rhzosperic soil occur mainly in the first three Cd-bearing phases due principally to the incorporation of roots exudates that modify pH and redox conditions of the rizhosphere. High levels of Cd (up to 9 mg·kg^{-1}) were found in shoots of three of the studied plants and may represent a mid-term hazard for animals and human health since these plants are used either for grazing of cattle or for medical purposes.

The phenomenon of natural enrichment of soils with geogenic Cd and its progressive accumulation in vegetation covers is suspected to have a widespread occurrence elsewhere, as a function of frequent outcrops of Cd-enriched carbonates of Bajocian and Oxfordian age in western and southern Europe principally in France, Spain and Italy.

Keywords: **Cadmium; Bioavailability; Geogenic; Natural pollution; Late-Bajocian carbonates; Plant; Rhizosphere; Soil; Sequential Extraction.**

GENERAL INTRODUCTION

CHAPTER 1

GENERAL INTRODUCTION

1.1 INTRODUCTION

In the framework of systematic soil-surveying studies carried out in the Swiss and French Jura Mountains during the early 1990's, anomalous high cadmium (Cd) concentrations were detected in a selection of soils. In a first approach, human activities were suspected to be at the origin of the Cd enrichments (Atteia et al., 1995). In subsequent studies, however, it was shown that the rates of incorporation of anthropogenic Cd by aerial deposition and application of sewage sludge, manure and phosphate fertilizers were not high enough to explain the anomalous Cd soil contents (Benitez, 1999), since most of the studied sites are remote from urban and industrial activity zones. As a consequence, natural sources of Cd were considered instead as a potential source of the observed Cd enrichments in soils, and further research was carried out with a focus on the underlying bedrocks. As such, it was determined that the excess of Cd in the soils under consideration is principally derived from the parent rock (Benitez, 1999; Dubois et al., 2002; Prudente et al., 2002; Rambeau, 2006).

The parent rocks consist of relatively shallow-water, mostly oolitic limestone, which dates from the Bajocian-Bathonian and Oxfordian-Kimmeridgian stages (Middle and early Late Jurassic). These rocks were shown to have anomalously high Cd concentrations reaching values as high as 8.15 $mg\cdot kg^{-1}$ (Baize and Sterckeman, 2001; Dubois et al., 2002) and exceptionally even up to 21.4 $mg\cdot kg^{-1}$ (Rambeau, 2006). This came rather as a surprise, since Cd contents in marine carbonate rocks were previously considered to range between 0.03 to 0.065 $mg\cdot kg^{-1}$ (Kabata-Pendias and Pendias, 1992; Alloway, 1995; Tuchschmid, 1995). Hitherto, they have not been described as a potential source of Cd to the soils.

Weathering of the Cd-enriched limestone under consideration triggers the release of Cd and subsequent pedogenesis promotes its incorporation into the resulting soil, which becomes enriched in this element. Cd concentrations in soils from specific sites have been reported to reach concentrations of up to 10 $mg\cdot kg^{-1}$ (Dubois et al., 1998; Benitez, 1999) and in one case even to 22 $mg\cdot kg^{-1}$ (Prudente, 1999), and these values largely exceed the official Swiss indicative guideline value for soils fixed at 0.8 mg·kg^{-1} (The Federal Authorities of the Swiss Confederation FASC, 1998). The concerned carbonate formations outcrop rather frequently in the French and Swiss Jura Mountains, and as such, this phenomenon of natural Cd pollution has a widespread occurrence, principally in France (Baize et al., 1999) and suspected in Spain and Italy (Rambeau, 2006).

The discovery of anomalic Cd enrichments in carbonate rocks, which were hitherto considered to be Cd depleted, and which are constituting important area sources in western and southern Europe, has consequences for our understanding of cadmium contaminations in soils and their possible impact on the environment. Geogenic sources of Cd were hitherto thought to be limited on specific and rarely occurring sedimentary rocks such as phosphate- and organic-rich sediments, and the addition of carbonates to the list of potential geogenic sources of Cd to soils fundamentally changes our perspective on this subject of environmental concern. This becomes all the more important since Cd is highly toxic, and this even for very low levels and both the physicochemical and mineralogical conditions as well as the pedogenic processes leading to its transfer from weathered rocks to soils, and its subsequent potential bioavailability, are in need of detailed geochemical assessments.

1.2 AIMS OF THE THESIS

In the present study we follow up on the aforementioned research works in order to investigate the geochemical and mineralogical conditions leading to the mobilization and transfer of cadmium from Cd-enriched carbonates to soils and associated vegetation cover by the process of weathering and soil formation. In order to achieve this goal, three specific objectives were established:

A) To highlight the occurrence of Cd in soils associated with Cd-enriched carbonates. The aim is to confirm the transfer of Cd from rocks, reported as containing anomalous Cd concentrations, to the associated soil by determining total Cd contents and the main physicochemical characteristics. We intend to determine the type of relationship between Cd contents in bedrock and Cd contents in the corresponding soil.

B) To understand the mechanisms of Cd transfer occurring in soils by constituting a solid database of the main physicochemical and mineralogical properties of soil profiles suspected to influence Cd speciation and bioavailability.

C) To study rock/soil/plant interactions by direct observations in the field. Cd contents in selected local plant species are measured and compared in order to determine the phytoavailability of Cd regarding the plant species and the main physicochemical characteristics of naturally enriched soils.

D) To assess the risk that the studied rock-soil-plant interactions may represent for the environment at a larger scale and more specifically with regard to Cd entering into the food chain.

1.3 METHODOLOGY

1.3.1 Fieldwork

Rock-soil interactions

Studies are performed on soils associated with middle and lower upper Jurassic carbonates enriched in cadmium outcropping in Switzerland where soils are in direct contact with this specific lithology. For this purpose, systematic sampling and measuring of soils and corresponding bedrocks were carried out in representative zones enriched in Cd. In addition, soils were characterized in the weathering profiles in order to precise pedogenic processes. Figure 1.1 show the location of the sites considered for this study. They are located at the Schleifenberg section near Liestal (canton Basel-Land) and at Le Gurnigel near La Chaux-de-Fonds (canton Neuchâtel).

Plant-soil interactions

Because of the accessibility and the topography of the Le Gurnigel site, fieldwork was carried out there on a parcel scale in determined sampling points.

Different aspects were taken into account for the choice of the experimental points such as a precise and systematic identification of plant species, their distribution relative to the Cd spatial variability in soils, the physicochemical characteristics of the soils and Cd speciation. The selected species were then collected with roots and shoots to be subsequently analyzed separately.

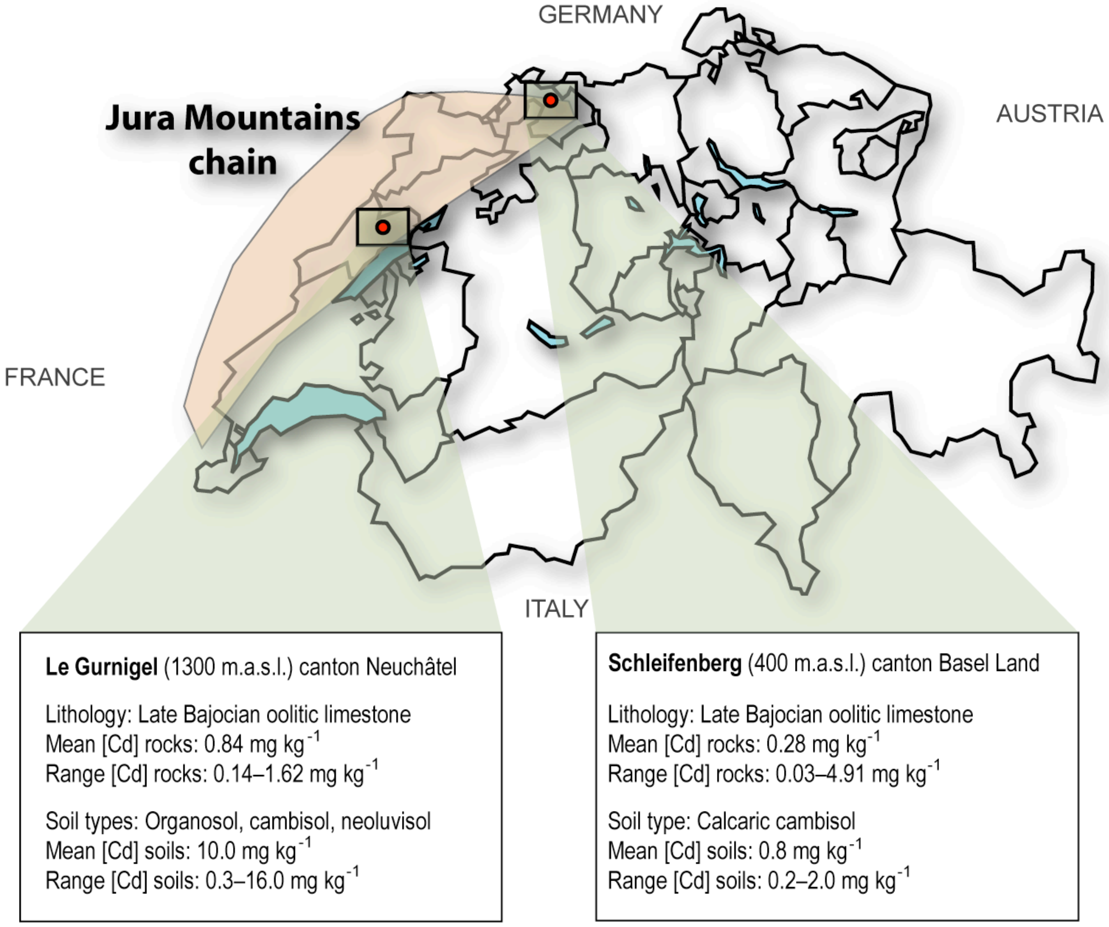

Le Gurnigel (1300 m.a.s.l.) canton Neuchâtel

Lithology: Late Bajocian oolitic limestone
Mean [Cd] rocks: 0.84 mg kg^{-1}
Range [Cd] rocks: 0.14–1.62 mg kg^{-1}

Soil types: Organosol, cambisol, neoluvisol
Mean [Cd] soils: 10.0 mg kg^{-1}
Range [Cd] soils: 0.3–16.0 mg kg^{-1}

Schleifenberg (400 m.a.s.l.) canton Basel Land

Lithology: Late Bajocian oolitic limestone
Mean [Cd] rocks: 0.28 mg kg^{-1}
Range [Cd] rocks: 0.03–4.91 mg kg^{-1}

Soil type: Calcaric cambisol
Mean [Cd] soils: 0.8 mg kg^{-1}
Range [Cd] soils: 0.2–2.0 mg kg^{-1}

Figure 1.1 Location of the Le Gurnigel and the Schleifenberg sites on the Switzerland map

1.3.2 Laboratory work

A) Physicochemical analyses of soil, rock, and plant samples using an ICP-MS (ELAN 6100, Perkin Elmer). The elements considered for the present study are:

- Total concentration of trace metals Cd, Zn, Pb, Cr, Ni, Cu
- Total concentration of major elements Ca, Fe, Al, Mn

B) Mineralogical analyses in soil samples and corresponding bedrocks using a Scintag XDS 2000 diffractometer (Cu-Kα radiation). The mineralogical fractions to study are:

- Bulk rock
- Fine-silt (2–16 µm)
- Clay fraction (<2 µm)

C) Principal physicochemical properties of soils:

- Total organic carbon (TOC) by Rock-Eval^{TM6}
- Mineral-carbon (C_{min}) by Rock-Eval^{TM6}
- Total carbon and nitrogen contents by Carlo Erba 1108
- Cation-exchange capacity (CEC) applying the French method AFNOR NF X31-130
- Soil $pH_{(KCl)}$ and $pH_{(H2O)}$ using a Metrohm 682 titroprocessor

D) Chemical sequential extractions of Cd and trace metals in selected soil samples using a modified Tessier's extraction protocol allowing for the separation of six bearing phases:

- Exchangeable
- Carbonates
- Organic matter
- Amorphous Fe and Mn oxides
- Crystalline Fe oxides
- Residual matrix

1.3.3 Statistical data analyses

Principal Component Analyses (PCA) were applied to the entire database obtained from the measured soil properties, chemical analyses and mineralogical assemblage. Correlation circles were used to discriminate the most significant variables from those that would not play an important role in Cd behaviour in the studied soil systems. Scatter distributions of soil samples were obtained to compare their variability according to the associations of the most significant properties of soils.

We attempted to produce a linear model to predict Cd behaviour in soils by means of multivariable linear regressions. Stepwise methods, both forward selection and backward elimination of variables, were used.

Statistical methods were also used to compare the different ways Cd is accumulated by the selected plant species in their roots and shoots and to evaluate the influence of the main physicochemical properties of soils on vegetal Cd accumulation.

1.4 STUDIED SITES

1.4.1 Schleifenberg

The first objective is treated in the third chapter of this work which deals with a soil developed on top of oolitic carbonates belonging to the Hauptrogenstein Formation of early Bajocian (Middle Jurassic) age, which outcrops along an approximately 330 m long trail cut into the SW-facing slope of the Schleifenberg hill, located northwest of Liestal, in canton Basel-Land (Switzerland; Fig. 1.1). The outcrop consists of a succession of mainly oolitic limestone beds in oblique position, which are partly interlayered by marly intervals (Gonzales, 1993). Rambeau (2006) carried out a detailed survey of Cd contents on this succession and several beds within these carbonates were found to be highly enriched in Cd. Six samples, from a total of 142 samples, showed Cd concentrations above 1 $mg \cdot kg^{-1}$ with a maximum value of 4.91 $mg \cdot kg^{-1}$. The soil is developed on a steep slope (on average 40%) at the SW flank of the Schleifenberg covering the succession of carbonate beds. The soils are rather thin; maximal depths do not exceed 60 cm. The topography of the hill suggests the possibility of soil creeping and incorporation of uphill allochthonous material.

1.4.2 Le Gurnigel

The fourth and fifth chapters are focused to study respectively the rock-soil and soil-plants interactions at Le Gurnigel. This site is a pasture that lies at 1300 m above sea level on the northern face of the Mont d'Amin located in the northern part of canton Neuchâtel (Switzerland; Fig.1.1). The geology of the region reveals that the majority of the site overlies late Bajocian limestone (Middle Jurassic). Aalenian and Bathonian marls are present in the northwestern part.

Cd contents in Bajocian limestone have been reported to range 0.14–1.62 $mg \cdot kg^{-1}$ with a mean value of 0.84 $mg \cdot kg^{-1}$ (Okopnik, 1997; Benitez, 1999; Dubois, 2002). The site present thin solums (13–40 cm deep) identified according to the French pedogenic reference system as organosols, rendosols and calcolsols, which are formed on top and on the flanks of the hills. Deeper soils (80–140 cm deep) are located in the accumulation zones or coombs that are formed by the conjunction of two hillocks. Deep soils are reported to present strong signs of allochthony suggesting that these soils were formed on postglacial aeolian silt deposits. Brunisols, calcisols and neoluvisols correspond to this group of soils. Both groups of soils lie on Bajocian carbonate. Soils formed on marl of Aalenian and Bathonian age show signs of hydromorphy, which increase with soil depth. The latter soils are not considered in the present study.

1.5 REFERENCES

Alloway, B. J., 1995. Cadmium. In: B.J. Alloway (Editor), Heavy Metals in Soils. Blackie Academic and Professional, Glasgow, 122-151.

Atteia, O., Thélin, Ph., Pfeifer, H.R., Dubois, J.P. and Hunziker, J.C., 1995. A search for the origin of cadmium in the soil of the Swiss Jura. Geoderma, 68: 149-172.

Baize, D., Deslais, W. and Gaiffe, M., 1999. Anomalies naturelles en cadmium dans les sols de France. Etude et Gestion des Sols, 2, 85-104.

Baize, D. and Sterckeman, T., 2001. Of the necessity of knowledge of the natural pedo-geochemical background content in the evaluation of the contamination of soils by trace elements. The Science of the Total Environment, 264, 127-139.

Benitez, L. N., 1999. Cadmium speciation and phyto-availability in soils of the Swiss Jura: hypothesis about its dynamics. Ph.D. Thesis, Ecole Polytechnique Fédérale de Lausanne, Switzerland.

Dubois, J. P., Benitez, N., Liebig, T., Baudraz, M. and Okopnik, F., 2002. Le cadmium dans les sols du haut Jura suisse. In D. Baize and M. Tercé (Editors), Les élements traces métalliques dans les sols. Approches fontionelles et spatiales. INRA, Orléans, 33-52.

Gonzales, R., 1993. Die Hauptrogenstein-Formation der Nordwestschweiz (mittleres Bajocien bis unteres Bathonien). Ph.D. Thesis, University of Basel, Switzerland.

Kabata-Pendias, A. and Pendias, H., 1992. Trace elements in soils and plants. CRC Press, Boca Raton.

Prudente, D., 1999. Distribution des teneurs naturelles en cadmium dans les sols de la forêt communale des Fourgs (Doubs, France). Ph.D. Thesis, Ecole Polytechnique Fédérale de Lausanne, Switzerland.

Prudente, D., Baize, D. and Dubois, J.P., 2002. Le cadmium naturel dans une forêt du haut Jura français. In: D. Baize and M. Tercé (Editors), Les élements traces métalliques dans les sols. Approches fontionelles et spatiales. INRA, Orléans, 53-70.

Rambeau, C., 2006. Cadmium anomalies in Jurassic carbonates (Bajocian, Oxfordian) in western and southern Europe. Ph.D. Thesis, University of Neuchâtel, Switzerland.

Tessier, A., Campbell, P.G.C., Bisson, M., 1979. Sequential extraction procedure for the speciation of particulate trace metals. Analytical Chemistry, 51 (7), 844-851.

The Federal Authorities of the Swiss Confederation (FASC), 1998. RS 814.12 Ordonnance sur les atteintes portées aux sols (OSol). Annexe 2., Valeurs indicatives, seuils d'investigation et valeurs d'assainissement pour les métaux lourds et le fluor dans les sols. Official Publications Centre, Switzerland.

Tuchschmid, M., 1995. Quantifizierung und Regionalisierung von Schwermetallen in bodenbildenen Gesteinen der Schweiz. Umwelt-Materialien N° 32. Office Fédéral de l'Environnement des Forêts et du Paysage, Berne.

CADMIUM, SOILS & ENVIRONMENT

CHAPTER 2

CADMIUM, SOILS & ENVIRONMENT

2.1 CADMIUM

References: Alloway (1995); EPA (1999); International Cadmium Association (2005); Rambeau (2006) and references therein

2.1.1 Geochemistry of cadmium in the environment

Cadmium is a naturally occurring chemical element with the symbol Cd, atomic number 48 and atomic weight 112.41. It belongs to group 12 of the Periodic Table below zinc (Zn) and above mercury (Hg). Its physical and chemical properties are similar to those of Zn (similar ionic structures and electronegativities) and to a lesser extent to Hg (similar metallic radii). In the environment, Cd exists in only one oxidation state (+2) and does not undergo oxidation-reduction reactions.

Natural levels of Cd in the environment depend on the specific compartment of consideration. The average concentration of Cd in the Earth's crust is between 0.1 and 0.5 $mg{\cdot}kg^{-1}$. Atmospheric levels of cadmium range from 0.01 to 1.0 $ng{\cdot}m^{-3}$, though it can be considered that in the past twenty years, Cd concentration in the air reach up to 5 $ng{\cdot}m^{-3}$ in rural areas, from 0.005 to 0.015 $\mu g{\cdot}m^{-3}$ in urban areas, and up to 0.06 $\mu g{\cdot}m^{-3}$ in industrial areas (WHO 1992). Concentrations may reach 0.3 $\mu g{\cdot}m^{-3}$ weekly mean values near metal smelters (WHO 1987). Atmospheric cadmium is generally associated with particulate matter of respirable size.

Fresh water typically contain levels of cadmium below 1 $\mu g{\cdot}L^{-1}$, normally in the 0.01–0.07 $\mu g{\cdot}L^{-1}$ range; but concentrations up to 10 $\mu g{\cdot}L^{-1}$ may occur on rare occasions due to environmental disturbances such as acid rain. Estimates for seawater range from 0.001 to 0.075 $\mu g{\cdot}L^{-1}$ and for rainwater from 0.0001 to 0.001 $\mu g{\cdot}L^{-1}$.

Most Cd in Earth's crust is present in zinc sulphide minerals, principally sphalerite and wurtzite (ZnS), as an atomic substitution for Zn making up less than 1% of the mineral in general, yet ZnS ores with 5% Cd are found. Only a few relatively pure Cd minerals are known, which appear as rather small crystals and are rare. Among these are the minerals greenockite (CdS) and otavite ($CdCO_3$). Igneous and metamorphic rocks have been reported with low concentrations of Cd that are in the 0.02–0.2 mg·kg^{-1} range (ICA, 200%). Cd may also occur as an impurity in phosphate minerals in concentrations of several hundred parts per million (ppm). As such, sedimentary rocks show a greater range of Cd contents than other rock types, with phosphorites (500 mg·kg^{-1}; WHO, 1992; Cook and Morrow, 1995), marine black shales and carbonates (0.030–0.065 mg·kg^{-1}; Kabata-Pendias and Pendias, 1992; Alloway, 1995, Tuchschmid, 1995). Recent studies have reported that specific carbonate rocks, in particular from the Swiss-French Jura Mountains, contain higher contents of Cd than the normally estimated for limestone, frequently above 1 mg·kg^{-1} (Benitez-Vasquez, 1999; Veuve, 2000; Baize and Steckerman, 2001; Dubois et al., 2002; Prudente et al., 2002, Rambeau, 2006).

In surface and groundwater, Cd is able to form a number of aqueous complexes, especially with dissolved carbonate. It may also exist in solution as the hydrated ion, and form other inorganic complexes such as chlorides, sulphates, hydroxides, and organic complexes with humic acids. Soluble forms of Cd may migrate in water. Cd mobility in solution may be controlled by either adsorption or precipitation/coprecipitation processes in associated sediments.

Cd's fate in soil depends on several factors such as soil pH, the availability of organic matter and environmental conditions. It is not likely that Cd undergoes significant transformation within the atmosphere. It exists in particulate form and sometimes in vapour form (emitted from high temperature processes), and as such, it may undergo atmospheric transport and eventually deposit onto soils and surface waters.

2.1.2 Cadmium in soils

Cd concentrations in uncontaminated soils are typically less than 1 mg·kg^{-1}. Analytical studies reported background levels in soils in the range of 0.06–1.1 mg·kg^{-1} (EPA, 1999), with a calculated worldwide mean of 0.53 mg·kg^{-1}. However, concentrations may be significantly higher due to both natural and anthropogenic sources of contamination. Natural sources comprise the weathering of parent material with high Cd concentrations, which may be autochthonous such as a solid rock substratum or transported parent material such as glacial till and alluvium. Anthropogenic inputs of Cd to soils are due to aerial deposition, non-ferrous metal production, sewage sludge and the use of phosphate fertilisers.

Soils are considered as a sink for Cd as the vast majority of Cd emissions of anthropogenic origin (80 to 90%) pass initially to the soil environment. The net flux into the soil is regarded as positive since the transfer of Cd occurs both from the atmosphere and water into this compartment and since this transfer is not counterbalanced by equal outputs such as soil leaching and biomass uptake. Within the solum, Cd is normally concentrated in the upper horizons due mainly to high organic-matter contents. Metals may also be retained in these horizons as a result of cycling through vegetation or from application of Cd-containing fertilisers or from wet and dry depositions from the atmosphere. Nevertheless, Cd has the tendency to move down the soil profile depending on various soil and site factors.

Cd speciation, adsorption, and distribution in soils are mainly governed by pH, soluble organic-matter content, hydrous metal-oxide content, clay content and type, presence of organic and inorganic binders, and competition from other metal ions. Figure 2.1 presents the effect of soil properties on the soil-solution distribution of Cd.

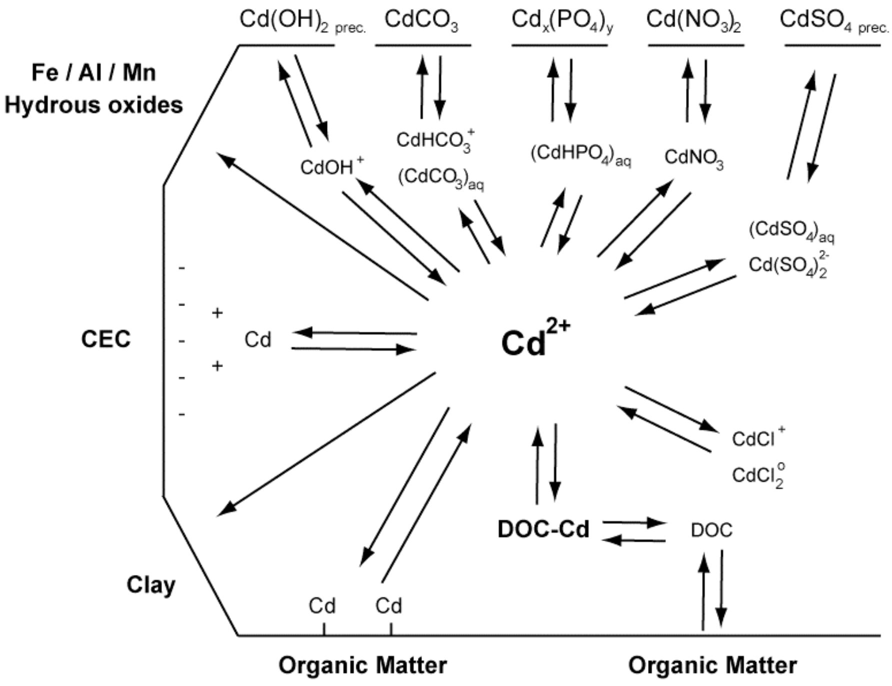

Figure 2.1 Effect of soil properties on soil-solution speciation of Cd (from Meers et al., 2005).

At pH values less than 7.5, most Cd minerals are more soluble than Cd concentrations found in freely drained (oxic) soils (10^{-7} M). At these concentrations Cd is not likely to precipitate. At pH levels greater than 7.5, the solubilities of $Cd_3(PO_4)_2$ or $CdCO_3$ (otavite) may control the concentrations of Cd in soils. It has been found that $CdCO_3$ precipitates in calcareous soils (pH > 7.8), whereas in neutral or acidic soils, adsorption is the predominate process for removal of Cd from solution.

The free ion Cd^{2+} in soil solution is more likely to be adsorbed on the surfaces of soil solids than other species in soil solution: $CdCl^{+}$, $CdOH^{+}$, $CdHCO_3^{+}$, $CdCl_3^{-}$, $CdCl_4^{2-}$, $Cd(OH)_3^{-}$ and $Cd(OH)_4^{2-}$ together with organic complexes. Chemical modelling programs have predicted the following species of Cd in oxic soil solution: Cd^{2+}, $CdSO_4^{o}$ and $CdCl_4^{+}$ in acid soils; Cd^{2+}, $CdCl^{+}$, $CdSO_4^{o}$ and $CdHCO^{+}$ in alkaline soils.

Relative significance of cadmium fractions in non-contaminated surface and subsoil horizons are often described as follow: Cd residual matrix >> Cd bound in/on Fe/Mn oxides > Cd exchangeable and specifically adsorbed > Cd complexed by organic matter >> water soluble Cd. Increasing anthropogenic soil contamination with cadmium, visible in surface horizons of soils located near smelters, manifests in a relative increase of non-residual fractions, the exchangeable and non-specifically adsorbed cadmium in particular (Kabała and Singh, 2006; Akkajita and Tongcumpoua, 2009).

2.2 THE SOIL SYSTEM

References: Alloway (1995); Gobat et al. (2003) and references therein

The soil is a complex heterogeneous medium comprising mineral and organic solids, aqueous and gaseous components. The minerals present are usually weathered rock fragments and secondary minerals such as phyllosilicates, Fe, Al, and Mn oxides (including hydrous oxides and oxyhydroxides) and sometimes carbonates (usually $CaCO_3$). Soil organic matter comprises living organisms (mesofauna and microorganisms), dead plant material (litter) and colloidal humus formed by the action of microorganisms on plant litter. These solid components are usually clustered together in the form of aggregates, thus creating a system of interconnected voids (pores) of various sizes filled with either water or air. The solid components have the ability to absorb ions; a feature, which depends on the type of building materials and which is strongly influenced by prevailing pH and redox conditions and relative concentrations of ions present in the aqueous soil solution.

The soil is a multifunctional crossway. As such, its main roles are:

- To support diverse life forms
- To stock organic matter and several minerals
- To be a regulator in the multiple energy and matter exchanges of the ecosystem

- To be the place where organic matter is degraded and transformed
- To recycle dead biomass
- To be a purifier system of toxic substances.

In the following lines, we present a brief bibliographic review of the main physicochemical properties of soils considered to have a significant effect on Cd distribution within the studied soil profiles, being the main subject of the present work.

2.2.1 Clay minerals

Clay minerals are products of rock weathering and have marked effects on both physical and chemical properties of the soils. Their contribution to soil chemical properties results from their comparatively large surface area and permanent surface negative charge. The soil textural class is dependent on the percentages of clay, silt and sand-sized particles. The clay fraction comprises dispersed minerals of less than two μm diameter. In most cases, this applies specifically to the mineralogically distinct group of clay minerals, although it can also include finely ground particles of other minerals.

The most common types of clay minerals include the kaolinites (0.7 nm thick constant) comprising one tetrahedral silica SiO_2 sheet and one octahedral gibbsite $Al(OH)_3$ sheet referred to as a 1:1 clay mineral; the illites (1 nm thick constant) and vermiculites (1–1.5 nm thick variable) comprising basically two silica sheets and one gibbsite (2:1), the smectites-montmorillonites (up to 2 nm thick when hydrated) also with two silica sheets and one gibbsite sheet (2:1); and the chlorites (1.4 nm thick) with a 2:1:1 sandwich structure: silica-gibbsite-silica sheets followed by an octahedral brucite $Mg(OH)_2$ sheet. In all minerals except kaolinites, isomorphous substitution within the mineral lattice gives rise to a net negative charge on the surface of the mineral. This is caused by trivalent Al^{3+} substituting for tetravalent Si^{4+} in tetrahedral sites and divalent Mg^{2+}, Fe^{2+} or trivalent Fe^{3+} substituting for Al. octahedral sites.

Mixed layer clay variations exist for most of the above groups. Ordering is described as random or regular ordering. Ordered illite-smectite would be regularly ordered in an ISISIS fashion. Mixed layer clay minerals which are perfectly ordered types often possess their proper names, e.g., ordered illite-smectite is known as rectorite, ordered chlorite-smectite is corrensite. Pedogenic integrades of type illite-vermiculite (illite-smectite are less common) may incorporate Al, Fe or Mg hydroxides in the interlayered water preventing them to expand. Due to this phenomenon, such inetrgrades are sometimes referred to as non-expandable or block mixed-layered complexes (IS-B). Their presence would suggest a more developed soil enriched with Al and Fe hydroxides. During soil formation, illite is transformed into illite-vermiculite mixed layers; chlorite is quickly weathered to give smectite layers. Kaolinite would be the most stable phyllosilicate. Vermiculite and smectite progressively desaturate, i.e. exchangeable cations (Ca, Mg) are removed and replaced by Al polycations; hydroxy-Al interlayered minerals are formed.

Most of the soils in temperate zones are developed from rocks, which contain phyllosilicates: granite, sedimentary rocks and metamorphic rocks, loess or glacial tills (muscovite, biotite and chlorite). In these soils the clay fraction is constituted of a mixture of relics of initial phyllosilicates with new clay minerals formed by weathering. In general, fine-clay fractions contain higher proportions of expandable clay minerals (vermiculite, smectite) than coarse fractions dominated by mica, kaolinite and quartz. Therefore, clay-rich horizons (horizons BT) have a higher cation exchange capacity (CEC).

Clay minerals rarely exist in pure form in soils; they usually have humic colloids and hydrous oxide precipitates linked to them. The combined organo-mineral colloidal complex plays a very important role in controlling the ion concentrations in the soil solution.

2.2.2 Soil organic matter

All soils contain organic matter (living organisms, organic debris and humus), though the amount and type may vary considerably. Colloidal soil organic matter has a major influence on the chemical properties of soils, and can be divided into non-humic and humic substances. The non-humic substances comprise unaltered biochemicals such as amino acids, carbohydrates, organic acids, fats and waxes that have not changed from the form in which they were synthesized by living organisms. Humic substances are a series of acidic, yellow to black coloured polyelectrolytes of moderately high molecular weight. They are formed by secondary synthesis reactions involving microorganisms and have characteristics which are dissimilar to any compounds in living organisms. They have a wide variety of functional groups, including carboxyl, phenolic hydroxyl, carbonyl, ester and possibly quinone and methoxy groups. While predominantly composed of humic substances, soil humus also contains some biochemicals bound to the humic polymers. The elemental composition of humus is typically (on an ash free-basis): 44–53% C, 3.6–5.4% H, 1.8–3.6% N and 40–47% O.

2.2.3 Hydrous oxides of Fe, Mn and Al

The term hydrous oxides refers to all oxides MO_x, hydroxides $M(OH)_x$, and oxyhydroxides MO_xOH_y of a metal M. The hydrous oxides are common crystalline and non-crystalline components of soils. They generally form by the weathering of primary or secondary silicate minerals and are some of the most stable minerals that occur in well-aerated soils. Al, Fe, and Mn hydroxides and oxyhydroxides all have several polymorphs. The chemical and physical conditions of the soil environment determine which polymorph will form. Isomorphous substitution is common in hydrous oxides, but only to a limited extent.

The hydrous oxides of Fe, Al and Mn play an important role in the chemical behaviour of metals in soils. They occur in the clay-size fraction (<2 μm) and are usually mixed with clays and have a disordered structure.

In oxic soils, oxides of Fe, Al and Mn, precipitate from solution and occur as:

- Coatings on soil particles where they are often intimately mixed with clays,
- Fillings in voids
- Concentric nodules.

Hydrous Fe oxide minerals tend to be the most abundant of all oxides in soils. Gibbsite $Al(OH)_3$ is a common form of Al hydroxide but is less abundant than Fe oxides. Initially, precipitation of Fe is usually in the form of gelatinous ferrihydrite ($Fe_5HO_8{\cdot}4H_2O$) and this gradually dehydrates to more stable forms such as goethite (α-FeOOH). Goethite is the most common Fe oxide found in soils and hematite (α-Fe_2O_3) is found mainly in tropical soils. Lepidocrocite (γ-FeOOH) is characteristic of the fluctuating redox conditions in gleyed soils.

Common Mn oxides in soils are birnessite $(Na_{0.3}Ca_{0.1}K_{0.1})(Mn^{4+},Mn^{3+})_2O_4{\cdot}$ $1.5H_2O$, hollandite $Ba(Mn^{4+},Mn^{2+})_8O_{16}$ and lithiophorite $(Al,Li)Mn^{4+}O_2(OH)_2$.

With regard to the dynamics of heavy metals in soils, Fe and Mn oxides co-precipitate and adsorb (scavenge) cations including Cd, Co, Cr, Cu, Mn, Mo, Ni, V and Zn, and anions such as HPO_4^{2-} and AsO_4^{3-}, from solution. This is due to a pH-dependent charge which, generally speaking, is negative in alkaline conditions and positive in acid conditions.

Little permanent charge has been attributed to the hydrous oxides, although this is very difficult to determine due to their small crystal size. The majority of charge is due to variable charge sites resulting from surface O, OH, and OH_2 groups. Variable charge is due to the presence of sites that can have their charge changed by potential determining ions. The most common potential determining ions include H^+ and OH^-, although other more complex ions such as SO_2^{4-} and PO_4^{3-} may also have an effect.

2.2.4 Soil pH

Soil pH is the measurement of hydrogen activity in the solution present in soil pores, which is in dynamic equilibrium with the predominantly negatively charged surfaces of the soil particles. Hydrogen ions are strongly attracted to the surface negative charges and they have the power to replace most other cations. Soil pH is affected by changes in redox potential. Reducing conditions generally cause a pH increase, and oxidation brings about a decrease.

Soil pH is the single most important factor affecting soil productivity. The reasons are: it affects the solubility and availability of nutrients and toxic elements, microbial activity, the ability of soils to hold nutrients and water, and physical properties of the soil. In general, heavy metal cations are most mobile under acid conditions and increasing the pH by liming usually reduces their bioavailability. At pHs below 7, most micronutrients such as Cu, Zn, and Fe and most toxic elements such as Pb and Cd are more soluble with the exception of Mo and thus available for plant uptake. At pHs above 7.5, most micronutrients become unavailable. Thus, the plants suffer from micronutrient deficiencies.

Most plants grow well in pH values between 5.5 and 7.5 with the notable exceptions of acid loving plants such as blueberries, which will grow at pHs below 5.5. pH also effects the amount of microbial activity which occurs in the soil. The higher the soil pH, the more overall microbial activity will be. Thus, organic-matter decomposition happens quicker at higher pHs. At low pHs, the primary organism involved in decomposition is fungi. Soils generally have pH values within the range 4–8.5 due to the buffering by Al at the lower end and by $CaCO_3$ at the upper end of the range.

The soil net ability to hold nutrients and water is higher with increasing pH. This is especially true with soils with high organic matter contents and also certain types of clays. The reason is that when the exchangeable acidity is removed, the exchange sites will be able to adsorb other ions. Thus, the cation exchange capacity (CEC) of the soil will vary with pH.

2.2.5 Cation Exchange Capacity CEC

Cation exchange capacity is defined as the degree to which a soil adsorbs and exchanges cations. Most heavy metals exist mainly as cations in the soil solution, and their adsorption depends therefore on the density of negative charges on the surfaces of the soil colloids. In order to maintain electroneutrality, the surface negative charge is balanced by an equal quantity of cations. Ion exchange refers to the exchange between the counter-ions balancing the surface charge on the colloids and the ions in the soil solution.

As it has been mentioned in §2.2.1, §2.2.2 and §2.2.3, soil particles and organic matter have negative charges on their surfaces. Mineral cations can adsorb onto inorganic and organic soil particles. Once adsorbed, these minerals are not easily lost when the soil is leached by water and they also provide a nutrient reserve available to plant roots.

These minerals can then be replaced or exchanged by other cations (i.e., cation exchange). CEC is highly dependent upon soil texture and organic-matter content. In general, the higher are the contents of clay and organic matter in the soil, the higher is the CEC. Clay content is important because these small particles have a high ratio of surface area to volume. Different types of clays also vary in CEC. Smectites have the highest CEC (80–100 $\mathrm{cmol \cdot kg^{-1}}$), followed by illites (15–40 $\mathrm{cmol \cdot kg^{-1}}$) and kaolinites (3–15 $\mathrm{cmol \cdot kg^{-1}}$).

2.3 THE JURA MOUNTAIN RANGE

References: Pochon (1978); Sommaruga (1997) and references therein

2.3.1 Geology

The Jura mountain range is a folded arc-shaped belt located in France, Switzerland and Germany in front of the western Alpine arc (Fig. 1.1). The highest peak in France is the Crête de la Neige (1720 m.a.s.l.) and in Switzerland the Mont Tendre (1679 m.a.s.l.). The outer arc of the Jura is 400 km long and the inner arc 340 km. The width between both arcs varies from 0 km at the eastern end, to 65 km between Neuchâtel (Switzerland) and Besançon (France). The external Jura located in France consists of flat areas or plateaux. The internal Jura arc or folded Jura runs through the northwestern part of Switzerland and consists of a well developed fold train representing a natural present-day northern limit to the Molasse Basin. A third zone, the Tabular Jura, is often associated with the Jura. This zone is located outside of the Jura arc and represents the Mesozoic cover of the southern Black Forest and Vosges basement.

The folded Jura comprise sedimentary formations from Triassic to Miocene in age. During the Mesozoic era, the Jura and Molasse Basin realm was part of the northern Alpine Tethys passive margin and comprises a total thickness of up to 2 km of alternating limestone and marl. The actual geomorphology of Jura landscapes takes the shapes of the described tectonic structures. Anticlines form the top of hills and synclines the valleys or accumulation zones.

2.3.2 The Jura soils

References: Pochon (1978); Benitez (1999); Gobat et al. (1997); Havlicek (1999) and references therein

Several soil types may be identified in the Jura Mountains. The most common soil types in the Swiss Jura are the following:

- Organosols (10–20 cm deep)
- Lithic leptosols (<10 cm deep)
- Rendzic leptosols (20–35 cm)
- Eutric cambisols and dystric cambisols (35–55 cm deep)
- Cambisol-neoluvisols (30–155 cm deep)

The pH of the Jura soils varies between fairly neutral (6.5–7.0) in shallow soils (<15 cm) and acidic values (4.5–6.0) in deep soils (>70 cm).

Jura soils may have developed directly on top of calcareous bedrock such as limestone and marl, and an important part was also formed on allochthonous aeolian deposits coming from the Würm glacial period (Pochon, 1978). As a general rule, autochthonous soils present a mineralogical composition similar to that of the dissolution residue of the associated bedrock. In this case, K-feldspars are much more abundant than plagioclase, chlorite is very low, and kaolinite is the dominating phyllosilicate. On the other hand, the mineralogical assembly of allochthonous soils contains plagioclases, which are not detected in bedrock. The same observation is true for chlorite in the clay-mineral fraction. Plagioclases are also much more abundant than K-feldspars in allochthonous soils.

Soils developed from loess material exhibit clay illuviation (movement of clay particles by transport in suspension in the soil water). Redeposition of translocated clay causes the formation of clay-rich horizons at certain depths in the soil profiles. The finest clay fraction (0.1 μm) is most affected by this dispersion while coarse clays are less mobile. Deep horizons change to a brownish colour, typical for cambisols (brunisols), develop a polyhedral soil structure, and show limited mechanical fragmentation of silt-sized phyllosilicates. Illite, chlorite, kaolinite and smectite are the major phyllosilicates in loess material.

2.3.3 Anomalous Cd enrichments in carbonate rocks of the Jura mountains

Cd contents in carbonate rocks are generally quite low (mean Cd concentrations range between 0.03–0.035 mg·kg^{-1}). Tuchschmid (1995), however, found higher Cd concentrations in carbonates of Switzerland (0.03–0.20 mg·kg^{-1}) with a maximal value of 2.42 mg·kg^{-1}. Benitez (1999) found Cd concentrations ranging between 0.09–1.32 mg·kg^{-1} in Bajocian rocks and 0.04–0.54 mg·kg^{-1} in Kimmeridgian rocks. Further research works reported anomalous Cd contents of up to 8.15 mg·kg^{-1} and even a highest record of 21.4 mg·kg^{-1} observed in carbonates of Bajocian and Oxfordian-Kimmeridgian ages (Prudente, 1999; Veuve, 2000; Baize and Sterckeman, 2001; Dubois et al., 2002; Rambeau, 2006).

Two possible models were proposed to explain the origin of these anomalous enrichments: Veuve (2000) and Rambeau (2006) established a model of synsedimentary and early diagenetic enrichment in Cd of shallow-water carbonate rocks in Jura mountains with organic matter as a vector of Cd transport. Efimenko et al. (2010) proposes instead a model of formation of Cd-bearing sphalerite mineralisations and cadmium incorporation into the Jurassic rocks during periods of tectonic and hydrothermal activity in the region.

2.3.4 Cd enrichments in soils associated to Cd-rich carbonate rocks

Surveying programs of the Swiss-French Jura soils and several research projects have established that soils with high Cd concentrations are consistently associated with carbonate rocks that are exceptionally rich in Cd (Atteia et al., 1994; Benitez, 1999; Baize and Sterckeman, 2001; Dubois et al., 2002; Prudente et al., 2002). These rocks as described in §2.3.2 have been assigned to the Bajocian (middle Juassic) and Oxfordian-Kimmeridgian (Late Jurassic) epochs. Soils associated with these carbonate rocks contain elevated Cd concentrations of up to 16 mg·kg^{-1} and even 22.3 mg·kg^{-1} in the topsoil (Prudente et al., 2002); values that largely exceed the Swiss and French official tolerance guideline values of 0.8 mg·kg^{-1} (Osol, 1998) and 2 mg·kg^{-1} (AFNOR, 1996), respectively.

Two sites in the Jura Mountains (Le Gurnigel, canton Neuchâtel, Switzerland; and Les Fourgs, department of Doubs, France) present soils that are enriched in cadmium by a factor of 10 to 20 relative to the rock substratum (Baudraz, 1995; Okopnik, 1997; Benitez, 1999; Baize et al., 1999; Prudente et al., 2002; Dubois et al., 2002). In a recent survey on natural cadmium enrichments in soils of France, which have formed on top of carbonate rocks, an average enrichment factor of approximately 10 was observed (Baize et al., 1999). At a site in the Frétoy forest (near Avallon, Burgundy, France), the enrichment factor ranged 4 to 8 in a soil associated with a fossil carbonate reef complex of late Oxfordian age (Rambeau et al., 2010).

Up to now, only a few selected soils in the Swiss and French Jura have been investigated with regards to their geogenic Cd enrichments (e.g., Les Fourgs, department of Doubs, France; Prudente et al., 2002; Dubois et al., 2002). These sites were also investigated relative to others parameters such as organic carbon, metal contents, CEC, pH, and particle size, and all results obtained have confirmed the geogenic origin of Cd and have also highlighted a Cd/Zn relation. However, the investigations were limited to the total Cd contents and the speciation of Cd was not analyzed. It is for this reason and probably also for the paucity of investigated sites that an empirical relation between the different physicochemical parameters could not be established. The authors of these studies concluded, therefore, that additional studies are necessary in order to precise the spatial distribution of Cd, its variability and speciation in these particular naturally enriched zones.

2.4 ENVIRONMENTAL RISKS

2.4.1 Toxicological profile of Cd

References: International Cadmium Association (2005); U.S. Department of Health and Human Services (2008) and references therein

Cd is one of the most toxic and mobile metallic elements found in soil. Cd and several Cd-containing compounds are known carcinogens. It inhibits important enzyme reactions in which zinc and calcium are involved, thereby causing different forms of cancer and damaging carriers of genetic information.

Cd is taken up by food, cigarette smoke, and by the skin. It is transported to the liver by means of the blood. Once in the liver, it bonds to proteins forming complex substances that are transported to the kidneys. Cadmium is stocked in the kidneys damaging their filtration mechanisms. Due to this, essential proteins and sugar are excreted out of the organism. Other serious problems that Cd may produce in the body are the following:

- Diarrhoea, stomach-aches, and vomiting,
- Fragile bones susceptible to break,
- It affects the reproductive capacity leading to infertility
- Damage the central nervous system
- Damage to the immune system
- Psychological disorders

- Likely to alter DNA or to induce to cancer.

It takes long to eliminate Cd out of the body. The toxic dose lies between 3 and 330 mg. One gram of cadmium is lethal.

2.4.2 Cadmium phytoavailability

References: Alloway (1995); Benitez (1999); International Cadmium Association (2005); Kim (2005); Kirkham (2005) and references therein

The concentrations of cadmium found in general in the environment do not cause acute toxicity. Nonetheless, even if Cd is an element that is not essential for plants, it has some properties which are partly similar to those of the essential micro-nutrient Zn, which is easily taken up by plants and that can be potentially bio-accumulated in the food web. In natural soils, cadmium toxicity to plants (phytotoxicity) is rare because Zn toxicity intervenes before it can develop (Kim, 2005). This means that concentrations of Cd can accumulate in plants that are not toxic to them, yet are toxic to the animals eating the plants.

The uptake of Cd in plants has been shown to be influenced by its speciation and thus, as mentioned previously, by a wide range of soil and plant variables. These include soil pH, soil organic matter, soil salinity, soil texture, total soil Cd, micro- and macro-nutrients and plants species and crops.

Various studies show that total soil cadmium content alone is not a good measure for short-term bioavailability and not a very useful tool to determine potential risks arising from soil contamination (Zhou et al., 1994; McBride, 2002). Actual prediction of Cd uptake by plants is based simultaneously on three parameters: total soil Cd, soil pH, and soil organic matter (Li et al., 2003) which allow generating numerous empirical relationships. Phytoavailability assessments were performed on anthropogenically polluted sites and rarely on geogenically contaminated sites. It is likely that Cd speciation and thus Cd mobility and bioavailability are quite different in the soils evolved from cadmium-enriched carbonates.

2.4.3 Environmental consequences of Cd-rich soils

According to the above bibliographical review on Cd geochemistry in soils and the research works conducted so far in the Jura Mountain range, it can be stated that the potential of soils developed from Cd-enriched carbonates of Middle to early Late Jurassic age to be naturally contaminated with regards to Cd is considerable, if the Swiss (0.8 mg·kg^{-1}) or French (2.0 mg·kg^{-1}) tolerance guideline values are applied. This is all the more important since Cd-enriched carbonates may reach stratigraphic thicknesses of several 10's of meters, which renders them diffuse area sources rather than point sources of Cd to the environment. In addition, the widespread occurrence of Cd-enriched carbonates of Middle to early Late Jurassic age in western and southern Europe suggests that this type of enrichment and the potentially associated Cd-enriched soils may not be limited to the investigated regions, but may also occur on a wider scale.

Considering that plants may transfer Cd from soils to their roots and leaves, an environmental risk linked to the occurrence of naturally enriched Cd in soils is related to potential Cd accumulation in the food web, with possible consequences on human health by direct ingestion (crops) or by indirect contamination (contaminated milk or cheese consumption).

2.5 REFERENCES

Akkajita and Tongcumpoua, 2009. Fractionation of metals in cadmium contaminated soil: Relation and effect on bioavailable cadmium. Geoderma, 156, 126–132

Alloway, B. J., 1995. Cadmium. In: B.J. Alloway (Editor), Heavy Metals in Soils. Blackie Academic and Professional, Glasgow, 122–151.

Atteia, O., Thélin, Ph., Pfeifer, H.R., Dubois, J.P. and Hunziker, J.C., 1995. A search for the origin of cadmium in the soil of the Swiss Jura. Geoderma, 68, 149–172.

Baize, D., Deslais, W. and Gaiffe, M., 1999. Anomalies naturelles en cadmium dans les sols de France. Etude et Gestion des Sols, 2, 85–104.

Baize, D. and Sterckeman, T., 2001. Of the necessity of knowledge of the natural pedo-geochemical background content in the evaluation of the contamination of soils by trace elements. The Science of the Total Environment, 264, 127–139.

Baudraz, M.,1995. Variabilité spatiale des métaux lourds à travers la chaîne jurassienne. Travail de diplôme, EPFL.

Benitez, L. N., 1999. Cadmium speciation and phyto-availability in soils of the Swiss Jura: hypothesis about its dynamics. Ph.D. Thesis, Ecole Polytechnique Fédérale de Lausanne, Switzerland.

Dubois, J. P., Benitez, N., Liebig, T., Baudraz, M. and Okopnik, F., 2002. Le cadmium dans les sols du haut Jura suisse. In D. Baize and M. Tercé (Editors), Les élements traces métalliques dans les sols. Approches fontionelles et spatiales. INRA, Orléans, 33–52.

Efimenko, N., Spangenberg, J.F., Schneider, J., Chiaradia, M., Adatte, T., Föllmi, K.B., submitted. Formation and age of cadmium-containing sphalerite mineralisations in carbonate rocks of Bajocian age in the Swiss Jura mountains. Geochimica et Cosmochimica Acta.

Gobat, J.M., Aragno, Matthey, 2006. Le Sol vivant. Presses polytechniques et universitaires romandes, Lausanne.

Havlicek, E., 1999. Les sols des paturages boisés du Jura suisse. Ph.D. Thesis, University of Neuchâtel, Switzerland.

International Cadmium Association, 2005. Available on http://www.cadmium.org/.

Kabała, C. and Singh, B.R., 2006. Distribution and forms of Cadmium in Soils near a Copper Smelter. Polish J. Environ. Stud. Vol. 15, No. 2a, 90–97.

Kabata-Pendias, A. and Pendias, H., 1992. Trace elements in soils and plants. CRC Press, Boca Raton, Florida, USA.

Kim, N., 2005. Cadmium accumulation in Waikato soils. Environment Waikato Technical Report 2005/51.

Kirkham, M.B., 2006. Cadmium in plants on polluted soils: Effects of soil factors, hyperaccumulation, and amendments. Geoderma 137, 19–32

Li, F., Okazaki, M. and Zhou, Q., 2003, Evaluation of Cd uptake by plants estimated from total soil Cd, pH, and organic matter. Bulletin Environmental Contamination and Toxicolology, 71, 714–721.

McBride, M.B., 2002, Cadmium uptake by crops estimated from soil total Cd and pH. Soil Science, 167, 62–67.

Okopnik, F., 1997. Relation entre la variabilité spatiale du Cd et la couverture pédologique de la region du Mon d'Amin. Master thesis, Ecole Polytechnique Fédérale de Lausanne, Switzerland.

Pochon, M., 1978. Origine et évolution des sols du Haut-Jura suisse. Ph.D. Thesis, University of Neuchâtel, Switzerland.

Prudente, D., 1999. Distribution des teneurs naturelles en cadmium dans les sols de la forêt communale des Fourgs (Doubs, France). Ph.D. Thesis, Ecole Polytechnique Fédérale de Lausanne, Switzerland.

Prudente, D., Baize, D. and Dubois, J.P., 2002. Le cadmium naturel dans une forêt du haut Jura français. In: D. Baize and M. Tercé (Editors), Les élements traces métalliques dans les sols. Approches fontionelles et spatiales. INRA, Orléans, 53–70.

Rambeau, C., 2006. Cadmium anomalies in Jurassic carbonates (Bajocian, Oxfordian) in western and southern Europe. Ph.D. Thesis, University of Neuchâtel, Switzerland.

Rambeau, C., Baize, D., Saby, N., Matera, V., Adatte, T. and Föllmi, K.B., 2010. High cadmium concentrations in Jurassic limestone as the cause for elevated cadmium levels in deriving soils: a case study in Lower Burgundy, France. Environmental Earth Sciences, in press.

Sommaruga, A., 1997 Geology of the Central Jura and the Molasse Bassin: New insight into an evaporite-based foreland fold and thrust belt. Thesis, University of Neuchâtel, Switzerland.

Tessier, A., Campbell, P.G.C., Bisson, M., 1979. Sequential extraction procedure for the speciation of particulate trace metals. Analytical Chemistry, 51 (7), 844–851.

The Federal Authorities of the Swiss Confederation, 1998. RS 814.12 Ordonnance sur les atteintes portées aux sols (OSol). Annexe 2., Valeurs indicatives, seuils d'investigation et valeurs d'assainissement pour les métaux lourds et le fluor dans les sols. Official Publications Centre, Switzerland.

Tuchschmid, M., 1995. Quantifizierung und Regionalisierung von Schwermetallen in bodenbildenen Gesteinen der Schweiz. Umwelt-Materialien N° 32. Office Fédéral de l'Environnement des Forêts et du Paysage, Berne.

U.S. Department of Health and Human Services, 2008. Draft toxicological profile for Cadmium. Available at www.atsdr.cdc.gov/.

World Health Organization (WHO), 1975. "Environmental Hazards of Heavy Metals: Summary Evaluation of Lead, Cadmium and Mercury." Environmental Health Criteria 20. Geneva.

World Health Organization (WHO), 1987. Air Quality Guidelines. Copenhagen: WHO Regional Office for Europe.

World Health Organization (WHO), 1992a. "Cadmium." Environmental Health Criteria 134. Geneva.

World Health Organization (WHO), 1992b. “Cadmium: Environmental Aspects.” Environmental Health Criteria 135. Geneva.

World Health Organization (WHO), 1993. Guidelines for Drinking Water Quality. Vol. 1: Recommendations. 2d ed. Geneva.

Zhou, Q.X., Wu, Y.Y. and Xiong, X. Z., 1994, Compound pollution of Cd and Zn and its ecological effect on rice plant. Chinese Journal of Applied Ecology, 5, 438–441.

CADMIUM DISTRIBUTION IN SOILS COVERING JURASSIC OOLITIC LIMESTONE WITH HIGH Cd CONTENTS IN THE SWISS JURA

The case of the Schleifenberg soils

Published in Geoderma 150 (2009) 287–301

CHAPTER 3

CADMIUM DISTRIBUTION IN SOILS COVERING JURASSIC OOLITIC LIMESTONE WITH HIGH Cd CONTENTS IN THE SWISS JURA

Raul Quezada-Hinojosa[1], Virginie Matera[1], Thierry Adatte[2], Claire Rambeau[3], Karl B. Föllmi[2]

[1] Institut de Géologie, Université de Neuchâtel, rue Emile-Argand 11, CP 158, CH-2009
Neuchâtel, Switzerland
[2] Institut de Géologie et Paléontologie, Université de Lausanne, Anthropôle 3172, CH-1015
Lausanne, Switzerland
[3] Department of Archaeology, University of Reading, Whiteknights Box 226 Reading RG6 6AB
United Kingdom.

Abstract

Oolitic carbonates belonging to the Hauptrogenstein Formation of Bajocian (Middle Jurassic) age have been shown to be anomalously enriched in cadmium (Cd) throughout the Jura Mountains. Soils associated with this type of rock substratum may be naturally polluted with regards to Cd. At Schleifenberg (Canton Basel Land, Switzerland) the Hauptrogenstein Formation is almost entirely exposed along a trail on its SW flank. Cadmium concentrations were systematically measured throughout this formation and Cd enrichments in rocks are shown to occur to a maximum content of 4.9 mg·kg^{-1}. We investigated associated soils, which cover the entire outcrop, and show that they have been formed through the weathering of the underlying bedrock and through the uptake of colluvial limestone fragments from the same and older formations. Cadmium contents in the soils reach a maximum value of 2.0 mg·kg^{-1}, thereby exceeding the official Swiss indicative guideline value for soils fixed at 0.8 mg·kg^{-1}. Mineralogical analyses on the soils and associated bedrock suggest that no allochthonous component related to aeolian transport is present. Sequential extractions applied to selected soil samples show that about half of the Cd resides in the carbonate fraction coming from the fractured parent-rock, while the Cd released from the weathered carbonates is associated either with organic matter (over 10%) or with Fe and Mn-oxyhydroxides (approximately 30%). No exchangeable Cd phase was found and this, together with the buffer capacity of this calcareous soil, suggests that the amount of mobile Cd is quite negligible in this soil, which also greatly reduce the amount of bioavailable Cd.

Keywords: **Anomalous enrichments; Cadmium; Geogenic; Natural pollution; Oolitic carbonates; Soil; Speciation.**

3.1 INTRODUCTION

Systematic soil-surveying studies carried out in the Swiss and French Jura Mountains during the past ten years have established a relationship between carbonates anomalously enriched with cadmium Cd (> 0.5 $mg \cdot kg^{-1}$; Bajocian and Oxfordian in age) and contaminated soils and vegetation covers (Atteia et al., 1995; Baize et al., 1999; Benitez, 1999; Veuve, 2000; Baize and Sterckman, 2001; Prudente et al., 2002; Dubois et al., 2002, Rambeau, 2006). These research works have determined that the excess of Cd in the soils under consideration was principally derived from weathering of Cd-enriched parent rocks.

Cd concentrations in soils from specific sites have been reported to reach concentrations of up to 10 $mg \cdot kg^{-1}$ (Dubois et al., 1998; Benitez, 1999) and in one case even to 22 $mg \cdot kg^{-1}$ (Prudente, 1999), and these values largely exceed the official Swiss indicative guideline value for soils fixed at 0.8 $mg \cdot kg^{-1}$ (The Federal Authorities of the Swiss Confederation, OSol, 1998).

It has been established that major factors governing the distribution and dynamics of Cd in soils are pH, organic-matter contents, inorganic ligands, hydrous metal oxides, specific clay mineralogy, and competition with other metal ions (Alloway, 1995). Benitez (1999) and Benitez and Dubois (1999) were the first who specifically analysed Cd contents in soils from the Jura Mountains and applied specifically adapted Cd speciation techniques, in order to define its bioavailability.

In the present study we describe the results of the mineralogical and geochemical analysis of Cd contents in a soil developed on top of Bajocian limestone, which outcrops along an approximately 330 m long trail cut into the SW-facing slope of the Schleifenberg, located northwest of Liestal, in canton Basel-Land (Figure 3.1). The outcrop consists of a succession of mainly oolitic limestone beds in oblique position, which are partly interlayered by marly intervals (Gonzales, 1993; Figure 3.2). A detailed survey of Cd contents has been performed on this succession and several beds within these carbonates were found to be highly enriched in Cd. Six samples, from a total of 142 samples, showed Cd concentrations above 1 $mg \cdot kg^{-1}$ with a maximum value of 4.91 $mg \cdot kg^{-1}$ (Rambeau, 2006). The goal of this study is to investigate the relations between these enriched beds and the Cd contents in the overlying soils, by applying systematic analyses of Cd speciation using a sequential extraction technique, organic matter contents, bulk-soil and clay mineralogy and trace-element contents. We specifically aimed at confirming the carbonate substratum as the main geogenic source of Cd at this site, given the possibility that these soils may potentially have been formed in loess or may have incorporated displaced calcareous fragments during soil formation. We furthermore compare the behaviour of natural Cd in these soils with soils that are enriched in this element by anthropogenic sources. Finally we assess the environmental risk associated with this natural pollution phenomenon.

3.2 MATERIAL AND METHODS

3.2.1 Soil sampling

The entire soil cover of the section is 330 m long. The soil is developed on a steep slope (on average 40%) at the SW flank of the Schleifenberg and is rather thin; maximal depths do not exceed 60 cm. A total number of 47 soils samples were taken from the entire soil cover. Sampling occurred along a main transect in the lower part of the section where the highest Cd concentrations in bedrock were found (Rambeau, 2006). Within this transect, two sub-transects were used to take samples systematically. The first sub-transect was 8 m long and had a sampling pace of 1 m. The second one was 15 m long with a sampling pace of 0.5 m approximately. Due to the steep relief, the middle and upper parts were less accessible for sampling. There, complementary sampling points were chosen where lower Cd concentrations or only isolated peaks of Cd enrichments were recorded in the underlying bedrock (Figs. 2 and 3). Sampling was carried out by drilling into soils to maximal depths of 40 cm with an auger tool, and taking representative soil samples from a depth of 20 to 30 cm. The first 10 cm (litter and carbonate colluviums) were discarded in each sampling point. The collected samples were subsequently homogenized, air-dried at 45°C and sieved through a 2 mm mesh.

Three samples taken from the second sub-transect (Figure 3.3) were used to study the speciation of Cd and selected trace elements (i.e. Zn, Pb, Cr, Ni, Cu) by means of sequential chemical extraction. The three samples were selected from the zone where bedrock presents important Cd enrichments, as a function of their Cd concentrations relative to the Swiss indicative guideline value of 0.8 $mg \cdot kg^{-1}$ (sample S14: 0.6 $mg \cdot kg^{-1}$ < indicative guideline value; sample S21: 1.2 $mg \cdot kg^{-1}$ > indicative guideline value; and sample S29: 0.8 $mg \cdot kg^{-1} \approx$ indicative guideline value).

3.2.2 Cadmium and other trace-metal concentrations

Chemical analyses of all soil samples were conducted following the Method 3051 developed by the U.S. Environmental Protection Agency EPA (1994). 250 mg of dried and grounded sample were subjected to microwave-assisted acid digestion (concentrated HNO_3) and samples were subsequently filtered before analysis. The filtrated solutions were analyzed by Inductively Coupled Plasma Mass Spectrometry (ICP-MS Perkin-Elmer Elan 6100). The concentrations measured by this method would exclude most trace metals trapped within silicate crystal lattices but it gives a reliable measure of the amounts of metals potentially available for natural leaching and biological processes (Soon and Abboud, 1993).

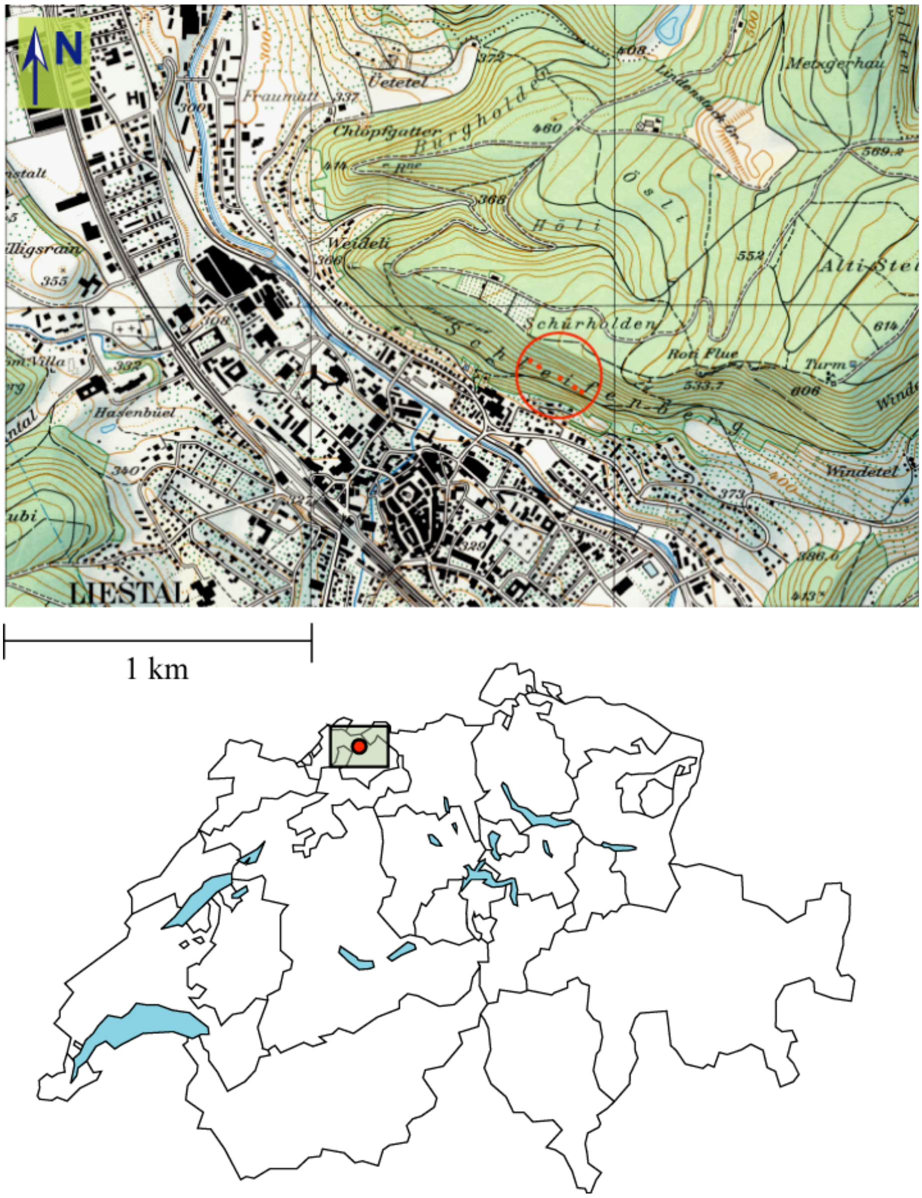

Figure 3.1 Topographic map of the Schleifenberg region (1:25'000), reproduced with the permission of the Swiss Federal Office of Topography (BA081056).

3.2.3 Soil mineralogy

The potential presence of allochthonous components in the here-investigated soil was checked by comparing the mineralogy of sampled soils and of the corresponding bedrock along the entire soil cover. Mineralogical analyses were carried out by X-Ray diffraction on bulk rock, and on the fine silt (2–16 μm) and clay fractions (<2 μm) using a diffractometer Scintag XDS 2000 with Cu-Kα radiation.

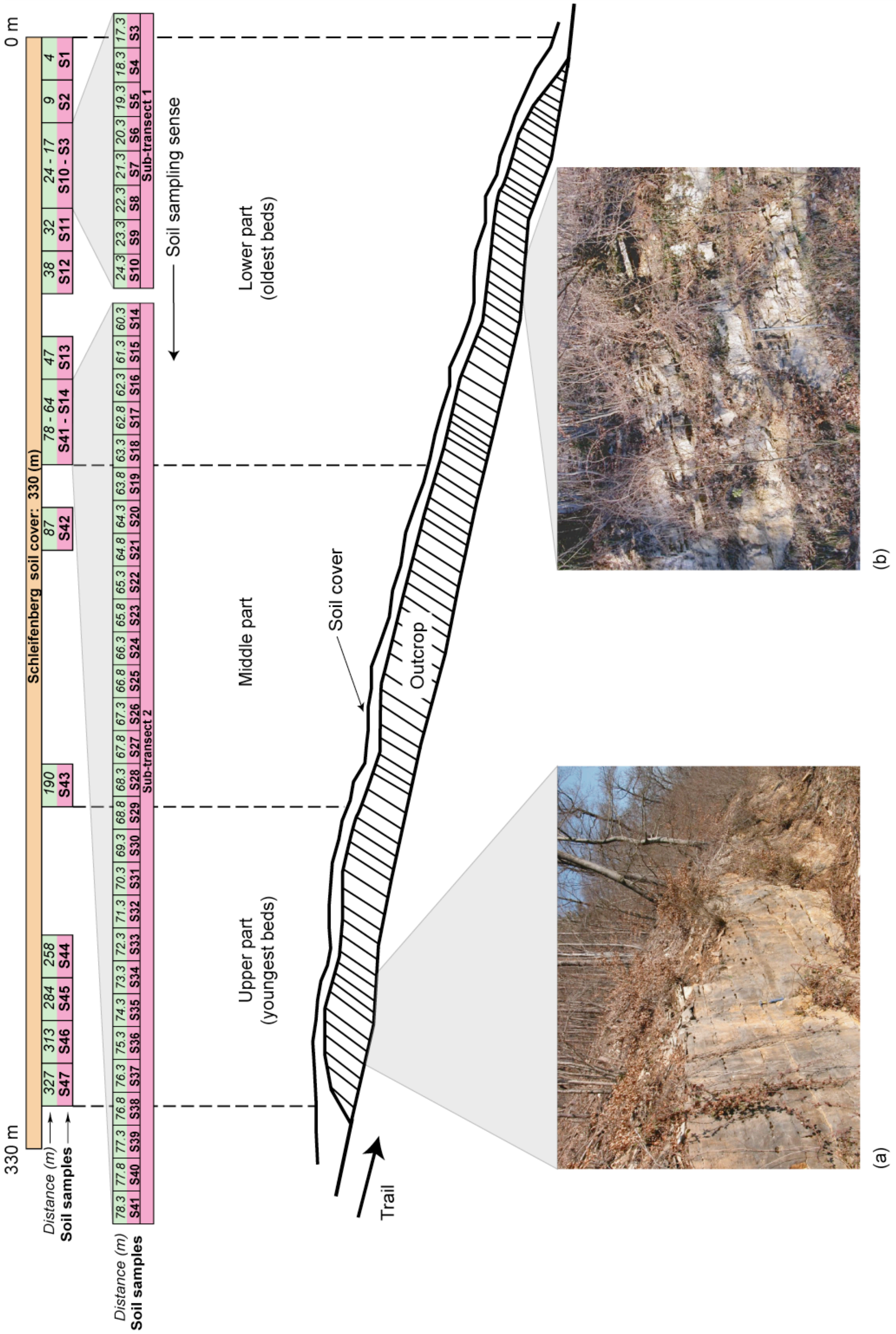

Figure 3.2 Sketch of the sampling sequences and their location with regards to the Schleifenberg section. A total of 47 soil samples coded from S1 to S47. The two photos show the upper and lower parts of the site. Pictures: (a) Upper part, oolitic-carbonate beds in oblique position; (b) Lower part, marly intervals intercalated with resedimented oolitic beds.

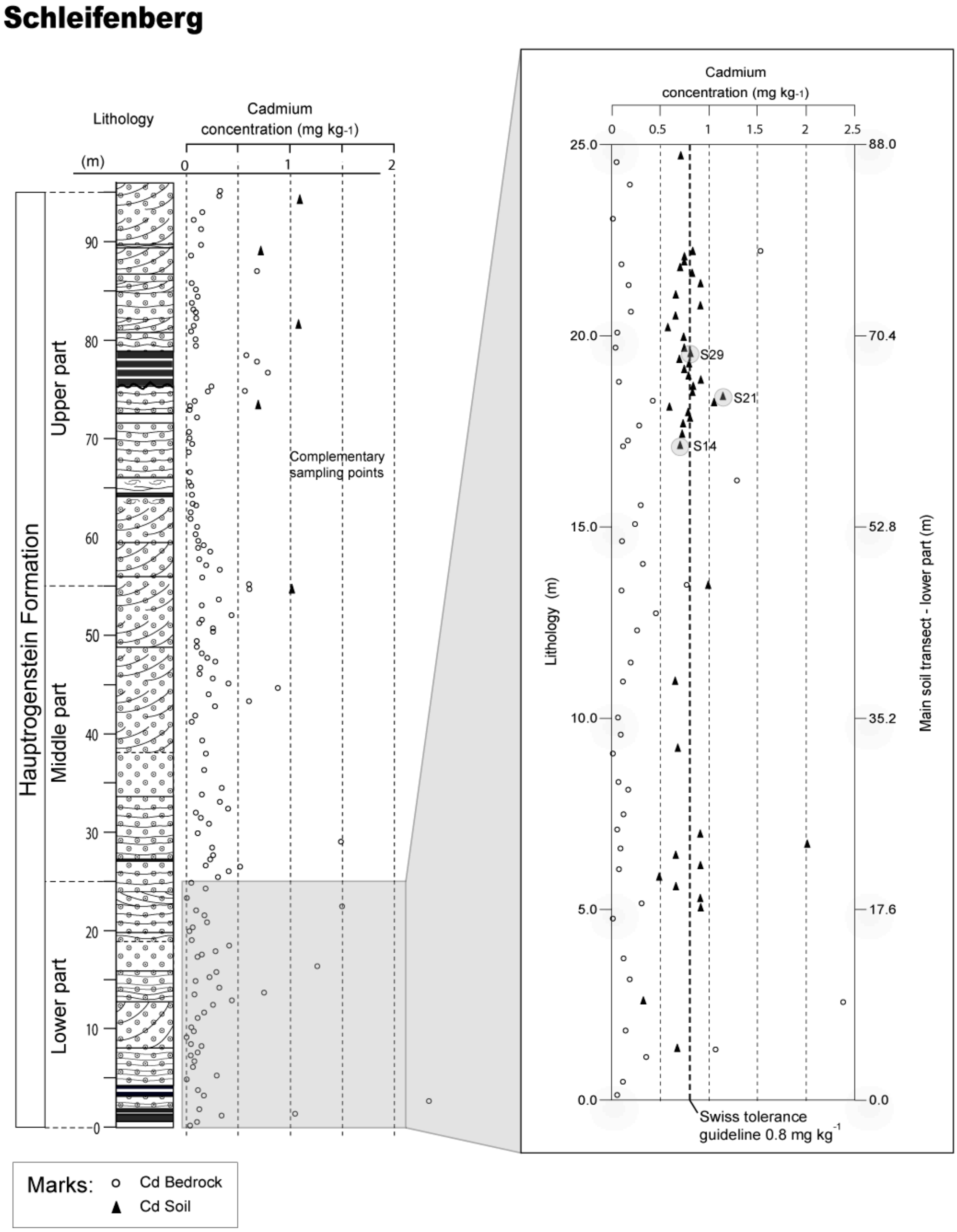

Figure 3.3 Cadmium concentrations in the Bajocian Hauptrogenstein Formation succession and corresponding soils at Schleifenberg. The diagram on the right side shows the lower zone of the outcropping carbonates for which associated soils were sampled in two sub-transects. Selected samples S14, S21, S29 were used for chemical sequential extractions.

The whole rock composition was determined based on methods described by Klug and Alexander (1974) and Kübler (1983). This method for semi-quantitative analysis of the bulk rock mineralogy (obtained by XRD patterns of random powder samples) used external standards. XRD analyses of oriented clay samples were performed after air-drying at room temperature and ethylene-glycol solvated conditions. The intensities of selected XRD peaks characterizing each clay mineral present in the size fraction (e.g. kaolinite, chlorite, mica, regular mica-smectite mixed-layers and illite-smectite mixed-layers) were measured for a semi-quantitative estimate of the proportion of clay minerals present in the size-fractions <2 µm and 2–16 µm. Therefore, clay minerals are given in relative percent abundance without correction factors (Moore and Reynolds, 1989; Adatte et al., 1996). Kaolinite was distinguished from chlorite by deconvolution of peak 24–25 Å aided by a Pearson 7 function.

3.2.4 Main chemical properties

Principal soil characteristics were determined for the three samples chosen for further sequential extractions of Cd. Total organic and mineral-carbon contents were measured in powdered samples by a Rock-Eval6^{TM} device. Total carbon and nitrogen contents were also analysed on powdered samples using an elemental analyzer Carlo Erba EAL 1108. Soil pH in KCl (1M) solution was measured using a Metrohm 682 titroprocessor. The cation-exchange capacity (CEC) was measured following the French protocol AFNOR NF X31-130: Soils samples were mixed with a solution of hexaamminecobalt(III) chloride and the concentration of free cobalt ions was measured in a calibrated UV spectrometer to 470 nm.

3.2.5 Cadmium and other trace-metal speciation

We used the sequential extraction procedure described by Benitez (1999), who specifically adapted the protocol developed by Tessier et al. (1979) for Cd in soils of the Swiss and French Jura (Figure 3.4). This method allows for the separation and identification of six fractions: (1) exchangeable; (2) carbonates; (3) organic matter; (4) amorphous Fe and Mn oxides; (5) crystalline Fe oxides; and (6) residual. The supernatants recovered in each extraction step after filtration were analyzed by quadrupole ICP-MS.

We modified the protocol used by Benitez (1999) in the following way: we used $NaNO_3$ instead of $MgCl_2$ for the exchangeable fraction since exchangeable Cd concentrations are overestimated by using chloride salts (Benitez, 1999). HNO_3 was used in step 4 instead of HCl to avoid interferences by Cl^- ions when analyzing solutions by ICP-MS., Because not all Cd is extracted from the residual mineral matrix by using concentrated HNO_3 in the last step, we needed to fit the mass balance since we applied the Method 3051 of the US-EPA to determine total Cd and trace elements concentrations in all samples.

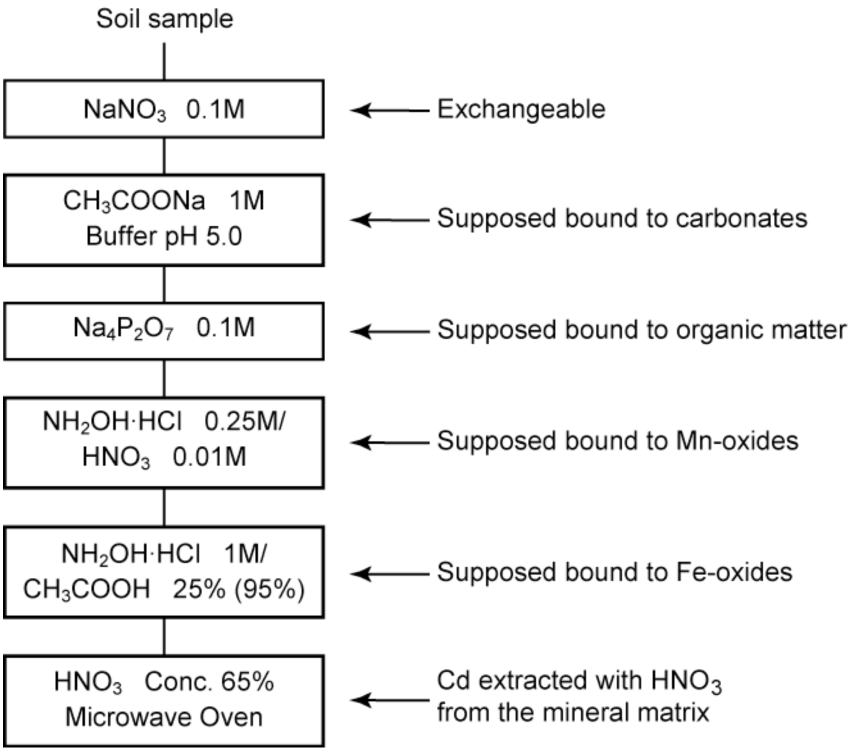

Figure 3.4 Sequential extraction procedure modified from Benitez (1999).

The main possible limitation of this operational technique is related to the lack of a specific selectivity of the chemicals used: some metallic ions are likely to be readsorbed on the remaining solid phases during each extraction step. Furthermore, drying of the soil sample and the applied speciation methodology (extraction time, liquid/solid proportions, agitation time, etc.) may induce chemical changes as well, This may explain the disagreement, which exists among authors with regards to the accuracy and reproducibility of the techniques employed for the different extraction protocols (Tessier et al., 1979; Bermond, 1992; Van der Sloot et al., 1997).

3.3 RESULTS

3.3.1 Description of the soil profile

The soil has been identified as calcaric cambisol (episkeletic) following the World Reference Base (WRB) for Soil Resources 2006, (Food and Agriculture Organization of the United Nations FAO, 2006). The soil contains 50 percent of pebbles within a depth of 50 cm from the soil surface. The soil is thus entirely calcareous, the pH measured *in situ* is alkaline (7.5–8). Three main horizons were identified (Figure 3.5) according to the French pedogenic reference (Baize and Boulaine, 1992).

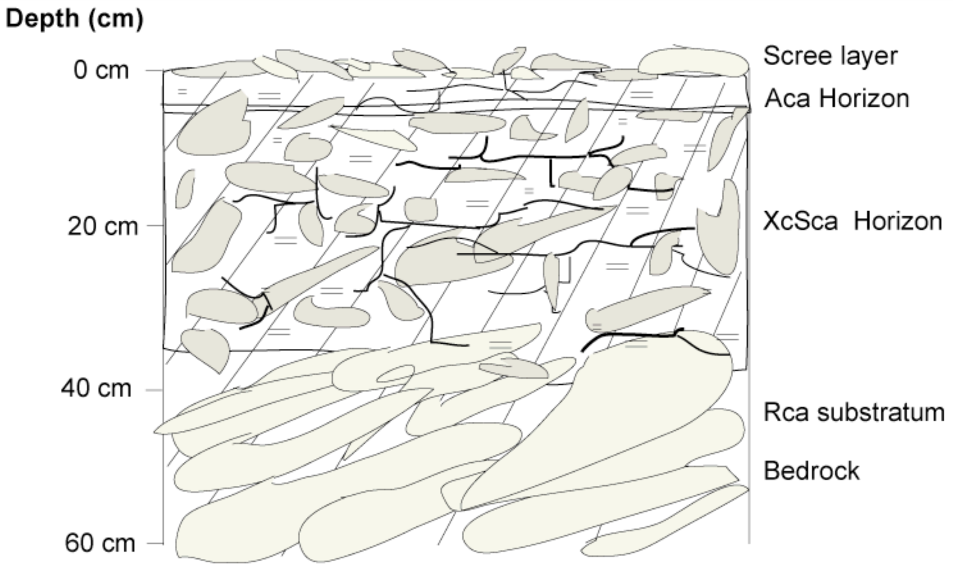

Horizons description:

Aca: Calcareous organo-mineral horizon
Sca: Calcareous structural horizon of alteration
Xc: Horizon containing > 50% fragmented rock pebbles (diametre > 2cm)
Rca: Fragmented limestone bed

Figure 3.5 Sketch of the soil profile morphology at Schleifenberg.

The upper holorganic horizon (Aca) is covered by scree layers consisting of displaced calcareous fragments. The presence of agglomerated particles suggests the evolution into a structural horizon. High quantities of organic matter are observed in the form of brown particles. The underlying horizon (X_cS_{ca}) was identified because of the presence of a polyhedral structure. This structure shows that the soil is relatively stable in this zone. Carbonate pebbles and organic matter are still abundant in this horizon. The substratum (R_{ca}) corresponds to slightly weathered bedrock with intact bed orientation and dip.

The soil developed in the upper part of the section on top of the youngest carbonate rocks shows small differences in its characteristics compared to those of the soil from the lower and middle parts of the section. The soil in the upper part is associated with a less steep slope giving the soil a better-developed structure than the lower soils. This soil is covered by a thicker holorganic horizon where black particles of organic matter are still in decomposition and is less covered by limestone fragments, thus less calcareous.

3.3.2 Total cadmium and other trace-metal contents

The results obtained for Cd, Zn, Pb, Cr, Ni and Cu are summarized in Table 3.1. Cd contents for all soil samples are compared with those of the bedrock and presented in Figure 3.3. The soils samples show mean total Cd concentrations of 0.8 mg·kg^{-1}. Even though the Cd contents found were lower than those reported for other sites, nearly 43% of the samples show concentrations that exceed the Swiss indicative guideline value of 0.8 mg·kg^{-1}. Table 3.2 presents calculated ratios between mean Cd concentrations of soils to those of the bedrocks. These ratios are quite variable: a ratio of 2.1 is calculated for the lower part of the section where a higher frequency of Cd anomalies in bedrock was found. The value 2.9 is the average ratio for the entire section and 4.2 for the entire section without taking into account the rock samples, which contain Cd concentrations higher than 1 mg·kg^{-1}. Anomalous contents were also found for Zn, Pb and Cr. Their concentrations exceed the corresponding indicative guideline values for soils of 150 mg·kg^{-1} for Zn, and 50 mg·kg^{-1} for Pb and Cr (OSol, 1998). Ni and Cu did not present any anomaly.

Table 3.1 Summary of Cd and selected trace-metal concentrations in the Schleifenberg soil samples (n = 47).

	Cd	**Zn**	**Pb**	**Cr**	**Ni**	**Cu**
	(mg·kg^{-1})					
Mean	0.8	190.4	49.6	52.6	28.2	13.8
Median	0.8	192.8	50.5	54.0	27.9	14.0
Standard Deviation	0.2	38.2	11.2	10.5	4.7	4.2
Minimum	0.3	46.6	10.3	22.5	17.3	6.7
Maximum	2.0	253.2	77.6	71.9	37.0	29.9
Osol guideline value	0.8	150.0	50.0	50.0	50.0	40.0
% Anomalous samples	43	87	57	62	0	0

Table 3.2 Variability of calculated Cdsoil / Cdrock ratio, as a function of mean Cd concentrations in bedrock, number of soil samples and location

	Cd concentration in bedrock (mg·kg^{-1})			**Cd concentration in soil (mg·kg^{-1})**			**Cd_{soil}/Cd_{rock}**
	N	**Mean**	**Range**	**N**	**Mean**	**Range**	
Entire section	147	0.28	0.03 – 4.91	47	0.82	0.33 – 2.00	2.9
Entire section without rock samples with Cd concentrations > 1 mg·kg-1	141	0.20	0.03 – 0.88	47	0.82	0.33 – 2.00	4.2
Lower part of the section	40	0.39	0.04 – 4.91	41	0.81	0.33 – 2.00	2.1

3.3.3 Bedrock mineralogy

Results of mineralogical analyses for bulk rock are presented in Table 3.3. Figures 3.6a, b, c illustrate bedrock mineralogy trends for bulk rock, and for the fine-silt (2–16 μm) and clay fractions (<2 μm) compared with those characterizing the soils sampled at the lower, middle and upper parts of the site. Nearly 90% of the bedrock is composed of calcite. Small contents were found for quartz (3%) and phyllosilicates (2.6%). Kaolinite is the principal clay mineral in the fine-silt fraction with a mean content of 86%. Mica contents correspond to 12% and chlorite 2%. Clays are composed by kaolinite (50%), mica (29%), regular mica-smectite mixed-layers (15%) and small quantities of illite-vermiculite clays (5%). Chlorite was not detected. As the fine-silt fraction shows the presence of chlorite, the presence of this mineral in the clay fraction is not excluded either, though in contents which are under the detection limits.

3.3.4 Soil mineralogy

Mineralogy data and trends for bulk soil are summarized in Table 3.3 and presented in Figure 3.6a. The mineralogy of the soil cover varies slightly in the different sampling zones. The main differences concern calcite contents ranging from 14 to 68%, and the non-quantified components (e.g., organic matter, amorphous compounds and poorly crystallized minerals), which vary widely (0.2 to 48.5%). The lower and upper parts of the section show less-calcareous soils, while the carbonate content increases in the middle part. Phyllosilicates (10–16%) and quartz contents (13–29%) do not show strong variations in the analysed samples. K-feldspar contents are generally low (up to 2.4%) and those of plagioclase are in most cases even lower.

Table 3.3 Distribution of minerals in bulk-rock samples (bedrock) and selected soil samples

Sample / Location		Phyllo-silicates	Quartz	K-Feldspars	Plagioclase	Calcite	Goethite	Non-quantified
					(%)			
Bedrock		2.6	3.0	< 0.2	< 0.2	92.2	0.3	1.7
Soil: Lower part of section	S14	11.1	13.4	0.4	< 0.2	26.1	2.0	46.9
	S22	11.8	20.2	0.6	0.2	18.0	0.8	48.5
Soil: Middle part of section	S42	10.3	9.4	< 0.2	< 0.2	67.6	1.0	11.6
	S43	11.8	31.2	2.4	0.5	50.5	1.9	1.1
Soil: Upper part of section	S44	16.4	19.9	< 0.2	0.3	48.3	1.3	13.9
	S45	12.6	25.8	0.6	1.5	13.8	1.5	44.2
	S46	10.3	27.8	1.4	0.9	13.8	1.5	44.4
	S47	14.7	29.1	0.8	2.9	49.0	3.0	0.2

ND = Non detected; Non-quantified = Organic matter, clay-humus complex + amorphous compounds and poorly crystallized minerals (e.g. Fe, Mn-oxihydroxides).

Results for the fine-silt fraction (2–16 μm) are presented in Figure 3.6b. Mean kaolinite contents amount to 80.5% while mica contents vary between 6.0% and 33.5% with a trend to

(a)

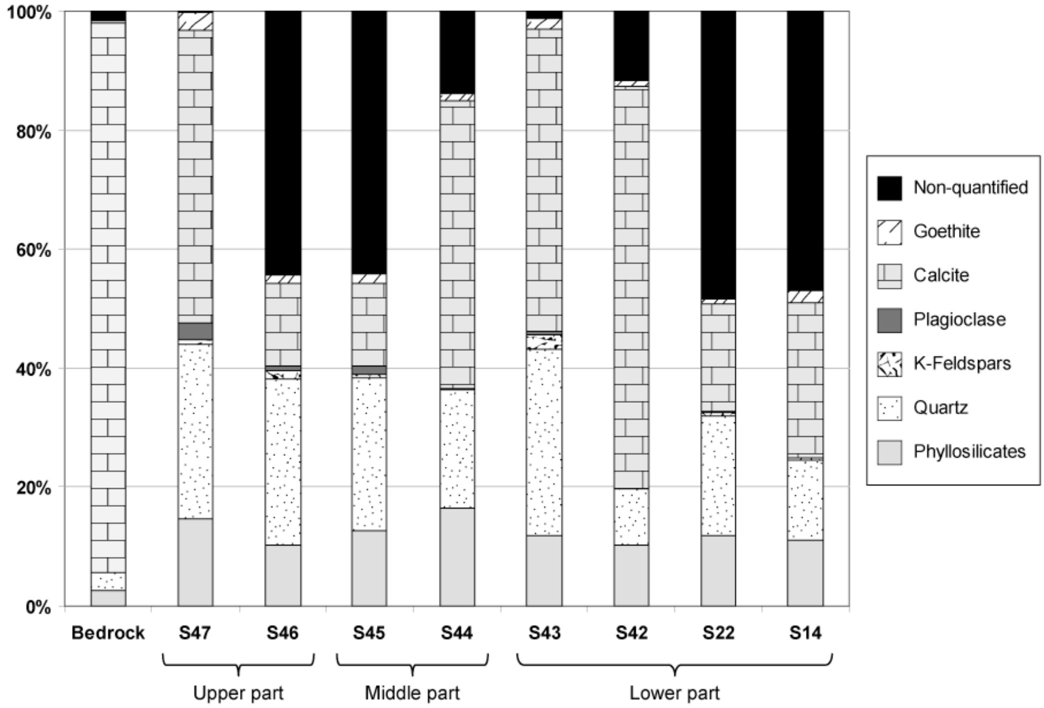
100%
80%
60%
40%
20%
0%
Bedrock
S47
S46
S45
S44
S43
S42
S22
S14
Upper part
Middle part
Lower part
Non-quantified
Goethite
Calcite
Plagioclase
K-Feldspars
Quartz
Phyllosilicates

(b)

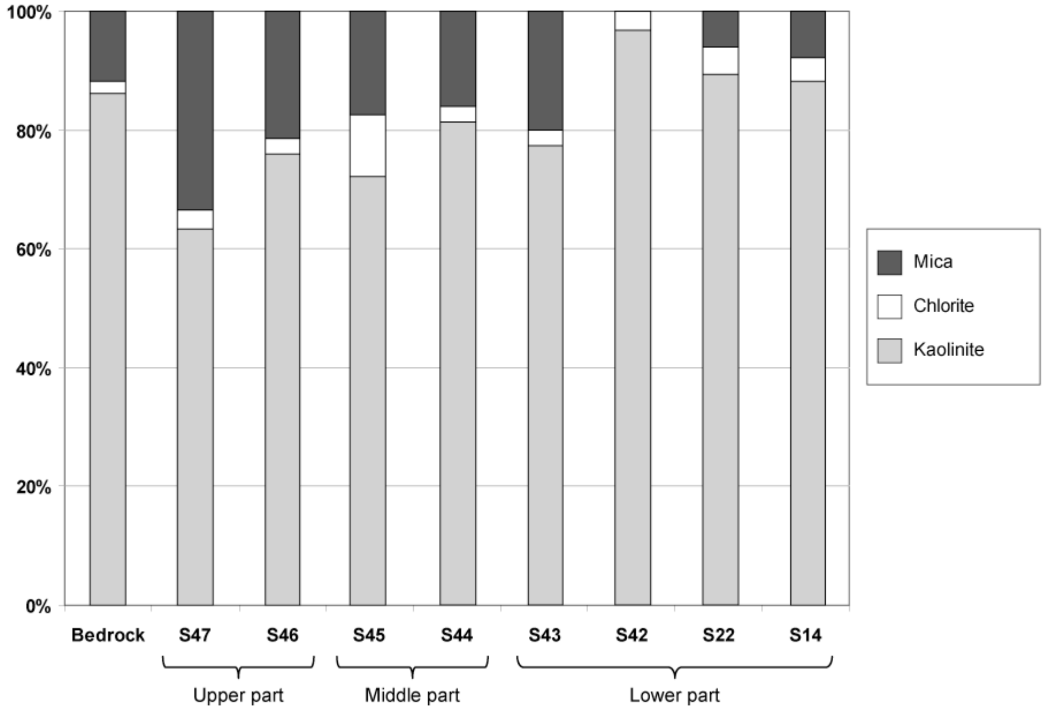
100%
80%
60%
40%
20%
0%
Bedrock
S47
S46
S45
S44
S43
S42
S22
S14
Upper part
Middle part
Lower part
Mica
Chlorite
Kaolinite

(Continued)

(c)

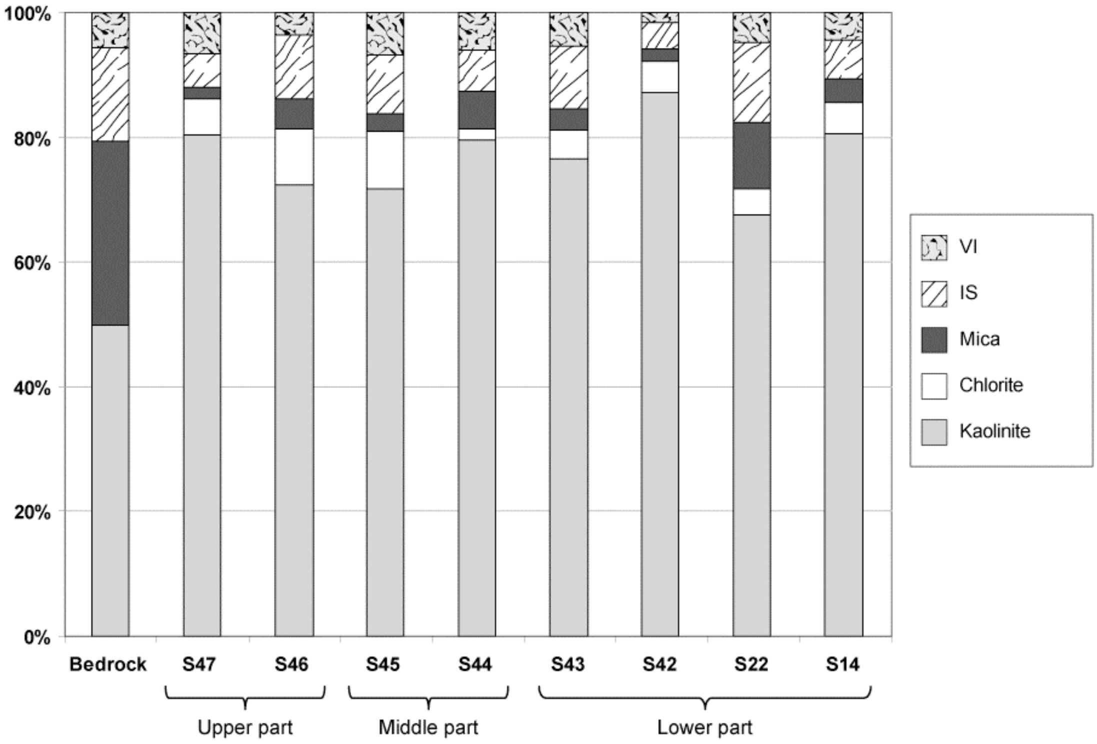

Figure 3.6 Identified mineral assemblages and their variations for bedrock and selected soils from three sampling zones. Non-quantified values correspond to organic matter contents, amorphous and poorly crystallized minerals. (a) Bulk rock; (b) fine-silt fraction (2–16 μm); (c) clay fraction (<2 μm). IS: Regularly mixed-layered mica-smectite; VI: Mixed-layered vermiculite-illite.

higher values in the upper part of the section. Low chlorite contents of up to 4% were measured, which do not show important variations. The clay distribution is presented in Figure 3.6c. As for the fine-silt fraction, kaolinite is the most abundant clay mineral with a mean content of 77%. Chlorite and mica contents reach mean values of 5.5 and 4.5%, respectively. Regular mica-smectite mixed layers (Moore and Reynolds, 1989) are present with mean values of 8.1%, while newly formed vermiculite-illite mixed layers amount to 4.9%. The distribution of the identified clay minerals is rather similar for all samples for this fraction.

3.3.5 Main chemical properties

The main characteristics for the three samples selected for sequential extractions are presented in Table 3.4. The differences amongst the three samples are not significant. pH values are neutral (7.2) and the mean CEC value corresponds to 20.3 cmol·kg^{-1}. The soils have total organic carbon (TOC) contents ranging from 10.5 to 16.4%. Organic matter (OM) contents have been calculated from TOC values (%OM = %TOC x 1.67; Alloway, 1995), and represent rather high values for these soil samples (17.6–27.5%). The C/N ratio of soils corresponds to a mean value of 17.

Table 3.4 Main chemical properties of selected soil samples

Sample	Cd ($mg \cdot kg^{-1}$)	pH_{KCl}	CEC ($cmol \cdot kg^{-1}$)	TOC (%)	OM (%)	C_{min} (%)	N (%)	C/N
S14	0.7	7.1	19.9	16.4	27.5	4.1	0.9	19.2
S21	1.2	7.2	20.2	13.9	23.2	2.2	0.9	16.0
S29	0.8	7.3	21.0	10.5	17.6	1.9	0.7	15.6

CEC = Cation exchange capacity; TOC = total organic carbon; OM = organic matter (%OM = %TOC x 1.67); C_{min} = Mineral carbon.

3.3.6 Cadmium and further trace-metal speciations

The identified Cd species in the three soil samples are presented in Table 3.5. Percent distributions of Cd in each fraction do not vary significantly in the three samples. Sample S14 delivered the lowest quantity of Cd bound to organic matter (only 6.4% Cd) while the other two samples recorded approximately 16% Cd bound to this fraction. The recovery of Cd by sequential extraction relative to the total Cd concentration is as follows: 81% for sample S14, 66% for S21 and 75% for S29. Only sample S29 delivered Cd in the residual phase giving a higher recovery. This implies that there is still a fraction of Cd trapped in the samples that is not released by the last step of the extraction protocol. The mean distributions of each Cd species in weight percent show that about half of total extracted Cd is bound to carbonate (49.3%), followed by Cd associations with crystalline Fe-oxides (31.7%), organic matter (12.7%), amorphous Mn-oxides (3.8%), and Cd extracted with HNO_3 from the residual matrix (2.4%). Exchangeable Cd was not detected.

Table 3.5 Results of Cd extraction for selected soil samples. Mass balance and percent distribution

Fraction	S14		S21		S29	
	Cd ($mg \cdot kg^{-1}$)	Distrib (%)	Cd ($mg \cdot kg^{-1}$)	Distrib (%)	Cd ($mg \cdot kg^{-1}$)	Distrib (%)
F1 Exchangeable	0.00 ± 0.00	0.0	0.00 ± 0.00	0.0	0.00 ± 0.00	0.0
F2 Carbonates	0.26 ± 0.03	52.9	0.34 ± 0.02	44.3	0.31 ± 0.04	50.8
F3 Organic Matter	0.03 ± 0.00	6.4	0.13 ± 0.01	17.1	0.09 ± 0.02	14.7
F4 Mn-oxides	0.02 ± 0.02	3.8	0.03 ± 0.01	3.9	0.02 ± 0.02	3.7
F5 Fe-oxides	0.18 ± 0.06	37.0	0.26 ± 0.02	34.8	0.14 ± 0.02	23.5
F6 HNO_3 extracted Cd (Residue)	0.00 ± 0.00	0.0	0.00 ± 0.00	0.0	0.04 ± 0.03	7.3
Sum of extracted fractions	**0.49 ± 0.02**	100	**0.76 ± 0.01**	**100**	**0.61 ± 0.03**	**100**
% Recovery	**81**		**66**		**75**	
Cd content (original sample)	**0.6 ± 0.01**		**1.2 ± 0.02**		**0.8 ± 0.01**	

Overall values and mean weight percent distributions of Cd and selected trace elements Zn, Pb, Cr, Ni, Cu within the extracted phases are summarized in Table 3.6 and presented in Figure 3.7a. The trace elements Zn, Cr, Ni and Cu are mainly contained in the residual fraction in association with silicates. Pb has a higher content in the crystalline Fe-oxide fraction than Zn, Cu and Ni. Organic matter is the next major fraction for Pb, Zn, Cr and Cu. The four elements have low contents in association with amorphous Mn oxides. Low contents of Pb, Zn, Ni and Cu were obtained in the fraction bound to carbonates. The exchangeable fraction also produced small concentrations for Pb, Cu, Cr and Ni while Zn was not detected. Cr did not appear in the Fe-oxide fraction and Ni bound to amorphous Mn-oxides was not detected.

Table 3.6 Mean percent distribution of Cd and other selected trace elements in soil samples

Fraction	Cd	Zn	Pb	Cr	Ni	Cu
	Mean distribution (%)					
F1 Exchangeable	0.0	0.2	3.8	2.3	1.1	2.7
F2 Carbonates	49.3	2.4	6.3	0.0	3.4	1.7
F3 Organic Matter	12.7	20.6	25.3	16.3	8.1	19.1
F4 Mn-oxides	3.8	3.1	1.3	3.4	0.0	3.4
F5 Fe-oxides	31.7	18.7	45.3	0.1	12.1	9.8
F6 Residue	2.4	55.0	18.0	77.9	75.3	63.2
% Mean recovery	**70**	**75**	**79**	**100**	**87**	**89**

In order to control the selectivity of the applied sequential extraction method, the major elements Ca, Fe, Mn and Al were also analysed and their distribution follows the main trends expected for each fraction (Figure 3.7b). The mass balance for each element (Table 3.7) shows high recoveries: Ca: 88%; Fe: 100%; Mn: 92.7%; and Al: 93%. Calcium shows the highest contents in the carbonate fraction (61%).

Table 3.7 Mean percent distribution of major elements in selected soil samples

Fraction	Ca	Fe	Mn	Al
	Mean distribution (%)			
F1 Exchangeable	6.6	0.3	0.6	1.0
F2 Carbonates	61.1	0.0	22.9	0.1
F3 Organic Matter	2.7	7.6	33.1	25.0
F4 Mn-oxides	4.5	1.4	9.5	6.0
F5 Fe-oxides	24.0	7.9	24.2	7.8
F6 Residue	1.2	82.8	9.7	60.1
% Mean recovery	**88**	**100**	**93**	**93**

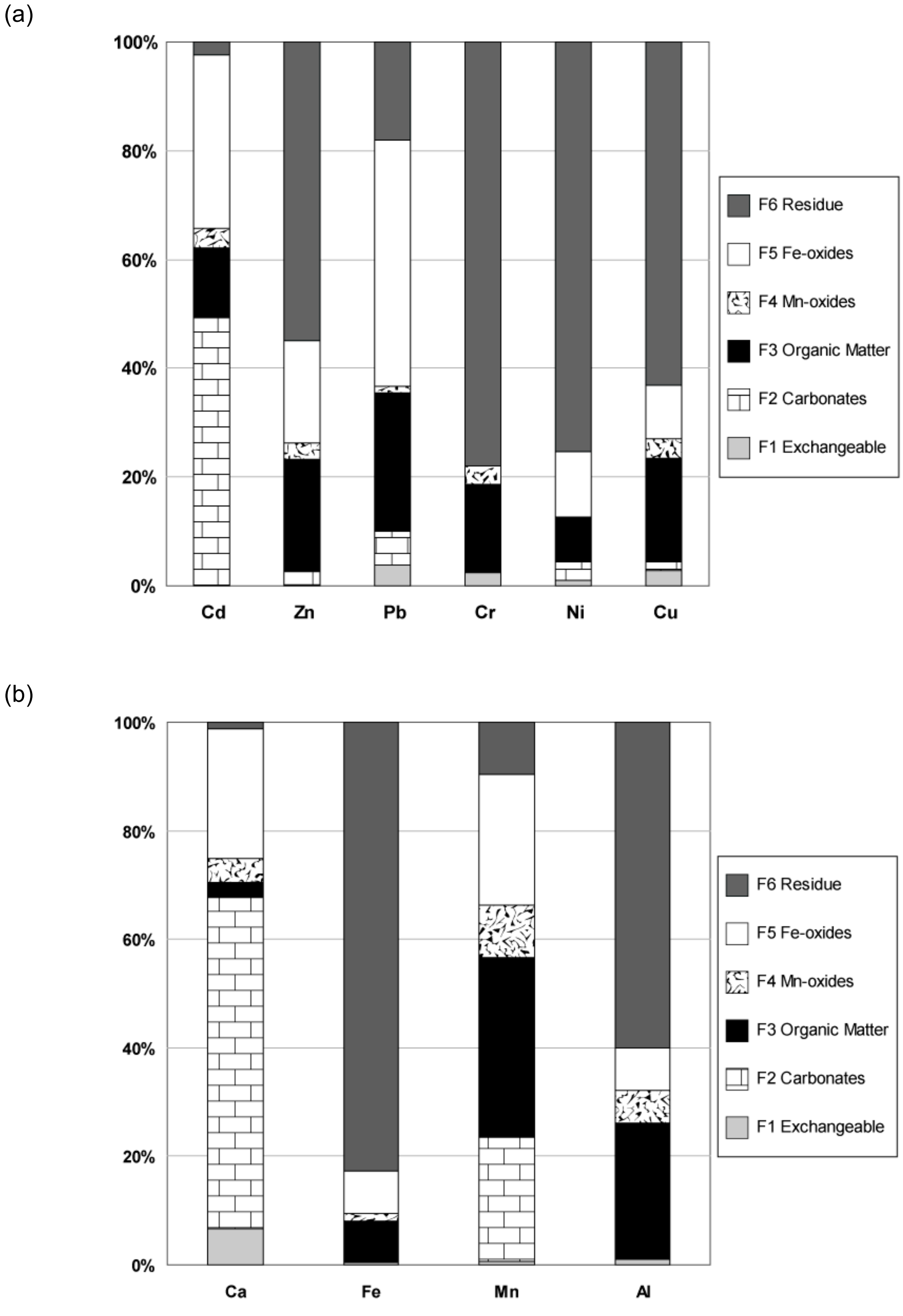

Figure 3.7 Mean percent distribution of extracted elements in soil: (a) Cd and selected trace elements; (b) Major elements.

Even if the residual sample was not entirely dissolved in the last step of the extraction protocol (51% non-dissolved soil), these results testify to the rather good reliability of the speciation method used here, except for Fe. The extraction efficiency for Fe in step 5 was limited since not all Fe is extracted in the Fe-oxide phase. A fraction of Fe remains in the residual silicate fraction (83%) and is extracted in the last step along with Al (60%). Aluminium bound to organic matter (25%) is also extracted. Kaiser and Zech (1996) and Kleber et al. (2004) observed that sodium pyrophosphate produces an alkaline dissolution of amorphous and peptized Al hydroxide phases associated with organic matter, thus extracting not only Al from humus complexes but also from mineral phases. Mn is distributed as follows: organic matter > carbonate > crystalline Fe-oxides > amorphous Mn oxides = silicates.

3.3.7 Correlation analysis

Trace- and major-element correlations in the soil samples were analysed by a multivariate approach. Chemical analyses of total Cd, Zn, Pb, Cr, Ni, Cu, Ca, Fe, Mn, and Al were considered for this purpose. Data for Zn, Pb, Cr, Ni, Cu, Ca, Fe, and Al have a normal distribution while data for Cd and Mn follow a Gaussian distribution that approximates a normal distribution.

Table 3.8 Correlation matrix of the concentrations of the elements in the Schleifenberg soil samples (n = 47). Significant correlations are in bold

Element	Cd	Zn	Pb	Cr	Ni	Cu	Ca	Fe	Mn	Al
Cd	1									
Zn	0.36	1								
Pb	0.36	**0.81**	1							
Cr	0.06	**0.78**	0.51	1						
Ni	0.06	0.57	0.46	0.68	1					
Cu	0.12	0.51	0.56	0.38	0.06	1				
Ca	-0.22	**-0.75**	**-0.73**	**-0.72**	**-0.74**	-0.34	1			
Fe	0.20	0.30	0.22	0.27	**0.73**	-0.10	-0.44	1		
Mn	0.19	-0.10	-0.07	-0.18	0.32	-0.23	0.02	**0.81**	1	
Al	0.12	0.22	0.05	0.47	0.60	-0.09	-0.39	**0.71**	0.54	1

Correlation coefficients for the ten elements are presented in Table 3.8. Cd is not correlated to any of the other measured elements. Instead, a strong correlation is observed between the pairs Zn-Pb, Zn-Cr and Fe-Mn. High correlation coefficients are present for the contents of Fe-Ni, and to some extent for Fe-Al contents as well. Moderate correlation exists between Cr and Ni contents. Calcium shows a negative correlation with Zn, Pb, Cr and Ni. No significant correlations are observed between Cu and the other elements.

3.3.8 Principal-component analysis

Analyses of principal components were applied to the variables in order to highlight the associations of Cd to selected trace and major elements within the whole system. The first three principal components were used as they explain 82% of the total variance.

Projections combining the three components give a clear image of the behaviour of the geochemical system. Figure 3.8a shows the projection of the first principal component (PC 1) and the second principal component (PC 2). A main group of elements composed by Pb, Zn and Cr appears with positive loadings on the PC 1. This component shows also Ni with a high positive load and Fe with a moderate load. Calcium is the only element showing a negative load on this component. Aluminium and copper do not show a definite tendency in the system, but it seems that Al is related to some extent to Fe, while Cu leans toward the Pb-Zn-Cr group. The second principal component is mainly loaded on Mn. Projection of the first principal component (PC 1) and the third principal component (PC 3) (Figure 3.8b) shows that PC3 is negatively loaded in Cd.

Scatter plots of soil samples were projected on the three principal components identified above (Figure 3.9a and b). These projections show that there is no preferential distribution of soil samples according to the geochemical dataset. Most samples coming from the two sub-transects of the lower part of the section are concentrated around the positive and negative sides of the first principal component. There is however an important load on the negative side of PC 1 of samples coming from the middle and the lower parts. These samples correspond to soils presenting higher carbonate contents. Samples from the upper part are mainly distributed along the second principal component corresponding to the amorphous Mn-oxides. As will be discussed later, these soils appear to be slightly different with regards to those soils sampled at the transects from the lower part of the outcrop. Relative to the third principal component (Cd), most samples are moderately distributed on this axis, showing the observed enrichments in Cd. Only one sample from sub-transect 1 has a high negative load on this axis, corresponding to the highest Cd concentration (2.0 mg·kg^{-1}) registered in the entire data set.

(a)

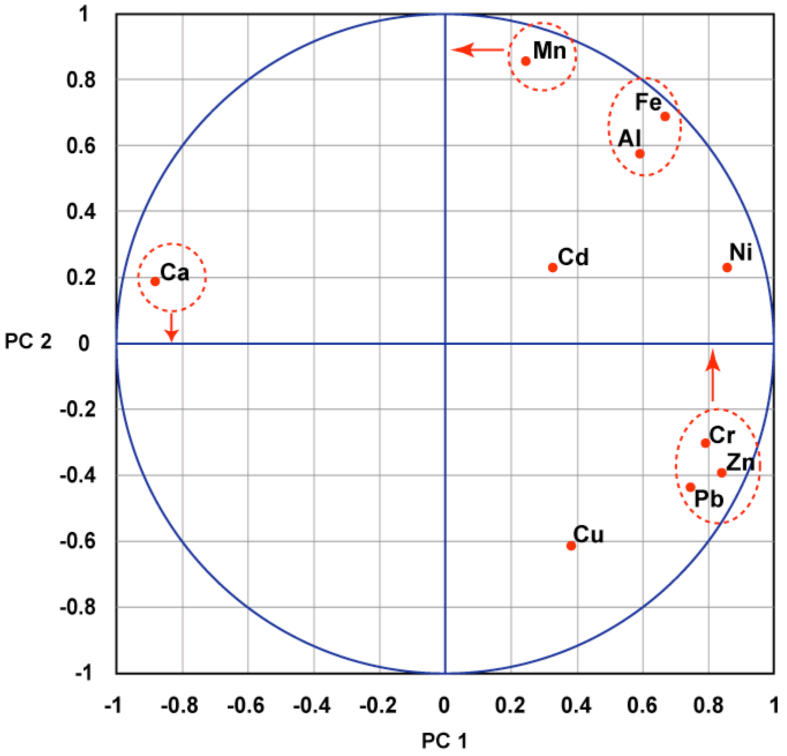

(b)

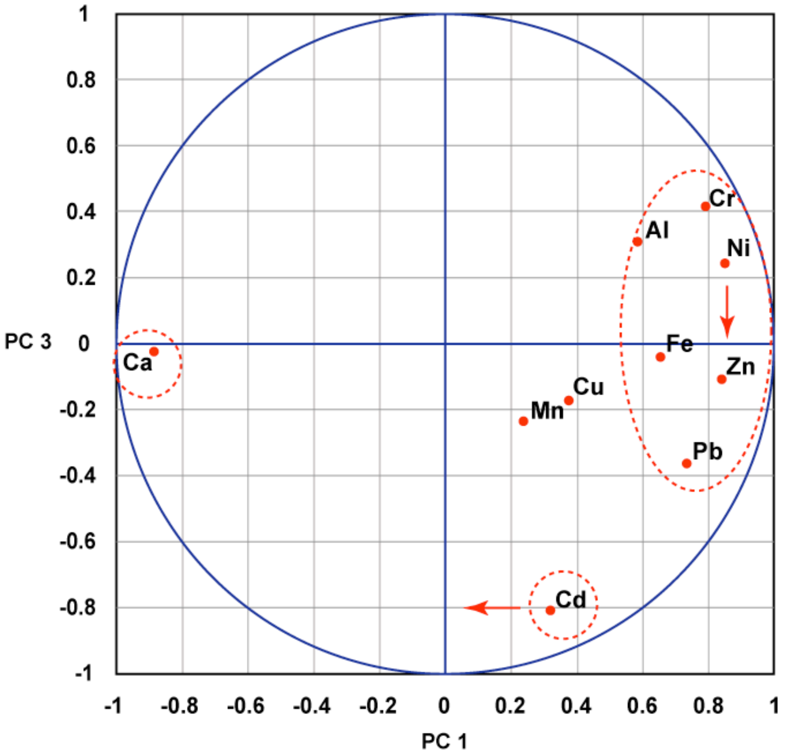

Figure 3.8 Correlation circles of the elemental concentrations measured. (a) Projection of principal components 1 and 2; (b) Projection of principal components 1 and 3.

(a)

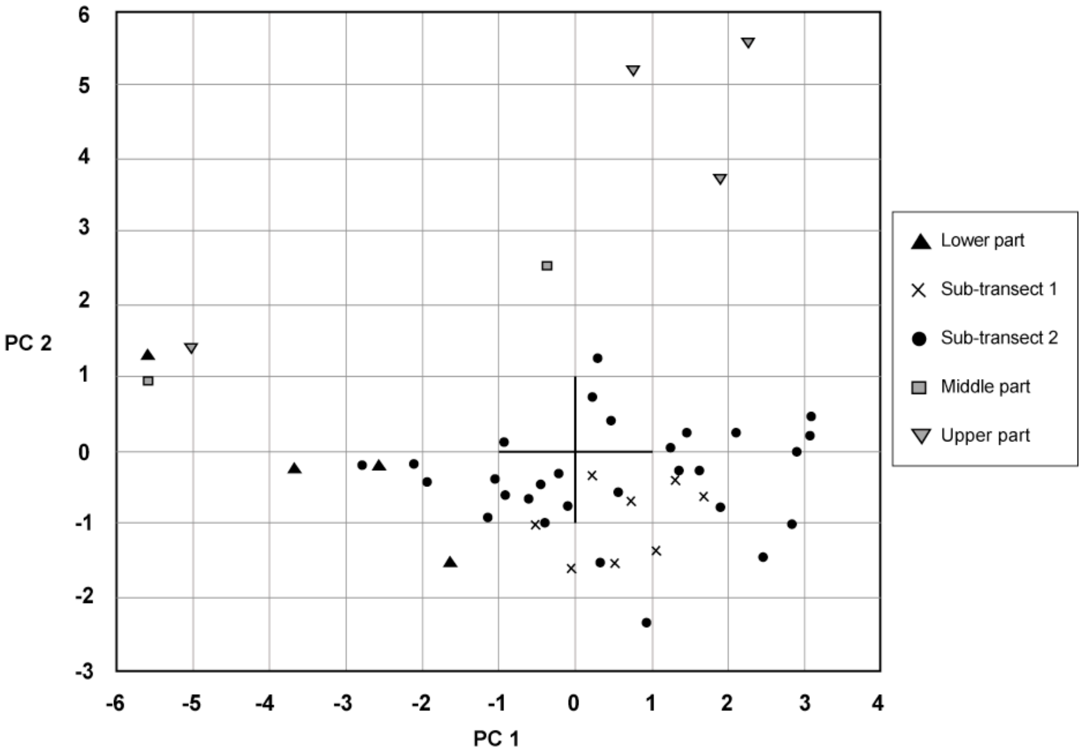

(b)

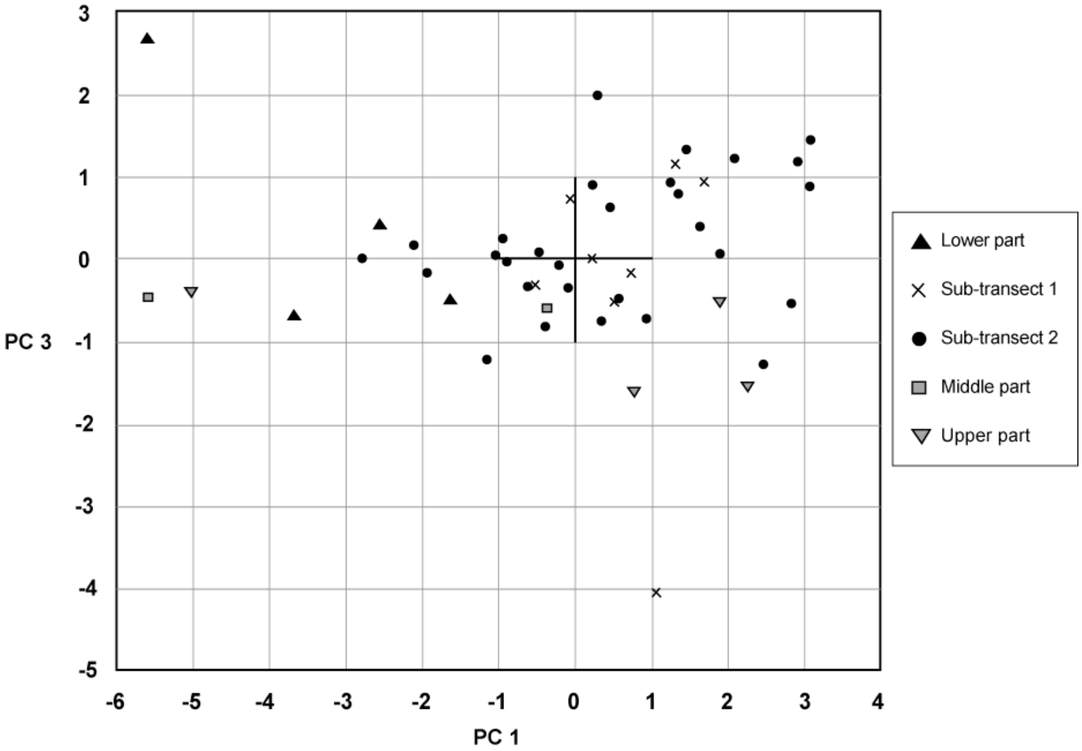

Figure 3.9 Scatter plot of sampling transects projected on principal components. (a) Projection of principal components 1 and 2; (b) Projection of principal components 1 and 3.

3.4 DISCUSSION AND INTERPRETATION

3.4.1 Soil characteristics

Due to its position on a rather steep sloop the soil described here is susceptible to creeping processes and will hardly accumulate. Furthermore, the presence of pebbles within and on top of the soil indicates that soil replenishment takes place by material falling and gliding down slope. This is especially true for soils of the middle and lower zones of the section, where high quantities of colluvial material are falling down. The soils in the upper part of the section are situated on a less steep slope. They show a more developed structure marked also by a darker colour due to greater quantities of organic matter. Nevertheless, due to the shallowness of the soil and the general topography, it is highly likely that these soils are also subjected to lateral movement. A comparison of the results of the mineralogical analyses of the soils and the underlying rock substratum is shown in Figures 10a, b and c. The mineralogical composition of bulk rock and the fine-silt fraction (2–16 μm) reveals a heritage of minerals from weathered bedrock to soils. Regular mica-smectite mixed layers (4–13%) in the clay fraction (<2 μm) of soils are inherited following rock weathering, while illite-vermiculite mixed-layer clays (2–7%) are a product of the transformation of mica minerals during soil evolution.

The soils lack long-distance allochthonous components, brought in, for instance, by aeolian transport of loess during previous phases of glaciation. Weathering of the underlying carbonate substratum is, therefore, the main source of mineralogical components in the soils, and minerals such as calcite, quartz and phyllosilicates are products inherited from the dissolution of limestone.

As for all rocks from the Jura Mountains, K-feldspar and plagioclase are present in trace quantities in bedrock; they are released during carbonate dissolution and incorporated into soils. Apart from a few exceptions, most soil and a few bedrock samples have higher contents of K-feldspar relative to plagioclase (Table 3.3). According to Benitez (1999) this fact is characteristic for the autochthony of the analysed soil. Chlorite in soils (mean content 4.2%) is also a product inherited from rock weathering since small chlorite contents (mean content 2.0%) are detected in the fine-silt fraction (2–16 μm) of both soils and corresponding bedrock (Figure 3.10b). Bolle et al. (1996) have already described the presence of trace quantities of chlorite in Bajocian-Bathonian rocks. As such, chlorite in the clay fraction (<2 μm) of soils may be either inherited from limestone dissolution, whose trace contents of chlorite were non detectable for the applied X-ray technique, or degraded chlorite from silt fraction 2–16 μm. Kaolinite represents the major clay mineral in the silt and clay fractions.

Despite its weak CEC (2–15 cmol·kg^{-1}), the slow evolution of mixed-layered illite-vermiculite clays and the formation of combined organo-mineral colloidal complexes would enhance the cation-exchange capacity of soils (Alloway, 1995).

(a)

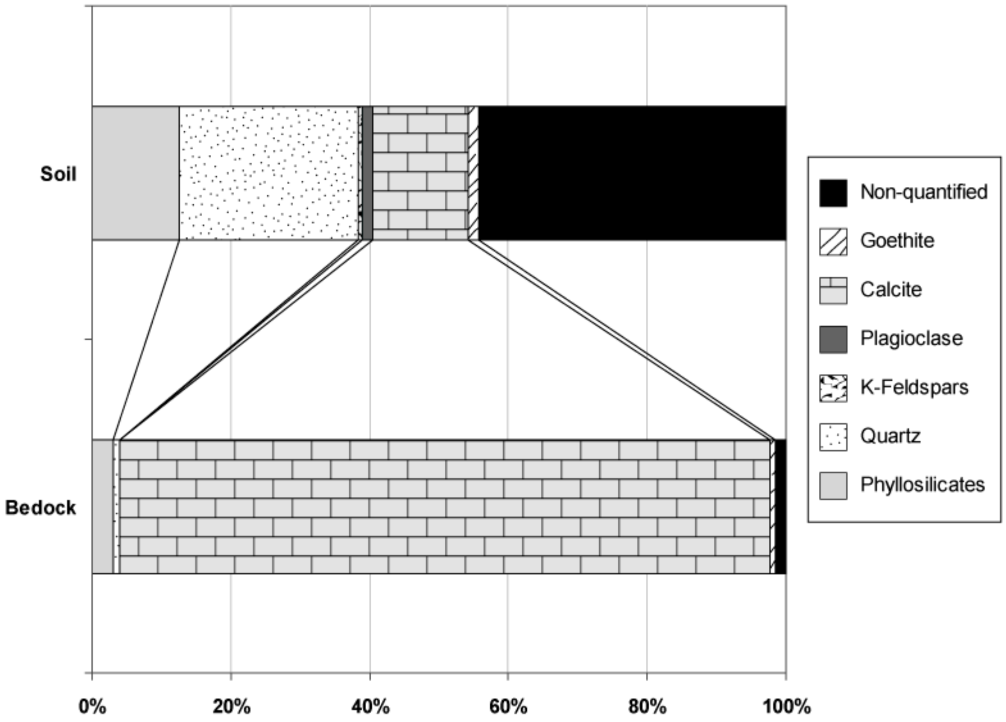

(b)

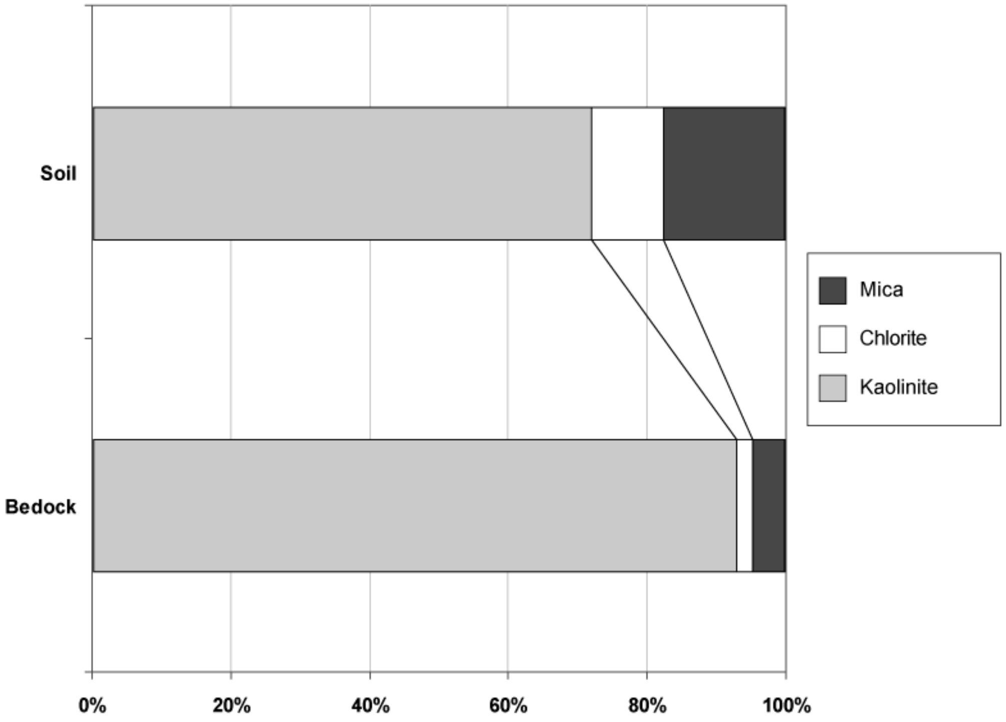

(Continued)

(c)

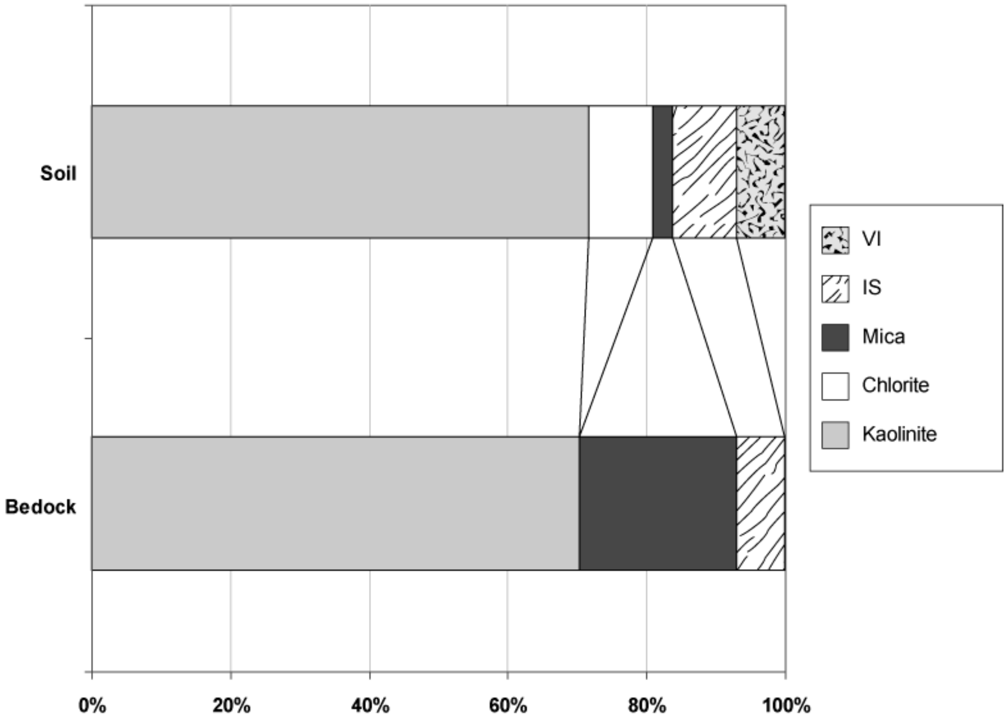

Figure 3.10 Comparison of the mean mineralogical composition of soil and bedrock: (a) bulk rock; (b) fine-silt fraction (2–16 μm); (c) clay fraction (<2 μm).

3.4.2 Cadmium distribution in soils

The mineralogical analyses suggest that the soil at Schleifenberg is issued from the underlying bedrock with the addition of an uphill carbonate colluvial component. In general, a genetic relation between the occurrence of Cd enrichments in the soils analysed here and the carbonate substratum is highly plausible, even though the Cd_{soil}/Cd_{rock} ratios calculated for the Schleifenberg (2.1–4.2) are low compared to those calculated by Rambeau (2006) for other sites of the Swiss Jura mountains such as 6.3 at Dornach, 7.3 at Le Gurnigel and 5.5–5.7 in Lower Burgundy. A close carbonate-bed to soil correlation in Cd contents is, however, not observed: soils on top of carbonates with high Cd contents are not necessarily related with high Cd contents in soils and vice versa (Figure 3.3). This observation and the somewhat low Cd_{soil}/Cd_{rock} ratios are probably partly explained by the fact that the soils undergo gravitational displacement and include displaced debris diluting the concentrations of Cd. Rambeau (2006) already mentioned the problems with the accuracy of soil/rock ratios due to frequent differences in the locations of rocks and soil sampling and mainly to the high heterogeneity in the Cd values measured in the underlying rocks.

The presence of peaks of Cd concentrations in bedrocks, especially in the lower part of the section, produces a higher mean value with low ratios (2.1–2.9). The calculation of ratios limited to bedrock Cd concentrations below 1 mg·kg^{-1} gives a higher ratio of 4.2.

During soil formation, the underlying Cd-enriched carbonates are weathered and disintegrated into pebbles and finer particles, which are gradually incorporated into the soil during pedogenesis. As not all carbonate particles become dissolved, a fraction of the Cd in the soil will remain associated with the carbonate phase (nearly 50%). On the other hand, the Cd released through the dissolution of carbonate particles becomes adsorbed onto organic matter and associated with newly formed Cd-bearing minerals. At Schleifenberg, 13% of the total amount of Cd released resides in the organic-matter fraction on average.

With regards to the association of Cd with newly formed minerals, several pathways may be envisaged in the case of Schleifenberg: 1) adsorption on hydrous iron oxides and eventual co-precipitation with octahedral Fe-oxides such as goethite by substitution of Fe^{3+} (Benitez, 1999; Prudente, 2002; Huynh et al., 2003); 2) Adsorption on amorphous Mn oxides and hydroxides; 3) Adsorption of minor amounts of Cd on clays. Association of Cd with organic matter and Fe and Mn compounds is by far the most important sink of Cd in soils once dissociated from carbonate parent rocks, as no exchangeable Cd was found. Adsorption of Cd on clay minerals is less important since other trace elements such as Pb, Zn, Cr, Ni and Cu may compete with Cd to occupy adsorption sites on clay minerals (Alloway, 1995). This behaviour was also observed by Benitez (1999) with regards to other soil occurrences in the Swiss Jura presenting geogenic enrichments in Cd. He stated that Cd was principally associated with organic matter and oxihydroxide compounds. As for other calcareous soils, Plassard et al. (2000) found carbonates and exchangeable fractions as the principal Cd-bearing phases. Anthropogenically polluted soils are characterized by large quantities of Cd and heavy metals in the exchangeable, carbonate bound and Fe-Mn oxides phases (Li and Thornton, 2001; Lee, 2006), while some polluted agricultural soils show Cd incorporation into the organic phase binding to the reactive sites of organic matter or binding to metal-organic complexes, residual fraction, Fe-oxides and to a lesser extent into amorphous colloidal compounds (Onyatta and Huang, 1999).

Cd contents in the soils investigated here represent a low risk with regards to their mobility. This interpretation is based on the observation that no exchangeable Cd was detected and that the soils are characterised by a rather neutral to alkaline pH. Furthermore, acidic rainfall is neutralised by the substantial amount of carbonate present in the soils. With these conditions in soils the bioavailability of Cd is also reduced. However, it is not possible to discard a direct Cd uptake by plants by the dissolution of calcareous particles in contact with roots. The mechanisms of Cd incorporation by plants are still in need of a more detailed research.

3.4.3 Geochemical behaviour of trace elements in the soil

The observations made with the help of sequential extractions are useful to identify the principal components of the multivariate analysis. The first principal component represents carbonates (Ca on the negative side of PC1), Fe-oxides and silicates (Fe-Al pair on the positive side of PC1) being two of the major soil bearing phases. This axe indicates also the fate of the trace metals Pb, Zn, Cr, Ni and to a lesser extent Cu released after carbonate weathering. These elements are known to have strong affinities to soil organic matter and organic complexes (Borůvka et al., 2005). This is especially the case for Pb (Lee and Touray, 1998). The negative load on Ca is also confirmed by the absence of Fe and Al in the carbonate fraction (Figure 3.7b). The second principal component represents the axis of amorphous Mn oxyhydroxides. Mn behaviour is opposite to Zn, Pb, Cr and Cu, whose lowest concentrations were registered in the amorphous Mn-oxide fraction. Mn is closely bound to organic matter and may form metal-organic complexes with high adsorption capacity. High Al contents are also registered in association with organic matter showing the presence of organo-clay complexes. These complexes may represent the phase where Cd may easily be adsorbed (Alloway, 1995; Onyatta and Huang, 1999). Finally, the third principal component represents the axis of Cd. Cadmium does not show any correlations to the other elements in the soil system and its major occurrence in the carbonate phase (Figure 3.7a) should not be considered as a correlation reference for the statistical analyse of the geochemical system. This is especially true when we analyse the lack of correlation of Cd to Ca. Rambeau (2006) stated that Cd and Zn are strongly associated in the chemical system of the bedrock. Nevertheless, their behaviour is not the same once both elements are released after limestone dissolution. Cadmium distribution in the soil phases is different to those of the other elements. In accordance with previous observations, Zn may compete with Cd to be adsorbed onto the silicate phase (Benjamin and Leckie, 1981). Pb and Cu reduce Cd adsorption by Fe-oxides (Benjamin and Leckie, 1980). Jalali (2007) found that Cu, Zn and Ni are more strongly adsorbed than Cd in calcareous soils and this mainly onto oxides and residual phases. The presence of anomalous contents of Pb and Cr may be related to pollution from atmospheric deposition as these elements occur in the exchangeable phase (Borůvka et al., 2005) and the site crops out not far from traffic roads.

Soils from the upper part of the outcrop contain higher contents of organic matter and Mn oxides, and are as such better able to concentrate Cd, while soils from the middle zone concentrate Cd in non-dissolved carbonates. The soils from the transect of the lower part of the outcrop show Cd distributions mainly in carbonates, organic matter and Fe oxides.

Where incorporated into the soil, colluviums will act as a dilution factor in Cd concentration. Cadmium behaviour in the soil at the Scheifenberg site is illustrated in Figure 3.11.

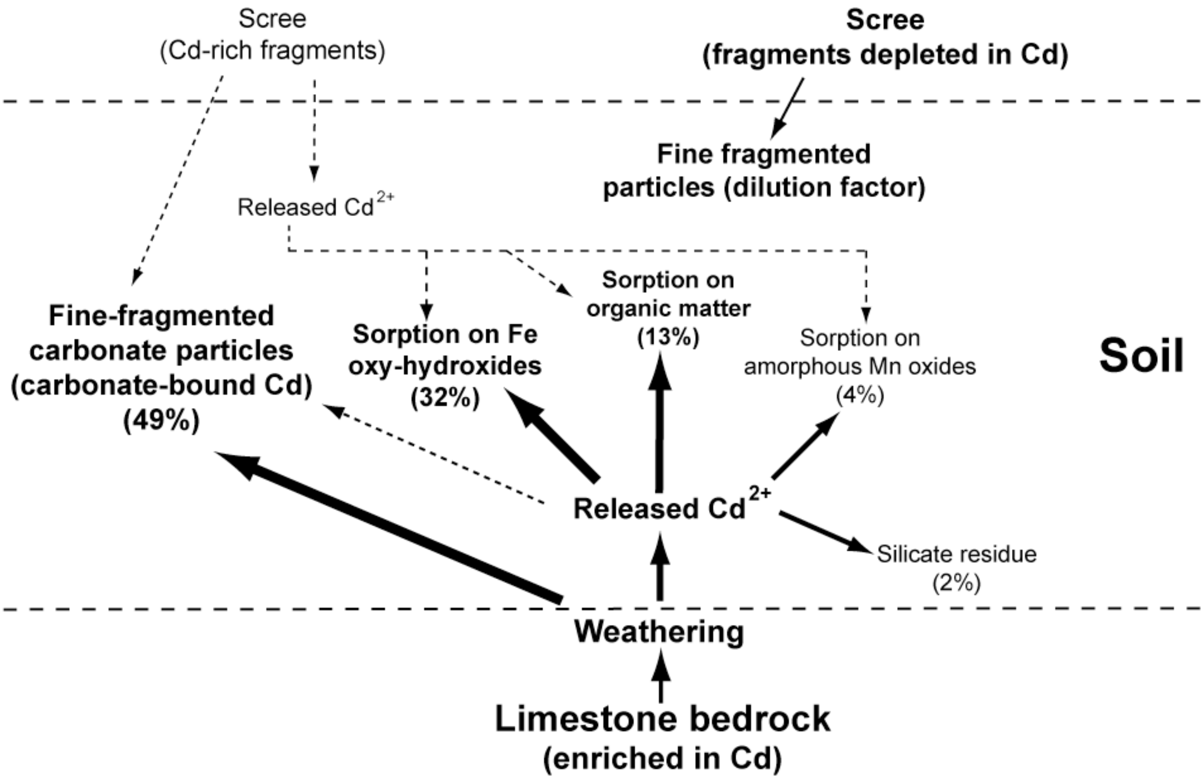

Figure 3.11 Cadmium distribution in soils at Schleifenberg.

3.5 CONCLUSIONS

Oolitic carbonates of the Bajocian Hauptrogenstein Formation crop out along the SW flank of the Schleifenberg. A well accessible section along a trail exposes almost the entire formation along a distance of 335 m. Systematic measurements of Cd concentrations in this section show the presence of anomalous enrichments in Cd of up 4.91 mg·kg^{-1} (Rambeau, 2006). A survey of the soils associated with this outcrop suggests that they are susceptible to be enriched in Cd as well, with a calculated Cd_{soil}/Cd_{rock} ratio of around 2.9. Even if Cd concentrations in these soils are lower in comparison to those found in other soils in association with the Hauptrogenstein Formation in the Jura mountains, it is evident that Cd pollution from a natural, geogenic source is taking place in this area (cf. also Benitez, 1999, Benitez and Dubois, 1999; Prudente, 1999; Dubois et al., 2002; Prudente et al., 2002). Vertical pedogenetic processes by weathering of the underlying bedrock and lateral inclusion of debris generated by the weathering and erosion of uphill carbonates are responsible for the origin of Cd in the soil. The short-distant allochthonous fragments act both as a Cd source when coming from Cd-rich carbonates as well as a dilution factor when Cd-lean pebbles roll downhill and cover the soil. Where developed on steep slopes above the here studied outcrop, the soil will hardly accumulate and displaced weathered material will constantly renew it.

Speciation of Cd in three soil samples suggests that a significant portion of Cd (nearly 50%) remains associated with carbonates. Cd dissociated from carbonates becomes associated with Fe-oxyhydroxides (approximately 30%), organic matter (over 10%), and a small fraction with Mn-oxides and clay minerals. As no Cd exchangeable phases were found in the soil, the risk that Cd becomes mobilised is low provided that the pH of the soil remains neutral. Under these conditions, the competition of other trace metals (Zn, Pb, Cr, Ni, Cu) and also Al is moderate and mainly concerns adsorption surfaces on clays and organic matter. Slightly acidic rainfall runoff becomes easily neutralized by the large amounts of calcareous material present in this area and its capacity to transfer Cd^{2+} ions into solution, or even to be leached out of the soil seems, therefore, quite negligible. The bioavailability of Cd is also reduced provided that the neutral conditions of soil do not change to more acidic pH values. Nevertheless, a direct uptake of Cd by plants through the dissolution of calcareous particles remains possible and this aspect needs further research.

3.6 REFERENCES

Adatte, T., Stinnesbeck, W., Keller, G., 1996. Lithologic and mineralogic correlations of near K/T boundary clastic sediments in NE Mexico: Implication for origin and nature of deposition. Sp. publications, Soc. Geol. of America, 307, 211–226.

Alloway, B. J., 1995. Cadmium. In: B.J. Alloway (Editor), Heavy Metals in Soils. Blackie Academic and Professional, Glasgow, 122–151.

Atteia, O., Thélin, Ph., Pfeifer, H.R., Dubois, J.P. and Hunziker, J.C., 1995. A search for the origin of cadmium in the soil of the Swiss Jura. Geoderma, 68, 149–172.

Baize, D., Deslais, W. and Gaiffe, M., 1999. Anomalies naturelles en cadmium dans les sols de France. Etude et Gestion des Sols, 2, 85–104.

Baize, D. and Sterckeman, T., 2001. Of the necessity of knowledge of the natural pedo-geochemical background content in the evaluation of the contamination of soils by trace elements. The Science of the Total Environment, 264,127–139.

Baize, D., and Boulaine, 1992. Peyrosols. In: D. Baize and M.C. Girard (Editors), Référentiel Pédologique. Principaux Sols d'Europe. INRA, Paris, 153–157.

Benitez, L. N., 1999. Cadmium speciation and phyto-availability in soils of the Swiss Jura: hypothesis about its dynamics. Ph.D. Thesis, Ecole Polytechnique Fédérale de Lausanne, Switzerland.

Benitez, L. N. and Dubois, J. P., 1999. Evaluation of the selectivity of sequential extraction procedures applied to the speciation of cadmium in soils. Environmental Pollution, Series B: Chemical and Physical, 11(2), 117–135.

Benjamin, M. M., and J. O. Leckie., 1980. Adsorption of metals at oxide interfaces: Effects on the concentration of adsorbate and competing metals. In: R. A. Baker (Editor), Contaminants and Sediments, Volume 2. Ann Arbor Science, Ann Arbor, Michigan, 305–332.

Benjamin, M. M., and J. O. Leckie., 1981. Multiple-site adsorption of Cd, Cu, Zn, and Pb on amorphous iron oxihydroxide. Journal of Colloid and Interface Science, 79, 209–221.

Bermond, A. P., 1992. Thermodynamics applied to the study of the limits of sequential extraction procedures used for the speciation of trace elements in sediments and soils. Environ. Technol. Lett.,13, 1175–1179.

Bolle, M.P., Adatte, T., Mangold, Ch., Remane.J.,1996. Microfacies, minéralogie et stratigraphie du Dogger de la région du Furcil (NE). Bull. Soc. Scie. Nat. Neuch. 119, 123–144.

Borůvka , L., Vacek, O., Jehlička, J., 2005. Principal component analysis as a tool to indicate the origin of potentially toxic elements in soils. Geoderma, 128, 289–300.

Dubois, J. P., Okopnik, F. Benitez, N. and Védy, J.C., 1998. Origin and spatial variability of cadmium in some soils of the Swiss Jura. 16th World Congress Soil Science. Montepellier.

Dubois, J. P., Benitez, N., Liebig, T., Baudraz, M. and Okopnik, F., 2002. Le cadmium dans les sols du haut Jura suisse. In D. Baize and M. Tercé (Editors), Les élements traces métalliques dans les sols. Approches fontionelles et spatiales. INRA, Orléans, 33–52.

Food and Agriculture Organization of the United Nations FAO, 2006. World reference base for soil resources 2006. A framework for international classification, correlation and communication. FAO, Rome.

Gonzales, R., 1993. Die Hauptrogenstein-Formation der Nordwestschweiz (mittleres Bajocien bis unteres Bathonien). Ph.D. Thesis, University of Basel, Switzerland.

Huynh, T., Tong, A.R., Singh, B., Kennedy, B.J., 2003. Cd-substituted goethites - A structural investigation by synchrotron X-Ray diffraction. Clays and Clay Minerals, 51, 397–402.

Jalali, M., Moharrami, S., 2007. Competitive adsorption of trace elements in calcareous soils of western Iran. Geoderma, 140 (1–2), 156–163.

Kabata-Pendias, A. and Pendias, H., 1992. Trace elements in soils and plants. CRC Press, Boca Raton, Florida, USA.

Kaiser, K., Zech, W., 1996. Defects in estimation of aluminium in humus complexes of podzolic soils by pyrophosphate extraction. Soil Science, 161, 452–458.

Kleber, M., Mikutta C., Jahn, R., 2004. Andosols in Germany - pedogenesis and properties. Catena, 56, 67–83.

Klug, H.P. & Alexander, L. (1974) - X-ray Diffraction Procedures for Polycrystalline and Amorphous Materials. John Wiley and Sons, Inc. First and Second editions, New York.

Kübler, B., 1983. Dosage quantitatif des minéraux majeurs des roches sédimentaires par diffraction X. Cahier de l'Institut de Géologie de Neuchâtel, Série AX N°1.1 &1.2

Lee, S., 2006. Geochemistry and partitioning of trace metals in paddy soils affected by metal mine tailings in Korea. Geoderma, 135, 26–37.

Lee, P.K. and Touray, J.C., 1998. Characteristics of a polluted artificial soil located along a motorway and effects of acidification on the leaching behaviour of heavy metals (Pb, Zn, Cd). Water research, 32 (11), 3425–3435.

Li, X. and Thornton, I., 2001. Chemical partitioning of trace and major elements in soils contaminated by mining and smelting activities. Applied Geochemistry, 16 (15), 1693–1706.

Moore, D. and Reynolds, R., 1989. X-Ray-diffraction and the identification and analysis of clay-minerals. Oxford University Press.

Onyatta, J.O., Huang, P.M., 1999. Chemical speciation and bioavailability index of cadmium for selected tropical soils in Kenya. Geoderma, 91, 87–101.

Plassard, F., Winiarski, T., Petit-Ramel, M., 2000. Retention and distribution of three heavy metals in a carbonated soil: comparison between batch and unsaturated column studies. Journal of Contaminant Hydrology, 42 (2–4), 99–111.

Prudente, D., 1999. Distribution des teneurs naturelles en cadmium dans les sols de la forêt communale des Fourgs (Doubs, France). Ph.D. Thesis, Ecole Polytechnique Fédérale de Lausanne, Switzerland.

Prudente, D., Baize, D. and Dubois, J.P., 2002. Le cadmium naturel dans une forêt du haut Jura français. In: D. Baize and M. Tercé (Editors), Les élements traces métalliques dans les sols. Approches fontionelles et spatiales. INRA, Orléans, 53–70.

Rambeau, C., 2006. Cadmium anomalies in Jurassic carbonates (Bajocian, Oxfordian) in western and southern Europe. Ph.D. Thesis, University of Neuchâtel, Switzerland.

Soon, Y.K. and Abboud, S., 1993. Cadmium, Chromium, Lead, and Nickel. In: M.R. Carter (Editor), Soil sampling and methods of analysis. Canadian Society of Soil Science, 101–107.

Tessier, A., Campbell, P.G.C., Bisson, M., 1979. Sequential extraction procedure for the speciation of particulate trace metals. Analytical Chemistry, 51 (7), 844–851.

The Federal Authorities of the Swiss Confederation, 1998. RS 814.12 Ordonnance sur les atteintes portées aux sols (OSol). Annexe 2., Valeurs indicatives, seuils d’investigation et valeurs d’assainissement pour les métaux lourds et le fluor dans les sols. Official Publications Centre, Switzerland.

Tuchschmid, M., 1995. Quantifizierung und Regionalisierung von Schwermetallen in bodenbildenen Gesteinen der Schweiz. Umwelt-Materialien N° 32. Office Fédéral de l'Environnement des Forêts et du Paysage, Berne.

U.S. Environmental Protection Agency (EPA), 1994. Test Methods for Evaluating Solid Waste, SW-846, 3rd ed., Office of Solid Waste and Emergency Response, Washington, D.C.

Van der Sloot, H.A., Heasman, L., and Quevauviller, Ph.,1997. Harmonization of leaching/extraction tests. Elsevier, Amsterdam, 281pp.

CADMIUM DISTRIBUTION IN A NATURALLY CONTAMINATED SITE OF THE SWISS JURA USING SEQUENTIAL EXTRACTIONS AND MULTIVARIABLE ANALYSES OF THE MAIN PHYSICOCHEMICAL SOIL PROPERTIES

The case of Le Gurnigel soils

Paper in preparation and will be submitted for publication shortly

CHAPTER 4

CADMIUM DISTRIBUTION IN A NATURALLY CONTAMINATED SITE OF THE SWISS JURA USING SEQUENTIAL EXTRACTIONS AND MULTIVARIABLE ANALYSES OF THE MAIN PHYSICOCHEMICAL SOIL PROPERTIES

Raul Quezada-Hinojosa[1], Virginie Matera[2], Séverine Vancolen[1], Eric Verrecchia[3],
Thierry Adatte[3], Karl B. Föllmi[3]

[1] *Institut de Géologie, Université de Neuchâtel, rue Emile-Argand 11, CP 158, CH-2009*
Neuchâtel, Switzerland
[2] *Institut National de Recherche et Sécurité Rue du Morvan CS 60027 54519*
Vandoeuvre Les Nancy, France
[3] *Institut de Géologie et Paléontologie, Université de Lausanne, Anthropôle 3172, CH-1015*
Lausanne, Switzerland

Abstract

Mineralogical, geochemical and principle-component analyses were performed on six closely spaced soil profiles, which are naturally enriched in cadmium (Cd) at le Gurginel, Swiss Jura Mountains. The soils consist of cambisols and cambic-neoluvisols and include an important allochthonous, aeolian fraction. All soils are associated with bedrock composed of middle Jurassic (Bajocian) oolithic carbonates, which have been identified as a source of geogenic Cd. Cadmium concentrations generally increase down the analysed soil profiles, showing maxima (up to 16.3 mg·kg^{-1}) near the soil-bedrock interface. A sequential extraction analysis suggests that most Cd resides in the carbonate and organic fractions in topsoils, whereas the amorphous iron and manganese oxyhydroxide fraction becomes the most important Cd-bearing phase in the middle and subsoils. The principal component analysis shows that Cd, Zn and Cr are positively correlated with comparable distributions in the soil profiles suggesting a common bearing phase such as Fe oxyhydroxides for these three elements. A complex transfer pattern of Cd is proposed for the analysed soil profiles, which starts with the release of Cd from the underlying bedrock, and its transfer into oxide, hydroxide, carbonate and organic phases. Additionally, the lateral advection of Cd-rich soils formed on neighbouring slopes acts as a local allochthonous input of Cd to these soils, which is transferred from the topsoil towards the deeper horizons by biological and pedogenic processes. The amount of readily exchangeable and therefore potentially bioavailable Cd is low in these soils (on average 0.2 mg·kg^{-1}) provided that the pH remains above 5. Under stronger acidic conditions the concentration of bioavailable Cd may increase in the topsoils of shallow cambisols (3.0 mg·kg^{-1}) and cambic-neoluvisols (1.2 mg·kg^{-1}). Under stronger acidic (pH < 4.5) and oxidizing conditions, Cd bound to organic matter may be mobilised in addition and the bioavailability of Cd would range between 3.3–5.4 mg·kg^{-1} in cambisols and reach up to 1.7 mg·kg^{-1} in cambic-neoluvisols.

Keywords: **Cadmium; Bioavailability; Geogenic; Jura Mountains; Late-Bajocian limestone; Oxyhydroxides; Multivariable regression, Soil; Sequential extractions.**

4.1 INTRODUCTION

Cadmium (Cd)-enriched carbonate rocks from the Bajocian-Bathonian and Oxfordian-Kimmeridgian stages (Middle and early Late Jurassic) crop out frequently in the French and Swiss Jura Mountains. Weathering of these rocks triggers the release of Cd and subsequent pedogenetic processes promote its incorporation into the resulting soil. As such, these rocks provide a natural source of anomalously high Cd concentrations in overlying soils (Benitez, 1999; Dubois et al., 2002; Prudente et al., 2002; Rambeau, 2006; Quezada et al., 2009), which have been reported to reach levels of up to 10 $mg \cdot kg^{-1}$ (Dubois et al., 1998; Benitez, 1999) and in one case even 22 $mg \cdot kg^{-1}$ (Prudente, 1999). These values largely exceed the official Swiss indicative guideline value for soils fixed at 0.8 $mg \cdot kg^{-1}$ (Federal Authorities of the Swiss Confederation, OSol, 1998).

The site called "Le Gurnigel" is located in the Jura Mountains northeast of the "col de la Vue des Alpes" (canton Neuchâtel, Switzerland: Figure 4.1). Soils at this site contain Cd concentrations with mean values, which are generally above 10 $mg \cdot kg^{-1}$. Such soils may be considered as naturally polluted and represent an environmental risk since the local herbaceous vegetation cover is susceptible to pump and stock this element in both roots and shoots, used by grazing ungulate livestock. As such, Cd is likely to gradually enter in the food chain jeopardizing animal and human health.

In this contribution, we aim at i) confirming the geogenic origin of Cd in the Le Gurnigel soils by means of a pedogenic and mineralogical approach and ii) confirming the geogenic origin of Cd and assessing Cd dynamics from a pedo/geochemical point of view completing the geochemical data obtained so far during previous studies (Okopnik, 1997; Benitez, 1999; Dubois et al., 2002). The pedogenic, physicochemical and mineralogical properties of a series of soil profiles are discussed here and multivariable analyses and linear regressions are applied to study the simultaneous effects on the transfer of Cd from the bedrock and its spatial distribution in these soils.

4.2 MATERIAL AND METHODS

4.2.1 Site description

Le Gurnigel is a pasture that lies at 1300 m above sea level on the northern face of the Mont d'Amin located in the northern part of canton Neuchâtel (Switzerland; Figure 4.1).

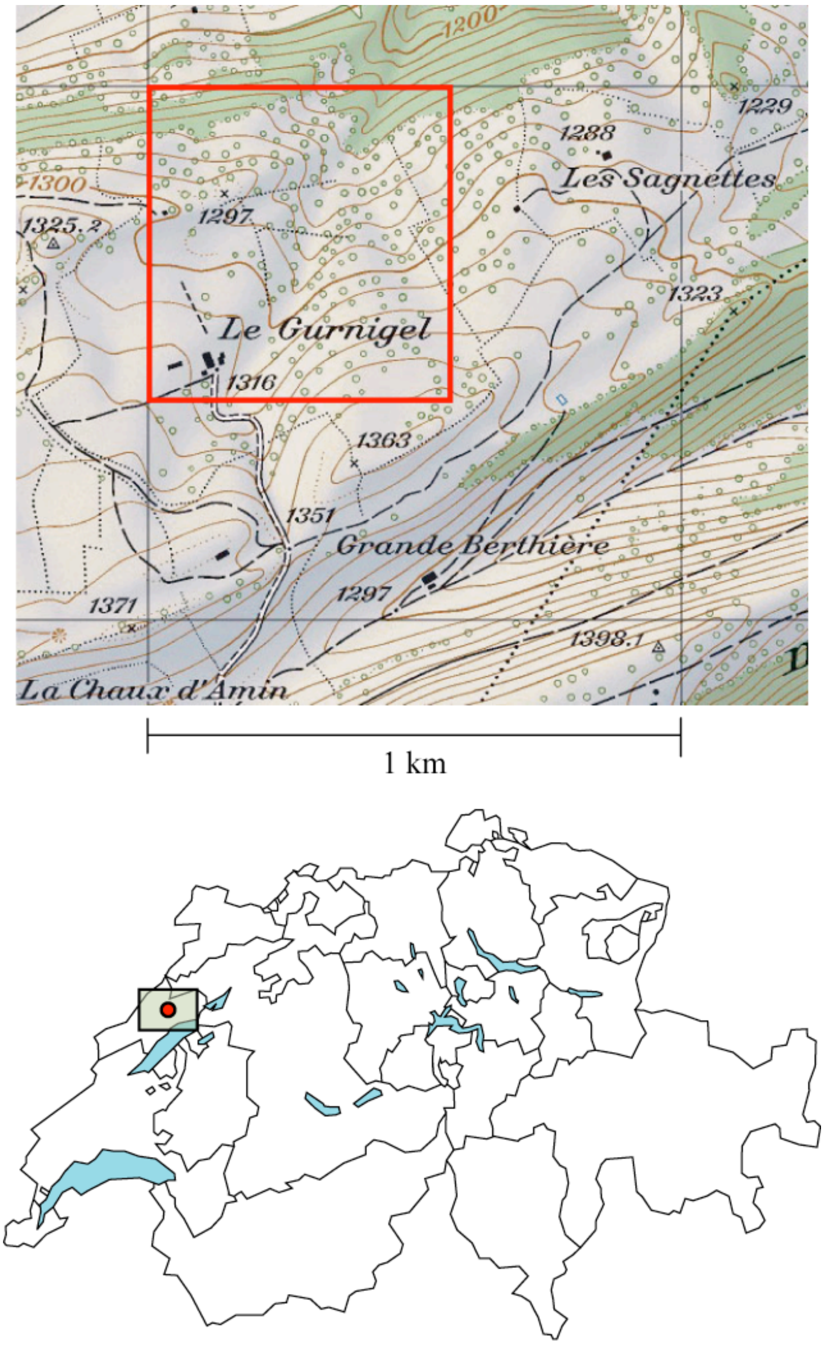

Figure 4.1 Topographic map of the Le Gurnigel site (1:25'000), reproduced with the permission of the Swiss Federal Office of Topography.

The geological map of the region (Figure 4.2a) reveals that the majority of the site overlies late Bajocian limestone (Middle Jurassic). Aalenian and Bathonian marls are present in the northwestern part. The geomorphology of the site consists of three main hillocks with slopes in their flanks ranging from 20% to 30%.

Okopnik (1997) established a pedogenic map of the Le Gurnigel area, which is shown in Figure 4.2b. Soils were classified following the French pedogenic reference system (Baize et al., 1995). The site present thin soils (13–40 cm deep) identified as organosols, rendosols and calcolsols, which are formed on top and on the flanks of the hills. Deeper soils (80–140 cm deep) are located in the accumulation zones or coombs that are formed by the conjunction of two hillocks. Deep soils present strong signs of allochthony suggesting that these soils were formed on postglacial aeolian silt deposits. Brunisols, calcisols and neoluvisols correspond to this group of soils. Both groups of soils lie on Bajocian carbonate. Soils formed on marl of Aalenian and Bathonian age show signs of hydromorphy, which increase with soil depth. These latter soils are not considered in the present study.

4.2.2 Soil sampling strategy

In a first approach, we used the pedogenic map of the Le Gurnigel site shown in Figure 4.2b to sample three main soil types in function of the degree of soil evolution, from the poorly developed AC-horizon soils to the better developed neoluvisols. In order to facilitate the sampling procedure, the three groups of soils were coded as follows: A = AC-horizon soils, C = brunisol-calcosol and E = brunisol-neoluvisol.

Okopnik (1997) determined the spatial distribution of Cd at the le Gurnigel site, which is reproduced on the map in Figure 4.2c. Based on this map, two intervals of Cd concentrations were considered for the present study: Interval X =1–8 mg kg^{-1} and interval Z = 8–16 mg kg^{-1}.

As a result of overlapping the pedogenic map with the Cd distribution map, a single map was obtained (Figure 4.3), on which it was possible to intersect the three types of soils with the two ranges of Cd concentrations hence producing six sample points: AX, AZ, CX, CZ, EX, EZ. The exact locations of these points were determined by means of a Garmin ETrex Sumit GPS device. A soil pit was dug at each sample point down to the weathered bedrock. Samples were taken from each soil profile at equidistant levels of 0.5 m for the shallowest soil AZ and 0.8 m wherever possible in the remaining five profiles. Special care was taken in sampling soils from each level in order to avoid taking a single sample from the interface of two different pedogenic horizons. All soil samples were air dried and sieved through a 2 mm mesh.

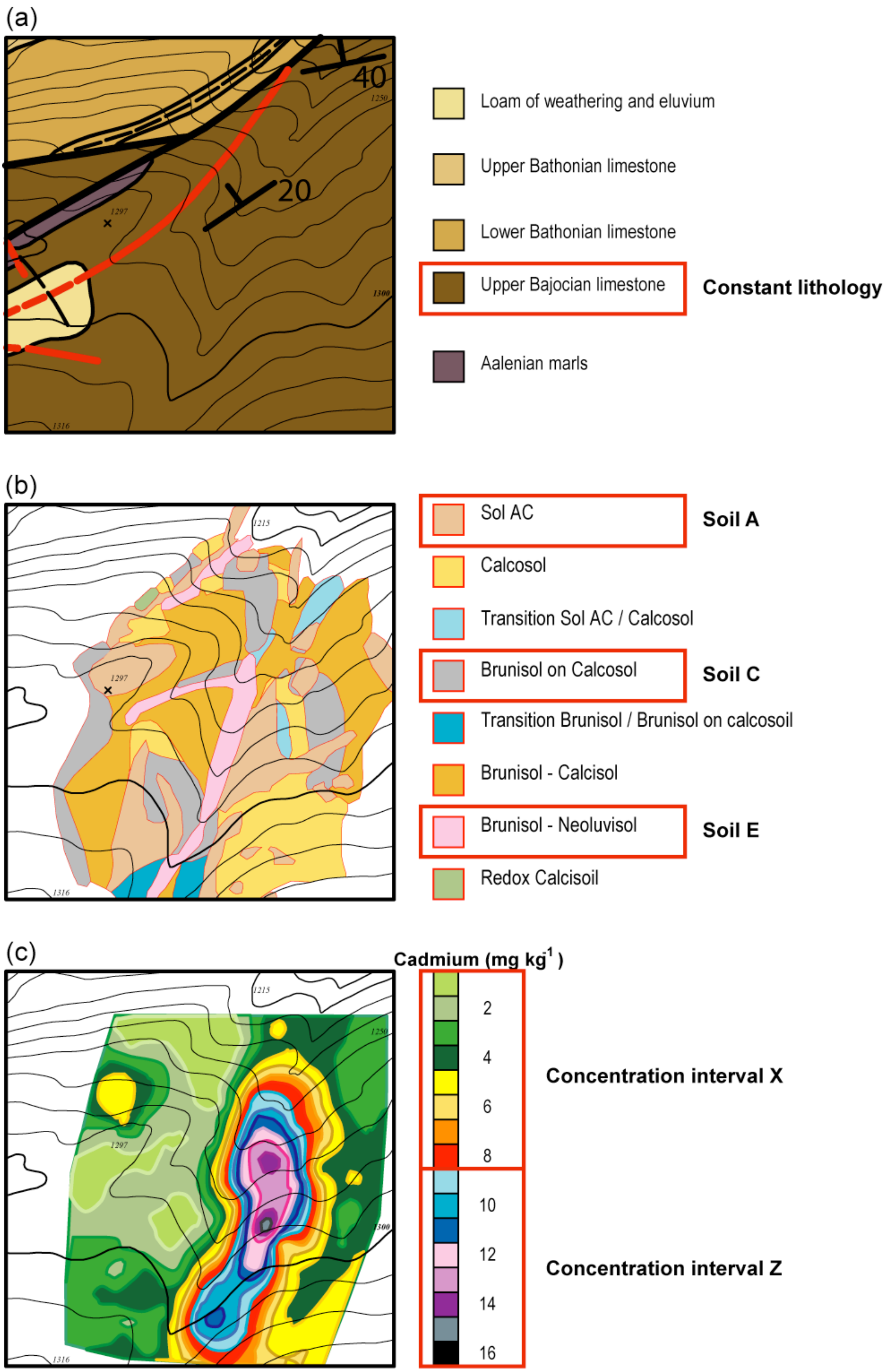

Figure 4.2 (a) Geological map of the Le Gurnigel site; (b) Soil distribution map of the site; (c) Cd spatial variability map from Okopnik (1997).

As most of the sampled soils did not match completely the soil type identified in the pedogenic map a new classification for each soil became necessary. In order to do so, we used the nomenclature of the World Reference Base (WRB) for Soil Resources 2006 (Food and Agriculture Organization of the United Nations FAO, 2006).

Samples were also taken from the underlying bedrock in sample points AX, AZ, CX, and CZ. We were unable to reach the bedrock in sample points EX and EZ, due to their depth. However, small solid aggregates, 2 cm in diameter approximately, were found in the deepest horizons of both soil profiles and were collected in order to identify and analyze them.

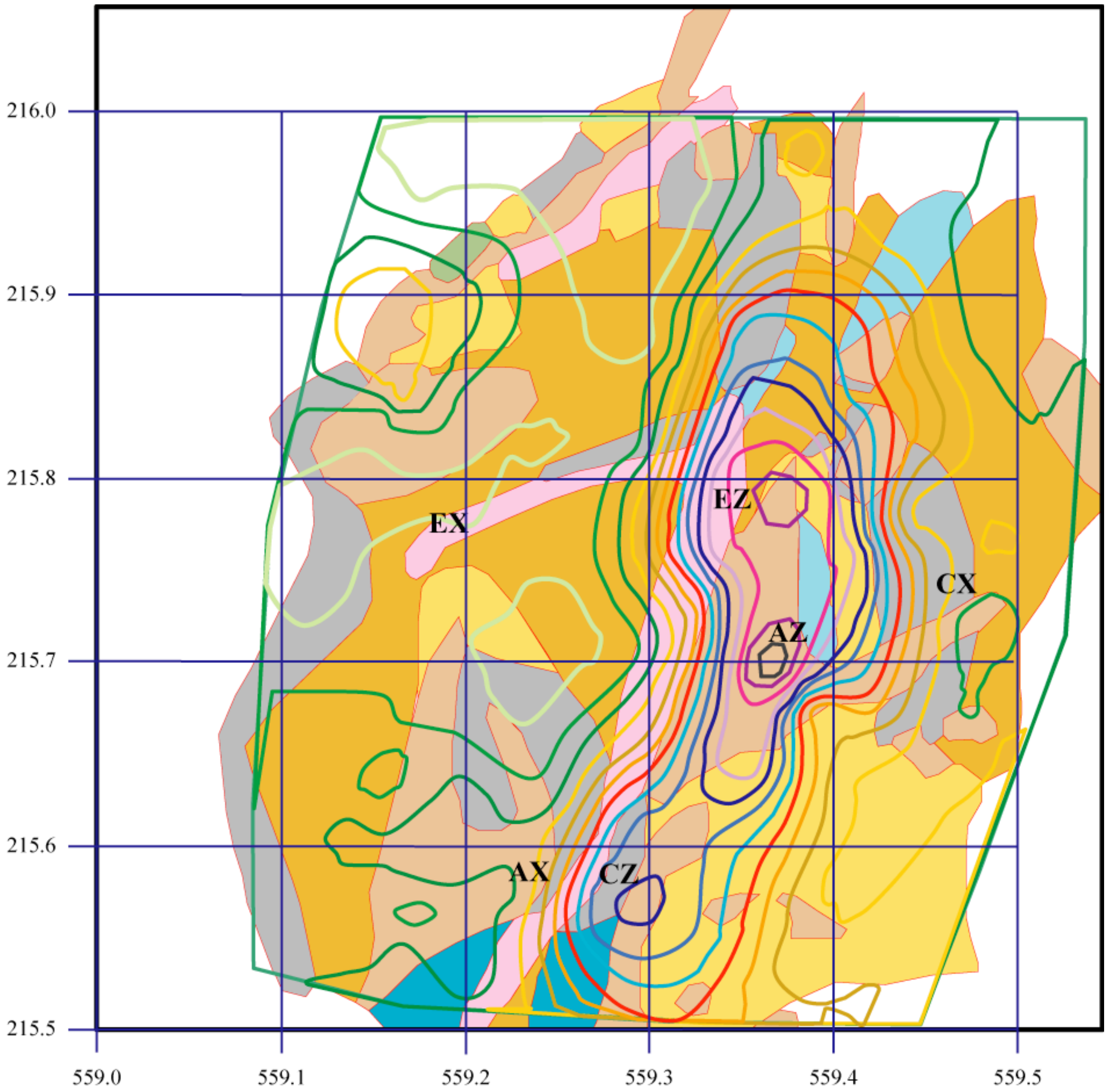

Figure 4.3 Map of the Le Gurnigel site where the 6 sampling points AX, AZ, CX, CZ, EX and EZ have been identified.

4.2.3 Main chemical soil properties

Total organic and mineral-carbon contents were measured in powdered samples by a Rock-Eval6^{TM} device. Total carbon and nitrogen contents were also analysed on powdered samples using an elemental analyzer Carlo Erba EAL 1108. Soil pH in H_2O was measured using a Metrohm 682 titroprocessor. The cation-exchange capacity (CEC) was measured following the French protocol AFNOR NF X31-130: Soils samples were mixed with a solution of hexaamminecobalt(III) chloride and the concentration of free cobalt ions was measured in a calibrated UV spectrometer to 470 nm.

4.2.4 Metals concentrations

Chemical analyses of trace metals Cd, Zn, Pb, Cr, Ni, Cu, and major elements Ca, Fe, Al, Mn in soil samples, rocks and mineral aggregates were conducted by Inductively Coupled Plasma Mass Spectrometry (ICP-MS). The samples were prepared by following the Method 3051 developed by the U.S. Environmental Protection Agency EPA (1994). 250 mg of dried and grounded sample were subjected to microwave-assisted acid digestion (concentrated HNO_3) and samples were subsequently filtered at 0.45 μm before analysis. The filtrated solutions were then analyzed by an ICP-MS Perkin-Elmer Elan 6100 device. The “total” concentrations measured by this method exclude most trace metals trapped within silicate crystal lattices of refractory minerals, but it gives a reliable measure of the amounts of metals potentially available for natural leaching and biological processes (Soon and Abboud, 1993).

4.2.5 Soils and rocks mineralogy

Mineralogical analyses were carried out by X-Ray diffraction on bulk rock and soil samples, and on their fine-silt (2–16 µm) and clay fractions (<2 µm) using a diffractometer Scintag XDS 2000 with Cu-Kα radiation.

The whole soil and rock compositions were determined based on methods described by Klug and Alexander (1974) and Kübler (1983). This method for semi-quantitative analysis of the bulk-soil and bulk-rock mineralogy (obtained by XRD patterns of random powder samples) used external standards. XRD analyses of oriented clay samples were performed after air-drying at room temperature and ethylene-glycol solvated conditions. The intensities of selected XRD peaks characterizing each clay mineral present in the size fraction (e.g. kaolinite, chlorite, mica, normal illite-smectite mixed layers and pedogenic intergrades were measured for a semi-quantitative estimate of the proportion of clay minerals present in the size-fractions <2 µm and 2–16 µm. Therefore, clay minerals are given in relative percent abundance without correction factors (Moore and Reynolds, 1989; Adatte et al., 1996).

Kaolinite was distinguished from chlorite by deconvolution of peak 24–25 Å aided by a Pearson 7 function.

4.2.6 Cadmium and trace-metal distribution in soils

We used the sequential extraction procedure described by Benitez (1999), who specifically adapted the protocol developed by Tessier et al. (1979) to extract Cd in soils of the Swiss and French Jura (Figure 4.4). This method allows for the separation and identification of Cd considered to be distributed in six major fractions: (1) exchangeable; (2) carbonates; (3) organic matter; (4) amorphous Fe-, Mn-oxyhydroxides which will be referred to as amorphous oxyhydroxides in this contribution; (5) crystalline Fe oxides; and (6) residual mineral matrix. The filtrated supernatants recovered in each extraction fraction were analyzed by quadrupole ICP-MS. In order to assure the accuracy of the results, three replicate analyses were carried out in the extraction protocol.

The extraction protocol was modified in step (1) and step (6) as follows: we used $NaNO_3$ instead of $MgCl_2$ for the exchangeable fraction since exchangeable Cd concentrations are overestimated by using chloride salts (Benitez, 1999). Concentrated HNO_3 was used in the last step, though not all of the Cd is extracted from the residual mineral matrix by using this chemical. We used this chemical, as we needed to fit the mass balance to adjust it to the “total” concentrations of Cd and trace elements measured by the US-EPA Method 3051.

The main possible limitation of this operational technique is related to the lack of a specific selectivity of the chemicals used: some metallic ions are likely to be readsorbed onto the remaining solid phases during each extraction step. Furthermore, drying of the soil sample and the applied speciation methodology (extraction time, liquid/solid proportions, agitation time, etc.) may induce chemical changes as well. This may explain the disagreement, which exists among authors with regards to the accuracy and reproducibility of the techniques employed for the different extraction protocols (Tessier et al., 1979; Bermond, 1992; Van der Sloot et al., 1997).

4.2.7 Statistical methods

Principal Component Analyses (PCA) were applied to the entire database obtained from the measured soil properties: concentrations of trace and major elements, chemical properties, mineralogy of bulk rock, and silt and clay fractions. Correlation circles were used to discriminate the most significant variables from those that would not play an important role in Cd behaviour. Scatter distributions of soil samples were also obtained to compare their variability according to the associations of the most significant properties of soils.

We subsequently attempted to establish a multivariable linear model to predict Cd behaviour in the Le Gurnigel soils based on the previously selected variables considered as the potential predictors. Stepwise methods, both forward selection and backward elimination, were used in removing any variable having an insignificant F statistic p-value that exceeded the specified cut-off value α fixed at 0.05, as a result of the multiple combinations of variables.

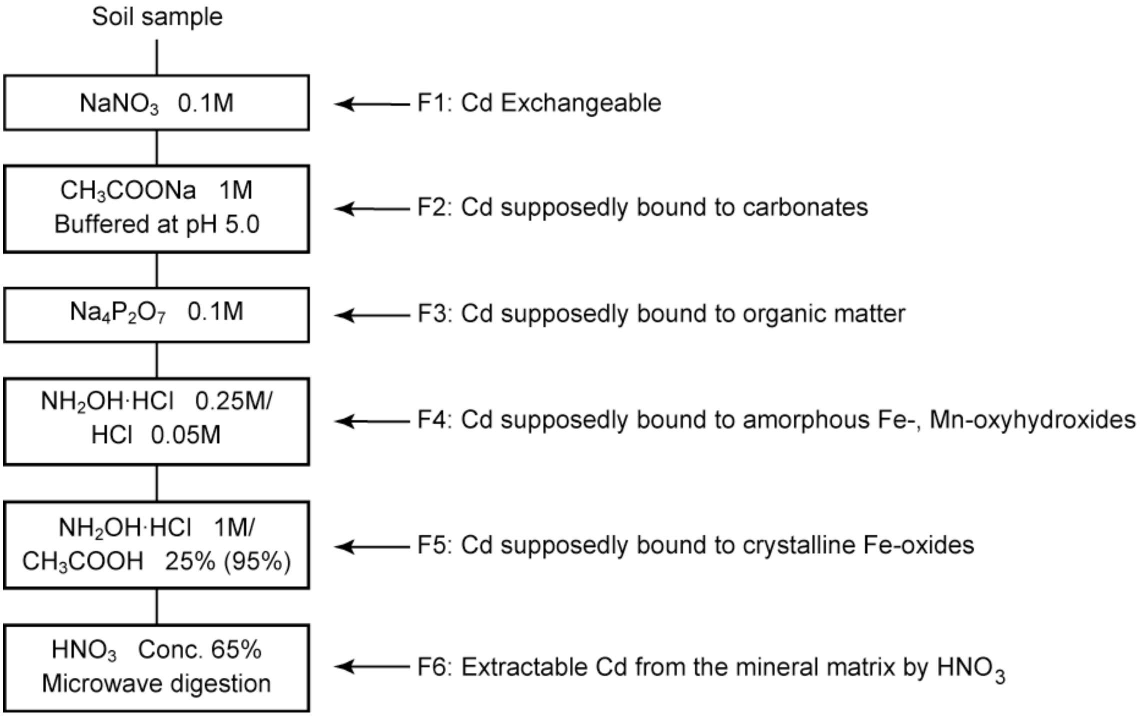

Figure 4.4 Sequential extraction scheme modified from Benitez (1999).

4.3 RESULTS

4.3.1 Soil descriptions

In Table 4.1, the soil identifications are given according to the WRB (FAO, 2006) and the French pedogenic reference system (Baize et al., 2008). Eutric-cambisols and cambic-neoluvisols are the two main soil groups identified at the sample sites. Figure 4.5 shows the soil profiles for each of the six sample sites including the distinguished soil horizons and sample depth.

Cambisols (soils AX, AZ, CX and CZ) were identified by the presence of an organic-mineral horizon A and chiefly by the presence of an underlying structural horizon S, which is recognised by the brownish discoloration and increasing clay percentage (FAO, 2006). These soils exhibit strong signs of carbonate removal along their entire profiles.

Soil AX, an eutric cambisol (humic), is 40 cm deep. Its topsoil horizon A_h is rich in organic matter (16.1%). Even though the horizons are not clearly differentiated, a slight colour change from dark brown to brownish ochre and a polyhedral texture suppose a structural horizon S_h. This horizon might be still in evolution as its organic-matter content is still important (7.5%).

Soil AZ, an eutric cambisol (leptic, humic), is the shallowest soil (16 cm depth). It presents features similar to soil AX. This soil is highly decarbonated, despite its depth.

Soil CX, an eutric-dystric cambisol (calcic), is 60 cm deep. Its horizons A_h and S are more easily recognisable by their texture and colour change. The S horizon is much more developed with a clear polyhedral texture and a yellow ochre colour. A more detailed analysis of its deeper horizons by means of thin sections suggests that this soil exhibits signs of clay illuviation. Figure 4.6a shows the presence of clay coatings on soil particles of level CX h7. As for the shallow cambisols, soil CX is decarbonated all along its profile. Nevertheless the lowest levels in the subsoil contain finely-grained weathered bedrock particles (horizon Sci?). The bedrock appears to be more fragmented than those of their shallow counterparts and has thus been identified as a horizon C. However, calcium contents measured in the last two levels are low (4.6–3.6%) and the pH is not higher than 5.8.

Soil CZ, an eutric-dystric cambisol, is 35 cm deep. Unlike soil AX, the horizon S is better developed and clearly visible by its yellowish coloration with low organic-matter contents. This soil is also entirely decarbonated.

Table 4.1 Classification of sampled soils

Soil code	Soil type	
	World Reference Base (2006)	**French Pedogenic Reference (1995)**
AX	Eutric cambisol (humic)	Brunisol saturé
AZ	Eutric cambisol (leptic, humic)	Brunisol saturé leptique
CX	Eutric-dystric cambisol (calcic)	Brunisol mesosaturé, horizon calcique profond
CZ	Eutric-dystric cambisol	Brunisol mesosaturé
EX	Cambic-neoluvisol	Brunisol-Neoluvisol
EZ	Cambic-neoluvisol	Brunisol-Neoluvisol

Cambic-neoluvisols EX and EZ are deeper than 70 cm. These soils show characteristics of cambisols in their upper horizons and neoluvisols in the middle and deeper horizons. The subsoil has higher clay contents than in the topsoil (including structural horizon S) principally due to clay migration and carbonate removal (FAO, 2006). It is difficult to identify an eluvial horizon E or AE related with a colour change in these soils. It is possible, however, to

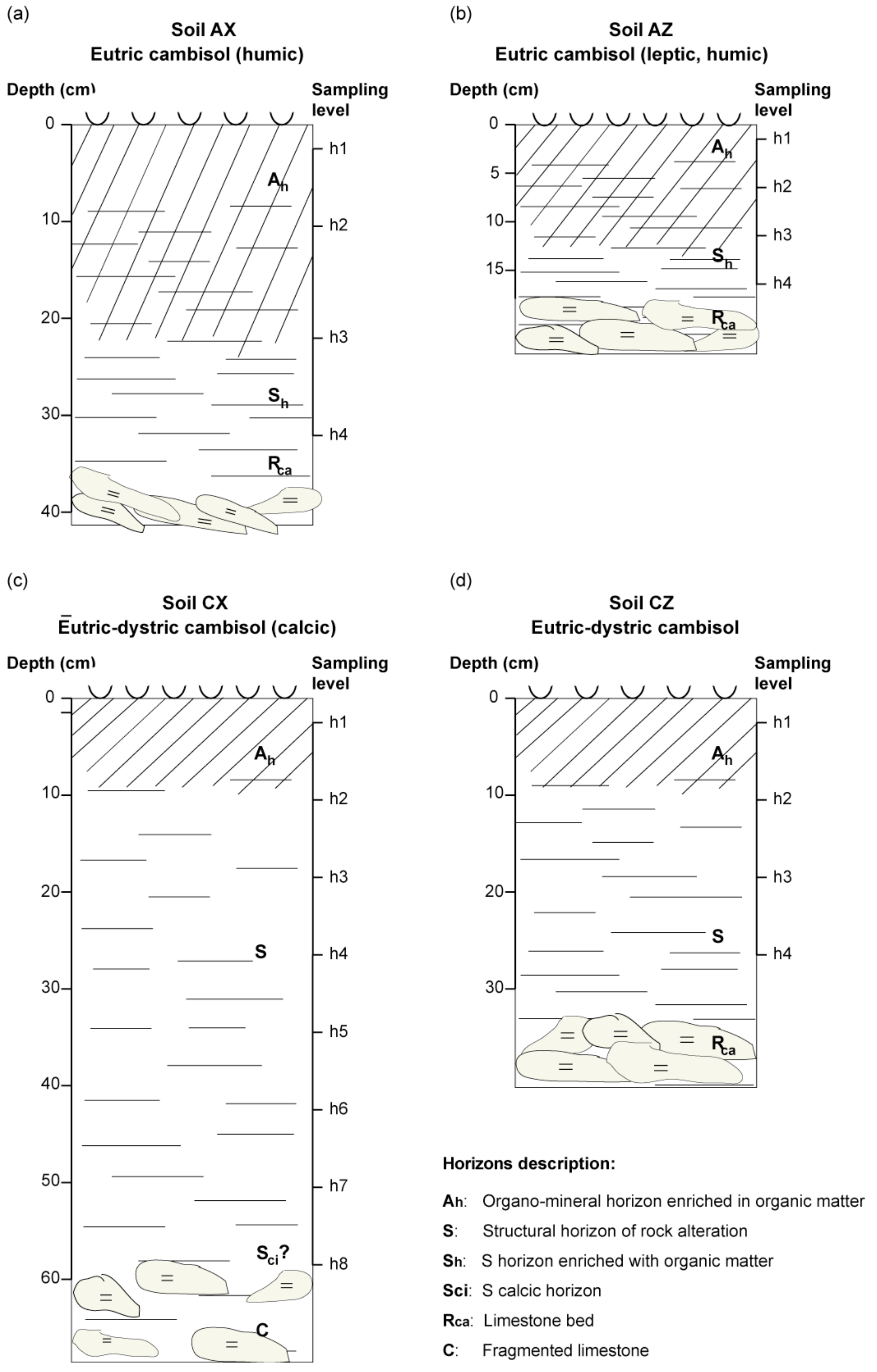

Horizons description:

Ah: Organo-mineral horizon enriched in organic matter

S: Structural horizon of rock alteration

Sh: S horizon enriched with organic matter

Sci: S calcic horizon

Rca: Limestone bed

C: Fragmented limestone

(Continued)

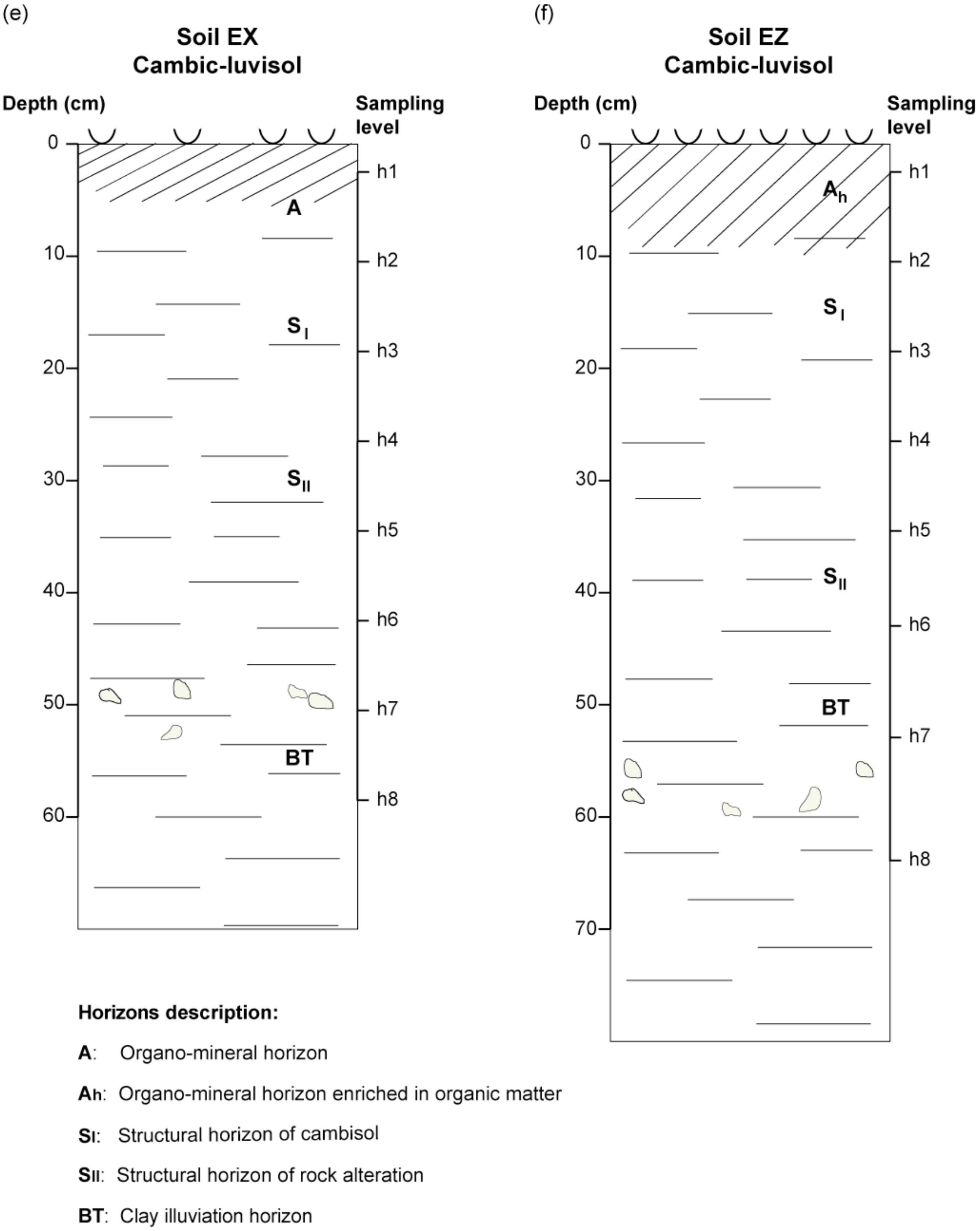

Horizons description:

A: Organo-mineral horizon

Ah: Organo-mineral horizon enriched in organic matter

SI: Structural horizon of cambisol

SII: Structural horizon of rock alteration

BT: Clay illuviation horizon

Figure 4.5 Soil profiles at the six sampling points. (a), (b) and (d) shallow cambisols; (c) deep cambisol; (e) and (f) deep cambic-neoluvisols.

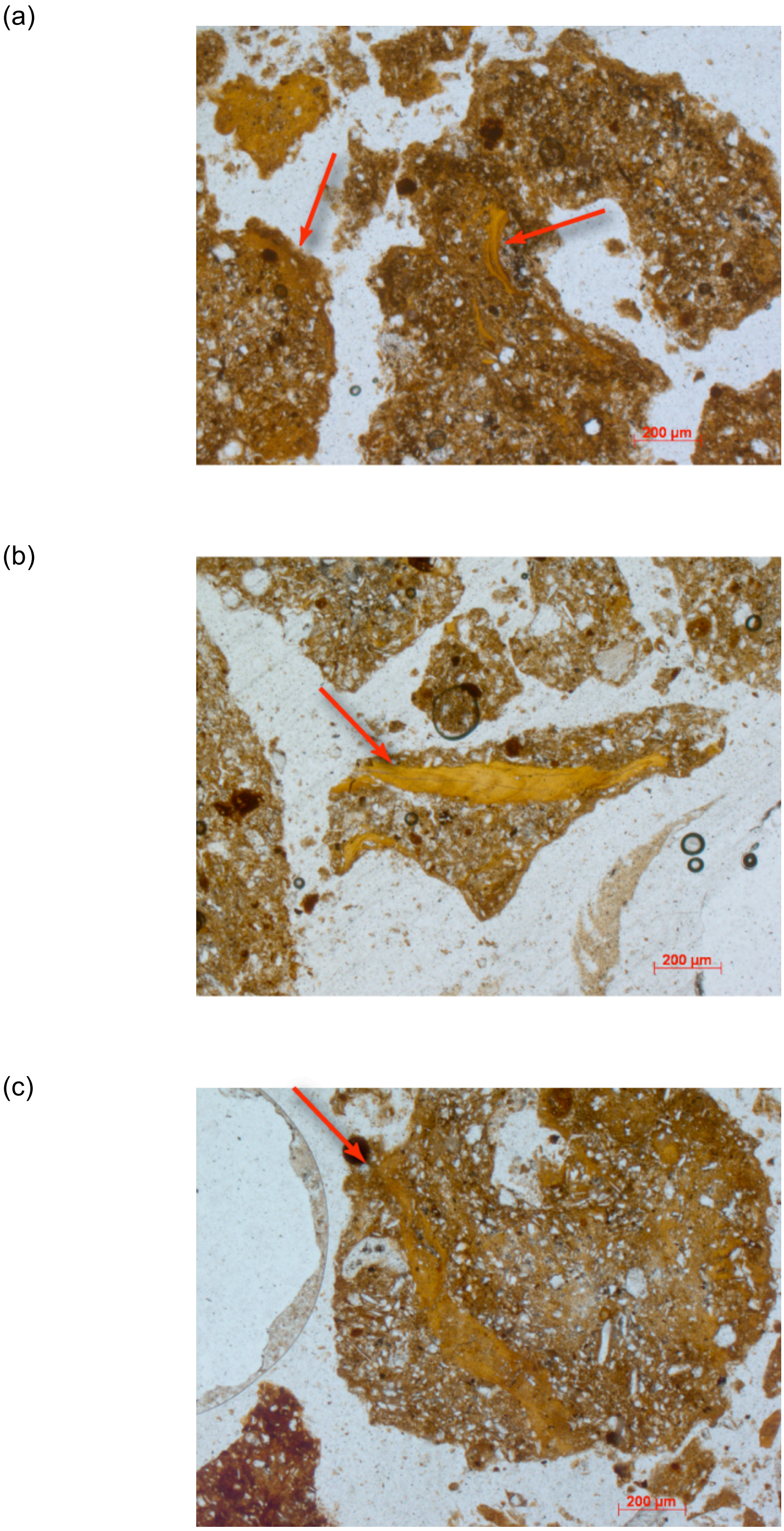

Fig. 4.6. Clay coatings identified by a red arrow on soil particles of subsoil, showing clay eluviation from upper horizons. (a) Cambisol CX level h7; (b) Neoluvisol EX level h7; (c) Neoluvisol EZ level h5. All images magnified 5x.

observe that the pH of the middle levels is slightly acidic (4.9 for both soils; Table 4.4). In thin sections, clay coatings on soil aggregates are observed in the deeper subsoil horizons (Figure 4.6b and c) in sampled levels of the subsoil. Several mineral aggregates are trapped in the deepest horizons B of the solum at nearly 50 to 60 cm. It was not possible to reach the underlying bedrock.

Based on soils depth and in order to simplify the nomenclature of soils in the following lines, soils with a maximal depth of 40 cm (AX, AZ, CZ) will be referred as shallow cambisols, whereas soils deeper than 40 cm will be referred as deep cambisol CX and deep neoluvisols EX, and EZ.

4.3.2 Main chemical soil properties

The main chemical characteristics for each sampling level of the six soil types are presented in Table 4.2. Higher values of total organic carbon (TOC) were measured in the upper levels of the shallow cambisols AX, AZ and CZ, which range from 9.0 to 10.6%. TOC contents in the upper levels of deep cambisol CX and deep neoluvisol EZ vary from 6.1 to 7.3%, respectively. Soil EX contains the lowest TOC values corresponding to 3.4% for the upper level and a mean value of 1.2% for the entire solum profile. All soils are highly decarbonated. Mineral-carbon contents are very low and range only from 0.1 to 0.5%. Mean pH values vary from neutral (6.3) in cambisol AX to slightly acidic in the other cambisols and neoluvisols (5.1–5.9).

As for TOC, high cation-exchange capacity (CEC) values were measured in the upper levels of shallow soils AX, AZ, CZ (19.4 cmol·kg^{-1}). They slightly diminish down section (up to 12.9). CEC values in the deep soils (CX, EX and EZ) are high in the upper levels (7.9, 17.3 and 14.8 cmol·kg^{-1}, respectively), decrease in the middle levels (3.0–7.5 cmol·kg^{-1}) and rise up again in the deeper levels (11.5–16.5 cmol·kg^{-1}).

The C/N ratio is rather uniform in the shallow soils varying from 9.8 to 13.4, with higher values in the upper levels. The C/N values in the deep soils diminish in a very moderate way with soil depth (from 13.5 to 7.7). The middle levels (h4, h5 and/or h6) contain the lowest C/N values in the soil profile.

Calcium contents are generally low in the soil profiles, and especially in the cambic-neoluvisols, they average only 2.0 g·kg^{-1}, whereas in the shallow soils, they average is in the narrow 4–7 g·kg^{-1} range. Iron and aluminium have a rather uniform distribution along the six profiles with mean values of 44.5 g·kg^{-1} and 26 g·kg^{-1}, respectively. Manganese contents are low (0.6–2.5 g·kg^{-1}).

Table 4.2 Main chemical properties of the six studied soils

Soil	Level	Depth	TOC	C_{min}	pH	CEC	C/N	Ca	Fe	Al	Mn
		(cm)	(%)	(%)		(cmol·kg^{-1})		(g·kg^{-1})*			
Eutric cambisol (humic) ***Soil code: AX***	**AX h1**	2.5	9.6	0.4	6.3	19.2	13.4	7.0	45.3	21.5	2.1
	AX h2	10.5	5.4	0.4	6.0	16.7	11.2	5.2	48.3	20.1	2.4
	AX h3	22.5	4.5	0.3	6.2	17.0	11.0	5.6	48.9	20.2	2.3
	AX h4	33.5	2.9	0.3	6.8	17.1	9.8	6.0	48.1	26.1	2.3
Eutric cambisol (leptic, humic) ***Soil code: AZ***	**AZ h1**	1.5	10.6	0.4	6.0	19.4	11.9	5.9	36.3	25.2	1.7
	AZ h2	6.5	5.4	0.3	5.6	12.8	10.7	3.8	40.9	28.0	1.5
	AZ h3	11.5	5.0	0.3	5.7	13.7	12.1	4.3	40.0	24.8	1.5
	AZ h4	16.5	4.9	0.3	6.0	19.8	10.5	14.3	47.2	15.3	1.9
Eutric-dystric cambisol (calcic) ***Soil code: CX***	**CX h1**	2.5	7.3	0.4	5.9	14.8	10.8	3.2	38.4	28.3	1.7
	CX h2	10.5	3.9	0.3	5.3	7.2	8.2	1.9	41.3	26.3	1.7
	CX h3	18.5	2.9	0.2	5.3	5.3	10.1	1.7	41.1	28.1	1.4
	CX h4	26.5	1.7	0.2	5.2	5.0	9.5	1.3	42.7	25.0	1.6
	CX h5	34.5	0.9	0.2	5.3	7.0	8.0	1.6	44.1	28.9	1.7
	CX h6	42.5	0.7	0.2	5.2	11.5	7.8	1.7	58.1	36.9	1.9
	CX h7	50.5	1.0	0.2	6.4	16.5	8.0	4.6	58.1	37.6	1.7
	CX h8	58.5	0.5	0.1	5.8	15.6	7.7	3.6	47.9	27.2	0.9
Eutric-dystric cambisol ***Soil code: CZ***	**CZ h1**	2.5	9.0	0.5	6.2	19.5	10.3	6.1	40.0	24.7	2.0
	CZ h2	10.5	4.6	0.3	5.7	14.8	11.2	4.0	48.3	25.0	2.6
	CZ h3	18.5	3.3	0.3	5.5	12.9	11.3	4.0	49.2	29.1	2.3
	CZ h4	26.5	2.6	0.3	6.2	14.7	11.9	4.8	47.8	25.9	2.2
Cambic-neoluvisol ***Soil code: EX***	**EX h1**	2.5	3.4	0.2	5.5	7.9	13.5	2.7	34.6	23.5	0.8
	EX h2	10.5	1.9	0.2	5.2	5.5	13.1	1.7	37.6	21.0	0.9
	EX h3	18.5	0.9	0.1	4.8	5.9	10.9	1.2	39.2	25.2	0.6
	EX h4	26.5	0.6	0.1	4.9	6.2	10.4	1.3	40.4	25.5	0.8
	EX h5	34.5	0.7	0.1	5.2	7.3	10.4	1.1	40.2	25.7	1.1
	EX h6	42.5	0.6	0.1	5.0	7.8	8.7	2.1	40.0	24.2	1.0
	EX h7	50.5	0.7	0.1	5.1	10.6	10.5	2.1	43.2	30.3	0.9
	EX h8	58.5	0.7	0.1	5.1	11.5	11.4	1.9	44.4	29.4	0.9
Cambic-neoluvisol ***Soil code: EZ***	**EZ h1**	2.5	6.1	0.3	6.2	17.3	12.8	4.7	37.2	25.5	1.6
	EZ h2	10.5	1.1	0.2	5.3	4.8	10.3	1.4	46.6	26.7	2.5
	EZ h3	18.5	1.1	0.2	4.9	3.0	12.4	1.3	42.6	23.4	2.1
	EZ h4	26.5	0.8	0.2	5.0	3.8	11.7	1.1	44.5	23.9	1.9
	EZ h5	34.5	0.8	0.2	4.9	4.7	9.9	1.2	46.4	26.5	1.8
	EZ h6	43.0	0.9	0.2	5.1	7.5	9.2	1.7	49.0	26.5	2.1
	EZ h7	53.0	1.3	0.2	5.1	12.3	9.8	2.9	53.4	33.0	2.0
	EZ h8	64.0	1.6	0.2	5.2	12.5	10.8	2.8	52.7	32.1	1.9

* = Concentration in g·kg^{-1} of the element extracted by concentrated HNO_3

TOC = Total organic carbon

C_{min} = Mineral carbon

CEC = Cation exchange capacity

C/N = Ratio between total organic carbon and total nitrogen

Table 4.3 Cadmium and selected trace metals concentrations in the six soils

Soil	Level	Cd		Zn		Pb		Cr		Ni		Cu	
		(mg·kg^{-1})											
		1	2	1	2	1	2	1	2	1	2	1	2
Eutric cambisol (humic) *Soil code: AX*	**AX h1**	**5.3**	**6.7**	**491.7**	**3.3**	**57.9**	**1.2**	**92.7**	**1.9**	48.1	1.0	25.9	0.6
	AX h2	5.7	7.1	495.8	3.3	61.7	1.2	94.3	1.9	48.9	1.0	24.2	0.6
	AX h3	5.4	6.7	503.3	3.4	51.1	1.0	96.1	1.9	48.3	1.0	19.2	0.5
	AX h4	5.4	6.7	540.8	3.6	48.2	1.0	104.1	2.1	50.0	1.0	16.8	0.4
Eutric cambisols (leptic, humic) *Soil code: AZ*	**AZ h1**	**7.3**	**9.1**	**683.2**	**4.6**	49.4	1.0	**97.4**	**1.9**	30.2	0.6	12.9	0.3
	AZ h2	6.2	7.8	758.7	5.1	64.1	1.3	113.1	2.3	35.6	0.7	10.3	0.3
	AZ h3	6.5	8.1	696.4	4.6	53.2	1.1	105.6	2.1	35.5	0.7	19.0	0.5
	AZ h4	10.2	12.7	862.3	5.7	54.8	1.1	124.2	2.5	46.4	0.9	13.4	0.3
Eutric-dystric cambisol (calcic) *Soil code: CX*	**CX h1**	**4.4**	**5.5**	**654.5**	**4.4**	49.6	1.0	**93.7**	**1.9**	34.8	0.7	11.8	0.3
	CX h2	4.3	5.3	643.7	4.3	49.8	1.0	95.2	1.9	33.5	0.7	11.9	0.3
	CX h3	2.6	3.3	641.2	4.3	43.9	0.9	95.3	1.9	35.9	0.7	9.0	0.2
	CX h4	2.8	3.4	586.9	3.9	45.6	0.9	87.1	1.7	33.6	0.7	12.4	0.3
	CX h5	4.0	5.0	659.0	4.4	45.4	0.9	99.9	2.0	39.1	0.8	10.8	0.3
	CX h6	9.3	11.6	914.9	6.1	46.0	0.9	133.4	2.7	55.7	1.1	14.0	0.4
	CX h7	16.3	20.4	939.1	6.3	45.1	0.9	149.1	3.0	54.0	1.1	13.4	0.3
	CX h8	7.7	9.7	631.1	4.2	34.2	0.7	110.0	2.2	44.2	0.9	12.7	0.3
Eutric-dystric cambisol *Soil code: CZ*	**CZ h1**	**6.1**	**7.7**	**626.9**	**4.2**	**54.7**	**1.1**	**81.5**	**1.6**	41.4	0.8	13.5	0.3
	CZ h2	5.2	6.5	614.9	4.1	48.0	1.0	86.5	1.7	43.6	0.9	12.1	0.3
	CZ h3	5.9	7.3	686.6	4.6	46.5	0.9	92.2	1.8	48.8	1.0	16.4	0.4
	CZ h4	6.6	8.2	679.3	4.5	36.4	0.7	89.1	1.8	56.0	1.1	16.4	0.4
Cambic-neoluvisol *Soil code: EX*	**EX h1**	0.6	0.7	**166.9**	**1.1**	39.8	0.8	52.4	1.0	33.1	0.7	10.5	0.3
	EX h2	0.4	0.5	133.3	0.9	27.9	0.6	50.6	1.0	34.7	0.7	8.4	0.2
	EX h3	0.3	0.4	146.0	1.0	22.9	0.5	59.9	1.2	42.0	0.8	10.9	0.3
	EX h4	0.6	0.7	165.0	1.1	21.6	0.4	58.2	1.2	49.5	1.0	13.6	0.3
	EX h5	1.3	1.6	156.0	1.0	28.2	0.6	55.1	1.1	53.6	1.1	14.5	0.4
	EX h6	1.3	1.6	170.0	1.1	24.1	0.5	55.4	1.1	50.9	1.0	16.6	0.4
	EX h7	1.6	2.0	178.9	1.2	27.9	0.6	65.6	1.3	60.3	1.2	24.1	0.6
	EX h8	1.2	1.5	169.6	1.1	23.8	0.5	65.7	1.3	57.0	1.1	16.8	0.4
Cambic-neoluvisol *Soil code: EZ*	**EZ h1**	**2.5**	**3.2**	**367.2**	**2.4**	46.5	0.9	**74.5**	**1.5**	31.2	0.6	10.6	0.3
	EZ h2	2.7	3.4	518.2	3.5	39.7	0.8	78.4	1.6	42.5	0.9	8.9	0.2
	EZ h3	1.5	1.9	382.2	2.5	35.0	0.7	69.6	1.4	34.2	0.7	11.0	0.3
	EZ h4	1.5	1.8	466.8	3.1	32.0	0.6	69.3	1.4	37.1	0.7	7.3	0.2
	EZ h5	2.4	3.0	504.3	3.4	36.7	0.7	73.4	1.5	42.7	0.9	9.4	0.2
	EZ h6	4.9	6.2	528.9	3.5	31.8	0.6	76.2	1.5	48.2	1.0	10.6	0.3
	EZ h7	8.2	10.2	671.5	4.5	35.1	0.7	101.8	2.0	58.4	1.2	11.5	0.3
	EZ h8	6.5	8.1	638.1	4.3	35.9	0.7	112.1	2.2	52.7	1.1	17.5	0.4

1 = Concentration in mg·kg^{-1}of metal extracted by concentrated HNO$_3$

2 = Comparative ratio between the metal concentration in soil and the corresponding official guideline value for non-polluted soils: Cd = 0.8 mg·kg^{-1}; Zn = 150 mg·kg^{-1}; Pb = 50 mg·kg^{-1}; Cr = 50 mg·kg^{-1}; Ni = 50 mg·kg^{-1}; Cu = 50 mg·kg^{-1}. Ratios with values higher than 1.0 in the first level (topsoil) of the profiles appear in bold.

4.3.3 Cadmium and trace-metal concentrations in soils and rocks

HNO_3-extractable concentrations of Cd, Zn, Pb, Cr, Ni and Cu are summarized in Table 4.3. In general, the shallow cambisols display higher concentrations in Cd and other trace metals, whereas the deeper cambic-neoluvisols and especially sample site EX contain lower Cd and trace-metal contents.

Ratios comparing the measured concentrations of Cd and trace metals to their respective guideline values were calculated for each sampled level and appear next to each element in Table 4.3. According to these ratios, Cd concentrations in most topsoils, i.e, first level, are significantly higher than its indicative guideline value of 0.8 mg·kg^{-1} (OSol, 1998). Cd contents exceed seven to nine times the guideline value in all measured levels of the shallow cambisols and even 13 times in the deepest level of soil AZ. The deeper cambisol CX shows a Cd concentration, which is 20 times higher than the guideline value. The deep cambic-neoluvisols and the four higher levels of soil EX display Cd contents lower than 0.8 mg·kg^{-1}, whereas their lower levels contain concentrations that surpass two to ten times the official indicative value. This is also valid for all sampled levels in soil EZ.

With the exception of soil EX, the measured Zn concentrations are anomalously high in all soils, and values exceed three to five times the indicative guideline value of 150 mg·kg^{-1} for Zn in soils (OSol, 1998). The measured concentrations of Cr surpass two to three times the guideline value of 50 mg·kg^{-1} for Cr (OSol, 1998). Soil EX shows Zn and Cr concentrations in its deeper horizons, which are 1.1 and 1.3 times higher than their guideline values, respectively. Pb concentrations in the upper horizons of the shallow cambisols are somewhat higher (1.3 times) than the corresponding Pb guideline value of 50 mg·kg^{-1} (OSol, 1998). No anomalous values have been observed for Ni and Cu.

Figure 4.7 shows the vertical evolution of Cd contents in the six soil profiles. As observed in Table 4.3, shallow cambisols AZ, AX and CZ present the highest Cd contents. These soils do not exactly match the Cd concentrations predicted in the spatial variability map established by Okopnik (1997; Figure 4.2c). Soil AZ presents the highest Cd contents (10 mg·kg^{-1}) for shallow soils at a maximum depth of 18 cm. This profile is situated in the zone considered as the hotspot with predicted concentrations of 16 mg·kg^{-1}. As for soil CX, the concentrations found in topsoil and in the middle part match the predicted Cd concentrations of the map quite well. Cd contents increase, however, with soil depth reaching the highest record of 16 mg·kg^{-1}. Cambic-neoluvisol EX presents the lowest Cd contents all along its profile as it was sampled in a zone with rather low Cd concentrations (Figure 4.2c). The maximum Cd concentration was measured in the subsoil with a value of 1.6 mg·kg^{-1}. The Cd distribution profile of soil EZ is analogous in shape to that of soil CX but with lower concentrations. The highest Cd concentration in the subsoil amounts to 8.2 mg·kg^{-1}. Figures 4.8 and 4.9 displays the chemical gradients of Zn and Cr along the studied solums showing a comparable vertical distribution with that of Cd. A more detailed interpretation of their correlation is given in the discussions.

HNO_3-extracted concentrations of trace metals and major elements in rocks and mineral aggregates are presented in Table 4.4. The bedrock of soils AZ and CX contain similar concentrations for all trace metals with the exception of Cu. Mean concentrations correspond to 1.5 mg·kg^{-1} for Cd, 75.4 mg·kg^{-1} for Zn, 0.4 mg·kg^{-1} for Pb, 11.2 mg·kg^{-1} for Cr and 0.8 mg·kg^{-1} for Cu. The bedrock of soils AX and CZ display Cd contents of 0.3 mg·kg^{-1} and 1.1 mg·kg^{-1}, respectively. Major elements are rather uniformly distributed in all bedrock samples with mean Ca contents of 371 g·kg^{-1}.

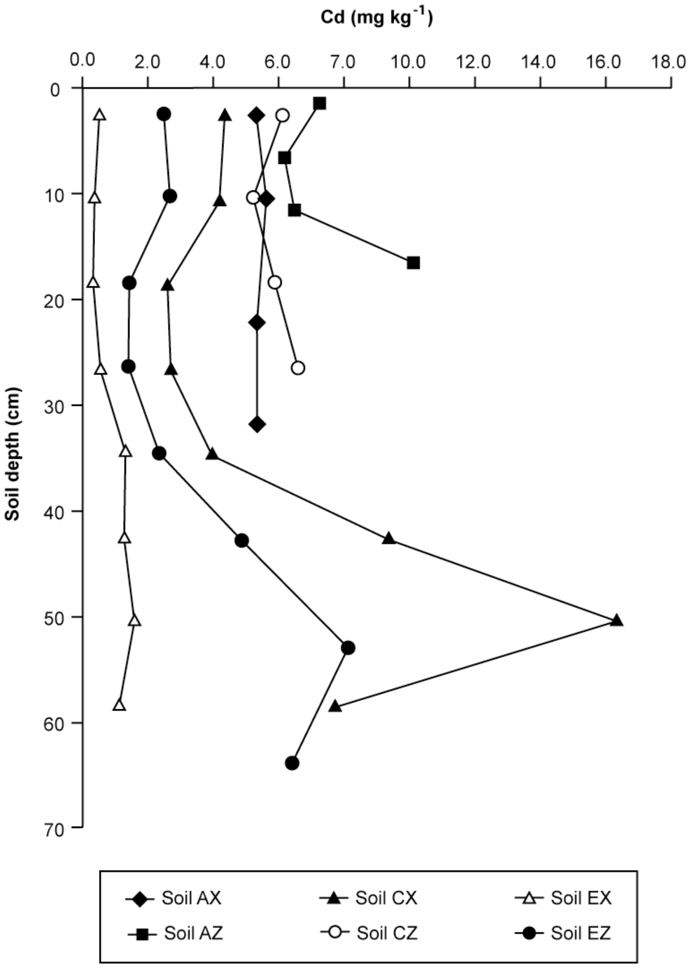

Figure 4.7 Vertical distribution profiles of Cd in the six studied soils.

Mineral aggregates display trace-metal and major-element concentrations, which greatly differ from those of the bedrock. Cd was not detected in aggregates of soil EX while those of soil EZ contain the highest Cd concentration (3.5 mg·kg^{-1}). Fe, Al and Mn contents are also higher in aggregates of soil EZ (2.4 g·kg^{-1}, 1.8 g·kg^{-1} and 1.0 g·kg^{-1}, respectively). The two samples show very low Ca contents (0.2 g·kg^{-1}and 0.7 g·kg^{-1}).

Table 4.4 Concentration of trace metals and major elements in bedrocks and mineral aggregates

Rock	Trace elements						Major elements			
	Cd	Zn	Pb	Cr	Ni	Cu	Ca	Fe	Al	Mn
	(mg·kg^{-1})						(g·kg^{-1})			
Bedrock AX	0.3	45.7	4.3	13.0	11.7	0.1	379.5	0.2	0.1	0.1
Bedrock AZ	1.5	74.6	0.4	12.1	9.6	0.8	364.4	0.4	0.2	0.1
Bedrock CX	1.5	76.2	0.4	10.3	15.0	0.7	366.4	0.1	0.2	0.1
Bedrock CZ	1.1	53.1	1.8	10.4	10.9	1.8	375.0	0.3	0.1	0.1
Mineral aggregates EX	< 0.02	14.9	3.1	4.0	2.1	1.4	0.7	0.7	1.0	0.1
Mineral aggregates EZ	3.5	50.3	4.7	7.4	7.6	1.4	0.2	2.4	1.8	1.0

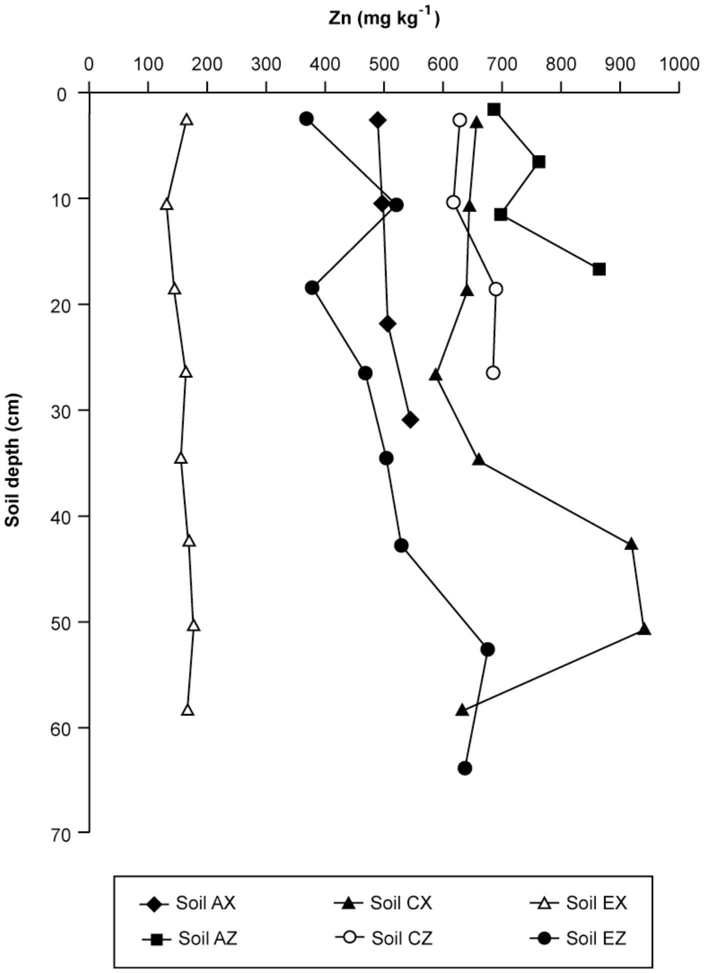

Figure 4.8 Vertical distribution profiles of Zn in the six studied soils.

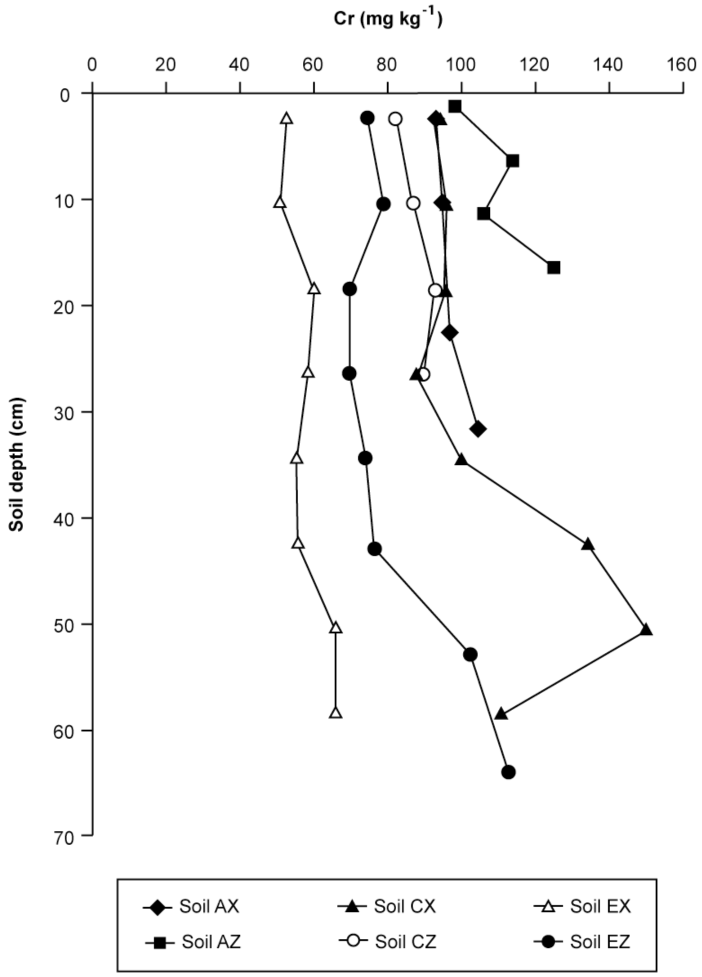

Figure 4.9 Vertical distribution profiles of Cr in the six studied soils.

4.3.4 Soil and rock mineralogies

Soils

The results of bulk-sample analyses of the mineralogy of soils are presented in Table 4.5. The main minerals show a rather uniform distribution regardless of the soil type. Quartz is the mineral with the highest percentage content reaching mean values of 44–51%, followed by the non-quantified compounds (which comprise poorly-crystallized minerals, amorphous compounds and organic matter; 22–36%). Phyllosilicates are present on an average level of 15% and goethite displays low values of 2%. All soils contain K-feldspar (2%) and plagioclase (2–8%). Calcite contents are below the detection limits of the X-ray diffraction method.

Table 4.6 resumes the measured clay-mineral distributions in soils. They display a quite high variability along all soil profiles. The fine-silt fractions (2–16 μm) are generally rich in chlorite with mean values between 31 and 44%, kaolinite (33–44%) and mica (19–30%).

Table 4.5 Distribution of main minerals in bulk-sample analyses of soils

Soil	Level	Bulk rock						
		Phyllo-silicates	Quartz	K-Feldspar	Plagioclase	Calcite	Goethite	Non-quantified
					(%)			
Eutric cambisol (humic) *Soil code: AX*	**AX h1**	7.6	34.3	1.2	1.3	< 0.1	0.0	55.6
	AX h2	23.7	55.0	1.1	3.0	< 0.1	3.8	13.4
	AX h3	8.7	38.1	3.8	1.9	< 0.1	1.7	45.9
	AX h4	15.9	50.3	2.5	1.1	< 0.1	1.6	28.7
	Mean	*14.0*	*44.4*	*2.1*	*1.8*	--	*1.8*	*35.9*
Eutric cambisol (leptic, humic) *Soil code: AZ*	**AZ h1**	13.8	40.9	2.0	2.2	< 0.1	1.8	39.4
	AZ h2	19.0	50.8	2.4	3.0	< 0.1	2.0	22.8
	AZ h3	13.9	60.3	6.4	10.8	< 0.1	2.3	6.4
	AZ h4	16.4	50.0	1.6	4.7	< 0.1	1.8	25.5
	Mean	*15.8*	*50.5*	*3.1*	*5.2*	--	*2.0*	*23.5*
Eutric-dystric cambisol (calcic) *Soil code: CX*	**CX h1**	9.2	39.8	3.6	28.3	< 0.1	2.3	16.7
	CX h2	9.8	47.7	1.9	1.5	< 0.1	2.1	37.0
	CX h3	10.7	69.2	1.6	4.0	< 0.1	2.9	11.7
	CX h4	15.2	67.0	2.5	3.9	< 0.1	1.9	9.5
	CX h5	11.9	62.2	2.5	3.0	< 0.1	2.4	17.9
	CX h6	15.2	30.9	2.7	17.4	< 0.1	2.2	31.6
	CX h7	13.2	39.2	1.0	2.3	< 0.1	4.2	40.1
	CX h8	19.0	62.1	1.9	0.9	< 0.1	2.5	13.7
	Mean	*13.0*	*52.3*	*2.2*	*7.7*	--	*2.6*	*22.3*
Eutric-dystric cambisol *Soil code: CZ*	**CZ h1**	16.1	47.2	1.5	0.9	< 0.1	2.5	31.8
	CZ h2	13.7	48.2	2.9	3.0	< 0.1	1.8	30.4
	CZ h3	12.5	37.0	2.5	2.7	< 0.1	2.1	43.2
	CZ h4	21.7	64.3	2.2	3.1	< 0.1	4.2	4.6
	Mean	*16.0*	*49.2*	*2.3*	*2.4*	--	*2.6*	*27.5*
Cambic-neoluvisol *Soil code: EX*	**EX h1**	15.0	51.4	1.2	1.5	< 0.1	1.4	29.5
	EX h2	19.0	47.5	3.0	2.3	< 0.1	2.8	25.4
	EX h3	10.7	39.0	1.9	2.9	< 0.1	0.0	45.5
	EX h4	14.6	48.1	2.0	2.1	< 0.1	1.4	31.8
	EX h5	18.8	52.6	2.0	3.3	< 0.1	1.3	22.0
	EX h6	15.1	58.9	1.8	5.3	< 0.1	2.2	16.7
	EX h7	10.8	35.5	2.3	2.1	< 0.1	0.0	49.2
	EX h8	13.4	49.3	1.9	2.0	< 0.1	1.8	31.6
	Mean	*14.7*	*47.8*	*2.0*	*2.7*	--	*1.4*	*31.5*
Cambic-neoluvisol *Soil code: EZ*	**EZ h1**	9.6	44.8	2.0	2.3	< 0.1	2.2	39.1
	EZ h2	16.3	51.4	2.4	1.9	< 0.1	1.1	27.0
	EZ h3	12.5	37.8	2.1	1.9	< 0.1	1.5	44.2
	EZ h4	9.4	47.6	1.5	2.3	< 0.1	1.6	37.5
	EZ h5	17.6	51.4	2.6	3.3	< 0.1	0.0	25.1
	EZ h6	19.6	40.9	1.4	4.5	< 0.1	1.4	32.1
	EZ h7	12.5	45.6	1.2	1.4	< 0.1	1.5	37.9
	EZ h8	15.2	48.6	1.8	1.4	< 0.1	1.9	31.1
	Mean	*14.1*	*46.0*	*1.9*	*2.4*	--	*1.4*	*34.2*

Table 4.6 Distribution of minerals in the fine-silt (2–16 µm) and clay (<2 µm) fractions of soils

Soil	Level	Fine-Silt (2–16 µm)			Clays (<2 µm)				
		Chlorite	Kaolinite	Mica	Chlorite	Kaolinite	Mica	IS-B	IS-N
			(%)				(%)		
Eutric cambisol (humic) *Soil code: AX*	**AX h1**	25.8	37.7	36.5	18.7	50.2	14.6	8.8	7.8
	AX h2	33.2	40.2	26.6	14.2	67.4	8.9	6.4	3.1
	AX h3	29.1	44.0	26.9	10.5	56.7	11.0	11.9	9.9
	AX h4	34.8	34.7	30.5	14.1	62.8	11.2	7.8	4.1
	Mean	*30.7*	*39.2*	*30.1*	*14.4*	*59.3*	*11.4*	*8.7*	*6.2*
Eutric cambisol (leptic, humic) *Soil code: AZ*	**AZ h1**	65.5	34.5	0.0	22.2	39.6	9.4	21.7	7.2
	AZ h2	48.7	37.3	14.0	27.4	47.8	6.2	12.2	6.4
	AZ h3	47.6	31.8	20.6	23.8	45.5	7.5	19.2	4.0
	AZ h4	12.8	65.0	22.2	26.1	46.4	7.2	12.0	8.3
	Mean	*43.7*	*42.1*	*18.9*	*24.9*	*44.8*	*7.6*	*16.3*	*6.5*
Eutric-dystric cambisol (calcic) *Soil code: CX*	**CX h1**	35.2	39.7	25.1	16.7	49.4	15.5	11.6	6.8
	CX h2	39.3	32.9	27.9	21.2	47.7	9.5	16.1	5.5
	CX h3	39.2	34.7	26.1	21.6	45.4	11.5	15.3	6.2
	CX h4	42.3	31.4	26.4	23.1	39.1	13.3	19.4	5.1
	CX h5	45.6	35.2	19.2	17.0	35.6	16.8	20.9	9.7
	CX h6	37.5	28.4	34.0	19.8	34.3	14.6	25.2	6.1
	CX h7	35.2	42.6	22.2	17.9	29.8	13.7	32.4	6.2
	CX h8	18.0	54.8	27.3	11.1	38.9	15.3	25.0	9.8
	Mean	*36.5*	*37.5*	*26.0*	*18.5*	*40.0*	*13.8*	*20.7*	*6.9*
Eutric-dystric cambisol *Soil code: CZ*	**CZ h1**	36.9	40.5	22.5	20.8	51.1	10.8	12.4	4.8
	CZ h2	29.0	43.2	27.9	16.5	56.0	9.9	13.0	4.7
	CZ h3	28.5	47.0	24.5	15.2	57.7	11.2	12.8	3.1
	CZ h4	30.0	46.1	23.9	15.8	59.0	12.1	8.2	5.0
	Mean	*31.1*	*44.2*	*24.7*	*17.1*	*55.9*	*11.0*	*11.6*	*4.4*
Cambic-neoluvisol *Soil code: EX*	**EX h1**	38.2	37.6	24.2	15.3	48.3	17.1	16.4	2.9
	EX h2	17.4	65.4	17.2	17.2	52.0	14.7	12.7	3.5
	EX h3	40.2	35.1	24.7	13.2	43.6	12.8	27.9	2.5
	EX h4	40.8	31.8	27.4	14.9	40.5	17.1	25.0	2.7
	EX h5	38.3	29.3	32.4	16.0	42.6	21.6	17.6	2.1
	EX h6	35.5	17.7	46.8	19.7	48.1	17.2	12.5	2.5
	EX h7	18.9	56.6	24.6	16.9	45.1	21.9	12.6	3.5
	EX h8	38.3	27.3	34.3	16.8	38.9	20.5	20.5	3.5
	Mean	*33.5*	*37.6*	*28.9*	*16.2*	*44.9*	*17.9*	*18.1*	*2.9*
Cambic-neoluvisol *Soil code: EZ*	**EZ h1**	38.2	28.9	32.9	18.5	53.7	16.8	8.6	2.4
	EZ h2	41.1	32.2	26.6	16.3	41.3	15.5	24.0	2.9
	EZ h3	38.0	40.5	21.6	16.3	38.1	14.2	28.4	2.9
	EZ h4	45.0	28.8	26.2	15.8	41.6	15.3	23.9	3.4
	EZ h5	33.8	44.1	22.1	17.0	36.2	18.5	24.2	4.1
	EZ h6	45.3	28.9	25.9	20.4	41.1	18.8	14.7	5.0
	EZ h7	50.3	24.4	25.4	15.5	36.9	20.4	17.3	9.9
	EZ h8	41.7	32.1	26.2	15.1	40.9	17.4	23.6	3.0
	Mean	*41.7*	*32.5*	*25.8*	*16.9*	*41.2*	*17.1*	*20.6*	*4.2*

IS-B = Pedogenic intergrades; IS-N = Normal illite-smectite mixed layers

The clay fractions (<2 µm) show kaolinite as the major mineral (41–59%), followed by chlorite (16–25%), and pedogenic intergrades IS-B (9–21%). Mica content varies from 8 to 14% in shallow cambisols and is around 17.5% in deep neoluvisols. Normal illite-smectite mixed layers (IS-N) contents are higher in cambisols (6.5%) than in neoluvisols (2–4%).

Rocks

Mineralogical results obtained from bulk-rock analyses of the bedrock and mineral aggregates, are summarized in Table 4.7. Bedrock samples display mean calcite contents of 98% and very low contents of non-quantified compounds (which comprise poorly-crystallized minerals, amorphous compounds and organic matter) ranging from 0.2 to 1.0%. In all rock samples, the contents of phyllosilicates, goethite and quartz are below detection limits. Neither feldspar nor plagioclase was detected. The mineral distribution of the aggregates found in the two deep cambic-neoluvisols is different from the bedrock samples. No calcite contents were detected but instead, important contents of quartz (60%) and of non-quantified compounds (38%) were measured.

Table 4.7 Distribution of minerals in bulk-rock samples (bedrocks and mineral aggregates)

Rock	Phyllosilicates	Quartz	K-Feldspar	Plagioclase	Calcite	Goethite	Non-quantified
				(%)			
Bedrock AX	< 0.3	3.9	< 0.2	< 0.2	96.0	< 0.2	0.0
Bedrock AZ	< 0.3	< 0.1	< 0.2	< 0.2	99.8	< 0.2	0.2
Bedrock CX	< 0.3	< 0.1	< 0.2	< 0.2	99.0	< 0.2	1.0
Bedrock CZ	< 0.3	0.6	< 0.2	< 0.2	98.7	< 0.2	0.8
Mineral aggregates EX	2.1	59.6	< 0.2	< 0.2	< 0.1	< 0.2	38.3
Mineral aggregates EZ	1.6	60.6	< 0.2	< 0.2	< 0.1	< 0.2	37.8

Non-quantified = Organic matter, clay-humus complex + amorphous compounds and poorly crystallized minerals e.g. Fe, Mn-oxyhydroxides

Table 4.8 Distribution of minerals in the fine silt (2–16 µm) and clay (<2 µm) fractions of bedrocks and mineral aggregates

Rock	Fine silt (2–16 um)			Clays (<2um)				
	Chlorite	Kaolinite	Mica	Chlorite	Kaolinite	Mica	IS-B	IS-N
		(%)				(%)		
Bedrock AX	ND	79.1	20.9	ND	28.7	37.7	19.9	13.7
Bedrock AZ	ND	80.5	19.5	ND	26.4	44.1	15.0	14.5
Bedrock CX	ND	87.2	12.8	ND	41.8	37.4	10.7	10.1
Bedrock CZ	ND	76.7	23.3	ND	17.9	45.2	30.1	6.9
Mineral aggregates EX	ND	55.4	44.6	ND	52.4	17.8	17.3	12.5
Mineral aggregates EZ	ND	ND	ND	ND	52.1	15.4	17.7	14.8

ND = Non detected
IS-B = Pedogenic intergrades
IS-N = Normal illite-smectite mixed layers

Clay-mineral distributions in the bedrocks are presented in Table 4.8. The fine-silt fractions (2–16 µm) in the bedrock of cambisols show kaolinite as the major mineral whose contents range from 76.7 to 87.2%. Mica contents vary between 12.8 and 23.3%. Chlorite is absent in all rock samples. The clay fraction (<2 μm) in bedrock displays mica as the most abundant mineral (37.4–45.2%). Kaolinite contents amount up to 41.8%. Pedogenic intergrades (IS-B) vary between 10.7 and 30.1%, and the normal illite-smectite mixed layers (IS-N) between 6.9 and 13.7%.

As observed before, the mineral aggregates of the two deep soils present a rather different distribution of clay minerals. The fine-silt fraction contains 55.4% kaolinite, which is lower than the contents found in bedrock, and 44.6% mica. The clay fraction contains 50% kaolinite, 17% IS-B, 16% mica and 13% IS-N.

4.3.5 Sequential extraction analyses of cadmium and trace-metal distributions

Sequential extraction analyses of Cd and trace-metal distributions were performed within the first five cm of the topsoils and within the 16 or 25 cm of the subsoil (depending on maximal soil depth) of the shallow soil profiles AX and AZ. As for the deeper soil profiles EX and EZ, the extractions were applied in the topsoils (5 cm), middle levels (25 cm) and subsoils (50 to 55 cm). An additional extraction was carried out on level CX h7 (subsoil) as this level contains the highest Cd concentration (16.3 $mg \cdot kg^{-1}$) recorded in all soils samples.

Shallow cambisols AX and AZ

Overall values and mean weight percent distributions of Cd and trace metals in the shallow cambisols are graphically represented in Figure 4.10 and summarized in Table 4.9.

The Cd distribution changes from the topsoil to the subsoil in these profiles. In the topsoil, Cd appears mainly in the fractions supposedly associated with carbonate (48%) and organic matter (24%), and to a lesser extent in fractions linked to amorphous oxyhydroxides (12%) and crystalline Fe-oxides (11.2%). Small quantities of Cd were extracted from the residual matrix phase (2.7%) and as exchangeable Cd (2%). In the subsoil, Cd is distributed mainly in the amorphous oxyhydroxide (33%) and the carbonate phases (26.4%). Organic matter (21.8%) and crystalline Fe-oxides (16.7%) are the next major Cd-bearing phases. Small fractions are extracted as exchangeable Cd (2%) and from the residual phase (2%).

Unlike Cd, the selected trace metals Zn, Pb, Cr, Ni and Cu have distributions in the bearing phases that do not considerably change along the soil profile. Zn, Cr, Ni and Cu were mainly extracted from the residual fraction. Crystalline Fe-oxides represent the second major phase hosting Zn and Ni, and organic matter is the second major phase for Cr and Cu. All four trace metals show low contents in association with amorphous oxyhydroxides and carbonate. The exchangeable fraction also produced small concentrations of Cr and Ni while Zn was not detected in this fraction. Pb appears with a rather different distribution compared to the other trace metals, as it was principally extracted from the fractions bound to crystalline Fe-oxides and amorphous oxyhydroxides. Organic matter and residual matrix are the next major fractions. Like the other trace metals, low Pb contents were obtained in the carbonate fraction.

Table 4.9 Mean percent distribution of cadmium and selected trace metals in soils AX and AZ

Fraction	Mean Percent Distribution (%)											
	Cd		Zn		Pb		Cr		Ni		Cu	
	Topsoil	Subsoil	Topsoil	Subsoil	Topsoil	Subsoil	Topsoil	Subsoil	Topsoil	Subsoil	Topsoil	Subsoil
F1 Exchangeable	1.9	0.0	0.0	0.0	0.0	0.4	0.2	0.7	0.7	0.1	2.4	0.6
F2 Carbonates	48.1	26.4	1.1	0.0	1.1	1.3	0.5	0.7	1.9	0.7	0.8	3.4
F3 Organic Matter	24.1	21.8	12.0	10.1	24.0	13.2	30.1	29.3	10.5	6.9	28.5	23.5
F4 Am. Oxyhydroxides	12.0	33.0	2.8	2.4	20.7	31.1	1.3	1.7	6.2	5.1	2.3	3.2
F5 Cryst. Fe oxides	11.2	16.7	22.8	21.3	39.3	37.5	7.5	19.1	25.9	14.0	26.3	26.4
F6 Residue	2.7	2.1	61.3	66.1	14.9	16.4	60.4	48.5	54.8	73.2	39.7	42.8
Recovery (%)	101.7	97.1	101.0	100.4	101.5	103.6	84.4	94.9	106.7	251.5	90.6	117.6

Table 4.10 Mean percent distribution of cadmium and selected trace metals in soils EX and EZ

Fraction	Mean Percent Distribution (%)								
	Cd			Zn			Pb		
	Topsoil	Middle	Subsoil	Topsoil	Middle	Subsoil	Topsoil	Middle	Subsoil
F1 Exchangeable	5.5	10.8	15.3	0	0.1	0	0	2.3	0
F2 Carbonates	40.2	7.4	14.8	0.4	0.9	0.3	6	5.8	1.5
F3 Organic Matter	20.1	7.4	12.5	20.1	23	22.2	29.1	16.5	15.8
F4 Am. Oxyhydrox	16.4	37.9	32.4	1.7	0.8	0.7	32	44.4	29.7
F5 Cryst. Fe oxides	16.5	27.6	23.6	31.8	27.2	16.2	32.9	29.7	40.8
F6 Residue	1.3	8.9	1.4	46.1	48.1	60.6	0	1.2	12.2
Recovery (%)	97	109.7	89.7	87.6	83.7	98.3	91.3	99.2	83.2

Fraction	Mean Percent Distribution (%)								
	Cr			Ni			Cu		
	Topsoil	Middle	Subsoil	Topsoil	Middle	Subsoil	Topsoil	Middle	Subsoil
F1 Exchangeable	0	0	0	0	0.2	0.1	2	3.7	1.2
F2 Carbonates	0	0	0	1.4	0.8	0.7	2.7	5.9	0.2
F3 Organic Matter	39.4	48.2	60.3	14.8	19.3	20.4	36.8	25	23.1
F4 Am. Oxyhydrox	1.6	1.8	1.7	3.3	2	2.9	3.9	7.6	2.6
F5 Cryst. Fe oxides	1.2	3.3	11.2	31.4	30.3	23.4	32.1	31.4	27.2
F6 Residue	57.9	46.7	26.8	49.1	47.4	52.5	22.4	26.2	45.8
Recovery (%)	69.3	63.3	57.3	93.5	92.7	92.7	93.2	107.1	88.6

Cambic-neoluvisols EX and EZ

Trace-metal distributions within the extracted phases of the cambic-neoluvisols are graphically presented in Figure 4.11 and summarized in Table 4.10.

Cd in the cambic-neoluvisols has a distribution similar to that of the shallow cambisols; Cd in the topsoil appears mainly bound to carbonate (40%), and subsequently to organic matter (20%), crystalline Fe-oxides (16.5%) and amorphous oxyhydroxides (16.4%). Rather small percentages of Cd were extracted from the exchangeable (5.5%) and residual fractions (1.3%). In the deeper horizons, its distribution changes and amorphous oxyhydroxides become the major Cd-bearing phase (38%), followed by crystalline Fe-oxides (28%). Cd contents bound to carbonate and organic matter decrease in the middle part to a value of 7.4% for both fractions and rise again in the subsoil to 14.8 and 12.5%, respectively. As a general rule, the proportion of exchangeable Cd increases with soil depth, 10.8% in the middle part up to 15.3% in the subsoil.

In the cambic-neoluvisols, Zn has a distribution, which is quite different from the one found in shallow cambisols: in the topsoil, it occurs principally in the residual fraction and bound to carbonate. Small quantities were extracted in the other four fractions. With regards to the middle of the profiles and the subsoil, most of Zn is linked to the residual fraction and the amorphous oxyhydroxides, followed by Fe-oxides. Small percentages of Zn were obtained from the carbonate and organic-matter fractions. As for Cd, the exchangeable Zn gradually increases in the deeper levels.

In the topsoil, Pb appears mostly bound to crystalline oxides, amorphous oxyhydroxides and organic matter. In the middle part and in the subsoil, the Pb distribution remains very similar, albeit with a diminution in the organic-matter phase while small quantities appear in the residual fraction.

Throughout the cambic-neoluvisol profiles, Cr has a distribution similar to the cambisols. It is mainly bound to organic matter and the residual fraction. Cr bound to organic matter increases with depth while its occurrence in the residual fraction decreases. No exchangeable Cr was found in these soils.

Ni is mainly extracted in the residual fraction followed by the Fe-oxides and the organic-matter fractions. Its distribution remains uniform along the soil profiles. Small quantities are bound to amorphous oxyhydroxides. No exchangeable Ni was extracted.

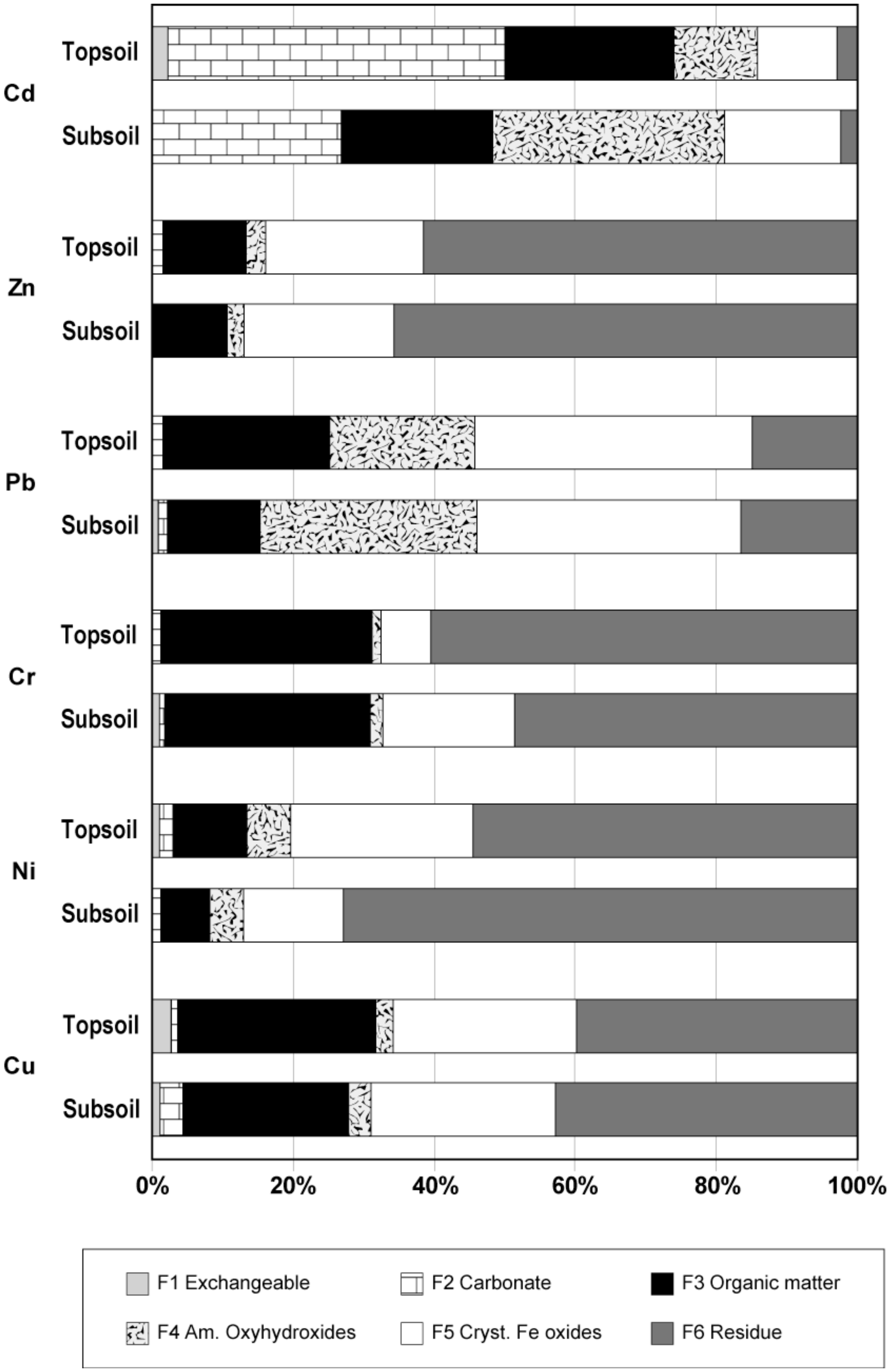

Figure 4.10 Mean percent distribution of Cd and selected trace elements extracted in shallow cambisols AX and AZ soils.

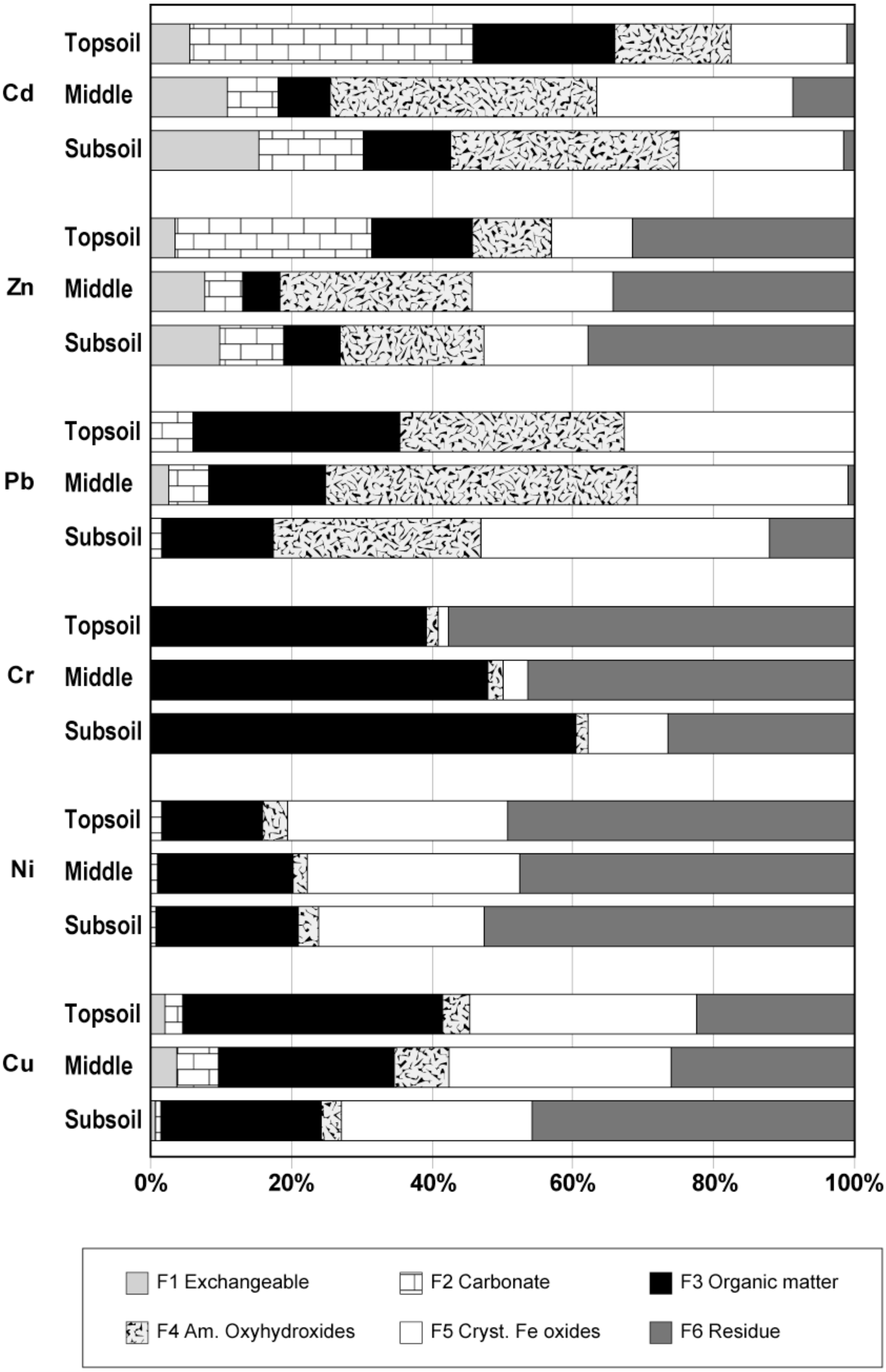

Figure 4.11 Mean percent distribution of Cd and selected trace elements extracted in deep cambic-neoluvisols EX and EZ.

Cu appears in organic-matter, crystalline Fe-oxides and in the residual fraction. The quantities of Cu bound to the mineral matrix are higher in the deeper horizons. In the topsoil and the middle horizons, small quantities are found in the exchangeable phase and bound to carbonate.

Deep Cambisol CX

Sequential extraction results for sample CX h7 are presented in Table 4.11. Cd is mainly extracted in the fractions corresponding to amorphous oxyhydroxides (40%), carbonate (26%), crystalline Fe-oxides (14.5%) and organic matter (11.6%). Low values were extracted for exchangeable Cd (3.3%) and the residual fraction (4.6%).

Table 4.11 Mean percent distribution of cadmium and selected trace metals in soil CX at the level CX h7

Fraction	Mean Percent Distribution (%)					
	Cd	Zn	Pb	Cr	Ni	Cu
	Subsoil					
F1 Exchangeable	3.3	0.6	0.0	1.3	0.6	4.5
F2 Carbonates	26.1	0.4	4.3	0.0	1.1	1.0
F3 Organic Matter	11.6	13.0	18.3	30.2	15.8	25.9
F4 Am. Oxyhydrox	39.9	1.5	33.3	1.5	4.3	4.9
F5 Cryst. Fe oxides	14.5	12.6	29.0	14.6	20.2	26.0
F6 Residue	4.6	71.9	15.1	52.3	58.0	37.6
Recovery (%)	96.5	93.1	99.1	82.6	99.8	103.6

4.3.6 Correlation and multivariable analyses

The following 24 variables were considered for the principal component analyses: trace metals: Cd, Zn, Pb, Cr, Ni and Cu; soil chemical properties: TOC, C_{min}, pH, CEC; major elements: Ca, Fe, Mn and Al; and the soil mineral distributions: bulk rock, fine-silt (2–16 μm) and clay (<2 μm) fractions. Figures 4.12 through 4.16 show the correlation circles used to represent the association of all the studied variables. Six principal components are necessary to explain 76.5 % of the cumulative variance of the geochemical system. An inner circle with a radius of 0.75 units has been placed as a limiting barrier to assure a good criterion to select only significant variables with correlation coefficients equal or higher than 0.75. Table 4.12 provides a summary of the identified principal components with the corresponding percentages of explained variance and the association of variables along their positive and negative extremes.

Table 4.12 Principal components identification explaining the variables of the entire geochemical system of the six studied soils

Component	Variance (%)	Cumulated Variance (%)	Variables as positive loads	Variables as negative loads	Geochemical information in the soil system
PC1	26.74	26.7	TOC, Cmin; pH, CEC, Ca, Pb	Mica (<2)	Soil main chemical properties, unweathered mica in clay fraction
PC2	17.29	44.0	Depth, Fe, Al	C/N	Influence of soil depth
PC3	11.76	55.8	Chl (2–16) (coeff coef. < 0.75)	--	Possibly allochthonous compounds in silt fraction
PC4	9.37	65.2	Quartz, Phyllosilicates	Non-quantified	Crystalline and amorphous minerals
PC5	6.21	71.4	Kaolinite (2–16)	--	Fine silt fraction
PC6	5.17	76.5	K-feldspars, Na-Plagioclase	--	Allochthonous compounds

The correlation circles show Cd, Zn and Cr positively correlated and grouped in a cluster whose projection remains relatively constant when combining the six principal axes. Figure 4.12 shows this cluster located at 45° between the positive extremes of the first and the second principal components (PC 1 and PC2). The first principal component (PC1) presents positive loads distributed in two main clusters of variables. The first cluster contains TOC and C_{min}; the second cluster contains pH, CEC, Ca and Pb. This component presents also a negative load of mica from the clay fraction (Mic(<2) in Figure 4.12). The distributions along this axis remain constant when compared to the other principal components. The second principal component (PC 2) is loaded on its positive extreme with soil depth, Fe and to some extent Al, while its negative side is loaded with the C/N ratio.

Concerning the correlation circles of the remaining four principal components, it is observed that Cd, Zn and Cr remain close to another and that their cluster appear orthogonal to the most significant variables represented by each principal component. An orthogonal projection implies that no correlation there exists between the involved variables. The third principal component (PC 3) does not present significant loads of any variable. Nevertheless, both chlorites from the fine-silt fraction (Chl (2–16)) and from the clay fraction (Chl (<2)) slightly lean towards the positive side of this component (Figure 4.13). The fourth principal component (PC 4) bears quartz (Qtz) and phyllosilicates as positive loads while the non-quantified compounds (N-Q) appear as a negative load (Figure 4.14). The fifth principal component (PC 5) contains positive loads of kaolinite from the silt fraction (Kao (2–16) in Figure 4.15). Finally, the sixth principal component (PC 6) presents K-feldspar and Na-plagioclase on its negative side (Figure 4.16).

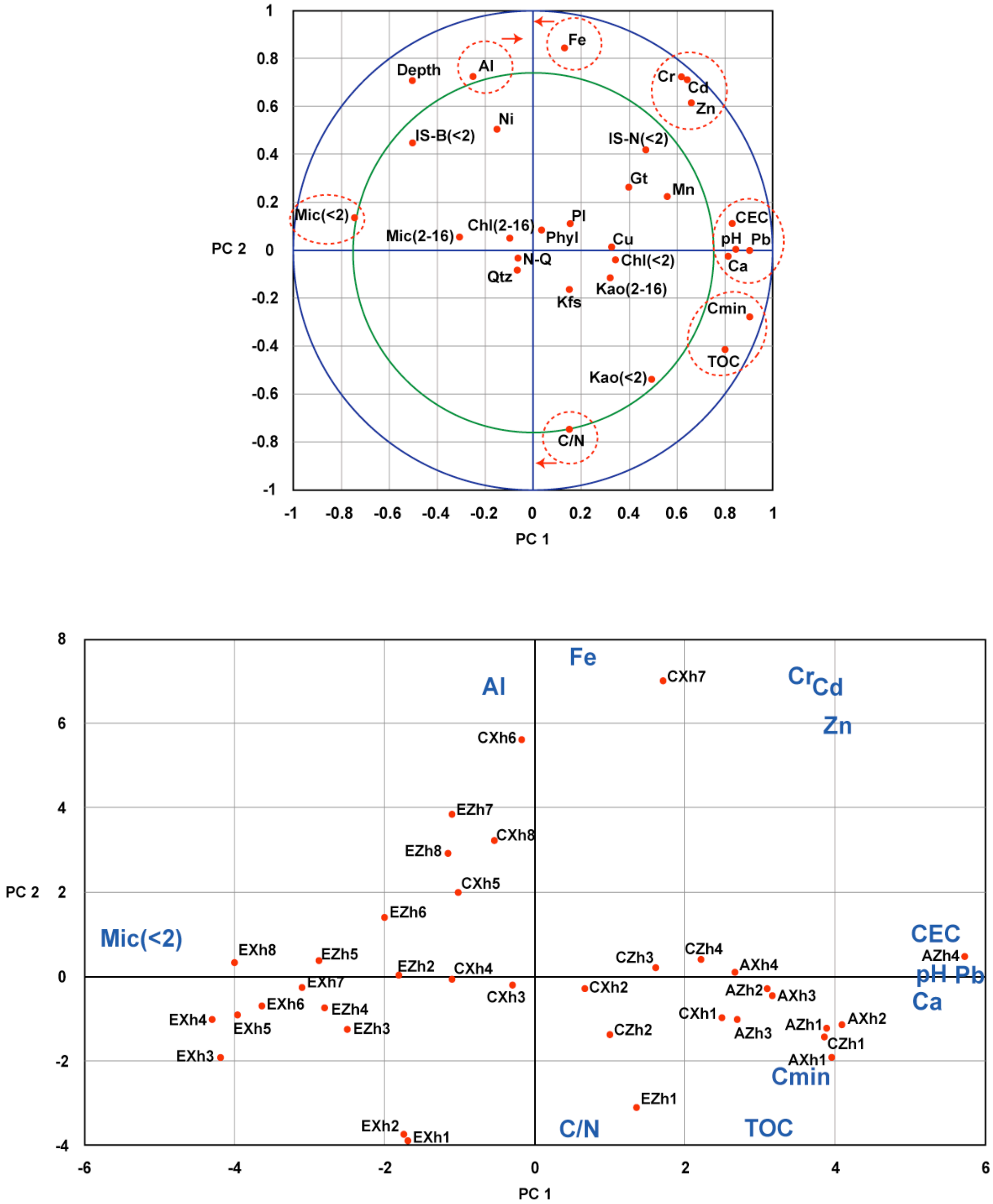

Figure 4.12 Correlation circles of the 30 variables studied and scatter plot of the 36 sampled soil-levels projected on principal components.

Projection of the first and the second principal components (PC 1 vs. PC 2).

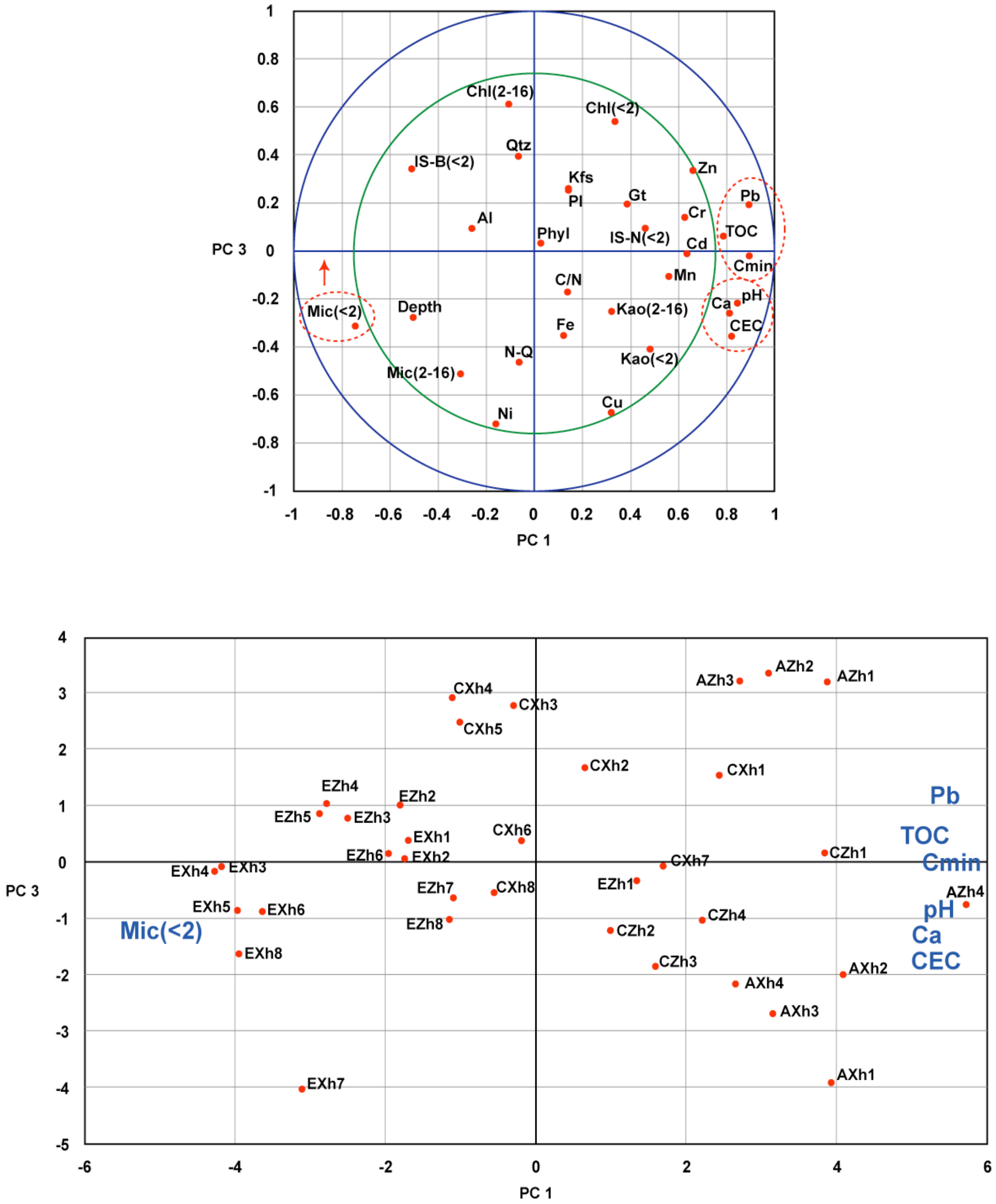

Figure 4.13 Correlation circles of the 30 variables studied and scatter plot of the 36 sampled soil-levels projected on principal components.
Projection of the first and third principal components (PC 1 vs. PC 3).

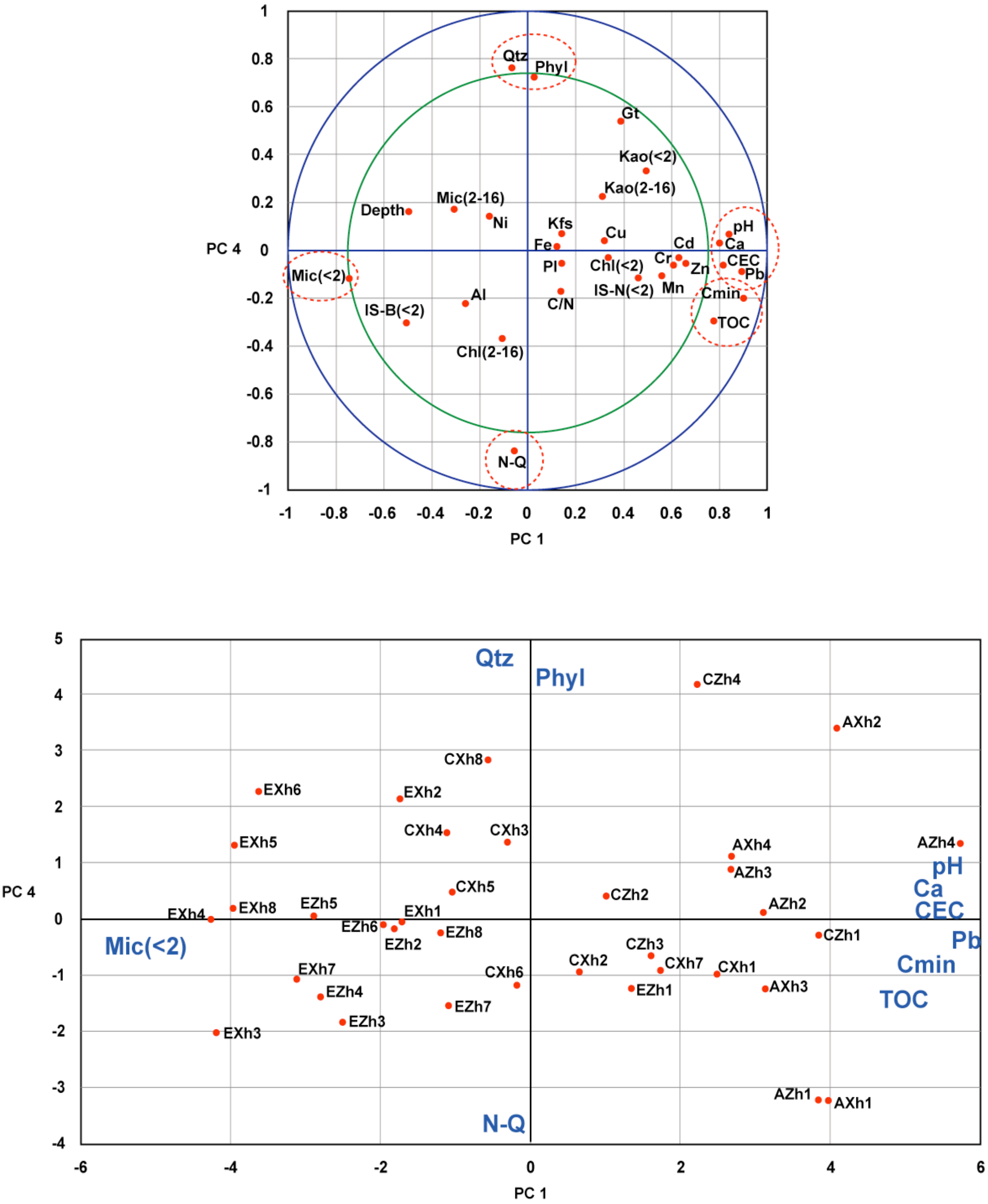

Figure 4.14 Correlation circles of the 30 variables studied and scatter plot of the 36 sampled soil-levels projected on principal components.

Projection of the first and fourth principal components (PC 1 vs. PC 4).

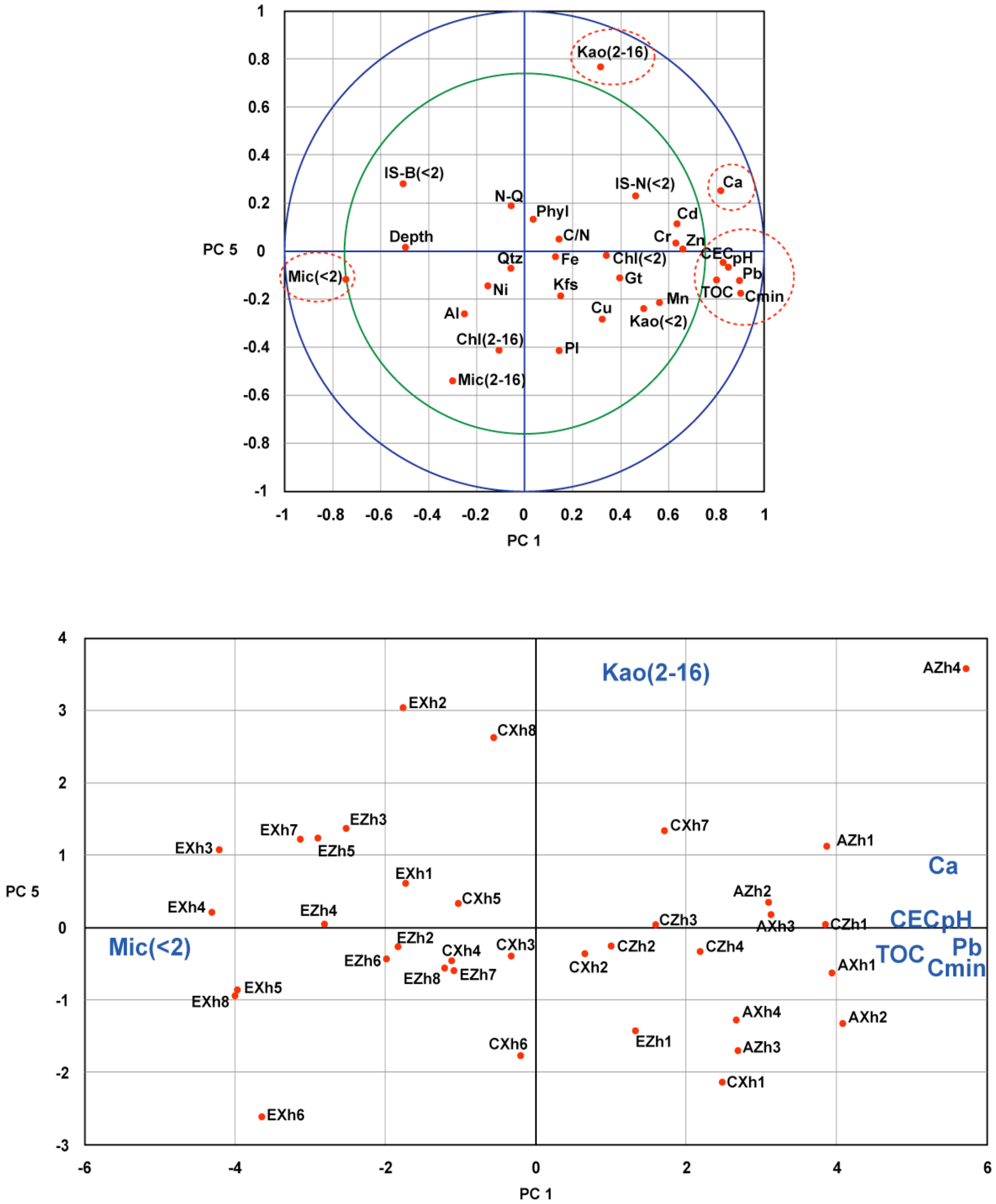

Figure 4.15 Correlation circles of the 30 variables studied and scatter plot of the 36 sampled soil-levels projected on principal components.

Projection of the first and fifth principal components (PC 1 vs. PC 5).

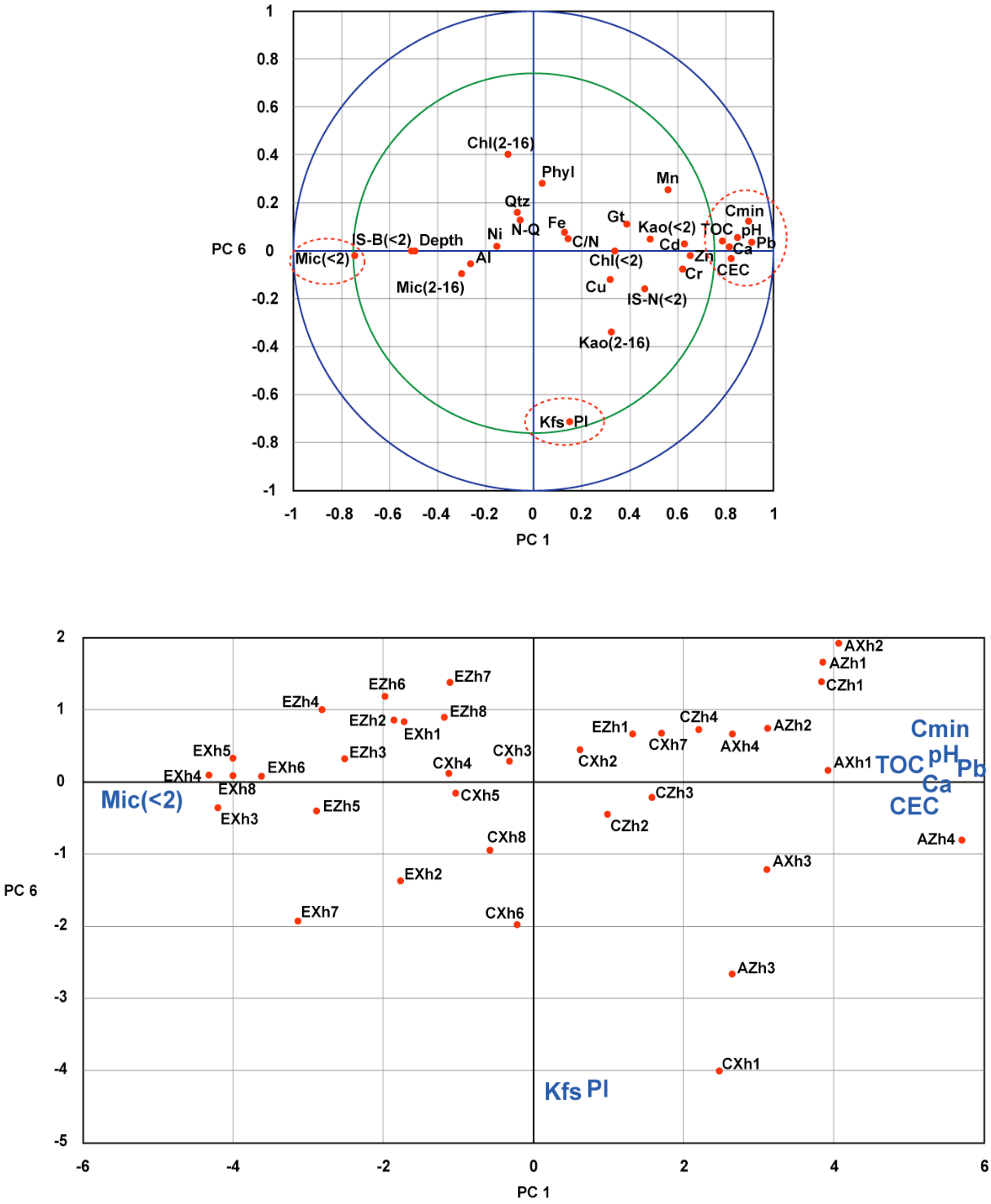

Figure 4.16 Correlation circles of the 30 variables studied and scatter plot of the 36 sampled soil-levels projected on principal components.

(e) Projection of the first and sixth principal components (PC 1 vs. PC 6)

4.3.7 Multiple linear regressions

14 out of 24 variables were identified as potential predictors: TOC, C_{min}, pH, CEC, C/N, Ca, Fe, Al, Mn, Gt, Kao(<2), Mic(<2), IS-B, IS-N. The variables considered to have an aeolian origin: Chl(2–16), Kao(2–16), Mic(2–16), Chl (<2), Qtz, K-feldspar and Na-plagioclase were discarded for this analyse since none of the trace metals showed any correlation to allochthonous minerals (see the chapter "discussions and interpretations" for a more detailed discussion). The non-quantified compounds were not considered either because the identification of their chemical composition and the exact Cd-bearing compound is not possible. In addition, the non-quantified, poorly crystallized compounds do not show any correlation to Cd as it can be observed in the corresponding correlation circle (Figure 4.14). The resulting models for Cd are presented in Table 4.13 and are discussed below.

Table 4.13 Multiple linear regression models for Cd

Proposed Model for Cd	S	R^2	$R^2_{(adj)}$
Cd = -17.7 + 0.978 Ca + 0.406 Al + 0.187 Fe	1.51	81.5	79.8
Cd = -15.2 + 0.829 Gt + 0.729 Ca + 0.366 TOC + 0.232 Al + 0.223 Fe + 0.126 IS-B - 0.333 C/N	0.98	93.2	91.5

S = Standard deviation; R^2 = Coefficient of determination; $R^2_{(adj)}$ = Adjusted coefficient of determination

4.4 DISCUSSION AND INTERPRETATION

4.4.1 4.1 Soils descriptions and assessment of allochthony

The mineralogical analyses of the soil profiles (Table 4.6) reveal the presence of important quantities of chlorite both in the fine-silt fraction (40% approximately) as well as in the clay fraction (14–25%), while no traces of chlorite were found in the bedrocks (Table 4.8). Figures 4.17 and 4.18 provide a general comparison of the mineralogical assemblies of the fine-silt and clay fractions of the sampled levels to that of the corresponding bedrock from soils AX and CX respectively in order to illustrate these observations. As no bedrocks were sampled in soil profiles EX and EZ, it is not possible to present a comparison of rock and soil mineralogies for those sections. Nevertheless, as the studied site is situated on the same geological formation, we infer that the previous observations are also applicable to both cambic-neoluvisol profiles.

Chlorite contents diminish between the fine-silt and the clay fractions. Havlicek (1999) related this to the possible presence of inherited, silt-sized chlorite particles. This material is interpreted to originate from crystalline rocks (granite, gneiss), which was brought to the Jura as an aeolian silt deposit (Pochon, 1978; Havlicek and Gobat, 1996). As no chlorite was found in the underlying rocks, we interpret the fine-silt and clay fractions of the Le Gurnigel soils to include a mixture of detrital phyllosilicates contained in allochthonous loess, “autochthonous” phyllosilicates derived from the underlying bedrock, and authigenic clay minerals formed by weathering and pedogenesis. Chlorite and mica undergo weathering processes leading to the formation of mixed-layered complexes, which are present in the clay fraction (Righi and Meunier, 1995; Havlicek, 1999). These processes explain also the decrease of percentages of chlorite and mica in the clay fraction compared to those of the silt fraction. It is not possible to determine the relative percentages of phyllosilicates derived from the rock substratum and from the allochthonous loess, but given the very pure carbonate composition of the bedrock (Table 4.7), the majority of the phyllosilicates is probably derived from loess. The presence of plagioclase and K-feldspar in soils and their absence in the corresponding bedrocks may also confirm the importance of allochthonous parent material during pedogenesis (Havlicek and Gobat, 1996; Benitez, 1999).

The Le Gurnigel soils are in continuous evolution after an early formation stage on aeolian silt material. Bedrock dissolution continues to provide inherited compounds such as kaolinite and normal illite-smectite mixed layers, while oxyhydroxides and pedogenic intergrades are newly formed. All soils undergo a decarbonation process that takes place along the entire soil profile. Calcium contents are hence quite low in the soils, a situation that favours dispersion of clays and their suspension in solution. Organic matter is mainly present in the topsoil whilst the subsoil is gaining a more structural configuration (brunification process) with the presence and the pedogenic formation of phyllosilicates and Fe-, Al-oxyhydroxides. This observation may explain the decrease of CEC values in the middle of all soil profiles. CEC may be related to the organo-mineral complexes in the upper horizons while it is thought to be related to the presence of clay minerals and oxyhydroxides in the deeper horizons.

Cambisols AX, AZ and CZ are not deeper than 30 cm because of their position on hill flanks. Despite their shallowness, they undergo a brunification process developing thus a structural horizon S rich in Fe and Al minerals. These soils are totally decarbonated. Soil profile CX shows a depth of 60 cm and is located in a rather flat topography allowing it to form a deeper and more developed structural horizon S. Clay illuviation signs are already detected by clay coatings on subsoil particles (Fig 6a) suggesting a possible further pedogenic evolution into a neoluvisol. Rock dissolution is witnessed in the deepest horizon and this process provides fresh mineral compounds.

The two cambic-neoluvisol profiles EX and EZ are located in the accumulation zones or coombs, which are formed by the conjunction of two hillocks. We were unable to measure the total depth of these soils. It is assumed that the underlying bedrock continues to weather while the already formed soil horizons undergo further transformation due to biological activity and mineral leaching. Illuviation processes are identified in the middle levels and consequently clays and Fe and Al oxyhydroxides are transported towards the subsoil.

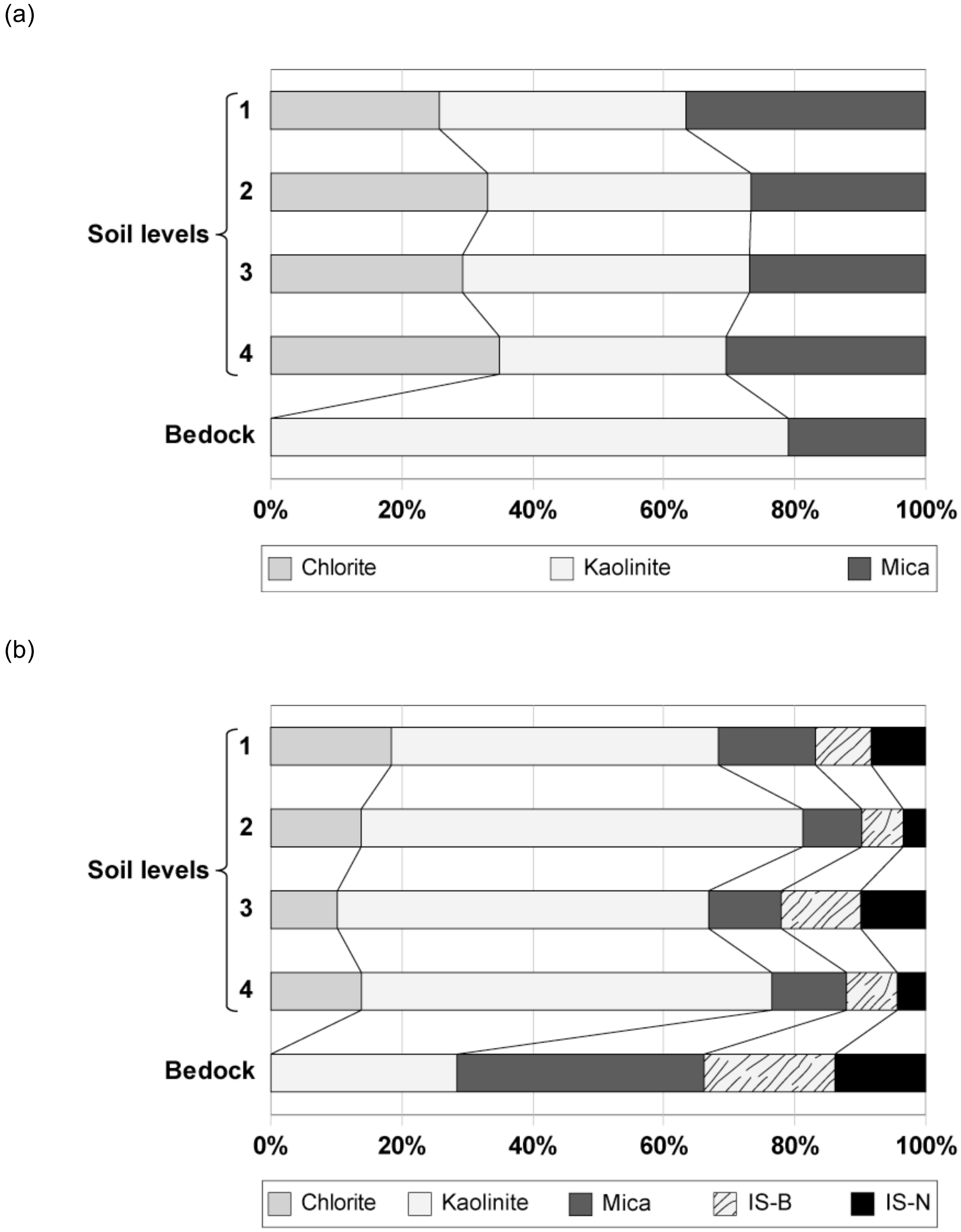

Figure 4.17 Comparison of the mean mineralogical composition of soil and corresponding bedrock. Shallow cambisol AX: (a) Fine-silt fraction (2–16 μm) (b) Clay fraction (<2 μm).

(a)

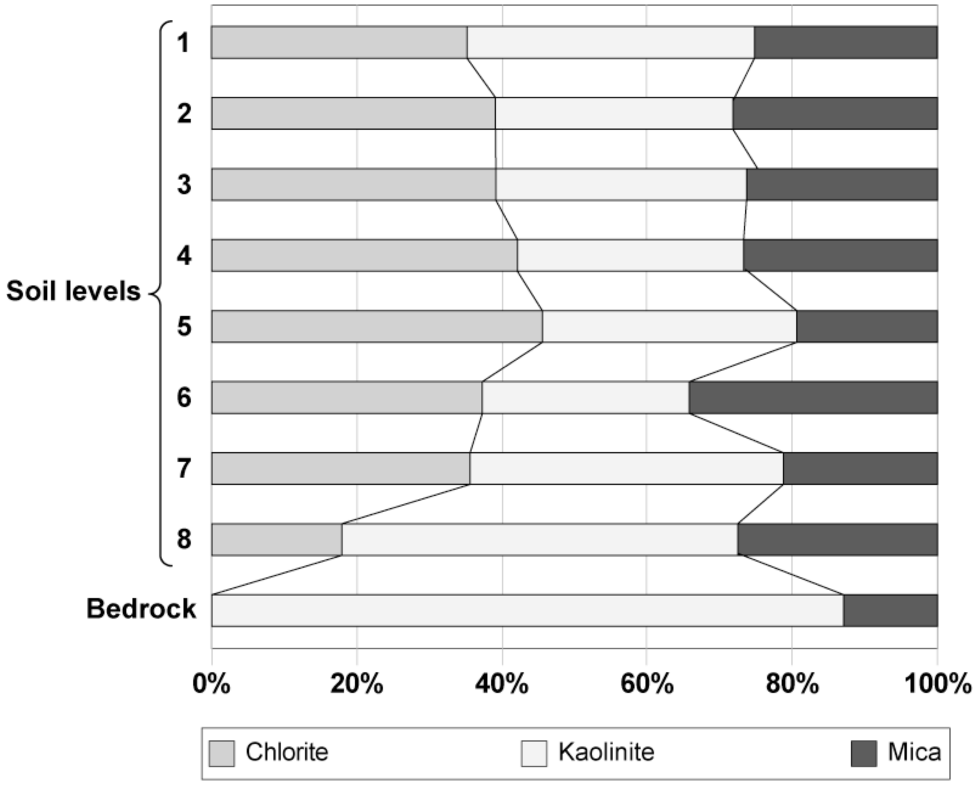

(b)

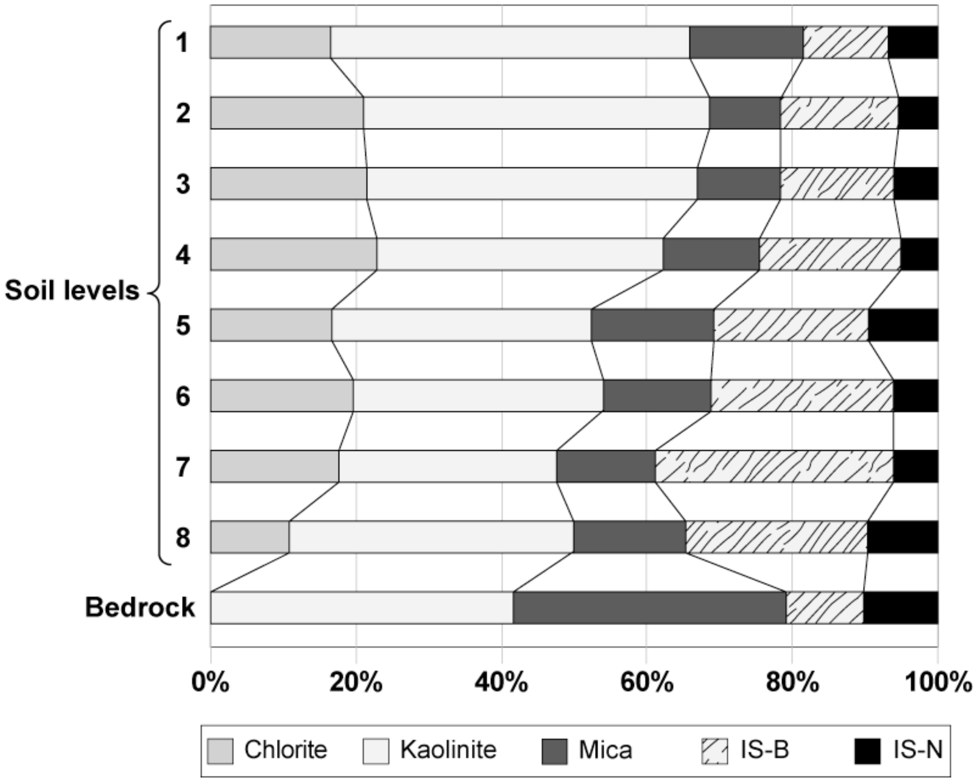

Figure 4.18 Comparison of the mean mineralogical composition of soil and corresponding bedrock. Deep cambisol CX: (a) Fine-silt fraction (2–16 μm); (b) Clay fraction (<2 μm).

As a result of these processes, mineral accretions such as the aggregates found in both soils are formed. These aggregates were identified on the basis of their mineralogical and chemical composition and their coloration. Aggregates in both soils have comparable bulk mineralogies (Table 4.7). Aggregates of soil EX present, however, a rather pale greyish coloration and are richer in phyllosilicates with kaolinite and mica in their silt fraction (Table 4.8), while those of soil EZ have a yellowish-ochre coloration and present higher Fe, Al and Mn contents. According to these observations, the latter were identified as iron-oxyhydroxide concretions. Following Gasparatos et al. (2004), such concretions are likely to be mainly composed of amorphous iron compounds such as poorly crystalline goethite and ferrihydrite whose diffraction patterns are not recognized by the applied XRD method. As such, the iron oxyhydroxides are reported as non-quantified compounds, which amount to 38% of the bulk mineralogy. Similarly, in thin section (Figure 4.6), we observe yellowish coatings on soil particles, which we consider to represent a mixture of clays with Fe-rich amorphous oxides which were formed by illuviation processes. Consequently, a mixture of quartz, phyllosilicates and amorphous oxyhydroxides constitutes the whitish concretions of soil EX. Clay coatings in deeper horizons of soils EX and EZ suggest that both soil sites undergo an evolution into fully developed neoluvisols with the presence of horizons BT in their subsoil.

4.4.2 Dynamics of cadmium in the soil profiles

The increasing Cd concentrations towards the bottom observed in each profile (Figure 4.7) may confirm the geogenic origin of Cd in these soils. The weathering of the underlying Cd-rich carbonates drives the release of Cd and other trace metals, which are subsequently incorporated into the different phases in the corresponding soils. It is assumed that the Cd concentrations in the analysed soil profiles are determined both by Cd concentrations in the underlying bedrock, where it is quite heterogeneously distributed on all scales (Rambeau, 2006; Efimenko et al., submitted), as well as by the physical-chemical properties of soils including depth, chemical composition and mineralogy, and pedogenetic processes. This renders a nonlinear relationship between Cd contents in bedrock and associated soil likely.

Shallow soils AZ, AX and CZ contain Cd, which is mainly distributed in the carbonate phase (48%) and the organic matter phase (24%; Figure 4.10). Care must be taken here as all analysed soils show a high decarbonation state with total carbonate amounts, which are mostly undetected by the applied X-Ray technique. This signifies that the amount of Cd extracted during the carbonate fraction is likely overestimated. Benitez-Vasquez (1999) already observed this problem in non-carbonated soils, and according to him, the acetate extraction step may release Cd bound to the amorphous oxyhydroxides and crystalline Fe-oxides containing 12% and 11% of total Cd, respectively. The amorphous oxyhydroxides become a more important Cd-bearing phase in the subsoil with 33% of the total Cd contents

(Fig 8a). As organic matter is still present in the subsoil, it becomes the third major Cd-bearing phase in the entire shallow cambisol profiles. The extracted quantities of exchangeable Cd and Cd bound to the residual phase are rather low, as was also reported by Benitez-Vasquez (1999).

A comparable Cd distribution is observed in the topsoil of the two cambic-neoluvisols, and especially in soil EZ. In the upper levels most Cd was extracted during the carbonate (40%) and the organic-matter fractions (20%), whereas in the middle part and deeper horizons the amorphous oxyhydroxides and the crystalline Fe-oxides are the most important Cd-bearing phases with mean percentage distributions of 35% and 25%, respectively.

It has been established that Cd is frequently adsorbed on non-crystalline iron oxyhydroxide minerals such as goethite (α-FeOOH), lepidocrocite (γ-FeOOH), akaganeite (β-FeOOH) and schwertmannite ($Fe_8O_8(OH)_6SO_4$), which represent some of the most stable minerals in well-aerated soils (Schwertmann et al., 1989; Randall et al., 1999; Mustafa et al., 2004). Based on this observation, we infer that the iron concretions found in the studied soils have a potential to adsorb and concentrate Cd, which would explain the enrichments in Cd, Fe and Al observed in the deeper BT horizons (Table 4.2). This enrichment in Cd is mainly observed in soil profile EZ, where its deeper levels EZ h6 to EZ h8 show the highest concentrations in Cd with a maximum value of 8.2 $mg\cdot kg^{-1}$ (Table 4.3; Fig 7a) and where associated iron concretions contain a measured Cd concentration of 3.5 $mg\cdot kg^{-1}$ (Table 4.4).

Soil profile CX contains the highest recorded concentration of Cd in its subsoil (16.3 $mg\cdot kg^{-1}$; Table 4.3; Fig 7a). Within this level Cd is both issued by the dissolution of the underlying rock as well as by a mixture of pedogenic processes, which not only distribute Cd towards the solum by biological activity but also translocate it from upper horizons by early clay and oxide illuviation processes during soil evolution. Consequently, amorphous oxyhydroxides, carbonates and crystalline Fe oxides are the three major Cd bearing phases in the subsoil.

As a synthesis of the previous discussions, it is assumed that the decrease in Cd contents in the middle part of deep soil profiles CX, EX, EZ is due to the beginning of eluviation processes with diminishing pH. An incipient horizon E is formed where clays, oxides and hydroxides are leached out and are dragged down the solum along with Cd into the illuviation horizons BT. The mineral phases in this horizon receive also Cd released by the dissolution of the underlying bedrock.

4.4.3 Principal component analyses

The positive correlation of Cd, Zn and Cr observed in the correlation circle of Figure 4.12 suggests that the three elements share information with regard to their distribution in soils that is likely to be controlled both by the CEC and soil pH as well as by Ca, Fe and to some extent by Al contents.

The first principal component (PC 1) represents the main chemical properties of the soils. CEC and pH are closely related since the latter will determine the absolute value of CEC in soils. At low pH values, positive charges are important due to the adsorption of H^+, which produces a high capacity to exchange anions, hence a low CEC. At higher pH values, the charge becomes negative due to adsorption of OH^- or loss of H^+ in solution, producing a high CEC. Trace metals will therefore be mobilised and removed from soils in soluble form at low pH values (Alloway, 1995). High CEC values will assure a higher capacity to retain trace metals in the diverse soil phases.

The relation between Ca and trace metals indicates that Cd, Zn and Cr are a product of carbonate dissolution. After rock weathering, trace metals will compete with Ca for places on newly formed mineral phases in soils such as clays. This observation could certainly explain the negative correlation between Cd, Zn, Cr and mica in the clay fraction Mic (<2), which has not yet been transformed into illite-smectite clays.

Even though the PC 1 carries important information with regards to TOC and C_{min} contents, these two variables appear projected orthogonally to the cluster of Cd, Zn and Cr. This implies that the distributions of these three trace metals in these soils are not primarily or directly controlled by organic-matter contents.

The second principal component (PC 2) comprises the compounds whose presence is mainly characterized by soil depth. On one hand, the C/N ratios are high in the upper horizons as a result of decaying organic matter, which is present in topsoil by the degradation of the biosphere: vegetal tissues due to the plant life cycle and micro and macrofauna. On the other hand, subsoils are rich in Fe-containing oxides, oxyhydroxides and Al-rich minerals (aluminosilicates and probably oxides). Cd, Zn and Cr are likely adsorbed on Fe and Al oxyhydroxydes and vertically distributed along the soil profile by illuviation processes starting in the middle horizons where a decrease in Fe and Al concentrations and the pH values has been observed, followed by an increase in the deepest levels. The scatter distribution of samples in Fig 9c shows how the deep levels h6–h8 of soil profiles CX and EZ lean towards the PC 2 axe. These levels show the highest peak in Cd, Zn and Cr in their respective profiles and also contain high quantities of Fe and Al.

The third principal component (PC 3; Fig 9b) is interpreted to represent the degree of allochthony within the soil profiles and particularly the presence of chlorite in the fine-silt fraction. The presence of allochthonous, aeolian components in the formation of these soils may also be observed in the projections of the fifth principal component (PC 5; Fig 9e), carrying kaolinite (2–16 μm) in the fine silt fraction, and the sixth principal component (PC 6; Fig 9f), which includes K-feldspar and Na-plagioclase. As already mentioned, Cd, Zn and Cr appear grouped and form angles of nearly 90° with all three axes with no significant correlation to all mentioned allochthonous components. The geogenic origin of these elements may hence be confirmed.

The fourth principal component (PC 4) is thought to mirror the distribution of minerals characterized by their degree of crystallinity, with perfectly crystalline quartz and phyllosilicates on one side and poorly crystalline, amorphous compounds on the other side. The cluster of Cd does not present any correlation and remains orthogonal to the variables of PC 4 suggesting that Cd, Zn and Cr are not correlated with any compound of crystalline origin and that these elements are only a product of carbonate rock dissolution. Despite of a lack of correlation with non-quantified components, we cannot neglect their distribution in badly crystalline, amorphous minerals such as the oxyhydroxides as already discussed.

Although the co-occurrence of Cd and Zn is rather common in rocks and soils (Alloway, 1995), the geochemistry of Cr is rather different and no particular association with Cd and Zn would be expected. Cd and Cr may share the same bearing phases such as the Fe oxyhydroxides, and this may explain their strong correlation.

4.4.4 Lateral advection in cambic-neoluvisol EZ

According to the scatter sample distributions in Figures 4.12 and 4.13, the upper level EZh1 in profile EZ leans towards the PC 1 that also contains the group of samples from soils CZ, AX, AZ, and upper levels of soil CX. As PC 1 represents the chemical characteristics of the investigated soils, this may suggest that level EZh1 shares geochemical information (TOC, CEC, pH and major elements contents) and display properties similar to the shallow soils formed on the hill flanks such as soil AZ. It is not excluded that lateral soil advection may take place due to the site topography. The cambic-neoluvisols formed in the accumulation zones are susceptible to receive material from the neighbouring hills. This phenomenon may explain the relatively high Cd concentrations in the upper horizons of these soils. This would imply a complex transfer pattern of Cd for these soils, which starts with the release of Cd from underlying rock, and its transfer into oxide, hydroxide, carbonate and organic phases. Additionally, the lateral advection of Cd-rich soils on top of these soils adds Cd to theses soils, which is transferred from the topsoil towards the deeper horizons by biological and pedogenic processes.

4.4.5 Models based on the principal components analyses

The first regression model presented in Table 4.13 used only the variables that correlated with Cd in the first and second principal components PC 1 and PC 2 circles. Only Ca, Al and Fe presented a significant mathematical fit yielding an acceptable adjusted coefficient of determination $R^2_{(adj)}$ = 79.8%. These three predictors could be related with the mineral phases considered as the main Cd-bearing phases in soils.

A second and a more pretentious regression model has been successfully established by combining the compounds and measured soil properties linked to Ca, Fe and Al that may play a major role in Cd distribution. The model presents a coefficient $R^2_{(adj)}$ = 91.5% which is a good fit of the potential predictors. In this model goethite (Gt) appears with the highest contribution confirming the already discussed adsorption of Cd on iron oxyhydroxides. The Ca contribution may be interpreted as being linked to the dissolution of carbonates releasing Cd into soils. TOC may explain the effect of organic matter, which counts as the third major bearing phase. Iron is likely to represent the adsorption on crystalline Fe-oxides and non-crystalline oxyhydroxides complementing the effect of goethite. Aluminium is likely to explain the effect of both, the organo-clay complex and certainly the aluminosilicates such as the pedogenic intergrades (IS-B), which are also predictors in the regression equation. Finally, the model comprises the negative contribution of the C/N ratio that might explain the plants uptake and biological activity stocking Cd in vegetal tissues and returning it to soil as part of the plant life cycle.

4.4.6 Normalized concentration profiles

In order to support the previous discussions, we applied the method described by Brantley et al. (2007) and generated element concentration profiles which are normalized to the parent rock as a function of depth. The concentrations of mobile elements were normalised to zirconium (Zr), which is considered as a nonreactive and immobile constituent found in both, bedrock and soil. The normalised concentrations are represented as $\tau_{i,j}$ where *i* is the concentration of Zr and *j* that of the mobile trace elements Cd, Zn, Cr and the major elements Ca, Fe, Al, Mn. Figures 4.19 and 4.20 depict the normalised concentrations $\tau_{Zr,j}$ in the soil profiles AX, AZ, CX and CZ. The soil profiles EX and EZ were not considered since it was not possible to sample bedrock in those profiles. As a general rule, Fe, Al and to some extent Mn are the most abundant major elements in the soils whose profiles present strong signs of translocation towards the deeper levels of the subsoil as a clear sign of eluviation-illuviation processes. Ca is completely depleted compared to bedrock in all profiles due to decarbonation and it appears with a constant value $\tau_{Zr,Ca}$= -1.0.

(a)

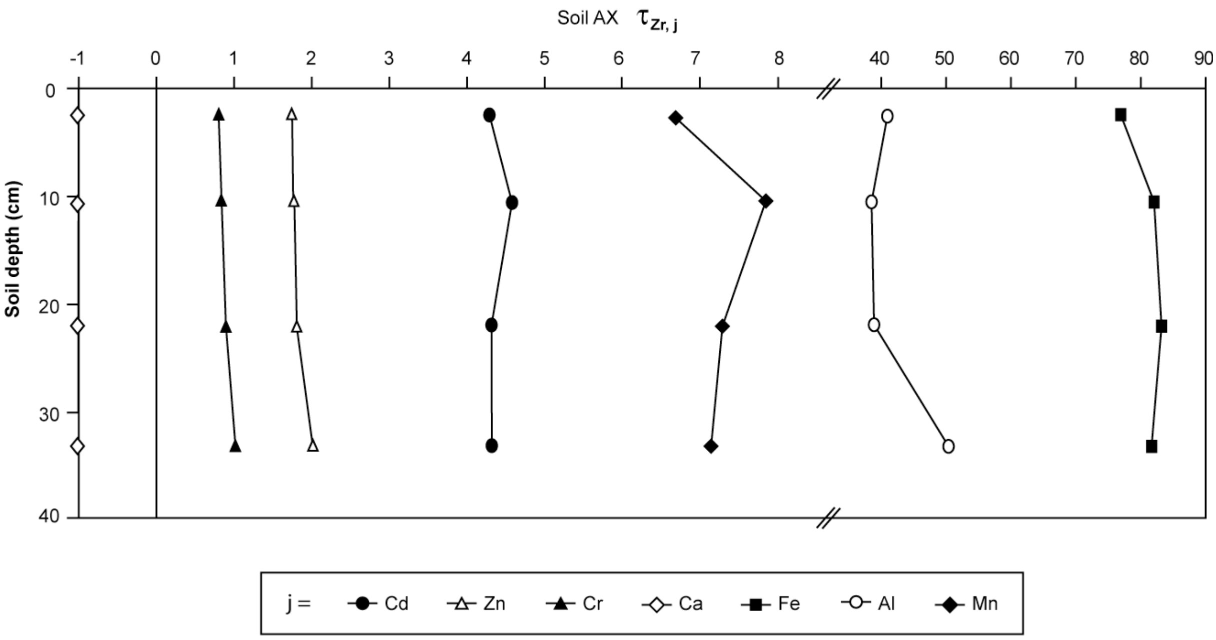
Soil AX $\tau_{Zr, j}$
-1
0
1
2
3
4
5
6
7
8
40
50
60
70
80
90
Soil depth (cm)
0
10
20
30
40
j =
Cd
Zn
Cr
Ca
Fe
Al
Mn

(b)

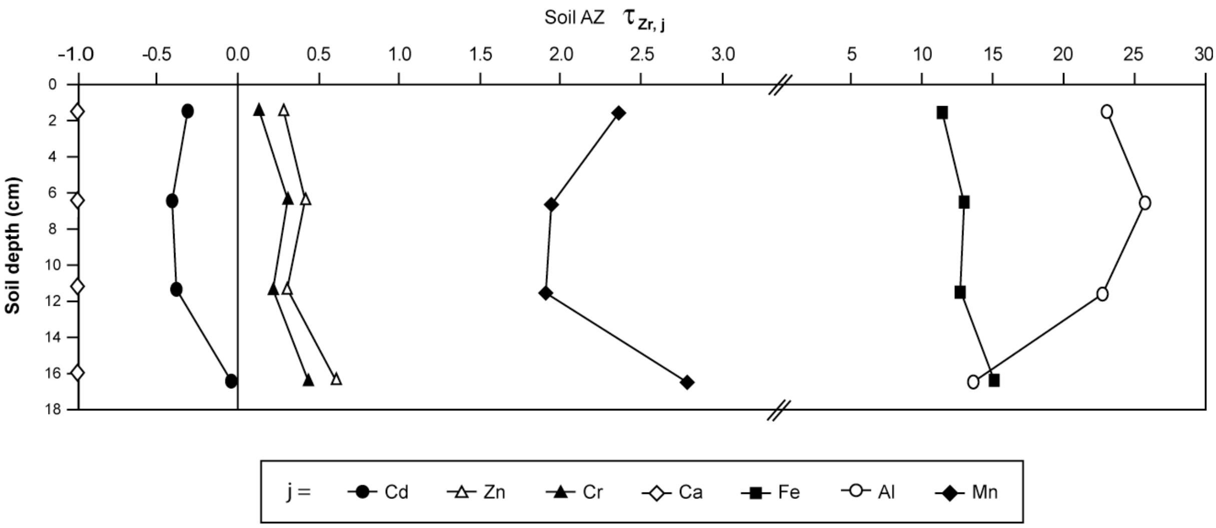
Soil AZ $\tau_{Zr, j}$
-1.0
-0.5
0.0
0.5
1.0
1.5
2.0
2.5
3.0
5
10
15
20
25
30
Soil depth (cm)
0
2
4
6
8
10
12
14
16
18
j =
Cd
Zn
Cr
Ca
Fe
Al
Mn

(Continued)

(c)

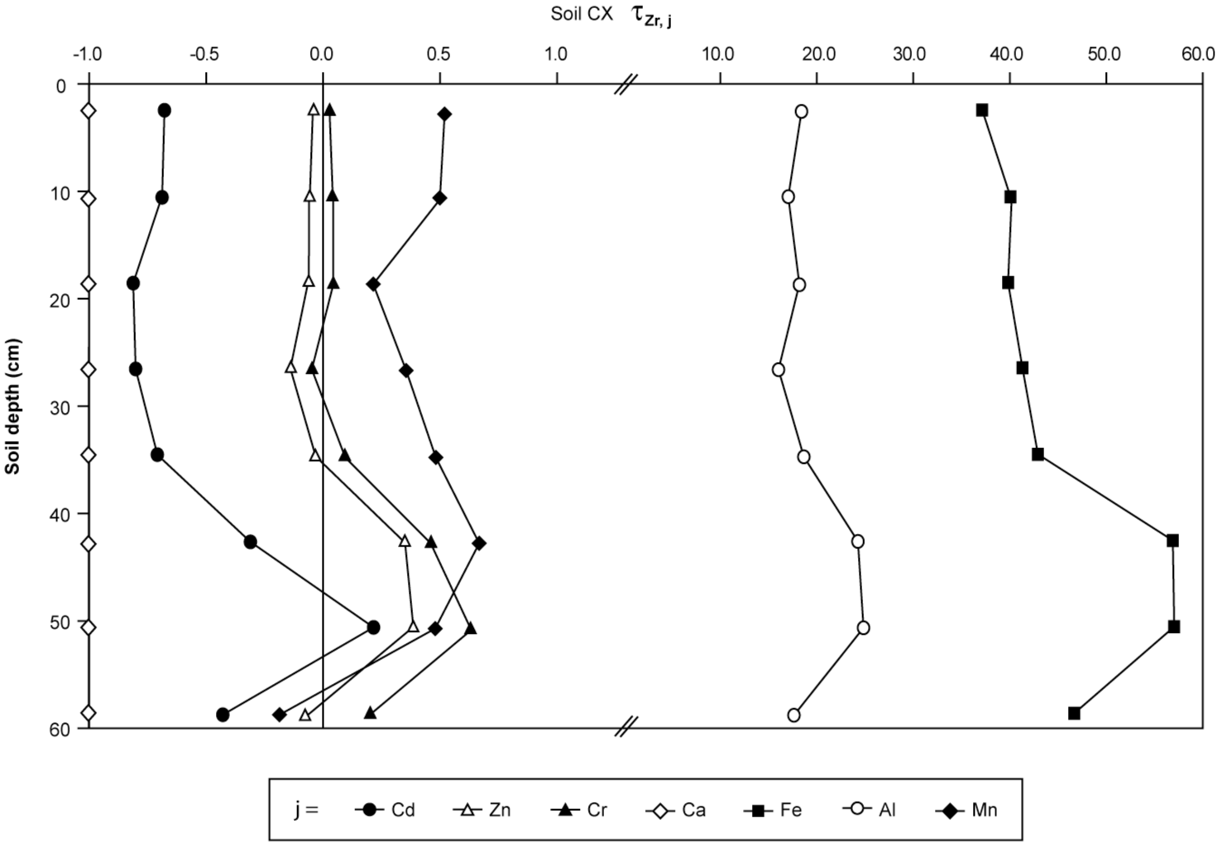

(d)

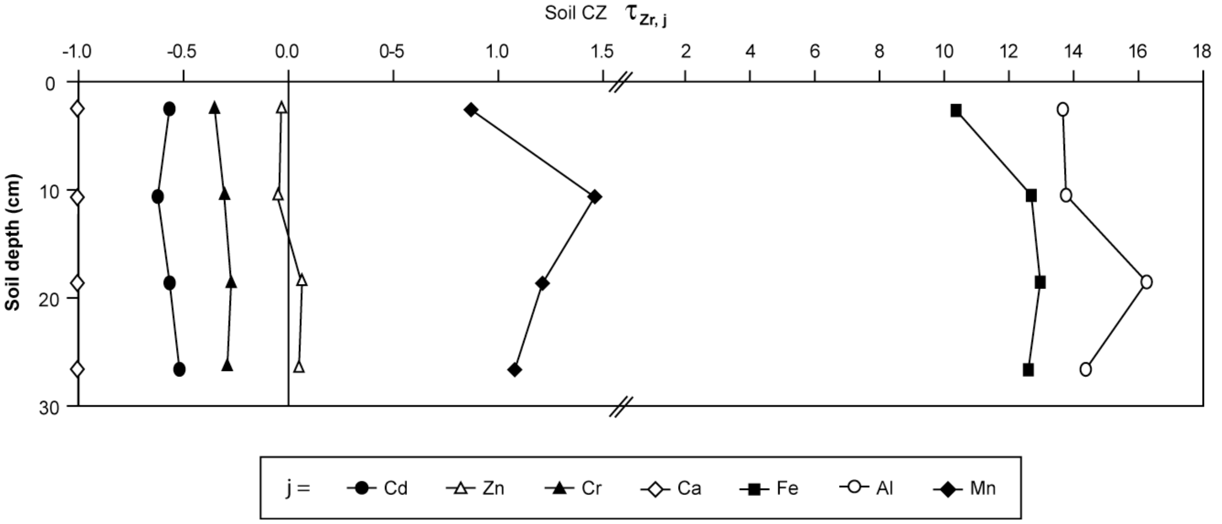

Figure 4.20 Concentration profiles of mobile elements: Cd, Zn, Cr, Ca, Fe, Al, Mn. Concentrations were normalized to Zr for for (a) soil AX; (b) soil AZ; (c) soil CX; (d) soil CZ.

Soil AX (Figure 4.19a) shows a fairly constant Cd profile, which is enriched compared to the concentration in the rock substratum. Cd in both profiles AZ (Figure 4.19b) and CZ (Figure 4.20b) displays a depletion gradient, which increases towards the bedrock confirming the geogenic origin of Cd in these soils. With regards to soil CX, cadmium shows a depletion-enrichment profile (Figure 4.20a). As explained above, its loss in the middle part of the solum is related to the eluviation of clay and hydrous oxides and associated decarbonation processes leading to the translocation of Cd towards the deeper horizons, where Cd input results also from bedrock weathering.

4.4.7 Risk assessment of cadmium at the Le Gurnigel site

The toxicity of trace metals in environmental systems depends not simply on their concentrations but also on their chemical species and their chemical and physical interactions with other soil components (Benitez, 1999). With this criterion, we evaluated the bioavailability of cadmium by taking into account the extracted contents in the first extraction phases, the exchangeable fraction and the carbonate phase. We also considered an extreme situation where strong acidity ($pH < 4.5$) and oxidizing agents would be able to release Cd bound to the organic matter phase. Table 4.14 shows the calculated concentrations of potentially bioavailable Cd both on the basis of total Cd concentrations measured in topsoils, middle and subsoils as well as the respective percentage distributions of extracted Cd in the first three fractions of the sequential extractions (Tables 4.9 thru 4.11).

The potentially bioavailable Cd issued by the readily exchangeable fraction is quite low along the soil profiles (mean value of 0.2 $mg \cdot kg^{-1}$) provided that the pH of soils remains above 5. It is not excluded that organic acids excreted by plant roots are implied in releasing additional Cd from the carbonate phase. In this situation, bioavailable Cd from the topsoil of all the cambisols (AX, AZ, CX, CZ) may amount to a mean concentration of 3.0 $mg \cdot kg^{-1}$ (maximum value recorded in topsoil AZ corresponding to 3.7 $mg \cdot kg^{-1}$) while in deep cambic-neoluvisols (EX, EZ) it would reach 0.8 $mg \cdot kg^{-1}$. The bioavailable Cd concentrations slightly decrease in subsoil AX, AZ and CZ with a mean value of 2.0 $mg \cdot kg^{-1}$. The potential of root-acid assisted increase in bioavailable Cd should not be neglected due to the shallowness of soils (maximum depths of 30 cm) as some plant roots could easily reach depths of 25 cm. Soil CX display high contents of bioavailable Cd in its subsoil (4.8 $mg \cdot kg^{-1}$) as a consequence of its maximum in total Cd (16.3 $mg \cdot kg^{-1}$) registered at 50 cm.

In cambic-neoluvisols EX and EZ bioavailable Cd is mostly located in the topsoil with contents of 0.3 and 1.2 $mg \cdot kg^{-1}$, respectively. It decreases in the middle part with mean low contents of 0.2 $mg \cdot kg^{-1}$, representing thus a lower risk compared to the cambisols. Under stronger acidity ($pH < 4.5$) and oxidizing conditions, Cd bound to the organic matter phase could be mobilised and the bioavailability of Cd could range between 3.3–5.4 mg·kg^{-1} in cambisols while it will amount to a maximum of 1.7 mg·kg^{-1} in cambic-neoluvisols.

Table 4.14 Potential bioavailable Cd in the Le Gurnigel soils

Soil	Soil level	Total Cd in soil level (mg·kg^{-1})	Potentially Bioavailable Cd Cd_{exch}	$Cd_{exch}+Cd_{carb}$ (mg·kg^{-1})	$Cd_{exch}+Cd_{carb}+Cd_{OM}$
AX	Topsoil	5.3	0.1	2.7	3.9
	Subsoil	5.4	0.0	1.4	2.6
AZ	Topsoil	7.3	0.1	3.7	5.4
	Subsoil	10.2	0.0	2.7	4.9
CX	Topsoil	4.4	0.1	2.2	3.3
	Subsoil	16.3	0.5	4.8	6.7
CZ	Topsoil	6.1	0.1	3.1	4.5
	Subsoil	6.6	0.0	1.7	3.2
EX	Topsoil	0.6	0.0	0.3	0.4
	Middle	0.6	0.1	0.1	0.2
	Subsoil	1.6	0.2	0.5	0.7
EZ	Topsoil	2.5	0.1	1.2	1.7
	Middle	1.5	0.2	0.3	0.4
	Subsoil	8.2	1.3	2.5	3.5

Cdexch = Cd extracted as easily exchangeable; Cdcarb = Cd supposed bound to the carbonate phase; CdOM = Cd supposed bound to organic matter

4.5 CONCLUSIONS

The site called “Le Gurnigel”, located in the Jura Mountains northeast of the “col de la Vue des Alpes” (canton Neuchâtel, Switzerland), overlies late Bajocian limestone, a local lithology present throughout the Jura Mountains, which is known for being enriched in Cd. The actual soils are in a continuous pedogenic evolution after an early formation stage on allochthnous aeolian silt material. The mineralogical analyses of the soil profiles reveal the presence of important quantities of chlorite both in the fine-silt fraction as well as in the clay fraction, while no traces of chlorite were found in the bedrocks. Nevertheless, pedogenic processes continue taking place and the dissolution of the bedrock continues to provide both inherited compounds as well as newly formed minerals such as illite-smectite mixed layers, oxides and amorphous oxyhydroxides.

The increasing Cd concentrations towards the bottom observed in each profile may confirm the geogenic origin of Cd in these soils. The weathering of the underlying Cd-rich carbonates drives the release of Cd and other trace metals, which are subsequently incorporated into the different phases in the corresponding soils. All analysed soils show a high decarbonation state.

Cambisols are rather shallow soils with a maxium depth of 40 cm because of their position on hill flanks. Their topsoil contains Cd, which is mainly distributed in the carbonate phase (48%) and the organic matter phase (24%). The amorphous oxyhydroxides become a more important Cd-bearing phase in the subsoil with 33% of the total Cd contents followed by the carbonate phase (26%) and crystalline Fe oxides (17%). Cambic-neoluvisols deeper than 70 cm are located in the accumulation zones or coombs, which are formed by the conjunction of two hillocks. The Cd distribution in the topsoil is comparable to the one in cambisols with carbonate (40%) and organic matter (20%) as the main bearing phases. It is not excluded that lateral soil advection may take place due to the site topography. The cambic-neoluvisols are susceptible to receive material from Cd-rich soils formed on the neighbouring hills. This phenomenon may explain the relatively high Cd concentrations in the upper horizons of these soils.

Amorphous oxyhydroxides and crystalline Fe-oxides in the middle part and deeper horizons are the most important Cd-bearing phases with mean percentage distributions of 35% and 25%, respectively. It is postulated that the Cd decrease in the middle part of the deep soils is due to the beginning of eluviation processes as the pH starts to diminish. As a consequence, clays, oxides and hydroxides are leached and dragged down the solum along with the adsorbed Cd into the deeper illuviation horizons, where Cd-bearing mineral concretions, composed of a variable mixture of quartz, phyllosilicates and amorphous oxyhydroxides, are formed.

A multiple linear regression model was obtained, in which the main predictors of Cd distribution in the Le Gurnigel soils are goethite (Gt), Ca, TOC, Fe, Al, pedogenic intergrades (IS-B) and the C/N ratio.

The potentially bioavailable Cd issued by the readily exchangeable fraction is quite low along the soil profiles (mean value of 0.2 $mg\cdot kg^{-1}$) provided that the pH of soils remains above 5. It is likely that organic acids, excreted by plant roots, have the capacity to dissolve additional Cd from the carbonate phase. This dissolution would produce higher contents of bioavailable Cd in the topsoil of cambisols reaching a mean concentration of 3.0 $mg\cdot kg^{-1}$. Bioavailable Cd in the cambic-neoluvisols is predominantly located in the topsoil, where maximum concentrations may amount to 1.2 $mg\cdot kg^{-1}$. It decreases in the middle part with mean low concentrations of 0.2 $mg\cdot kg^{-1}$, representing thus a lower risk compared to the cambisols. Under stronger acidic ($pH < 4.5$) and oxidizing conditions, Cd bound to organic matter would be mobilised and the bioavailability of Cd would range between 3.3–5.4 $mg\cdot kg^{-1}$ in cambisols and around 1.7 $mg\cdot kg^{-1}$ in cambic-neoluvisols.

Zn and Cr show a positive correlation to Cd with comparable vertical distributions along the soil profiles. Cd, Zn and Cr may share the same bearing phases such as Fe oxyhydroxides, and this may explain their strong correlation. Further studies should be considered in order to study the speciation and the potential risk presented by these two elements.

4.6 REFERENCES

Alloway, B. J., 1995. Cadmium. In: B.J. Alloway (Editor), Heavy Metals in Soils. Blackie Academic and Professional, Glasgow.

Baize, D., Girard, M.C., 2008. Référentiel Pédologique 2008. Association française pour l'étude du sol AFES, Nancy.

Benitez, L. N., 1999. Cadmium speciation and phyto-availability in soils of the Swiss Jura: hypothesis about its dynamics. Ph.D. Thesis, Ecole Polytechnique Fédérale de Lausanne, Switzerland.

Benitez, L. N., Dubois, J. P., 1999. Evaluation of the selectivity of sequential extraction procedures applied to the speciation of cadmium in soils. Environmental Pollution, Series B: Chemical and Physical, 11(2), 117–135.

Bermond, A. P., 1992. Thermodynamics applied to the study of the limits of sequential extraction procedures used for the speciation of trace elements in sediments and soils. Environ. Technol. Lett.,13, 1175–1179.

Brantley, S., Goldhaber, M., Ragnarsdottir, K.V., 2007. Crossing Disciplines and Scales to Understand the Critical Zone. Elements, Vol. 3, 307–314.

Dubois, J. P., Okopnik, F. Benitez, N., Védy, J.C., 1998. Origin and spatial variability of cadmium in some soils of the Swiss Jura. 16th World Congress Soil Science. Montepellier.

Dubois, J. P., Benitez, N., Liebig, T., Baudraz, M., Okopnik, F., 2002. Le cadmium dans les sols du haut Jura suisse. In D. Baize and M. Tercé (Editors), Les éléments traces métalliques dans les sols. Approches fonctionelles et spatiales. INRA, Orléans, 33–52.

Efimenko, N., Spangenberg, J.F., Schneider, J., Chiaradia, M., Adatte, T., Föllmi, K.B., submitted. Formation and age of cadmium-containing sphalerite mineralisations in carbonate rocks of Bajocian age in the Swiss Jura mountains. Geochimica et Cosmochimica Acta

Federal Authorities of the Swiss Confederation, 1998. RS 814.12 Ordonnance sur les atteintes portées aux sols (OSol). Annexe 2., Valeurs indicatives, seuils d'investigation et valeurs d'assainissement pour les métaux lourds et le fluor dans les sols. Official Publications Centre, Switzerland.

Food and Agriculture Organization of the United Nations FAO, 2006. World reference base for soil resources 2006. A framework for international classification, correlation and communication. FAO, Rome.

Gasparatos, D., Haidouti, C., Tarenidis, D., 2004.Characterization of iron oxides in Fe-rich concretions from an imperfectly-drained Greek soil: a study by selective-dissolution techniques and X-ray diffraction. Archives of Agronomy and Soil Science, Vol. 50, Issue 4 & 5, 485–493.

Havlicek, E., 1999. Les sols des paturages boisés du Jura suisse. Ph.D. Thesis, University of Neuchâtel, Switzerland.

Havlicek, E., Gobat, J.-M., 1996. Les aports éoliens dans les sols du Jura. Etat des connaissances et nouvelles données en pâturages boisés. Etude et Gestion des Sols, Paris, 3, 3, 167–178.

Moore, D., Reynolds, R., 1989. X-Ray-diffraction and the identification and analysis of clay-minerals. Oxford University Press.

Mustafa, G., Singh, B., Kookana, R.S., 2004. Cadmium adsorption and desorption behaviour on goethite at low equilibrium concentrations: effects of pH and index cations. Chemosphere, 57(10), 1325–33.

Okopnik, F., 1997. Relation entre la variabilité spatiale du Cd et la couverture pédologique de la region du Mon d'Amin. Master thesis, Ecole Polytechnique Fédérale de Lausanne, Switzerland.

Pochon, M., 1978. Origine et évolution des sols du Haut-Jura suisse. Ph.D. Thesis, University of Neuchâtel, Switzerland.

Prudente, D., 1999. Distribution des teneurs naturelles en cadmium dans les sols de la forêt communale des Fourgs (Doubs, France). Ph.D. Thesis, Ecole Polytechnique Fédérale de Lausanne, Switzerland.

Prudente, D., Baize, D., Dubois, J.P., 2002. Le cadmium naturel dans une forêt du haut Jura français. In: D. Baize and M. Tercé (Editors), Les élements traces métalliques dans les sols. Approches fonctionelles et spatiales. INRA, Orléans, 53–70.

Quezada-Hinojosa, R.,P., Matera V., Adatte, T., Rambeau, C., Föllmi, K.,B., 2009. Cadmmium distribution in soils covering Jurassic oolitic limestone with high Cd contents in the Swiss Jura. Geoderma Volume 150, Issues 3–4, 287–301.

Rambeau, C., 2006. Cadmium anomalies in Jurassic carbonates (Bajocian, Oxfordian) in western and southern Europe. Ph.D. Thesis, University of Neuchâtel, Switzerland.

Randall, S., Sherman, D., Ragnarsdottir, V., Collins, C., 1999. The mechanism of cadmium surface complexation on iron oxyhydroxide minerals. Geochimica et Cosmochimica Acta, Vol. 63, No. 19/20, 2971–2987.

Righi, D., Meunier, A., 1995. Origin of clays by rock weathering and soil formation. In: B. Velde (Editor), Origin and Mineralogy of Clays. Springer, Berlin, 43–157.

Schwertmann, U., Taylor, R. M., 1989. Iron Oxides. Ch.8. In: J. B. Dixon and S.B. Weed (Editors), Minerals in Soil Enironments, 2nd Edition.

Soon, Y.K., Abboud, S., 1993. Cadmium, Chromium, Lead, and Nickel. In: M.R. Carter (Editor), Soil sampling and methods of analysis. Canadian Society of Soil Science, 101–107.

Tessier, A., Campbell, P.G.C., Bisson, M., 1979. Sequential extraction procedure for the speciation of particulate trace metals. Analytical Chemistry, 51 (7), 844–851.

U.S. Environmental Protection Agency (EPA), 1994. Test Methods for Evaluating Solid Waste, SW-846, 3rd ed., Office of Solid Waste and Emergency Response, Washington, D.C.

Van der Sloot, H.A., Heasman, L., Quevauviller, Ph.,1997. Harmonization of leaching/extraction tests. Elsevier, Amsterdam, 281pp.

Zhang, M., Karathanasis, A. D., 1997. Characterization of iron-manganese concretions in Kentucky Alfisols with perched water tables. Clays and Clay Minerals, Vol. 45, No. 3, 428–439.

CADMIUM ACCUMULATION IN SIX COMMON PLANT SPECIES ASSOCIATED WITH SOILS CONTAINING HIGH Cd CONCENTRATIONS OF GEOGENIC ORIGIN

The case of Le Gurnigel plants

Paper in preparation

CHAPTER 5

CADMIUM ACCUMULATION IN SIX COMMON PLANT SPECIES ASSOCIATED WITH SOILS CONTAINING HIGH Cd CONCENTRATIONS OF GEOGENIC ORIGIN

Raul Quezada-Hinojosa[1], Virginie Matera[2], François Gillet[3], Karl B. Föllmi[4]

[1] Institut de Géologie, Université de Neuchâtel, rue Emile-Argand 11, CP 158, CH-2009 Neuchâtel, Switzerland
[2] Institut National de Recherche et Sécurité Rue du Morvan CS 60027 54519 Vandoeuvre-Les Nancy, France
[3] UMR 6249 Chrono-environment, Université de Franche- Comté, 16, route de Gray Besançon, France
[4] Institut de Géologie et Paléontologie, Université de Lausanne, Anthropôle 3172, CH-1015 Lausanne, Switzerland

Abstract

The uptake of cadmium (Cd) was analyzed for six different plant species growing in a pasture of the Swiss Jura, where the soils are enriched in geogenic Cd (10 mg·kg^{-1} on average). The six selected plants - *Hypericum maculatum, Alchemilla xanthochlora*, *Cynosurus cristatus, Ranunculus acris*, *Dactylis glomerata and Acer pseudoplatanus* - show variable Cd contents between the species and between individuals from the same family (Poaceae). Average Cd concentrations in the selected individuals are in the 2–6 mg·kg^{-1} range and exceed the maximal Cd concentration tolerated in vegetal food for animals established at 1 mg·kg^{-1} as such. High Cd concentrations in the soil result in a reduction of Cd accumulation in the shoots and a corresponding increase in the accumulation of Cd in the roots. This implies that Cd transfer coefficients from the soil / rhizosphere to the plant are inversely proportional to the total Cd concentrations in soils and do not depend on plant species but instead on soil type. Sequential chemical extractions reveal that variations in Cd distribution between the distant soil and the corresponding rhizosperic soil occur mainly in the Cd-bearing phases, which are exchangeable, bound to carbonates, and associated with organic matter. This is principally due to the incorporation of roots exudates, which modify pH and redox conditions of the rizhosphere. Elevated Cd concentrations in the shoots of *Alchemilla x.* (up to 8 mg·kg^{-1}), *Cynosurus c.* (maximum 9 mg·kg^{-1}) and *Hypericum m.* (3 mg·kg^{-1}) may represent a long-term hazard for animals and human health since these plants are used either by grazing livestock or for medicinal purposes. *Ranunculus a., Acer p.,* and especially *Dactylis g.,* on the contrary, show lower Cd concentrations and are of minor concern with regards to their environmental impact.

Keywords: **Bioaccumulation; Bioavailability; Cadmium; Geogenic; Plant; Rhizosphere; Soil; Sequential Extraction**

5.1 INTRODUCTION

In the French and Swiss Jura Mountains, Middle Jurassic (Bajocian) carbonates contain intervals, which are highly enriched in geogenic cadmium (Cd). As a consequence, associated soils are naturally incorporating this element into their different mineralogical phases (Okopnik, 1997; Benitez, 1999; Dubois et al., 2002; Rambeau, 2006; Quezada et al., 2009; Quezada et al., *in preparation*). This is the case at the site called “Le Gurnigel”, which is located in the Jura Mountains, northeast of the “Col de la Vue des Alpes” (canton Neuchâtel, Switzerland). Soils at this site contain Cd concentrations with mean values, which are generally above 10 $mg \cdot kg^{-1}$ (maximum value recorded in the subsoil = 16 $mg \cdot kg^{-1}$; Quezada et al., *in preparation*). These values largely exceed the official Swiss indicative guideline value for soils fixed at 0.8 $mg \cdot kg^{-1}$ (Federal Authorities of the Swiss Confederation: OSol, 1998). As such, these soils may represent an environmental risk since the local herbaceous vegetation cover is susceptible to pump and stock this element in both roots and shoots, which are again used by grazing ungulate livestock. Consequently, Cd may gradually enter the food chain and jeopardize animal and human health.

Wermeille (1999) analyzed the total aerial biomass of a large set of local plant species and reported Cd accumulations of up to 9 $mg \cdot kg^{-1}$ dry matter (DM), especially in some grass species. With this contribution, we follow up on this research and focus on the individual behaviour of six different plant species growing on soils with variable Cd concentrations at the Le Gurnigel site, and analyze Cd accumulations in roots and shoots separately for each species. *Hypericum maculatum, Alchemilla xanthochlora*, *Cynosurus cristatus, Ranunculus acris*, *Dactylis glomerata and Acer pseudoplatanus* were collected for this purpose. A statistical approach by means of ANOVA Kruskal-Wallis rank sum tests, is used to correlate the data and trace the variability in Cd behaviour in plants.

5.2 MATERIAL AND METHODS

5.2.1 Site description

Le Gurnigel is a pasture, which lies at 1300 m above sea level on the northern face of the Mont d’Amin located in the northern part of canton Neuchâtel, Switzerland (Figure 4.1). The majority of the site overlies Upper Bajocian limestone (Middle Jurassic). The geomorphology of the site consists in three main hillocks with slopes ranging from 20 to 30%. Soils at the site include thin solums (13–40 cm deep) formed mainly on top of the hill flanks, and deeper soils (80–140 cm deep), which are located in the accumulation zones or coombs formed by the conjunction of two hillocks. The soils at this site present strong signs of allochthony suggesting that they were formed on aeolian silt deposits of glacial origin (Okopnik, 1997;

Quezada et al., *in preparation*). Table 5.1 shows the six selected soils classified according to the World Reference Base (WRB) for Soil Resources 2006 (Food and Agriculture Organization of the United Nations FAO, 2006).

Table 5.1 Classification of sampled soils

Soil code in sampling map	**World Reference Base (2006)**
AX	Eutric cambisol (humic)
AZ	Eutric cambisol (leptic, humic)
CX	Eutric-dystric cambisol (calcic)
CZ	Eutric-dystric cambisol
EX	Cambic-neoluvisol
EZ	Cambic-neoluvisol

5.2.2 Plant sampling strategy

We used the sampling points described in chapter 4 (Quezada et al., *in preparation*), and shown in Figure 4.3. The sampling points were coded as AX, AZ, CX, CZ, EX and EZ. The exact locations of these points were determined by means of a Garmin ETrex Sumit GPS device. The selection of plant species was based on their ubiquity in each of the six sampling points in order to compare the behaviour of the same species at each point whenever possible. Following this criterion, six major species of plants were collected (roots and shoots), which are presented in Table 5.2. In order to control the accuracy of the analyses, three individuals of each species were collected at each sampling point.

Table 5.2 Plant classification

Plant Species		**Symbol**	**Group**	**Family**	**Duration**	**Growth Habit**
Scientific name	**Common name**	**Alt. symbol***				
***Hipericum maculatum* Crantz**	Spotted St. Johnswort	**HYMA** **Hm**	Dicotyledonous	Clusiaceae Mangosteen family	Perennial	Forb/herb
Alchemilla xanthochlora	Lady’s mantle	**ALXA** **Ax**	Dicotyledonous	Rosaceae Rose family	Perennial	Forb/herb
Cynosurus cristatus	Crested dogstail grass	**CYCR** **Cc**	Monocotyledonous	Poaceae Grass family	Perennial	Graminoid
Ranunculus acris	Tall buttercup	**RAAC** **Ra**	Dicotyledonous	Ranunculaceae Buttercup family	Perennial	Forb/herb
Dactylis glomerata	Orchardgrass	**DAGL** **Dg**	Monocotyledonous	Poaceae Grass family	Perennial	Graminoid
Acer pseudoplatanus	Sycamore maple	**ACPS** **Ap**	Dicotyledonous	Aceraceae Maple family	Perennial	Tree

* Alt. symbol: Alternative symbol for each species of plant used in some figures in order to facilitate their interpretation

All plant individuals were separated from other species, soil particles were washed away and roots were separated from shoots to analyze them individually. We also separated the distant soil from the roots and carefully collected samples of the rhizospheric soil in direct contact with the roots of each of the six plant species. Due to the maximal depth of 20 cm reached by the roots, we consider the topsoil levels down to the first 20 cm of each soil profile as distant soil (Figure 4.5).

5.2.3 Chemical analyses of trace metals in plants

Roots and shoots were dried by lyophilisation during 63 hours at -40°C and a pressure of 0.05 Pa. Each part was weighed separately in order to measure its respective dried matter (DM) biomass.

Cd concentrations were determined separately in roots and shoots for each plant species as follows: Dried samples were milled and sieved through a 0.5 mm mesh. 150 mg of milled sample were subjected to microwave-assisted acid digestion in PTFE vessels under oxidizing conditions with a mixture composed of 6 ml of concentrated HNO_3 and 2 ml of H_2O_2. Dissolved samples were subsequently filtered through a 0.45 μm HVLP-Millipore filter before analysis. The filtrated solutions were analyzed by Inductively Coupled Plasma Mass Spectrometry (ICP-MS Perkin-Elmer Elan 6100).

5.2.4 Cd concentration in distant and rhizospheric soils

Chemical analyses of Cd, selected trace metals Zn, Pb, Cr, Ni, Cu, and major elements Ca, Fe, Al, Mn in distant soil and in rhizospheric soil samples were conducted following the Method 3051 developed by the U.S. Environmental Protection Agency EPA (1994). 250 mg of dried and grounded sample were subjected to microwave-assisted acid digestion (concentrated HNO_3) and samples were subsequently filtered before analysis. The filtrated solutions were analyzed by Inductively Coupled Plasma Mass Spectrometry (ICP-MS Perkin-Elmer Elan 6100).

5.2.5 Main chemical soil properties

Total organic and mineral-carbon contents were measured in powdered samples by a Rock-Eval6^{TM} device. Total carbon and nitrogen contents were also analyzed on powdered samples using an elemental analyzer Carlo Erba EAL 1108. Soil pH in H_2O was measured using a Metrohm 682 titroprocessor. The cation-exchange capacity (CEC) was measured following the French protocol AFNOR NF X31-130: Soils samples were mixed with a solution of hexaamminecobalt(III) chloride and the concentration of free cobalt ions was measured in a UV spectrometer calibrated to 470 nm.

5.2.6 Cd distribution in rhizospheric soils

We applied the sequential extraction protocol used by Benitez (1999) and described in §4.2.6 (Figure 4.4). This method allows for the separation and identification of Cd, which is presumed to be distributed in six major fractions: (1) exchangeable; (2) carbonates; (3) organic matter; (4) amorphous Fe-, Mn-oxyhydroxides; (5) crystalline Fe oxides; and (6) residual mineral matrix. The filtrated supernatants recovered in each extraction step were analyzed by Inductively Coupled Plasma Mass Spectrometry (ICP-MS Perkin-Elmer Elan 6100). In order to assure the accuracy of the results, three replicates for each sample were used in every extraction step.

5.3 RESULTS

5.3.1 Total Cd contents in plants

Table 5.3 summarizes both the mean concentrations measured in roots and shoots as well as the concentrations in the entire plants at the six sampling points. As a general rule, Cd concentrations in roots are higher than those of the respective shoots for each plant. *Alchemilla xanthochlora* (ALXA) shows the highest Cd concentrations for the entire plant (3.1–13.4 mg·kg^{-1}), followed by *Cynosurus cristatus* (CYCR) with Cd concentrations in the range of 2.3–9.7 mg·kg^{-1}. *Hypericum maculatum* (HYMA) and *Ranunculus acris* (RAAC) present lower Cd contents with maximum values of 3.2 mg·kg^{-1} and 4.5 mg·kg^{-1}, respectively. *Dactylis glomerata* (DAGL) and *Acer pseudoplatanus* (ACPS) possess the lowest Cd concentrations of all analyzed plants ranging from 0.6 to 2.2 mg·kg^{-1} in *Dactylis g.* and from 1.0 to 2.1 mg·kg^{-1} in *Acer p*.

Cynosours c. appears to be the main Cd accumulator in aerial biomass (maximum value 9.4 mg·kg^{-1}), followed by *Alchemilla x.* (8.1 mg·kg^{-1}), *Hypericum m.* (2.9 mg·kg^{-1}) and *Ranunculus a.* (2.9 mg·kg^{-1}). *Dactylis g.* and *Acer p.*, present the lowest Cd contents (maximum value 0.8 mg·kg^{-1}). The Cd concentrations in plants from soil AX and CZ might not be fully representative as data from the triplicates were lost due to technical problems with the ICP-MS during the analyses (Table 5.3).

Table 5.3 Mean cadmium contents in roots, shoots and total plant

Soil	***Hypericum maculatum***			***Alchemilla xanthochlora***			***Cynosurus cristatus***		
	$[\mathrm{Cd}]_{\mathrm{root}}$	$[\mathrm{Cd}]_{\mathrm{shoots}}$	$[\mathrm{Cd}]_{\mathrm{plant}}$	$[\mathrm{Cd}]_{\mathrm{root}}$	$[\mathrm{Cd}]_{\mathrm{shoots}}$	$[\mathrm{Cd}]_{\mathrm{plant}}$	$[\mathrm{Cd}]_{\mathrm{root}}$	$[\mathrm{Cd}]_{\mathrm{shoots}}$	$[\mathrm{Cd}]_{\mathrm{plant}}$
	(mg kg^{-1})			(mg kg^{-1})			(mg kg^{-1})		
AX	2.8 ± 1.1	2.5 ± 1.7	2.6 ± 1.5	3.8 ± 1.1	1.2 ± 0.7	3.1 ± 0.8	5.7 ± 1.6	4.5 ± 2.8	4.9 ± 2.3
AZ	2.8 ± 0.5	0.2 ± 0.0	1.1 ± 0.4	9.2 ± 1.3	1.5 ± 0.1	7.0 ± 1.5	8.7 ± 0.1	2.7 ± 0.0	5.0 ± 1.0
CX	4.7 ± 1.0	2.9 ± 0.5	3.2 ± 0.2	14.8 ± 2.0	5.6 ± 0.9	10.3 ± 2.2	7.6 ± 1.7	3.4 ± 1.2	5.4 ± 3.0
CZ	Not found at sampling point			16.2	8.1	13.4	9.9	9.4	9.7
EX	1.5 ± 0.1	0.9 ± 0.2	1.1 ± 0.2	5.6 ± 0.6	3.0 ± 0.4	4.9 ± 0.9	2.9 ± 0.4	1.4 ± 0.2	2.3 ± 0.5
EZ	1.8 ± 0.3	1.5 ± 0.3	1.6 ± 0.3	5.7 ± 0.5	1.2 ± 0.1	4.5 ± 0.9	7.5 ± 1.0	3.0 ± 0.5	4.6 ± 0.2

Soil	***Ranunculus acris***			***Dactylis glomerata***			***Acer pseudoplatanus***		
	$[\mathrm{Cd}]_{\mathrm{root}}$	$[\mathrm{Cd}]_{\mathrm{shoots}}$	$[\mathrm{Cd}]_{\mathrm{plant}}$	$[\mathrm{Cd}]_{\mathrm{root}}$	$[\mathrm{Cd}]_{\mathrm{shoots}}$	$[\mathrm{Cd}]_{\mathrm{plant}}$	$[\mathrm{Cd}]_{\mathrm{root}}$	$[\mathrm{Cd}]_{\mathrm{shoots}}$	$[\mathrm{Cd}]_{\mathrm{plant}}$
	(mg kg^{-1})			(mg kg^{-1})			(mg kg^{-1})		
AX	2.1	0.8	1.2	3.3	0.5	2.2	3.4	0.6	1.5
AZ	6.6 ± 0.7	0.5 ± 0.3	3.3 ± 0.9	2.3 ± 0.2	0.3 ± 0.0	0.9 ± 0.3	5.5 ± 1.7	0.6 ± 0.3	2.1 ± 0.3
CX	4.1 ± 0.8	0.9 ± 0.4	2.2 ± 0.6	2.0 ± 0.2	0.8 ± 0.1	1.3 ± 0.3	Not found at sampling point		
CZ	6.8	2.9	4.5	2.4	0.6	1.4	2.5	0.4	1.4
EX	2.0 ± 0.6	1.7 ± 0.9	1.8 ± 0.8	2.4 ± 0.8	0.6 ± 0.2	1.5 ± 0.2	1.3 ± 0.5	0.7 ± 0.4	1.0 ± 0.5
EZ	2.4 ± 0.4	1.4 ± 0.5	1.7 ± 0.3	1.1 ± 0.2	0.3 ± 0.1	0.6 ± 0.0	3.1 ± 1.0	0.6 ± 0.3	1.7 ± 0.9

5.3.2 Chemical analyses of rhizospheric and distant soils

The variability in Cd contents in the six soil profiles has been already described in §4.3.3 and presented in Figure 4.7. Table 5.4 summarizes the Cd concentrations measured in the rhizospheric soils of each plant species and the corresponding distant soils for each profile. Cd concentrations range from 0.3 to 14.3 mg·kg^{-1}. Cd concentrations in the soils decrease in the following order: AZ > CZ > AX > CX > EZ > EX.

Due to the shallowness of soil AZ (16.5 cm deep; Figure 4.7), Cd contents in the rhizosphere equal the mean Cd concentration measured in its deepest level (10 mg·kg^{-1}) rather than the mean value of the topsoil (7.5 mg·kg^{-1}).

The main chemical properties of the topsoils at the six sampling profiles are presented in Table 5.5. As observed in §4.3.2, Total Organic Carbon (TOC) contents are higher in cambisols AX (6.5%), AZ (6.5%) and CZ (5.6%) than in cambic-neoluvisols EX (2.1%), EZ (2.8%). A comparable difference is observed for the cation-exchange capacity (CEC) with the highest values observed in soils AX (17.6 cmol·kg^{-1}), AZ (16.4 cmol·kg^{-1}) and CZ (15.6 cmol·kg^{-1}). The soil pH is rather acidic in the topsoils from the deep soil profiles CX (5.5), EZ (5.5) and especially EX (5.2). As observed before, all soils are highly decarbonated with low Ca contents, with a minimum value recorded in soil EX (1.9 g·kg^{-1}) and a maximum value of 7.1 g·kg^{-1} in shallow soil AZ.

Table 5.4 Mean Cd concentrations in rhizospheric and distant soils for all profiles

Plant species	Cd (mg kg^{-1})					
	AX	AZ	CX	CZ	EX	EZ
HYMA	6.7	12.3	4.4	NF	0.3	2.4
ALXA	4.9	12.0	4.2	6.7	0.4	2.4
CYCR	5.9	12.4	4.9	8.1	0.2	2.0
RAAC	4.6	14.3	4.3	7.7	0.5	1.7
DAGL	5.1	13.8	3.9	9.6	0.4	2.5
ACPS	5.6	14.3	NF	8.3	0.5	2.0
Distant topsoil	5.5	7.5	3.8	5.7	0.4	2.2

NF = Plant species not found at the sampling point

Table 5.5 Main chemical properties of topsoil at the six sampling points

Soil code	TOC (%)	Cmin (%)	pH	CEC (cmol·kg^{-1})	C/N	Ca (g·kg^{-1})	Fe (g·kg^{-1})	Al (g·kg^{-1})	Mn (g·kg^{-1})
AX	6.5	0.4	6.1	17.6	11.9	5.9	47.5	20.6	2.3
AZ	6.5	0.3	5.8	16.4	11.3	7.1	41.1	23.3	1.6
CX	4.7	0.3	5.5	9.1	9.7	2.3	40.3	27.6	1.6
CZ	5.6	0.3	5.8	15.7	10.9	4.7	45.8	26.2	2.3
EX	2.1	0.2	5.2	6.4	12.5	1.9	37.1	23.2	0.8
EZ	2.8	0.2	5.5	8.4	11.8	2.5	42.1	25.2	2.1

5.3.3 Cd distribution in rhizospheric soils

One of the goals of this study was to determine if a significant difference is present between the distribution of Cd and trace metals in the rhizosphere of a plant accumulating high quantities of Cd and that of a plant accumulating low quantities of Cd. For this purpose sequential extractions were applied to the rhizosperic soils of *Alchemilla xanthochlora* and *Dactylis glomerata.* Moreover, we compared these distributions in two groups of soils with different Cd concentrations - the shallow cambisols AX and AZ, and deep cambic-neoluvisols EX and EZ. The results are summarised in Table 5.5 for *Alchemilla x.* and Table 5.6 for *Dactylis g.*

Table 5.6 Distribution of Cd in rhizospheric soil of *Alchemilla xanthochlora* collected in cambisols AX, AZ and cambic-neoluvisols EX, EZ

Soil fraction	Rhizospheric soil of *Alchemilla xanthochlora*			
	Percent distribution of Cd (%)			
	Soil AX	Soil AZ	Soil EX	Soil EZ
F1 Exchangeable	0.8	0.3	21.4	5.8
F2 Carbonates	32.4	29.9	39.7	48.8
F3 Organic Matter	36.0	38.5	14.9	17.8
F4 Amorphous Oxyhydroxides	18.0	18.2	13.2	9.6
F5 Crystalline Fe oxides	10.5	11.5	10.8	14.8
F6 Residue	2.3	1.6	0.0	3.2
Recovery (%)	118.8	99.6	105.7	88.9

Table 5.7 Distribution of Cd in rhizospheric soil of *Dactylis glomerata* collected in cambisols AX, AZ and cambic-neoluvisols EX, EZ

Soil fraction	Rhizospheric soil of *Dactylis glomerata*			
	Percent distribution of Cd (%)			
	Soil AX	Soil AZ	Soil EX	Soil EZ
F1 Exchangeable	1.4	1.1	16.4	0.0
F2 Carbonates	33.2	34.4	48.2	32.2
F3 Organic Matter	32.9	48.7	12.0	28.9
F4 Amorphous Oxyhydroxides	18.7	8.8	5.2	19.2
F5 Crystalline Fe oxides	11.4	5.8	12.9	17.6
F6 Residue	2.4	1.2	5.2	2.1
Recovery (%)	95.4	102.9	114.3	94.2

Graphical comparisons between mean Cd and trace-metals distributions in the rhizosphere and the distant soil for *Alchemilla x.* and *Dactylis g.* in soil profiles AX, AZ, EX and EZ are presented in Figure 5.1.

Soil AX

Cd bound to the carbonate phase (F2) decreases from 45% in the distant soil to 32% in the rhizosphere of *Alchemilla x.* and *Dactylis g*. The opposite is observed in the organic matter phase (F3) where the percentage of Cd rises from 26% in the distant soil to 32% for *Dactylis g*. and 36% for *Alchemilla x.* Rather small changes are observed for amorphous oxyhydroxides (F4) where Cd rises from 15% to 18.5% in both rhizospheres. The exchangeable fraction (F1) does not seem to be greatly modified with a reduction from 2% to 1.4% (*Dactylis g.*) and 0.8 (*Alchemilla x.*). Cd associated with Fe-oxides remains constant while Cd residing in the silicate matrix slightly increases from 1.5% to 2.4% in the rhizosphere of both plants.

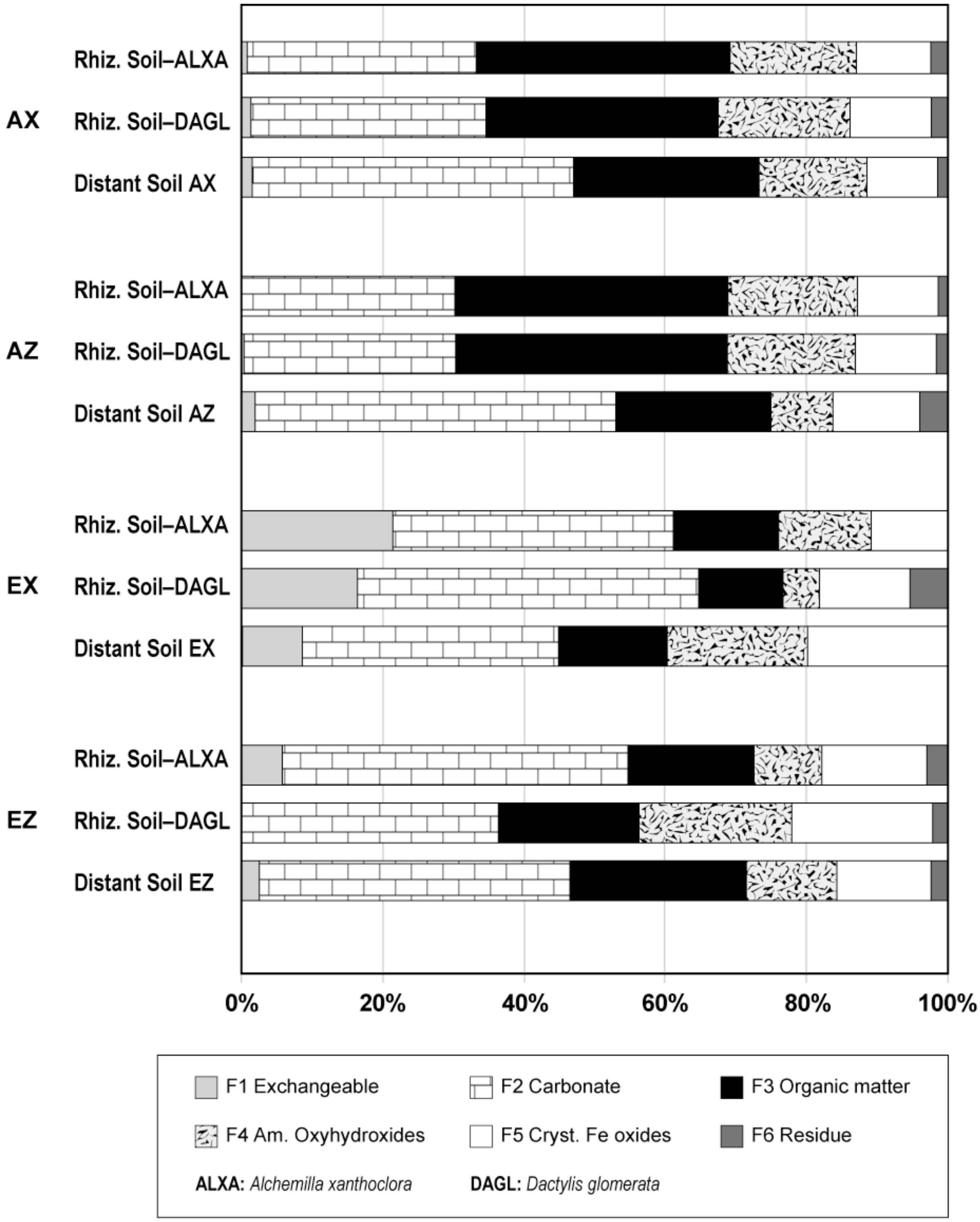

Figure 5.1 Mean percent distribution of Cd extracted in rhizospheric and distant soils. Data are compared between *Alchemilla xanthochlora* and *Dactylis glomerta* in soil profiles AX, AZ, EX and EZ.

Soil AZ

This soil presents changes in its Cd distribution similar to that in soil AX. Cd percentage in the carbonate fraction diminishes from 51% to 34% for *Dactylis g*. and 30% for *Alchemilla x.* Cd-bound to organic matter rises from 22% to 38.5% (*Alchemilla x.*) and 49% (*Dactylis g*.), respectively. Cd in amorphous oxides doubles from 9% to 18% in both rhizospheres. The exchangeable fraction is reduced from 2% to 1% in *Dactylis g*. and 0.3% in *Alchemilla x.* Cd in the residual matrix is reduced from 4% to nearly 1.5% in the rhizosphere. Cd in crystalline Fe-oxides remains constant.

Soil EX

The exchangeable Cd rises considerably if compared to the other soils, incrasing from 8.5% in distant soil to 16% in rhizospheric soil of *Dactylis g*. and 21% in *Alchemilla x.* The carbonate phase remains rather constant. Cd-bound to organic matter decreases from 15% to 12% in *Dactylis g*. but remains constant in *Alchemilla x.* Cd in amorphous oxyhydroxides is reduced from 20% to 12% for *Alchemilla x.* and to 5% in *Dactylis g*. Cd in Fe-oxides diminish from 20% to 12% in both rhizospheres. The rhizosphere of *Dactylis g*. presents 5% Cd in the residual phase while it is absent in its distant soil and in that of *Alchemilla x.*

Soil EZ

Exchangeable Cd appears only in the distant soil (2.5%) and in the rhizospheric soil of *Alchemilla x.* (5.8%). Cd bound to the carbonate fraction is higher in *Alchemilla x.* (50%) than in distant soil (44%). Cd bound to organic matter and to residual matrix remains on a level of 29% in *Dactylis g*. and 18% in *Alchemilla x.* Cd in amorphous oxyhydroxides varies from 13% in distant soil to 19% (*Dactylis g*.) and 10% (*Alchemilla x.*), respectively. Cd bound to Fe-oxides does not show a significant variation.

5.4 DISCUSSION AND INTERPRETATION

5.4.1 Cd uptake by plants

In a first approach, we studied global concentrations of Cd in the vegetation cover at Le Gurnigel. For this purpose, we plotted mean Cd concentrations for all plants, with no distinction of species, against Cd contents in the six soils (Figure 5.2a). Global concentrations of Cd in plants are in the range of 2–6 mg·kg^{-1} for dried matter (DM). As such, these levels exceed the maximal Cd concentration tolerated in plant food for animals, established at 1 mg·kg^{-1} (OSEC, 1995). However, these concentrations are within the range of limit values of 5–10 mg·kg^{-1} DM for plants and are lower than the critical values, which range from 10 to 20 mg·kg^{-1} DM (Agence de l'Environnement et de la Maîtrise de l'Energie AEME, 2010).

The variations in Cd concentrations in soils appear to have a direct influence on the accumulation of Cd by plants. It would be expected that a rise in the concentration of Cd in a given soil would produce a stronger accumulation in a plant growing in it. This may be true for the increasing concentrations in the sequence of 0.5; 2.6 and 4.3 mg·kg^{-1} observed in soils EX, EZ and CX respectively. However, plants from soils AX and AZ, which present higher levels of Cd in the topsoil (5.5 and 6.7 mg·kg^{-1} respectively), appear to accumulate lower quantities of Cd than their counterparts in soil CX and soil CZ (mean Cd contents of 5.7 mg Cd·kg^{-1}). Care should however be taken with the high standard deviation of plants in soil CZ (Figure 5.2a) due to the lack of triplicates.

Cd uptake by plants is a process controlled not only by the concentration and speciation of the metal in the soil solution, but also by the movement of the metal from the bulk soil to the root surface, the transport of the metal from the root surface into the root, and its translocation from the root to the shoots (Chaney and Giordano, 1977, Alloway, 1995). Wild (1988) found that plant uptake of mobile ions in the soil solution is largely determined by the total quantity of this ion in the soil. However, in the case of strongly adsorbed ions, absorption rates are more dependent upon the amount of root produced and result in yield reduction. Figures 5.2b and c present global Cd concentrations in roots and shoots as a function of total concentrations in the topsoil. As a general rule, roots accumulate higher Cd concentrations than shoots (Sauerbeck, 1991; Cieslinski et al., 1996; Lehoczky et al., 1996). The varietal influence may depend on whether a given plant species retains Cd taken up in the roots or translocates it to the shoots as it has been demonstrated in maize plants (Florijn and van Beusichem, 1993, Chizzola et al., 2005).

It has been observed that a rise in the concentration of Cd in the soil progressively reduces the transport of Cd toward shoots. In this way, plants growing in non-polluted soils will easily transfer ions from the roots towards the leaves. The opposite occurs in Cd-rich soils where roots will accumulate higher quantities of Cd while only a low percentage is transferred to shoots (Cieslinski et al., 1996).

Plants show a similar behaviour with regards to micronutrients such as Cu, Fe, Mn and Zn (Kabata-Pendias and Pendias 1992; Alloway, 1995). The supply of a micronutrient may increase until a lower critical concentration level is reached. Below this level, the plant grows normally and no deficiencies occur in yield production.

(a)

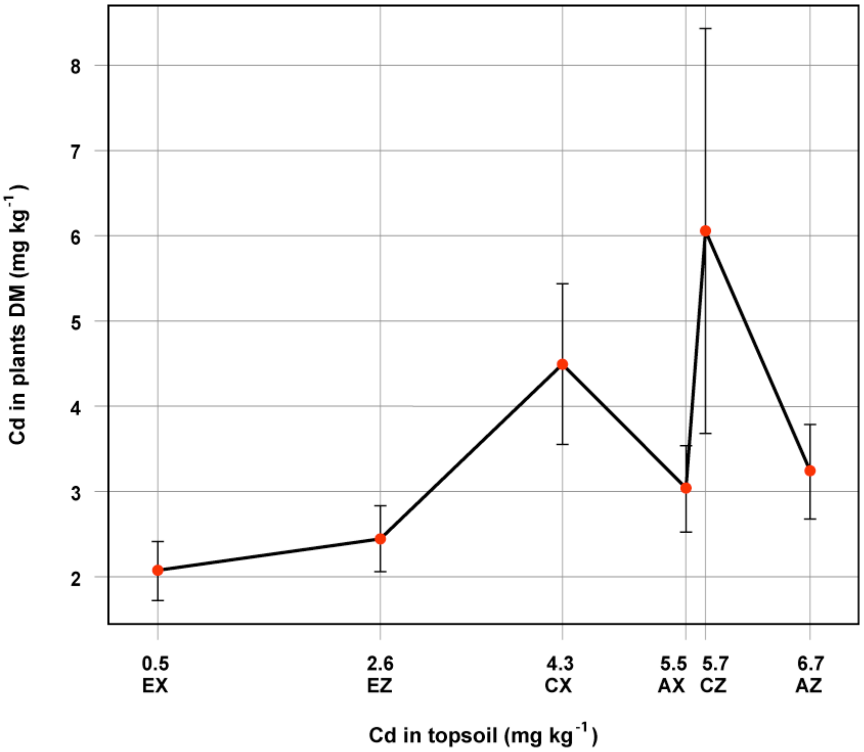
Cd in plants DM (mg kg^{-1})
8
7
6
5
4
3
2
0.5 EX
2.6 EZ
4.3 CX
5.5 AX
5.7 CZ
6.7 AZ
Cd in topsoil (mg kg^{-1})

(b)

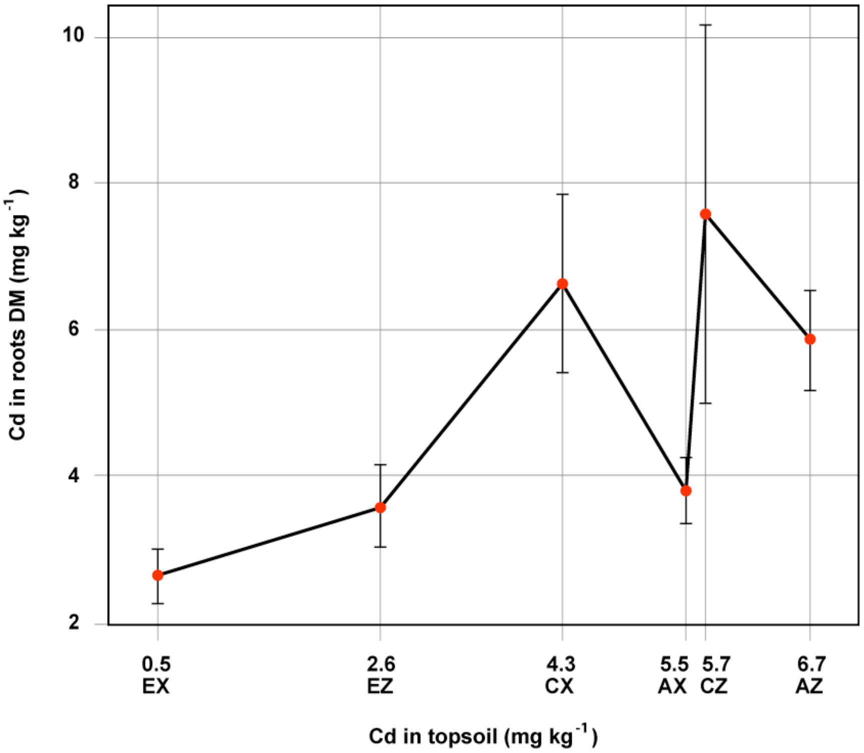
Cd in roots DM (mg kg^{-1})
10
8
6
4
2
0.5 EX
2.6 EZ
4.3 CX
5.5 AX
5.7 CZ
6.7 AZ
Cd in topsoil (mg kg^{-1})

(Continued)

(c)

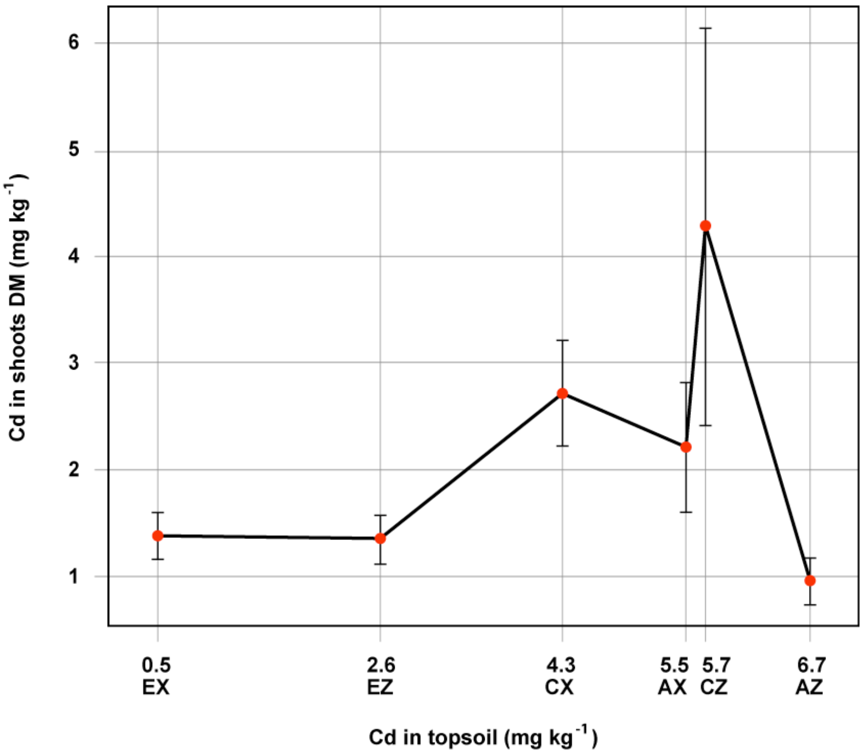

Figure 5.2 Global Cd concentrations in plants measured in (a) entire plant; (b) roots; (c) shoots

Above the upper critical concentration level, a yield reduction occurs due to toxicity (Alloway, 1995). When growing in soils with high Cd concentrations, the plant may control its Cd household by stocking the excess Cd in roots and reducing the yield production. This is the case in soils AX and AZ where Cd concentrations in shoots drop (from 2.7 mg·kg^{-1} DM in soil CX) to 2.2 mg·kg^{-1} DM and 1 mg·kg^{-1} DM, respectively (Figure 5.2c). This mechanism of detoxification may well depend on genetic differences within plant species (Wermeille, 1999).

5.4.2 Cd uptake by plants as a function of species identity

Figure 5.3 depicts global Cd concentrations measured for each plant species as a function of the total Cd concentration in the topsoil. *Alchemilla xathochlora* appears with the highest concentrations followed by *Cynosusurs cristatus* (Table 5.3). It has been reported that the transfer of Cd from the soil into the plant may vary greatly with the plant species and even with the variety or genotype within a given species (Malko, 2002; Schneider et al., 2002). This is case for *Cynosusurs cristatus* and *Dactylis glomerata*, both of the family poaceae, which behave differently in the same soil and show two extremes, with *Cynosusurs c.* as an important and *Dactylis g.* as a subordinate Cd accumulator (Table 5.3).

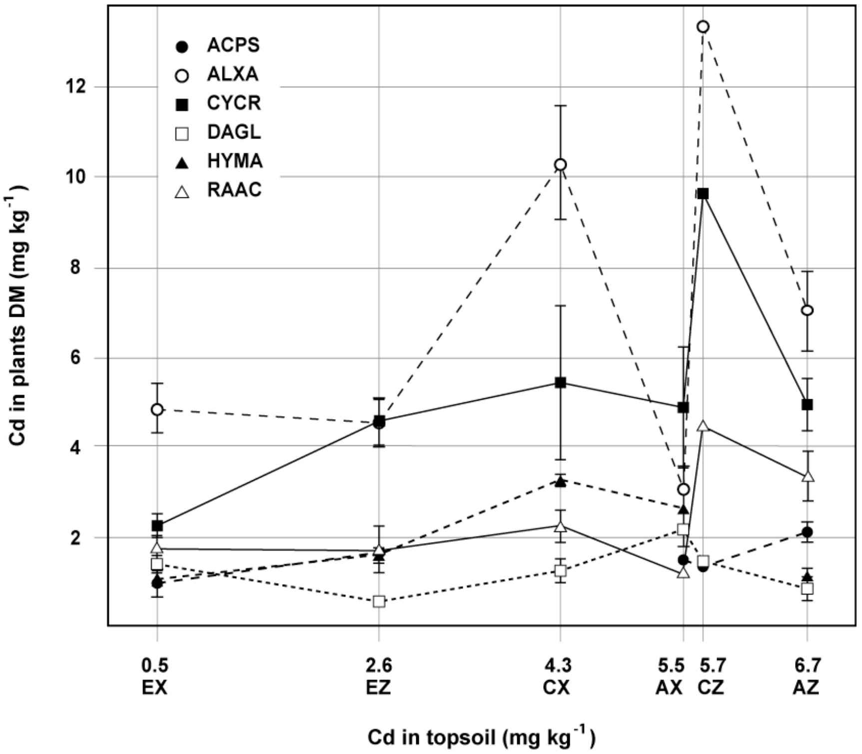

Figure 5.3 Global Cd concentrations in plants separated by species identity.

Figure 5.3 shows that Cd levels in all plant species gradually increase until they reach a maximum value in soil CX. They consequently drop to lower levels in soil AX as the detoxification mechanisms exposed in §5.4.1 may stop the transfer of Cd towards the shoots. The Cd uptake by plants in soil AZ raises again, which is probably due to the high levels present in the rhizosphere (over 10 mg·kg^{-1}). In this case the Cd is stocked mainly in the roots.

5.4.3 Cd uptake by plants as a function of soil type

Figures 5.4a and b depict Cd concentrations in each plant species plotted against soil type. A progressive increase in Cd uptake is observed for *Alchemilla x*. going from soils AX, AZ, CX to CZ, where a maximum value of 13.4 mg·kg^{-1} is reached. This may be explained by the decreasing concentrations in Cd as is discussed in §5.4.1. Cd levels in *Alchemilla x*. decreases in soils EX and EZ, which is mainly due to their lower Cd concentrations. A similar situation is observed for *Cynosurus c.*, with a maximum value of 9.7 mg·kg^{-1} in soil CZ. *Hypericum m.* appears to follow the same trend though the values do not change as clearly as for the two previous potential accumulators. *Ranunculus a.*, *Acer p.* and *Dactylis g*. do not follow a discernible trend.

(a)

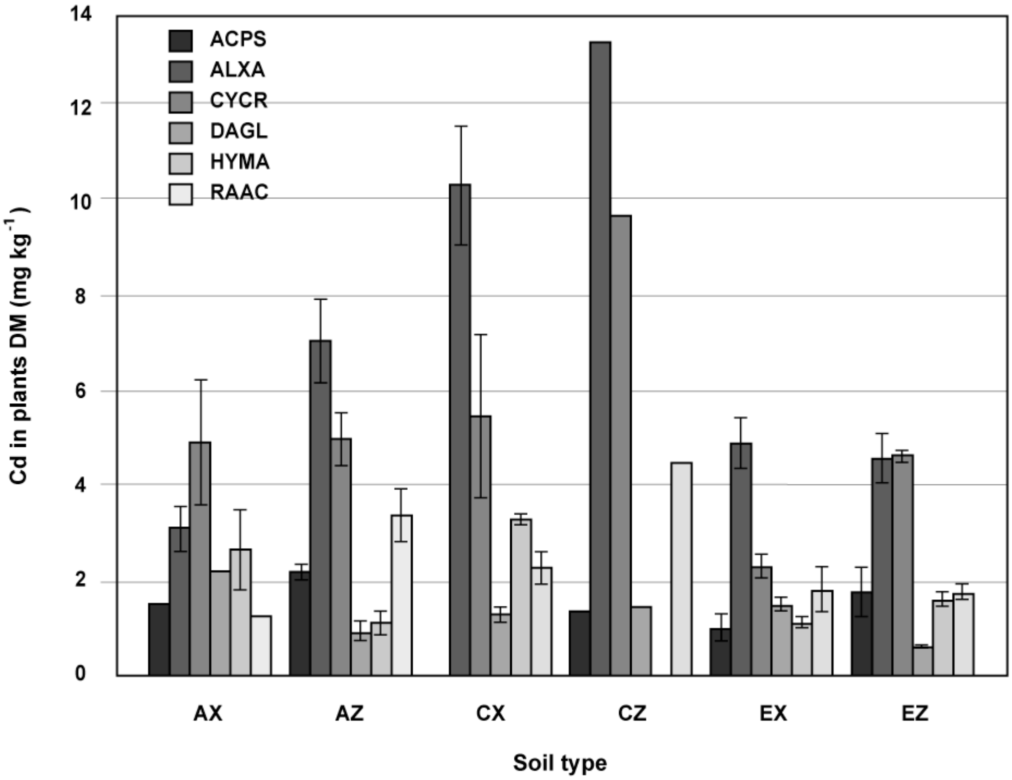

(b)

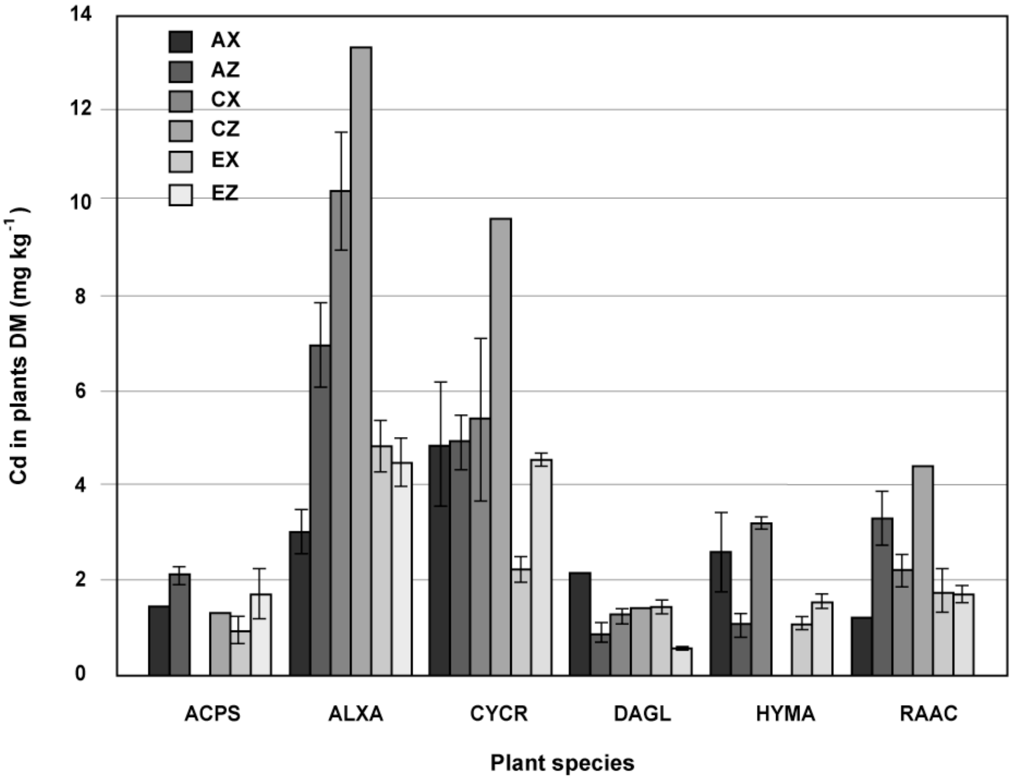

Figure 5.4 Cd concentration in plants as a function of (a) soil type; (b) species identity.

Table 5.8 summarizes estimations of Cd percentage in roots and shoots of each plant species for the six soil profiles. Soils are arranged by increasing Cd concentrations in the soil in order to compare the changes in Cd distribution between roots and shoots.

Table 5.8 Estimated percentages for the Cd distribution in roots and shoots. Soils are arranged by increasing mean Cd concentrations in the topsoils

Soil	Mean Cd	*Hypericum maculatum*		*Alchemilla xanthoclora*		*Cynosurus cristatus*	
		Cd_{roots}	Cd_{shoots}	Cd_{roots}	Cd_{shoots}	Cd_{roots}	Cd_{shoots}
	$mg\ kg^{-1}$	%		%		%	
EX	0.5	60.5	39.5	89.1	10.9	79.2	20.8
EZ	2.6	26.1	73.9	96.3	3.7	63.4	36.6
CX	4.3	15.4	84.6	81.2	18.8	45.6	54.4
AX	5.5	32.6	67.4	86.9	13.1	52.8	47.2
CZ	5.7	Not found		78.4*	21.6*	62.0*	38.0*
AZ	7.0	93.4	6.6	96.1	3.9	73.4	26.6

Soil	Mean Cd	*Ranunculus acris*		*Dactylis Glomerata*		*Acer pseudoplatanus*	
		Cd_{roots}	Cd_{shoots}	Cd_{roots}	Cd_{shoots}	Cd_{roots}	Cd_{shoots}
	$mg\ kg^{-1}$	%		%		%	
EX	0.5	47.0	53.0	84.0	16.0	60.5	39.5
EZ	2.6	60.2	39.8	71.7	28.3	77.5	22.5
CX	4.3	70.4	29.6	69.7	30.3	Not found	
AX	5.5	58.3*	41.7*	91.1	8.9	74.0	26.0
CZ	5.7	59.9*	40.1*	76.6*	23.4*	85.8*	14.2*
AZ	7.0	85.1	14.9	81.3	18.7	88.6	11.4

* Data calculated with only one individual

The soil composition, pH, organic matter, CEC and available mineral elements and interdependencies between these parameters may decrease or increase the availability of Cd for plants (Chizzola and Lukas, 2005; Kirkham, 2006). Plescher et al. (1995) reported that at lower soil pH, higher Cd bioaccumulation has been recorded in various medicinal plants, including a variety of *Hypericum maculatum*. Chizzola et al. (2005) found that in regression analyses, soil pH, soil organic carbon and soil Cd content were the main factors influencing Cd accumulation in the plant shoots. Despite these observations, Wermeille (1999) found that the pH of Le Gurnigel soils does not have a direct influence on Cd uptake by plants.

5.4.4 Transfer coefficents

The soil-plant transfer coefficient is obtained from the ratio of each detected metal concentration in plant tissues to that in soil (Kloke et al., 1984). It quantifies the relative differences in bioavailability of soil metal to plant and is a function of both soil and plant properties (Alloway, 1995). Typical transfer coefficients for Cd and other selected metals are shown in Table 5.9.

Table 5.9 Soil-plant transfer coefficients for Cd and selected trace elements

Element	Soil-plant transfer coefficient
Cd	1–10
Zn	1–10
Pb	0.01–0.1
Cr	0.01–0.1
Cu	0.1–10
Ni	0.1–1.0

From Kloke et al, 1994. Adapted from Alloway, 1995

Transfer from topsoil to rhizosphere

One of our goals was to determine whether the transfer of Cd from the topsoil to the rhizosphere depends on the total Cd concentration in the topsoil. Following the definition of a transfer coefficient, we calculated the transfer ratio from the distant soil (topsoil) to the rhizosphere as $[Cd]_{rhiz}/[Cd]_{topsoil}$ and plotted the obtained ratios as a function of Cd in the distant topsoil in Figure 5.5.

A significant linear regression (p-value = 2.319×10^{-7}, $R^2_{adj} = 0.5584$) and a positive Spearman's rank correlation (p-value = 1.814×10^{-10}; rho = 0.851) suggest that there exists a direct relation between these two variables. A rise in the Cd levels in the topsoil will produce an augmentation of Cd in the rhizosphere.

With regard to the influence of the plant species, a Kruskal-Wallis rank sum test (p-value = 0.9911) proves that the transfer of Cd from the topsoil to the rhizosphere does not depend on species identity, and only the physicochemical soil properties and changes therein will determine the degree of Cd mobilisation across the distant soil-rhizosphere interface.

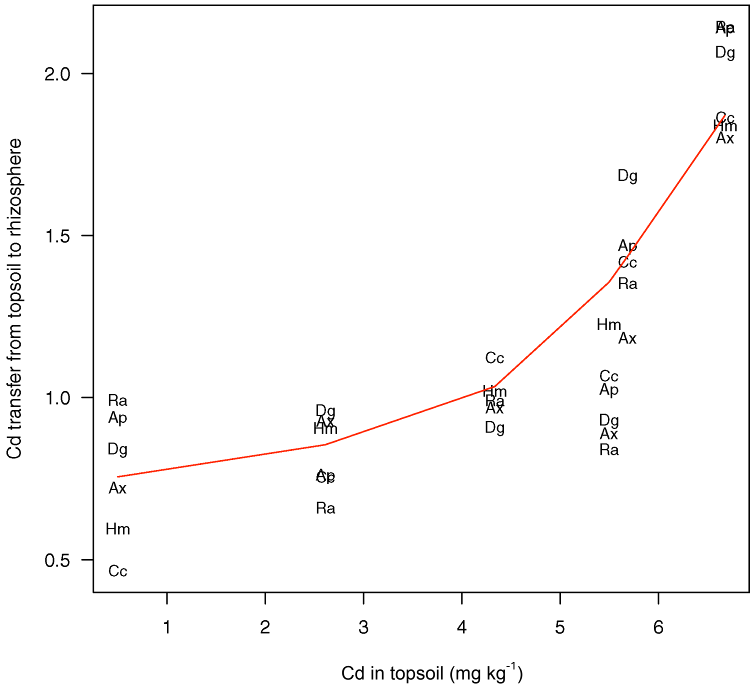

Figure 5.5 Effect of total Cd concentrations in the topsoil on the transfer from topsoil to the rhizosphere.

In order to determine whether the transfer of Cd from the topsoil to the rhizosphere depends on specific Cd-bearing fractions of the topsoil, linear regressions were applied by which the Cd transfer ratio as a function of Cd concentration in each soil fraction was kept as an independent variable. The results are presented in Figure 5.6. The horizontal red line proves that Cd associated with crystalline Fe-oxides, the residual phase, the exchangeable and carbonate phases provides significant fractions, which explain 80% of the variance. Organic matter has a reduced effect probably due to the binding of Cd to organic substances in the soil. Chizzola and Lukas (2005) reported that higher organic carbon content in the soil may result in lower Cd concentrations in the plant. Variations in the Cd distribution in rhizospheric soils (Fig. 5.1) are mainly observed for the first three fractions and especially for the exchangeable and carbonate fractions, which may be mainly due to their sensibility to an increase in pH in the rizhosphere. Changes in Cd concentrations bound to these fractions may therefore depend on a complex combination of plant physiological characteristics, initial Cd concentrations in the soil, and soil properties. Organic matter has a mixed influence on the transfer of Cd from the soil to the rhizosphere because in the rhizosphere this phase receives appreciable amounts of organic material from the roots, including exudates, mucilage, sloughed-off cells and their lysates. This is associated with a general rise in the microbial and biochemical activity (Dong et al., 2007). The addition of organic material in the rhizosphere will either dilute or increase Cd percentages derived from distant soils.

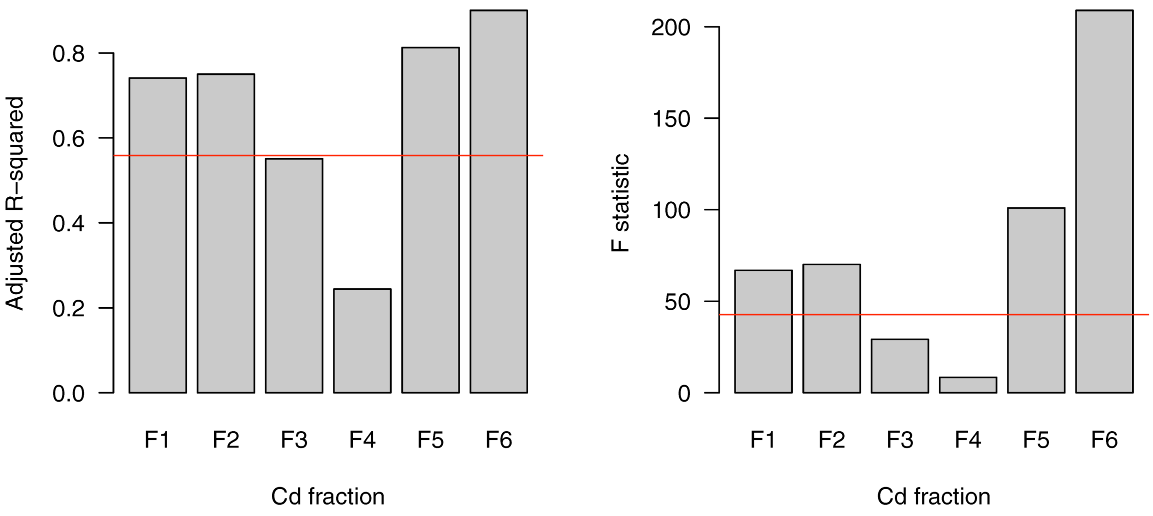

Figure 5.6 Evaluation of linear regressions between Cd transfer from the topsoil to the rhizosphere and Cd concentrations in each soil-bearing fraction. The horizontal red line corresponds to the R^2_{adj} coefficient (right) and F-value (left).

Amorphous oxyhydroxides appear to have a reduced influence because they are less important as a Cd-bearing phase in the topsoil in comparison to the in the subsoil. Cd percentages in these compounds are likely to increase when roots enter in contact with the subsoil as is the case in the shallow soils. This explains the increase in Cd bound to amorphous oxides observed in the rhizospheres of soil AZ. With regards to the deeper soils, the presence of Cd bound to this phase mainly depends on whether the roots reach the subsoil horizons rich in Cd adsorbed to amorphous oxyhydroxides. Deeper soils with lower pH and low CEC may favour the presence of bioavailable Cd with higher contents in the easily exchangeable phase. Furthermore, carbonates and organic matter will still be fractions susceptible to release Cd for plant uptake, especially in the case of a decrease of the pH in the rhizosphere. pH and redox conditions in the rhizosphere are not sufficient to mobilize Cd-bound to crystalline Fe-oxides (fraction 5) and residual matrix (fraction 6).

Transfer from rhizosphere to plants

The transfer coefficient of Cd from the rhizosphere to plants $[Cd]_{plant}/[Cd]_{rhiz}$ is presented in Figures 5.7 and 5.8 as a function of total Cd concentrations in the topsoil and the rhizosphere. We observe in both figures that the transfer coefficient is inversely proportional to both parameters. It has been already discussed in §5.4.1 that increasing concentrations of Cd in soils will lead to a decrease in its transfer rate towards the upper parts of plants.

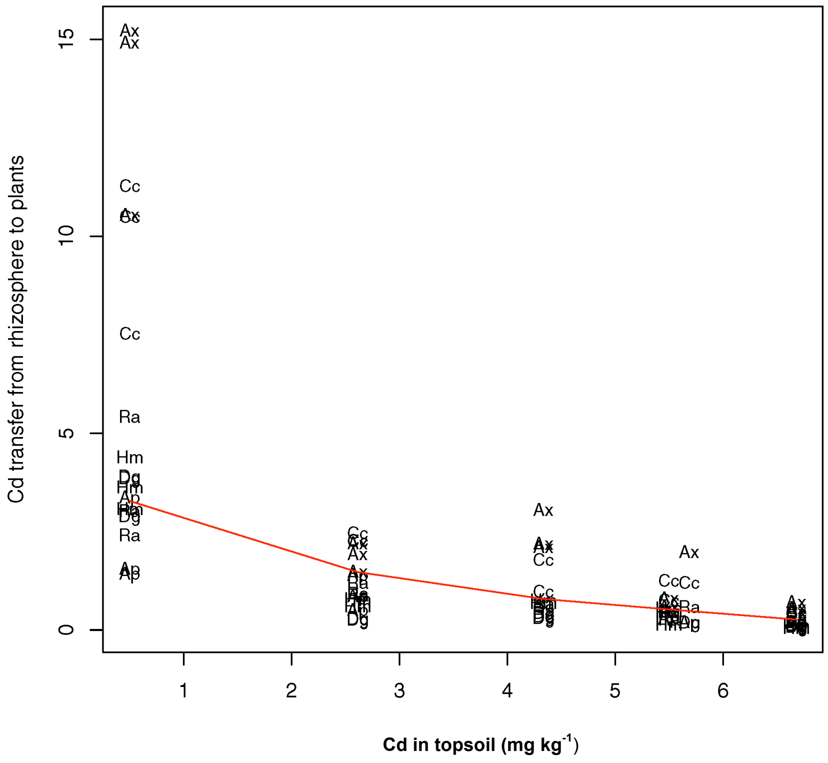

Figure 5.7 Effect of total Cd concentrations in the topsoil on the transfer of Cd from the rhizosphere to the plants.

Transfer from topsoil to plant

The transfer coefficient of Cd from topsoil to plant $[Cd]_{plant}/[Cd]_{topsoil}$ is presented in Figure 5.9 as a function of total Cd concentrations in the topsoil. As in Figure 5.7, the relation between the transfer from soil to plant is inversely proportional to Cd concentrations in the soil.

In order to determine whether the transfer from topsoil to plant depends on species identity, we applied a Kruskal-Wallis rank sum test. The obtained p-value = 0.0002841 (<0.05) suggests that the species identity plays an important role in Cd uptake.

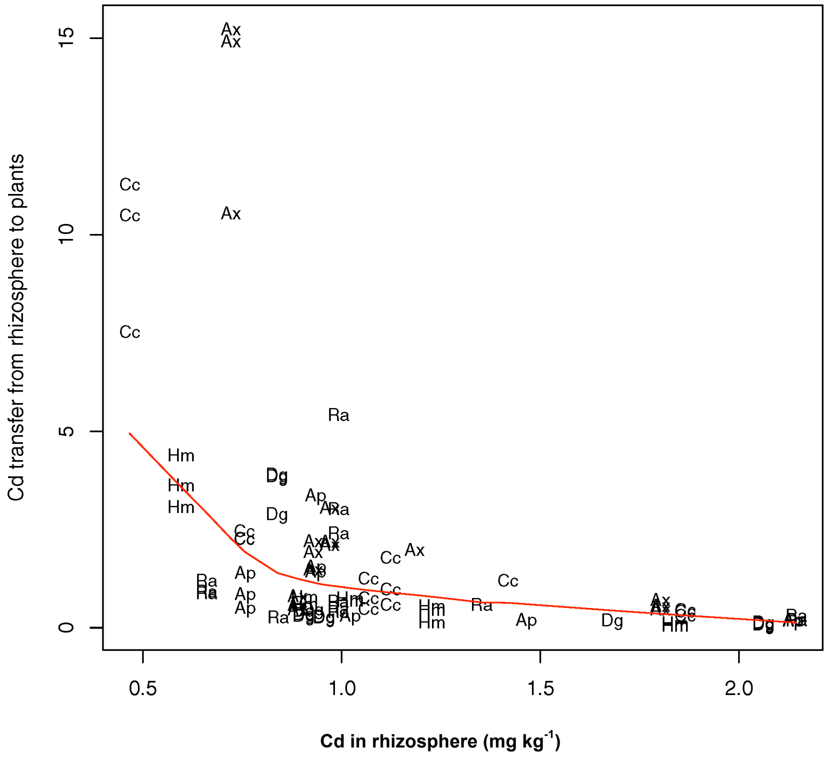

Figure 5.8 Effect of total Cd concentrations in the rhizosphere on the transfer of Cd from the rhizosphere to the plants.

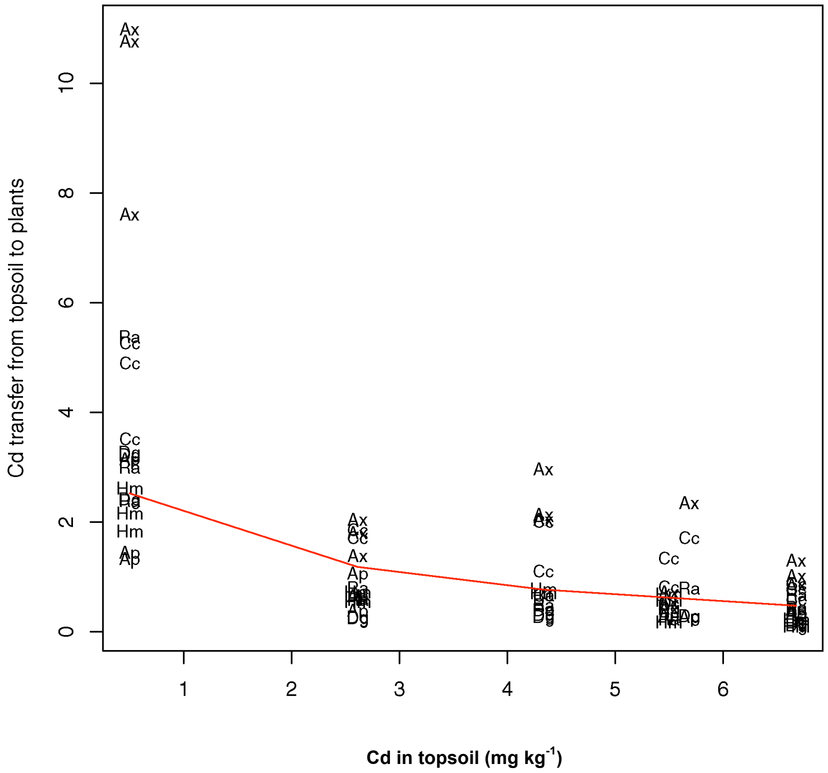

Figure 5.9 Effect of total Cd concentrations in the topsoil on the transfer of Cd from the topsoil to the plants.

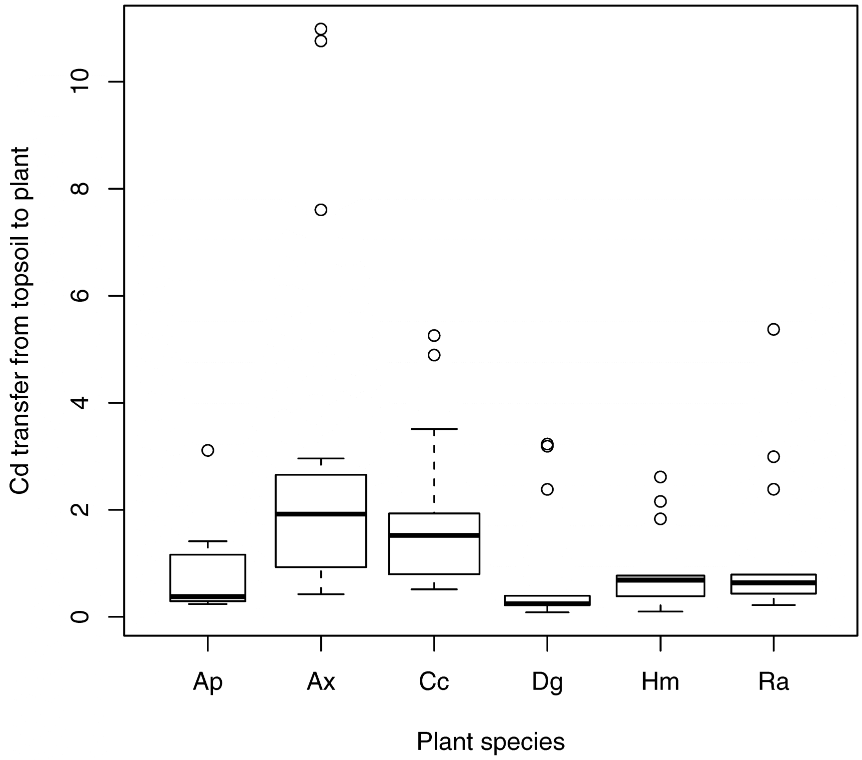

Figure 5.10 Box diagram showing the effect of species identity on the transfer from topsoil to plant.

The nearly symmetrical distributions of the box plots of *Alchemilla x.* and *Cynosurus c.* (Figure 5.10) confirm that these two plants have strong abilities to absorb and transfer Cd to the plant tissues since their coefficients reach the highest values, whereas the coefficient of *Dactylis g.* is the lowest. A further Kruskal-Wallis rank test (p-value = 3.606 x 10^{-08}; Fig. 5.11) confirms that the transfer from the topsoil to the plant depends on the soil type. Soil EX shows the highest transfer rate even though the plants growing in this soil record low concentration levels compared to those of the other soils. This may be explained by the low CEC value (6.4 cmol·kg^{-1}), the low pH (5.2) and the high percentages of exchangeable Cd in the rhizosphere (up to 21%) despite the low Cd concentrations in the topsoil (0.4 mg·kg^{-1}).

It has already been observed that plants growing on Cd-contaminated soils may present lower Cd bioaccumulation rates than when growing on soils with low Cd concentrations (Plescher et al., 1995; Hooda et al., 1997). In the evaluation of bioaccumulation rates, one has to consider, however, that higher rates may result for plant samples low in Cd when the corresponding soils are very low in Cd (Chizzola et al., 2005).

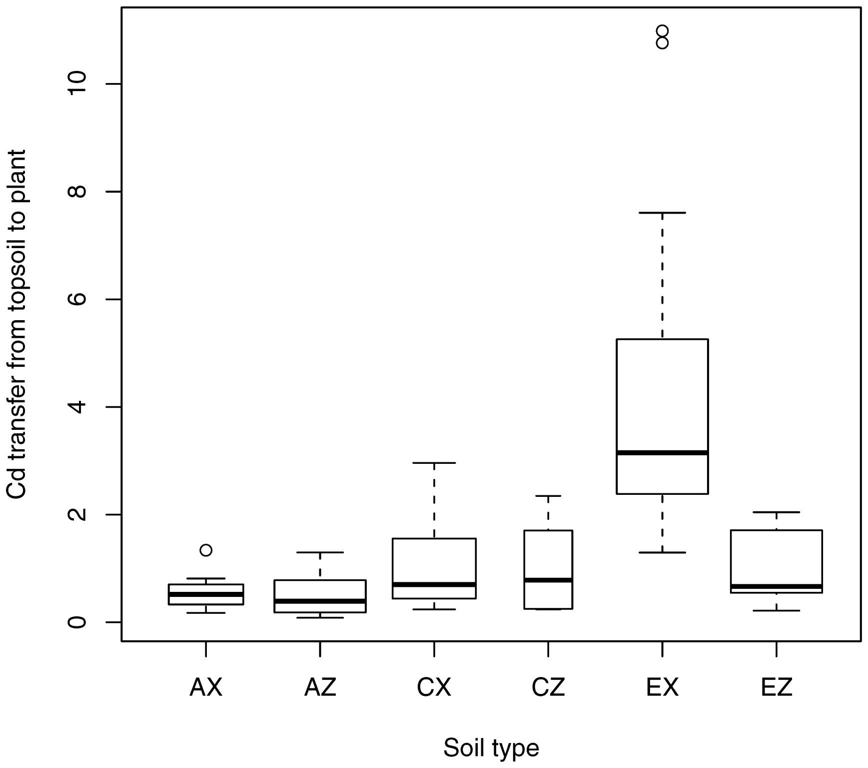

Figure 5.11 Box diagram showing the effect of soil type on the transfer from the topsoil to the plant.

5.4.5 Risk assessment of Cd in plants

Plants at the Le Gurnigel pasture are revealed to accumulate rather high levels of Cd in their roots and shoots. The main risk is represented by three species which happen to occur in high density in comparison to the other plant species selected here and which are used either by grazing livestock or as medicinal plants to treat specific health problems. The Cd concentrations observed in these plants exceed the official maximum concentration for animal food fixed at 1 mg·kg^{-1} and the tolerance limit value for cattle food (0.5 mg·kg^{-1}). However, the measured concentrations do not surpass the concentration level fixed at 30 mg·kg^{-1} (OSEC, 1995), above which a toxicity risk for animals is given. Yet they are likely to menace animal and human health on a long-term period by entering the food chain.

Alchemilla xanthochlora (Lady's Mantle)

This plant has been found to accumulate the highest cadmium concentrations. Mean values are in the 3–10 mg·kg^{-1} range. 81–96% of Cd is accumulated in roots (maxima 15 mg·kg^{-1}) though shoots present also important Cd contents (maxima 6 mg·kg^{-1}). As such, this plant represents a serious threat to human health since it is used because of its medicinal virtues. It has astringent and anti-inflammatory properties, controls bleeding and is taken as an infusion for menstrual and menopausal problems. It is also possible to use young leaves of this plant to prepare a variety of "salad of bitters".

Cynosurus cristatus (Crested Dog's-tail)

Being a typical species in grassland, it is used by grazing ungulate livestock. Cows ?? and sheep eat the young leaves eagerly, but leave the stiff, hard stems. It withstands the cold and drought and remains green during the winter. Since shoots of this plant contain Cd levels which range from 1.4 to 4.5 $mg \cdot kg^{-1}$, there exists a possible menace for animals by the long-term input of Cd to the food chain.

Hypericum maculatum (Spotted St. Johnswort)

The species of the genus *Hypericum* have been used as a remedy since ancient times, in particular to treat ulcers, burns, wounds, abdominal pains and bacterial diseases. Shoots of this plant contain Cd concentrations of up to 3.0 $mg \cdot kg^{-1}$, hence providing a risk for human health.

Ranunculus acris (Tall buttercup)

Shoots of this plant possess Cd concentrations in the 0.5–2.0 $mg \cdot kg^{-1}$ range. Even though these concentrations are somehow higher than the official limit values for animal food, the plant is not considered of risk since cattle pass it up. This plant, as well as other buttercups, contains ranunculin, which breaks down to the toxin protoanemocin, a chemical that can cause dermatitis and vomiting.

Dactylis glomerata (Orchard grass)

Orchard grass is ranked below other popular grass species for its nutritive value and is considered by many farmers to be poor. The low concentrations of Cd in shoots (up to 0.8 $mg \cdot kg^{-1}$) render this plant of minor concern.

Acer pseudoplatanus (Sycamore maple)

Young maple trees present rather low concentrations in Cd in their stems and leaves (0.7 $mg \cdot kg^{-1}$), though the root is able to uptake larger quantities of Cd (up to 5.5 $mg \cdot kg^{-1}$). The plant samples analyzed here do not present any signs of visible toxicity in the young leaves and root itself.

5.5 CONCLUSIONS

Plants growing at the Le Gurnigel pasture are susceptible to accumulate high levels of geogenic Cd. The six species analyzed here - *Hypericum maculatum, Alchemilla xanthochlora*, *Cynosurus cristatus, Ranunculus acris*, *Dactylis glomerata and Acer pseudoplatanus* - show global mean Cd concentrations, which range from 2 to 6 mg·kg^{-1}. The variability in Cd concentrations is related to soil type and its Cd content. The Cd concentrations in plants measured here exceed the maximal concentration tolerated in vegetal food for animals (1 mg·kg^{-1}). As a general rule, relative to the mean concentrations, the percentages of Cd concentrations in roots are higher than in shoots, and are a function of Cd concentrations in soil, though the proportions may strongly vary from one species to another. Nevertheless, shoots of some plants (*Alchemilla xanthochlora*, *Cynosurus cristatus, Hypericum maculatum*) may reach maximum concentrations in the 3–13 mg·kg^{-1} range, depending on species identity. As such, these plant species may represent a long-term hazard for animals and human health given that they are used either by grazing livestock or for medicinal purposes. *Ranunculus acris*, *Acer pseudoplatanus* and *Dactylis glomerata* are of lower concern.

It is estimated that plants in soils containing up to 4 mg Cd·kg^{-1} will progressively accumulate Cd in their different parts. However, when growing in soils with higher concentrations, plants are thought to use a detoxification mechanism which induces them to stock Cd in roots by a series of organic-ligand complexation mechanisms, and as such reduce the transport of Cd ions toward the shoots, thereby also reducing the yield production. This may explain the inverse relationship between Cd transfer coefficients from the distant soil / rhizosphere to the plants and the total Cd concentration in soils. Yet the Cd transfer coefficients will also depend on soil type. Soils with low CEC and low pH (5) will favour the transfer of Cd from the soil to the plant. The transfer of Cd from the topsoil to the rhizosphere does not depend on species identity, but on the physicochemical changes at the soil-rhizosphere interface. The exchangeable, carbonate and organic-matter fractions associated with Cd are mainly affected by the incorporation of roots exudates, which modify pH and redox conditions in the rhizosphere, thereby increasing the bioavalaibility of Cd.

5.6 REFERENCES

Agence de l'Environnement et de la Maîtrise de l'Energie, 2010. Sites pollués et sols. Phytoextraction. Available on http://www2.ademe.fr/.

Alloway, B. J., 1995. Cadmium. In: B.J. Alloway (Editor), Heavy Metals in Soils. Blackie Academic and Professional, Glasgow, pp. 122–151.

Benitez, L. N., 1999. Cadmium speciation and phyto-availability in soils of the Swiss Jura: hypothesis about its dynamics. Ph.D. Thesis, Ecole Polytechnique Fédérale de Lausanne, Switzerland.

Chaney, R. L. and Giordano, P.M., 1977. In: L.F. Elliot and F.J. Stevenson (Editors), Soils for the management of organic wastes and waste waters. Soil Sci. Soc. Am., Am. Sox. Agron & Crop Sci. Soc. Am., Madison, pp. 235–279.

Chizzola, R. and Lukas, B., 2005. Variability Of The Cadmium Content In Hypericum Species Collected In Eastern Austria. Water, Air & Soil Pollution, Vol. 170, No. 1–4, pp. 331–343.

Cieslinski, G., Neilsen, G.H., & Hogue, E.J. (1996). Effect of soil cadmium application and pH on growth and cadmium accumulation in roots, leaves and fruit of strawberry plants (Fragaria X ananassa-Duch.). Plant and Soil, 180 (2), 267–276.

Dong, J., Mao, W.H., Zhang, G.P., Wu, F.B., Cai, Y. Root excretion and plant tolerance to cadmium toxicity – review. Plant Soil Environment, 53 (5), pp. 193–200.

Dubois, J. P., Benitez, N., Liebig, T., Baudraz, M. and Okopnik, F., 2002. Le cadmium dans les sols du haut Jura suisse. In D. Baize and M. Tercé (Editors), Les élements traces métalliques dans les sols. Approches fonctionelles et spatiales. INRA, Orléans, pp. 33–52.

Florijn, P. J. and van Beusichem, M. L., 1993. Uptake and distribution of cadmium in maize inbred lines. Plant and Soil 150, 25–32.

Food and Agriculture Organization of the United Nations FAO, 2006. World reference base for soil resources 2006. A framework for international classification, correlation and communication. FAO, Rome.

Hooda, P. S., McNulty, D., Alloway, B. J. and Aitken, M. N., 1997. Plant availability of heavy metals in soils previously amended with heavy applications of sewage sludge. J. Sci. Food Agric. 73, 446–454.

Kirkham, M.B., 2006. Cadmium in plants on polluted soils: Effects of soil factors, hyperaccumulation, and amendments. Geoderma 137, pp. 19–32

Kloke, A., Sauerbeck, D.R. and Vetter, H., 1994. In: J., Nriagu (Editor), Changing Metal cycles and human health. Springer-Veriag, Berlin, pp. 113.

Krauss, M., Wilcke, W., Kobza, J. and Zech, W., 2002. Predicting heavy metal transfer from soil to plant: potential use of Freundlich-type functions. Journal of plant nutrition and soil science, Vol. 165, No.1, pp. 3–8

Lehoczky, E., Szabados, I., & Marth, P. (1996). "Cadmium content of plants as affected by soil cadmium concentration". Communication in Soil Science and Plant Analysis, 27 (5–8), 1765–1777.

Malko, A., 2002, Untersuchung zum Wirkstoffgehalt, zur Cadmiumaufnahme und Rotwelkeanfälligkeit von Hypericum perforatum L. Dissertation Justus-Liebig-Universität Gießen, Germany, 2002, 163 pp.

McBride, M.B., 2002, Cadmium uptake by crops estimated from soil total Cd and pH. Soil Science, 167, 62–67.

Okopnik, F., 1997, Relation entre la variabilité spatiale du Cd et la couverture pédologique de la region du Mon d'Amin. Diploma thesis, Ecole Polytechnique Fédérale de Lausanne, Switzerland.

Prudente, D., 1999. Distribution des teneurs naturelles en cadmium dans les sols de la forêt communale des Fourgs (Doubs, France). Ph.D. Thesis, Ecole Polytechnique Fédérale de Lausanne, Switzerland.

Prudente, D., Baize, D. and Dubois, J.P., 2002. Le cadmium naturel dans une forêt du haut Jura français. In: D. Baize and M. Tercé (Editors), Les élements traces métalliques dans les sols. Approches fonctionelles et spatiales. INRA, Orléans, pp. 53–70.

Puschenreiter, M. and Horak, O., 2000. Influence of different soil parameters on transfer factor soil to plant of Cd, Cu and Zn for wheat and rye, Die Bodenkultur 51, 3–9.

Sauerbeck, D.R. (1991). "Plant, element and soil properties governing uptake and availability of heavy metals derived from sewage sludge". Water Air and Soil Pollution, 57–58, 227–237.

Schneider, E., Pank, F., Koball, G., Foltys de Garcia, E., Dehe, M. and Blüthner, W. D., 2002. Einfluss von Genotyp und Umwelt auf die Cadmiumaufnahme des Johanniskrautes (Hypericum perforatum L.), Z. Arnzei- und Gewürzpflanzen 7, 329–335.

Soon, Y.K. and Abboud, S., 1993. Cadmium, Chromium, Lead, and Nickel. In: M.R. Carter (Editor), Soil sampling and methods of analysis. Canadian Society of Soil Science, pp. 101–107.

The Federal Authorities of the Swiss Confederation, 1995. Département fédéral de l'intérieur, Ordenance fédérale sur les substances étrangères et les composants dans les denrées alimentaires. Ordonnance sur les substances étrangères et les composants, OSEC. Official Publications Centre, Switzerland.

The Federal Authorities of the Swiss Confederation, 1998. RS 814.12 Ordonnance sur les atteintes portées aux sols (OSol). Annexe 2., Valeurs indicatives, seuils d'investigation et valeurs d'assainissement pour les métaux lourds et le fluor dans les sols. Official Publications Centre, Switzerland.

U.S. Environmental Protection Agency (EPA), 1994. Test Methods for Evaluating Solid Waste, SW-846, 3rd ed., Office of Solid Waste and Emergency Response, Washington, D.C.

Wermeille, C., 1999. Biodisponibilité du cadmium dans les sols du Gurnigel (Jura neuchâtelois). Diploma thesis, Ecole Polytechnique Fédérale de Lausanne, Switzerland.

Wild, A. (Editor), 1988. Russell's soil conditions and plant growth. 11th edition. Longman, London.

CONCLUSIONS

CHAPTER 6

CONCLUSIONS

6.1 ROCK–SOIL INTERACTIONS

6.1.1 Origin of Cd in soils

Oolitic carbonates of Bajocian age in the Swiss Jura Mountain chain show the presence of anomalous enrichments in cadmium of up 4.91 mg·kg^{-1}. Soils associated with these rocks are susceptible to be enriched in Cd. As such, cadmium contents in the soils of Scheleifenberg reach a maximum value of 2.0 mg·kg^{-1} while Cd concentrations in Le Gurnigel soils reach higher values up to 16 mg·kg^{-1}, thereby exceeding the official Swiss indicative guideline value for non polluted soils fixed at 0.8 mg·kg^{-1}. This phenomenon is observed even in soils formed after an early formation stage on allochthonous aeolian silt material. The continuous dissolution of the underlying Cd-rich carbonates drives the release of Cd and other trace metals, which are subsequently incorporated into different phases in the corresponding soils by actual pedogenic processes in the ongoing soil evolution. The weathering of the bedrock provides both inherited compounds as well as newly formed minerals such as mixed-layer clays (illite-smectite, vermiculite-illite), hydrous oxides and amorphous oxyhydroxides which will retain trace metals by adsorption phenomena, in addition to organic matter.

Additional aeolian Cd input during early soil formation on top of allochthonous loess deposits of crystalline origin is excluded since no correlation exists between Cd contents in soils and the minerals considered of allochthonous origin (chlorite in the silt and clay fractions, K-feldspar and Na-plagioclase in the bulk mineralogy). Moreover, the increasing Cd concentrations towards the bottom observed in shallow and deep soil profiles is a signature of the geogenic origin of Cd.

6.1.2 Cd_{rock} and Cd_{soil}

It is hard to establish a direct relationship between the concentrations of Cd in soil and that of the underlying rock. It is assumed that the Cd concentrations in the analysed soil profiles are determined by the following variables:

- Cd concentrations in the bedrock, where Cd is quite heterogeneously distributed on all scales. Vertical pedogenetic processes will incorporate Cd in soils after parent rock dissolution.

- The physical-chemical properties of soils including depth, chemical composition and mineralogical assembly.

- The topography of the site or ground relief. Where developed on steep slopes the soil will hardly accumulate and displaced weathered material will constantly renew it.

- Lateral inclusion of debris generated by the weathering and erosion of uphill carbonates. The short-distant allochthonous fragments may act both as a Cd source when coming from a Cd-rich source (carbonates or soils) as well as a dilution factor when Cd-lean material roll downhill and cover the soil.

These components render a nonlinear relationship between Cd contents in bedrock and associated soil likely.

6.2 CD DYNAMICS IN SOILS

A complex transfer pattern of Cd is proposed for the analysed soil profiles, which starts with the release of Cd from the underlying bedrock, and its transfer into oxide, hydroxide, carbonate and organic phases. Additionally, the lateral advection of Cd-rich particles released from neighbouring slopes acts as a local allochthonous input of Cd, which is transferred from the topsoil towards the deeper horizons by biological and pedogenic processes.

6.2.1 Calcaric cambisol at the Schleifenberg hill

At the Schleifenberg hill (canton Basel-land) Fragmented calcareous material is incorporated in soils and pH of soils remains neutral (7.2). Under such conditions 50% of Cd remains associated with carbonates while Cd released after carbonates weathering becomes associated with Fe-oxyhydroxides (approximately 30%), organic matter (over 10%), and a small fraction with Mn-oxides (4%) and clay minerals (2%). As no Cd exchangeable phases were found in the soil, the risk that Cd becomes mobilised is low provided that the pH of the soil remains neutral. The competition of other trace metals (Zn, Pb, Cr, Ni, Cu) and also Al will be moderate and mainly concerns adsorption surfaces on clays and organic matter.

6.2.2 Shallow cambisols at Le Gurnigel

Soils at Le Gurnigel are in a continuous pedogenic evolution after an early formation stage on allochthonous aeolian silt material. All analysed soils show a high decarbonation state. Shallow cambisols are not deeper than 40 cm because of their position on hill flanks. Their topsoil contains Cd, which is mainly distributed in the carbonate phase (48%) and the organic matter phase (24%). The amorphous oxyhydroxides become a more important Cd-bearing phase in the subsoil with 33% of the total Cd contents followed by the carbonate phase (26%) and crystalline Fe oxides (17%).

6.2.3 Deep cambic-neoluvisols at Le Gurnigel

Cd in the topsoil is mainly bound to the carbonate phase (40%) and organic matter (20%). Amorphous oxyhydroxides and crystalline Fe-oxides in the middle part and deeper horizons are the most important Cd-bearing phases with mean percentage distributions of 35% and 25%, respectively. The beginning of eluviation processes along with a diminution of the pH in the middle of the profile could explain the observed decrease in Cd. As a consequence, clays, oxides and hydroxides are leached and dragged down the solum along with the adsorbed Cd into the deeper illuviation horizons, where Cd-bearing mineral concretions, composed of a variable mixture of quartz, phyllosilicates and amorphous oxyhydroxides, are formed.

Cd distribution in the Le Gurnigel soils may therefore be governed by the following soil components: goethite (Gt), calcium (Ca), total organic carbon (TOC), iron (Fe), aluminium (A)l, block mixed-layer illite-smectite clays (IS-B) and the C/N ratio.

6.3 CD BIOAVAILABILITY

6.3.1 Schleifenberg soils

Slightly acidic rainfall runoff becomes easily neutralized by the buffer capacity of this soil due to the large amounts of calcareous material present in this area. Under these conditions the capacity to transfer Cd^{2+} ions into solution, or leach it out of the soil seems quite negligible. The bioavailability of Cd is therefore reduced provided that the neutral conditions of soil do not change to more acidic pH values. Nevertheless, a direct uptake of Cd by plants through the dissolution of calcareous particles remains possible and this aspect needs further research for this site.

6.3.2 Le Gurnigel soils

The potentially bioavailable Cd issued by the readily exchangeable fraction is quite low along the soil profiles (mean value of 0.2 mg·kg^{-1}) provided that the pH of soils remains above 5. It is likely that organic acids, excreted by plant roots, have the capacity to dissolve additional Cd from the carbonate phase. This dissolution would produce higher contents of bioavailable Cd in the topsoil of cambisols reaching a mean concentration of 3.0 mg·kg^{-1}. Bioavailable Cd in the cambic-neoluvisols is predominantly located in the topsoil, where maximum concentrations may amount to 1.2 mg·kg^{-1}. It decreases in the middle part with mean low concentrations of 0.2 mg·kg^{-1}, representing thus a lower risk compared to the cambisols. Under stronger acidic ($pH < 4.5$) and oxidizing conditions, Cd bound to organic matter would be mobilised and the bioavailability of Cd would range between 3.3–5.4 mg·kg^{-1} in cambisols and around 1.7 mg·kg^{-1} in cambic-neoluvisols.

6.4 SOIL-PLANT INTERACTIONS

Plants growing at the Le Gurnigel pasture are susceptible to accumulate high levels of geogenic Cd. Global mean concentrations of Cd in the vegetation range from 2 to 6 mg·kg^{-1}; a variability that changes according to soil type and the in Cd concentrations. Cd levels in plants exceed the maximum concentration tolerated in vegetal-food for animals (1 mg·kg^{-1}). As a general rule, the percentage of Cd in roots are higher than that of shoots, though the proportions may strongly vary from one species to another, as a function of Cd concentrations in soil. Nevertheless shoots of Crested dogstail grass, Spotted St. Johnswort, and Lady's mantle in particular, appeared with maximum concentrations in the 3–13 mg·kg^{-1} range depending on species identity. Under these considerations, the site may result in a mid-term hazard for animals and human health given that dogstail grass is used mainly for grazing of cattle and both herbs are used for medicinal purposes. Tall buttercup, Orchardgrass and Sycamore maple are plants of lower concern.

It is estimated that plants in soils containing up to 4 mg Cd·kg^{-1} will progressively accumulate Cd in their different parts. However, when growing in soils with higher concentrations, plants are thought to use a detoxification mechanism which induces them to reduce the transport of Cd ions toward the shoots, thereby reducing also the yield production and stocking Cd in roots by a series of organic-ligands complexation mechanisms. Soils with low CEC contents and acidic ph (5) will favour the transfer of Cd from soil to plant. The transfer of Cd from the topsoil to the rhizosphere does not depend on species identity, but on the physicochemical changes in the soil-rhizosphere interface. The exchangeable, carbonates and organic matter fractions are mainly affected by the incorporation of roots exudates that modify pH and redox conditions in the rhizosphere increasing thus the bioavalaibility of Cd.

ACKNOWLEDGMENTS

Special thanks to:

Karl Föllmi (Director) and Virginie Matera (Supervisor) for guiding my work from the beginning, providing advice and assistance in numerous ways. The Commission fédérale des bourses pour étudiants étrangers for financing the first two years of my Ph.D.

I gratefully acknowledge:

Claire Le Bayon, Denis Baize, Eric Verrecchia, François Gillet, Jean-Michel Gobat, Thierry Adatte for their help answering my questions in their field of expertise.

I am deeply grateful to:

Aline Michaud, Andrea Stadler, Andreea Uta, Anita Serrano, Beat Strittmatter, Brizeida Mendieta, Carla Santos, Carolina Briñez, Cécile Guex-Joris, Christina Glunk, Claire Rambeau, Cristina Bossi, Delphine Bavarel, Diego Villagomez, Edba Ritz, Elodie Nogues, Eric Bouchaud, Eric Rios, Fabian Blobel, Fabienne Luisier, Fabio Arandia, Familia Acosta-Lamas, Familia Arandia-Loayza, Familia Arellano-Pericon, Familia Cortés, Familia Garcia-Alvarez, Familia Hinojosa-Ledezma, Familia Montero-Tavera, Familia Pericon-De Chazal, Familia Rios-Ardaya, Familia Tapia-Ochoa, Federica Galliotto, Federica Orlando, Fernando Subilibia, Francesca Ciulli, Francesca De Gaspari, Francesco Venturin, Gilles Farron, Gordana Botalla, Grégoire Phyton, Haydon Mort, Herbert Müller, Igor Loayza, Ivette Loayza, Ivonne Prado, Jeannette Jornod, Jesus Garcia, Joëlle Farine, Katia Ferro, Khadija, Laura Elmiger, Leonardo Fonseca, Lise Dummermuth, Luis Maldonado, Marcia Arandia, Mario Andrade, Marta Bogino, Martina Mangold, Melanie Meyer, Michell Alvez, Monica Sanchez, Montse Cazorla, Narel Loayza, Natalia Efimenko, Nataliya Tertychna, Nicole Jeanneret, Octavio Hinojosa, Olivier Jacquat, Pamela Loza, Paola Loayza, Pascal Linder, Peter Andres, Rébecca Geissbühler, Regula Brenz, Ronal Gainza, Rosario Revollo, Salomé Bruneau, Sandrine Gungerich, Sandro Quezada, Serena Traversa, Séverine Vancolen, Silvano Quezada, Silvia Minuzzo, Sopna Kalapurakal, Stephan Ritz, Stéphanie Meylan, Tiffany Monnier, Veronica Garcia, Véronique Miéville, Wilson Acosta and Xenia Boutsiadou...each of whom has brought to my thesis strengths that have helped make this a successful project.

And a very special thank to:

Maria René Zuna for her beloved support, patience and creative talent to design the covers of the present work.

APPENDIX

APPENDIX A

Table A.1 Schleigfenberg: Location of soil samples according to the stratigraphical section depth.

Rock Sample	[Cd]rock (mg kg^{-1})	Section depth (m)	Soil sample	[Cd]soil (mg kg^{-1})
R 1	0.33	94.95		
R 2	0.32	94.55		
		92.91	**S47**	**1.10**
R 5	0.16	92.80		
R 7	0.08	92.00		
R 9	0.14	91.15		
R 12	0.14	89.40		
		88.79	**S46**	**0.73**
R 14	0.06	88.35		
R 16	0.68	86.85		
R 18	0.05	85.55		
R 19	0.09	84.95		
R 20	0.11	84.30		
R 21	0.05	83.55		
R 22	0.07	82.90		
R 23	0.10	82.70		
R 24	0.09	82.00		
R 25	0.07	81.20		
		80.75	**S45**	**1.07**
R 26	0.04	80.70		
R 27	0.09	79.90		
R 28	0.09	79.30		
R 29	0.58	78.30		
R 30-1	0.68	77.70		
R 32-1	0.78	76.50		
R 33	0.24	75.05		
R 34	0.57	74.65		
R 34	0.21	74.60		
R 35	0.08	73.60		
		73.22	**S44**	**0.67**
R 36	0.03	73.00		
R 37	0.03	72.80		
R 38	0.10	71.95		
R 39	0.04	70.50		
R 40	0.04	69.80		
R 41	0.06	69.25		
R 42	0.03	68.45		
R 45	0.04	66.35		
R 46	0.03	65.25		
R 47	0.04	64.95		
R 48	0.06	64.05		
R 49	0.07	63.20		
R 50	0.09	63.00		
R 51	0.04	62.25		
R 52	0.04	61.60		
R 53	0.10	60.90		
R 54	0.09	60.05		
R 55	0.12	59.40		
R 56	0.17	58.90		
R 57	0.12	58.70		
R 58	0.23	58.30		
R 59	0.13	57.55		
R 60	0.19	56.90		
R 61	0.32	56.40		
R 62	0.16	55.70		
R 63	0.60	55.00		
R 64	0.61	54.50		
		54.05	**S43**	**1.02**
R 65	0.31	53.45		
R 66	0.15	52.85		
R 67	0.45	51.85		
R 68	0.15	51.30		
R 69	0.13	51.10		
R 70	0.26	50.40		
R 71	0.26	50.20		
R 72	0.11	49.20		
R 73	0.11	48.70		
R 74	0.16	48.00		
R 75	0.21	47.50		
R 76	0.28	47.10		
R 77	0.13	46.50		
R 78	0.13	45.90		
R 79	0.25	45.45		
R 80	0.41	44.90		
R 81	0.88	44.40		
R 82	0.22	43.80		
R 83	0.60	43.10		
R 84	0.28	42.60		
R 85	0.09	41.70		
R 86	0.05	41.00		
R 89	0.15	39.20		
R 91	0.19	37.75		
R 94	0.17	36.10		
R 97	0.34	34.30		
R 98	0.15	33.60		
R 99	0.33	32.85		
R 100	0.40	32.20		
R 101	0.09	31.75		

Table A.1 (continued)

Rock Sample	[Cd]rock (mg kg^{-1})	Section depth (m)	Soil sample	[Cd]soil (mg kg^{-1})
S 102	0.14	31.25		
R 103	0.22	30.65		
R 104	0.11	29.70		
R 105	1.49	28.80		
R 106	0.25	28.20		
R 107	0.26	27.45		
R 108	0.24	27.05		
R 109	0.19	26.45		
R 110	0.51	26.25		
R 111	0.41	25.80		
R 112	0.30	25.20		
		24.77	**S42**	**0.71**
R 113	0.04	24.60		
R 114	0.19	24.00		
R 115	0.00	23.10		
R 116	1.50	22.25		
		22.24	**S41**	**0.83**
		22.10	**S40**	**0.75**
		21.96	**S39**	**0.75**
R 117	0.10	21.90		
		21.82	**S38**	**0.71**
		21.67	**S37**	**0.83**
		21.39	**S36**	**0.92**
R 118	0.17	21.35		
		21.11	**S35**	**0.67**
		20.82	**S34**	**0.92**
R 119	0.20	20.65		
		20.54	**S33**	**0.67**
		20.25	**S32**	**0.58**
R 120	0.06	20.10		
		19.97	**S31**	**0.75**
R 121	0.04	19.70		
		19.69	**S30**	**0.75**
		19.54	**S29**	**0.81**
		19.40	**S28**	**0.70**
		19.26	**S27**	**0.79**
		19.12	**S26**	**0.75**
		18.98	**S25**	**0.80**
		18.83	**S24**	**0.92**
R 122	0.06	18.80		
		18.69	**S23**	**0.84**
		18.55	**S22**	**0.83**
		18.41	**S21**	**1.14**
R 123	0.42	18.30		
		18.27	**S20**	**1.05**
		18.12	**S19**	**0.60**
		17.98	**S18**	**0.79**
		17.84	**S17**	**0.81**
		17.70	**S16**	**0.74**
R 124	0.28	17.65		
		17.41	**S15**	**0.73**
R 125	0.15	17.25		
		17.13	**S14**	**0.71**
R 126	0.12	17.10		
R 127	1.26	16.20		
R 128	0.30	15.55		
R 129	0.23	15.05		
R 130	0.09	14.60		
R 131	0.32	14.00		
		13.45	**S13**	**1.00**
R 132	0.75	13.45		
R 133	0.09	13.30		
R 134	0.44	12.70		
R 135	0.26	12.25		
R 136	0.18	11.40		
		10.90	**S12**	**0.67**
R 137	0.11	10.90		
R 138	0.05	9.95		
		9.18	**S11**	**0.69**
R 139	0.08	9.50		
R 140	0.00	9.00		
R 141	0.06	8.25		
R 142	0.16	8.05		
R 143	0.11	7.40		
R 144	0.04	7.00		
		6.91	**S10**	**0.92**
		6.62	**S9**	**2.00**
R 145	0.08	6.50		
		6.34	**S8**	**0.67**
		6.05	**S7**	**0.92**
R 146	0.06	5.95		
		5.77	**S6**	**0.50**
		5.49	**S5**	**0.67**
		5.20	**S4**	**0.92**
R 147	0.29	5.05		
		4.92	**S3**	**0.92**
R 148	0.00	4.65		
R 149	0.11	3.60		

Table A.1 (continued)

Rock Sample	[Cd]rock (mg kg^{-1})	Section depth (m)	Soil sample	[Cd]soil (mg kg^{-1})
R 150	0.17	3.05		
		2.45	**S2**	**0.33**
R 151	2.34	2.45		
R 152	0.13	1.70		
		1.22	**S1**	**0.68**
R 153	1.04	1.20		
R 154	0.34	1.00		
R 155	0.10	0.35		
R 156	0.04	0.00		

Cd concentrations in rocks and section depth were measured by Rambeau (2006)

Table A.2 Schleifenberg: Geometrical relation between soil cover length and bedrock section depth

Sampling Transect	Sample	Section depth (m)	Soil cover (m)	[Cd]soil (mg kg^{-1})
Upper Points	S47	92.91	327.11	1.10
	S46	88.79	312.61	0.73
	S45	80.75	284.31	1.07
	S44	73.22	257.81	0.67
	S43	54.05	190.31	1.02
	S42	24.77	87.21	0.71
T1	S41	22.24	78.31	0.83
	S40	22.10	77.81	0.75
	S39	21.96	77.31	0.75
	S38	21.82	76.81	0.71
	S37	21.67	76.31	0.83
	S36	21.39	75.31	0.92
	S35	21.11	74.31	0.67
	S34	20.82	73.31	0.92
	S33	20.54	72.31	0.67
	S32	20.25	71.31	0.58
	S31	19.97	70.31	0.75
	S30	19.69	69.31	0.75
	S29	19.54	68.81	0.81
	S28	19.40	68.31	0.70
	S27	19.26	67.81	0.79
	S26	19.12	67.31	0.75
	S25	18.98	66.81	0.80
	S24	18.83	66.31	0.92
	S23	18.69	65.81	0.84
	S22	18.55	65.31	0.83
	S21	18.41	64.81	1.14
	S20	18.27	64.31	1.05
	S19	18.12	63.81	0.6
	S18	17.98	63.31	0.79
	S17	17.84	62.81	0.81
	S16	17.70	62.31	0.74
	S15	17.41	61.31	0.73
	S14	17.13	60.31	0.71
	S13	13.45	47.36	1.00
	S12	10.90	38.38	0.67
	S11	9.18	32.31	0.69
T2	S10	6.91	24.31	0.92
	S9	6.62	23.31	2.00
	S8	6.34	22.31	0.67
	S7	6.05	21.31	0.92
	S6	5.77	20.31	0.50
	S5	5.49	19.31	0.67
	S4	5.20	18.31	0.92
	S3	4.92	17.31	0.92
Lower Points	S2	2.45	8.63	0.33
	S1	1.22	4.31	0.68

Table A.3 Schleifenberg: HNO_3 extracted concentration of trace metals in soils samples

Sample	Trace elements (mg kg^{-1})					
	Cd	**Zn**	**Pb**	**Cr**	**Ni**	**Cu**
S1	0.68	154.99	41.38	41.42	27.41	9.26
S2	0.33	46.56	10.26	44.86	18.78	8.76
S3	0.92	215.65	50.20	58.79	27.07	17.42
S4	0.92	209.77	46.61	60.18	26.32	14.00
S5	0.67	226.44	49.34	64.91	30.34	15.71
S6	0.50	218.20	56.61	54.53	24.39	18.13
S7	0.92	230.26	55.24	56.17	24.98	17.22
S8	0.67	253.20	53.02	65.11	27.91	14.90
S9	2.00	232.61	54.82	54.94	24.06	15.51
S10	0.92	202.22	46.01	50.72	25.06	13.59
S11	0.69	146.51	43.66	30.81	21.78	11.05
S12	0.67	173.90	56.10	43.73	21.71	18.03
S13	1.00	166.35	51.31	49.18	24.06	17.32
S14	0.71	134.56	40.83	38.40	22.81	9.81
S15	0.73	191.64	52.25	55.73	31.58	9.92
S16	0.74	170.21	50.34	45.55	30.54	8.42
S17	0.81	192.53	59.16	46.50	26.88	11.39
S18	0.79	199.77	57.18	49.76	28.00	29.94
S19	0.60	190.90	36.31	63.39	32.86	6.69
S20	1.05	241.95	77.64	61.20	31.31	12.45
S21	1.14	233.76	70.18	55.58	31.41	18.76
S22	0.83	178.11	46.09	51.08	24.22	12.99
S23	0.84	189.58	51.94	48.89	28.64	11.16
S24	0.92	216.24	59.95	59.10	33.28	16.62
S25	0.80	190.03	39.29	58.64	31.69	8.69
S26	0.75	209.58	49.86	67.73	33.70	15.51
S27	0.79	209.71	62.31	57.99	31.76	12.35
S28	0.70	204.56	55.27	59.77	32.99	15.62
S29	0.81	244.68	60.12	66.60	36.01	12.17
S30	0.75	226.44	54.90	71.95	36.96	13.90
S31	0.75	223.20	54.82	70.30	35.96	17.42
S32	0.58	206.83	50.03	63.00	33.11	16.21
S33	0.67	205.56	50.46	61.26	33.28	16.21
S34	0.92	198.01	55.42	55.30	30.01	17.52
S35	0.67	164.48	42.33	48.41	25.31	14.00
S36	0.92	194.09	56.19	54.01	25.82	16.21
S37	0.83	191.64	48.75	53.96	25.40	15.91
S38	0.71	170.64	45.24	44.12	24.72	13.59
S39	0.75	188.79	44.81	54.58	24.56	14.30
S40	0.75	192.79	51.57	53.98	26.99	15.26
S41	0.83	215.75	62.00	53.50	24.31	18.93
S42	0.71	111.55	27.53	28.37	17.29	7.06
S43	1.02	147.58	41.26	41.30	28.00	9.85
S44	0.67	117.45	24.85	22.46	21.49	7.45
S45	1.07	171.43	48.32	46.53	35.23	9.46
S46	0.73	169.02	54.12	43.98	32.58	12.96
S47	1.10	179.67	37.37	45.72	30.86	8.41

Table A.4 Schleifenberg: HNO_3 extracted concentration of major elements in soils samples

Sample	**Major elements (g kg^{-1})**			
	Ca	**Fe**	**Mn**	**Al**
S1	138.91	23.46	0.43	11.24
S2	171.38	15.35	0.22	21.91
S3	100.29	31.56	0.54	17.93
S4	110.43	30.52	0.55	17.72
S5	89.23	31.73	0.56	19.39
S6	99.17	26.31	0.46	15.46
S7	90.28	28.07	0.46	15.15
S8	76.62	33.27	0.54	19.42
S9	93.44	27.64	0.48	15.92
S10	83.64	26.54	0.44	13.40
S11	165.36	26.04	0.60	8.80
S12	120.58	22.21	0.68	12.34
S13	124.90	25.46	0.80	12.88
S14	102.86	24.33	0.56	10.99
S15	89.85	34.00	0.72	15.59
S16	100.67	30.52	0.61	11.15
S17	67.25	30.25	0.57	11.89
S18	73.26	30.03	0.56	13.08
S19	91.05	34.79	0.64	18.32
S20	51.73	29.04	0.55	20.63
S21	52.56	30.97	0.61	16.65
S22	92.78	25.37	0.54	15.23
S23	82.68	28.59	0.61	14.09
S24	65.85	29.98	0.59	18.12
S25	80.41	33.93	0.67	15.49
S26	69.52	35.11	0.67	21.27
S27	59.79	32.20	0.64	17.89
S28	81.56	33.23	0.63	17.28
S29	53.86	36.72	0.69	20.82
S30	59.15	37.46	0.72	22.06
S31	60.67	36.27	0.73	20.83
S32	88.13	35.09	0.79	19.39
S33	93.05	34.29	0.77	17.46
S34	112.31	31.58	0.74	15.37
S35	160.30	26.79	0.74	12.73
S36	126.12	27.48	0.76	13.18
S37	120.76	27.79	0.76	14.18
S38	136.03	25.89	0.71	12.28
S39	131.09	27.70	0.76	14.42
S40	129.49	27.27	0.71	16.39
S41	101.80	28.24	0.70	14.36
S42	212.18	23.38	0.63	12.65
S43	108.80	38.70	1.05	23.91
S44	179.37	25.25	0.89	11.73
S45	96.58	55.45	2.91	25.85
S46	64.11	51.00	2.24	22.96
S47	134.75	47.48	2.81	25.58

APPENDIX B

Table B.1 Le Gurnigel: Geographical coordinates of the six sampling points

Sampling point	Coordinates (map)			Coordinates at the site			Precision	Sampling Date	
	X (km)	Y (km)	Altitude (m)	X (km)	Y (km)	Altitude (m)	(m)	Plants	Soils
AX	559.193	215.815	1290	559.225	215.590	1300	5	29/8/06	15/11/06
AZ	559.367	215.707	1285	559.382	215.693	1298	12	21/7/06	15/11/06
CX	559.437	215.733	1280	559.437	215.733	1276	5	21/7/06	15/11/06
CZ	559.285	215.574	1300	559.280	215.560	1304	6	29/8/06	15/11/06
EX	559.200	215.774	1285	559.235	215.787	1284	4	10/8/06	16/11/06
EZ	559.341	215.781	1265	559.342	215.773	1233	18?	21/7/06	21/11/06

Table B.2 Le Gurnigel: Correlation matrix between Cd and chemical properties of soils and selected trace elements

Variable	Cd	Depth	TOC	C_{min}	pH	CEC	C/N	Ca	Fe	Al	Mn	Zn	Pb	Cr	Ni	Cu
Cd	1															
Depth	0.19	1														
TOC	0.22	**-0.72**	1													
Cmin	0.36	**-0.66**	**0.94**	1												
pH	0.56	-0.36	0.64	**0.75**	1											
CEC	0.64	-0.17	**0.68**	**0.75**	**0.85**	1										
C/N	-0.38	-0.55	0.43	0.35	0.13	0.10	1									
Ca	0.56	-0.28	0.59	**0.65**	**0.72**	**0.80**	0.17	1								
Fe	**0.67**	0.59	-0.34	-0.12	0.12	0.21	-0.48	0.13	1							
Al	0.36	0.57	-0.36	-0.33	-0.15	-0.08	-0.50	-0.43	0.50	1						
Mn	0.43	-0.19	0.29	0.50	0.40	0.32	-0.01	0.34	0.52	-0.04	1					
Zn	**0.85**	0.01	0.26	0.40	0.43	0.43	-0.40	0.43	0.55	0.32	0.59	1				
Pb	0.52	-0.54	**0.72**	**0.82**	**0.66**	0.59	0.05	0.59	0.09	-0.17	0.56	**0.67**	1			
Cr	**0.91**	0.17	0.18	0.33	0.49	0.53	-0.45	0.47	**0.65**	0.39	0.44	**0.92**	0.62	1		
Ni	0.27	**0.67**	-0.39	-0.27	-0.02	0.21	-0.28	0.05	**0.67**	0.37	0.09	-0.03	-0.32	0.13	1	
Cu	0.17	0.11	0.26	0.31	0.35	0.51	0.14	0.34	0.22	-0.10	0.15	-0.05	0.23	0.14	0.53	1

Table B.3 Le Gurnigel: Correlation matrix between Cd and soil mineralogical assemblage

Variable	Cd	Phyll	Qtz	Kfs	Pl	Gt	N-Q	Chl (2–16)	Kao (2–16)	Mic (2–16)	Chl (<2)	Kao (<2)	Mic (<2)	IS-B	IS-N
Cd	1														
Phyll	0.12	1													
Qtz	-0.15	0.40	1												
Kfs	-0.06	-0.11	0.08	1											
Pl	0.12	-0.13	-0.16	0.46	1										
Gt	0.47	0.36	0.38	-0.01	0.13	1									
N-Q	0.00	-0.57	**-0.85**	-0.29	-0.29	-0.53	1								
Chl (2–16)	-0.02	-0.10	0.07	0.02	0.03	-0.02	-0.03	1							
Kao (2–16)	0.18	0.19	-0.09	0.09	-0.09	0.09	0.03	**-0.75**	1						
Mic (2–16)	-0.22	-0.14	0.03	-0.15	0.08	-0.10	0.01	-0.33	-0.38	1					
Chl (<2)	0.21	0.06	0.16	0.10	0.17	0.08	-0.22	0.25	-0.06	-0.26	1				
Kao (<2)	-0.14	0.16	0.06	0.12	-0.06	0.22	-0.10	-0.34	0.23	0.14	-0.17	1			
Mic (<2)	-0.37	-0.09	-0.12	-0.27	-0.03	-0.36	0.18	-0.01	-0.26	0.39	-0.41	-0.44	1		
IS-B	0.09	-0.12	-0.10	-0.05	-0.04	-0.14	0.14	0.31	-0.18	-0.18	-0.13	**-0.84**	0.24	1	
IS-N	0.55	-0.18	0.03	0.02	0.10	0.14	-0.02	-0.05	0.21	-0.24	0.09	-0.18	-0.21	-0.05	1

APPENDIX C

Figure C.1 Sampling points at the Le Gurnigel and picture of the six plant species

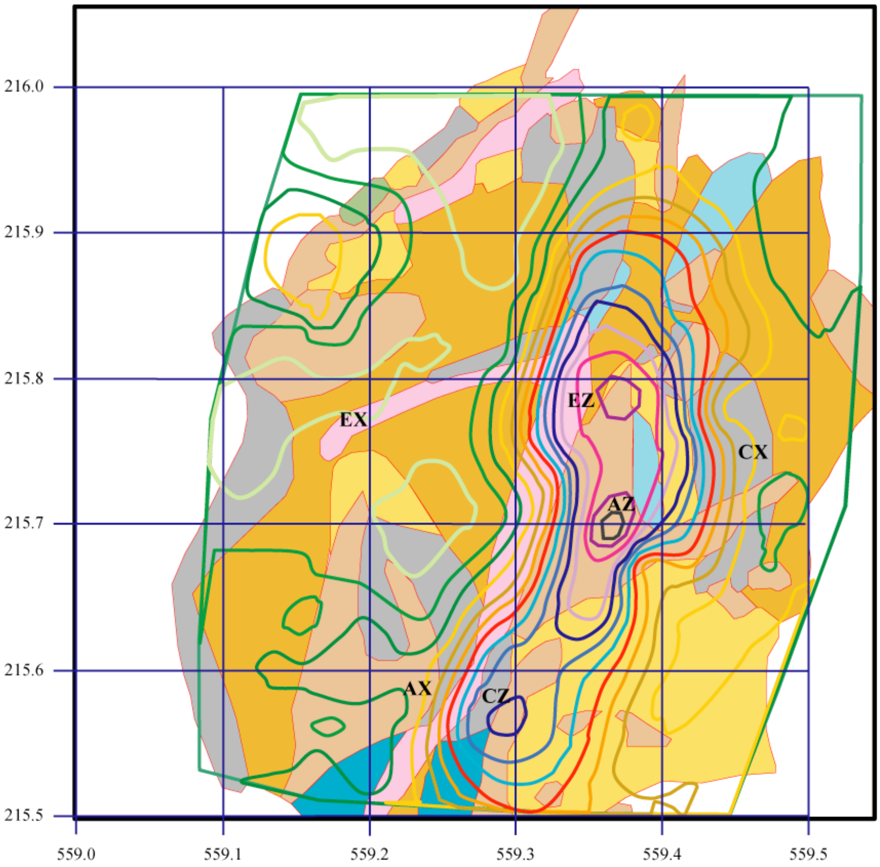

Hipericum maculatum

Alchemilla xanthochlora

Cynosurus cristatus

Ranunculus acris

Dactylis glomerata

Acer pseudoplatanus

Table C.1 Le Gurnigel: Cadmium concentrations data and dried-matter (DM) biomass of roots and shoots of the plants (triplicates)

Sampling point	***Hypericum maculatum*** **(HYMA)**											
	HYMA (1)				**HYMA (2)**				**HYMA (3)**			
	[Cd] root mg·kg^{-1}	**DM root mg**	**[Cd] shoots mg·kg^{-1}**	**DM shoots mg**	**[Cd] root mg·kg^{-1}**	**DM root mg**	**[Cd] shoots mg·kg^{-1}**	**DM shoots mg**	**[Cd] root mg·kg^{-1}**	**DM root mg**	**[Cd] shoots mg·kg^{-1}**	**DM shoots mg**
AX	2.68	0.10	3.35	0.18	3.92	0.36	3.69	0.72	1.79	0.09	0.54	0.17
AZ	2.87	0.08	0.17	0.38	2.20	0.13	0.16	0.17	3.18	0.31	0.14	0.39
CX	4.53	1.03	3.14	6.05	3.88	0.25	3.29	2.32	5.83	0.65	2.35	2.57
CZ	**Not found at the sampling point**											
EX	1.65	1.40	0.68	2.00	1.51	0.90	1.10	0.90	1.49	0.30	0.79	1.40
EZ	2.10	0.25	1.29	1.11	1.89	0.20	1.87	0.59	1.50	0.16	1.40	0.39

Sampling point	***Alchemilla xanthoclora*** **(ALXA)**											
	ALXA (1)				**ALXA (2)**				**ALXA (3)**			
	[Cd] root mg·kg^{-1}	**DM root mg**	**[Cd] shoots mg·kg^{-1}**	**DM shoots mg**	**[Cd] root mg·kg^{-1}**	**DM root mg**	**[Cd] shoots mg·kg^{-1}**	**DM shoots mg**	**[Cd] root mg·kg^{-1}**	**DM root mg**	**[Cd] shoots mg·kg^{-1}**	**DM shoots mg**
AX	3.27	1.09	1.70	0.35	3.04	0.68	0.48	0.26	5.03	0.87	1.56	0.38
AZ	7.99	0.88	1.65	0.21	9.04	0.99	1.47	0.80	10.49	1.27	1.35	0.32
CX	14.72	1.48	6.37	3.47	16.74	1.70	5.73	0.94	12.81	1.15	4.64	0.89
CZ	16.21		0.69		8.15		0.38		**Missing data**			
EX	6.10	1.00	2.91	0.30	5.84	1.70	3.40	0.30	4.98	0.90	2.60	0.90
EZ	6.24	1.65	1.14	0.35	5.25	0.86	1.25	0.14	5.56	0.54	1.34	0.47

Sampling point	***Cynosurus cristatus*** **(CYCR)**											
	CYCR (1)				**CYCR (2)**				**CYCR (3)**			
	[Cd] root mg·kg^{-1}	**DM root mg**	**[Cd] shoots mg·kg^{-1}**	**DM shoots mg**	**[Cd] root mg·kg^{-1}**	**DM root mg**	**[Cd] shoots mg·kg^{-1}**	**DM shoots mg**	**[Cd] root mg·kg^{-1}**	**DM root mg**	**[Cd] shoots mg·kg^{-1}**	**DM shoots mg**
AX	7.10	0.25	7.68	0.21	5.98	0.33	3.47	0.50	3.95	0.22	2.28	0.45
AZ	8.60	0.07	2.64	0.25	8.75	0.13	2.66	0.18	8.78	0.28	2.73	0.28
CX	9.48	7.60	4.36	1.36	7.12	0.21	3.70	0.45	6.07	0.13	2.01	0.51
CZ	9.92	0.38	9.38	0.25	**Missing data**				**Missing data**			
EX	2.92	0.50	1.63	0.30	2.51	1.10	1.28	1.80	3.36	1.30	1.24	0.70
EZ	6.36	0.65	3.48	0.71	8.28	1.09	3.07	2.98	7.76	0.26	2.53	0.43

Table C.1 (continued)

Sampling point	***Ranunculus acris* (RAAC)**											
	RAAC(1)				**RAAC(2)**				**RAAC(3)**			
	[Cd] root mg·kg^{-1}	**DM root mg**	**[Cd] shoots mg·kg^{-1}**	**DM shoots mg**	**[Cd] root mg·kg^{-1}**	**DM root mg**	**[Cd] shoots mg·kg^{-1}**	**DM shoots mg**	**[Cd] root mg·kg^{-1}**	**DM root mg**	**[Cd] shoots mg·kg^{-1}**	**DM shoots mg**
AX	**Missing data**				**Missing data**				2.06	0.94	0.77	1.80
AZ	7.41	0.44	0.13	0.30	6.12	0.16	0.71	0.24	6.36	0.31	0.65	0.55
CX	4.96	0.58	1.25	0.73	3.34	0.24	0.47	0.29	4.02	0.96	1.09	1.88
CZ	**Missing data**				6.85	0.11	2.93	0.17	**Missing data**			
EX	2.63	0.90	2.72	1.00	2.03	0.30	0.87	0.80	1.36	1.20	1.63	1.10
EZ	2.03	0.51	1.24	0.62	2.89	0.21	1.88	0.92	2.24	0.60	0.98	0.80

Sampling point	***Dactylis Glomerata*(DAGL)**											
	DAGL(1)				**DAGL(2)**				**DAGL(3)**			
	[Cd] root mg·kg^{-1}	**DM root mg**	**[Cd] shoots mg·kg^{-1}**	**DM shoots mg**	**[Cd] root mg·kg^{-1}**	**DM root mg**	**[Cd] shoots mg·kg^{-1}**	**DM shoots mg**	**[Cd] root mg·kg^{-1}**	**DM root mg**	**[Cd] shoots mg·kg^{-1}**	**DM shoots mg**
AX	**Missing data**				3.30		0.96		0.48		0.64	
AZ	2.25	0.28	0.35	0.33	2.13	0.24	0.37	2.03	2.58	0.74	0.29	1.88
CX	2.09	2.08	0.86	1.67	1.76	0.71	0.75	0.94	2.05	0.61	0.81	2.67
CZ	2.39		0.67		0.61		0.80		**Missing data**			
EX	1.52	4.30	0.51	2.10	3.05	1.10	0.82	2.10	2.51	2.00	0.61	1.80
EZ	1.25	0.51	0.44	2.00	0.88	0.55	0.35	0.65	1.05	1.57	0.23	2.29

Sampling point	***Acer pseudoplatanus* (ACPS)**											
	ACPS(1)				**ACPS(2)**				**ACPS(3)**			
	[Cd] root mg·kg^{-1}	**DM root mg**	**[Cd] shoots mg·kg^{-1}**	**DM shoots mg**	**[Cd] root mg·kg^{-1}**	**DM root mg**	**[Cd] shoots mg·kg^{-1}**	**DM shoots mg**	**[Cd] root mg·kg^{-1}**	**DM root mg**	**[Cd] shoots mg·kg^{-1}**	**DM shoots mg**
AX	3.42		0.13		0.56		0.28		**Missing data**			
AZ	5.29	0.04	0.88	0.13	7.34	0.07	0.30	0.15	4.01	0.08	0.49	0.11
CX	**Not found at the sampling point**											
CZ	**Missing data**				2.48		0.13		0.37		0.14	
EX	1.86	0.11	1.23	0.10	0.94	0.20	0.50	0.40	1.05	0.20	0.47	0.30
EZ	4.06	0.15	0.90	0.12	3.23	0.05	0.56	0.08	2.00	0.05	0.33	0.09

Figure C.2 Mean percentage distrbution of trace metals in rhizospheric and distant soil AX

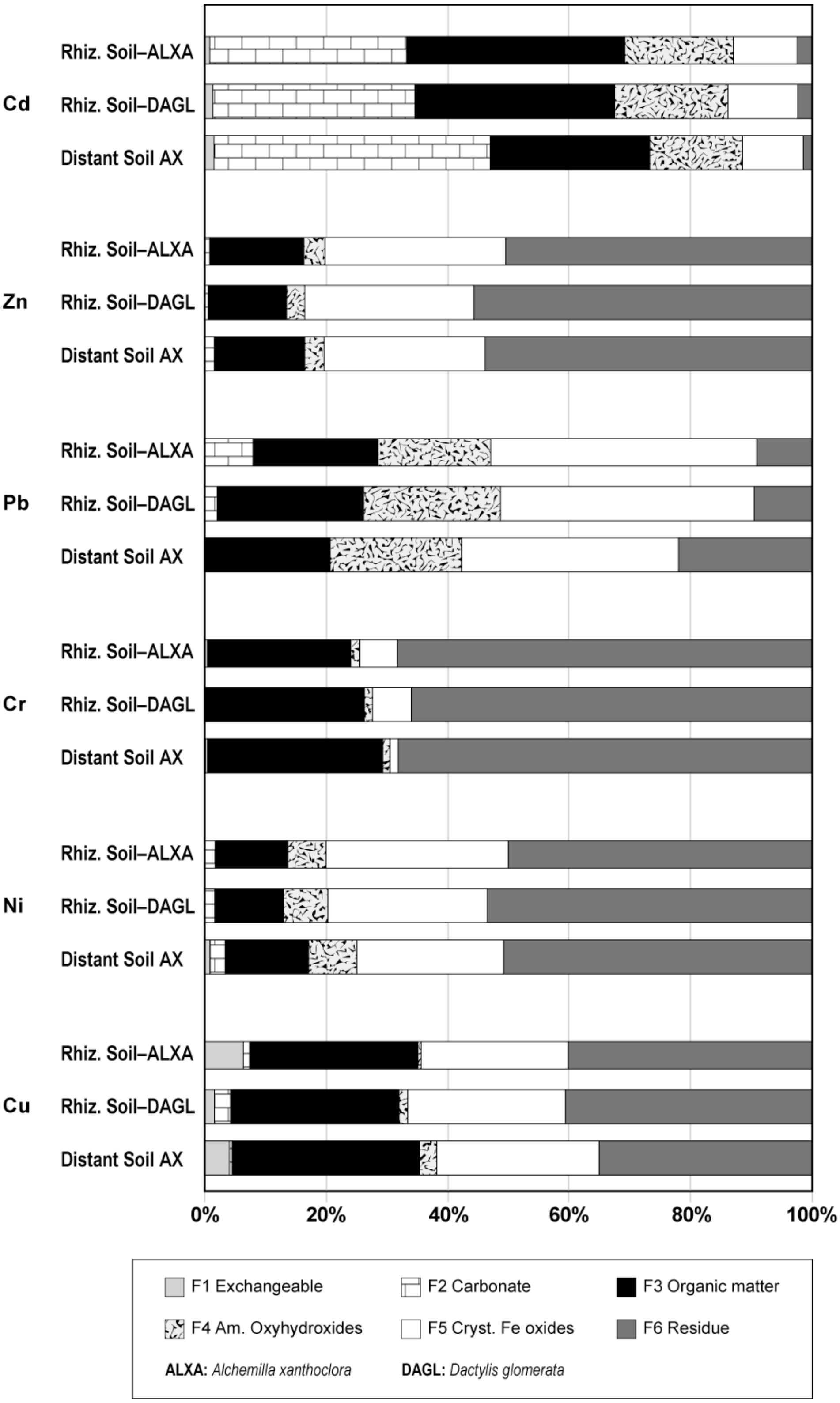

Figure C.3 Mean percentage distrbution of trace metals in rhizospheric and distant soil AZ

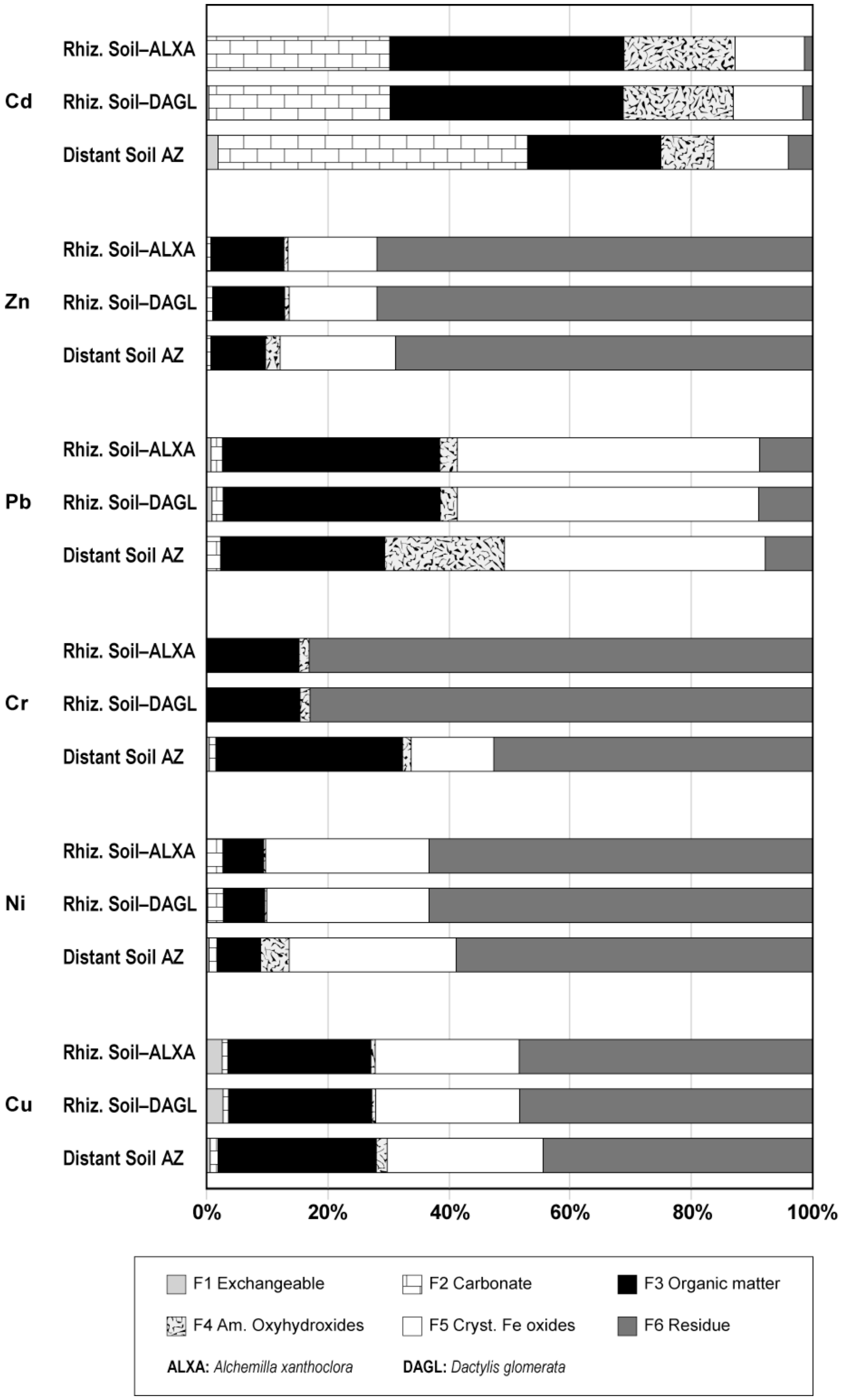

Figure C.4 Mean percentage distrbution of trace metals in rhizospheric and distant soil EX.

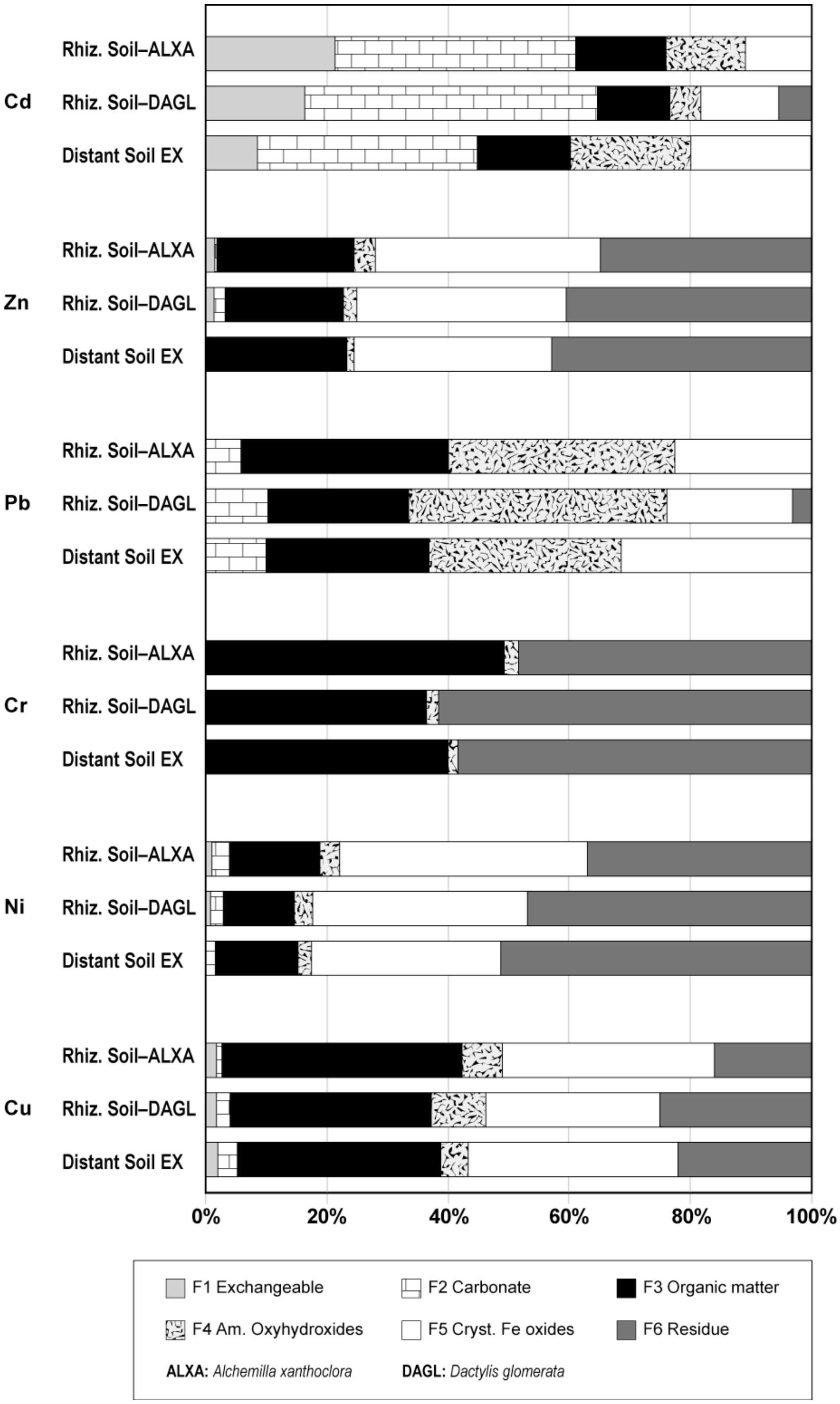

Figure C.5 Mean percentage distrbution of trace metals in rhizospheric and distant soil EZ.

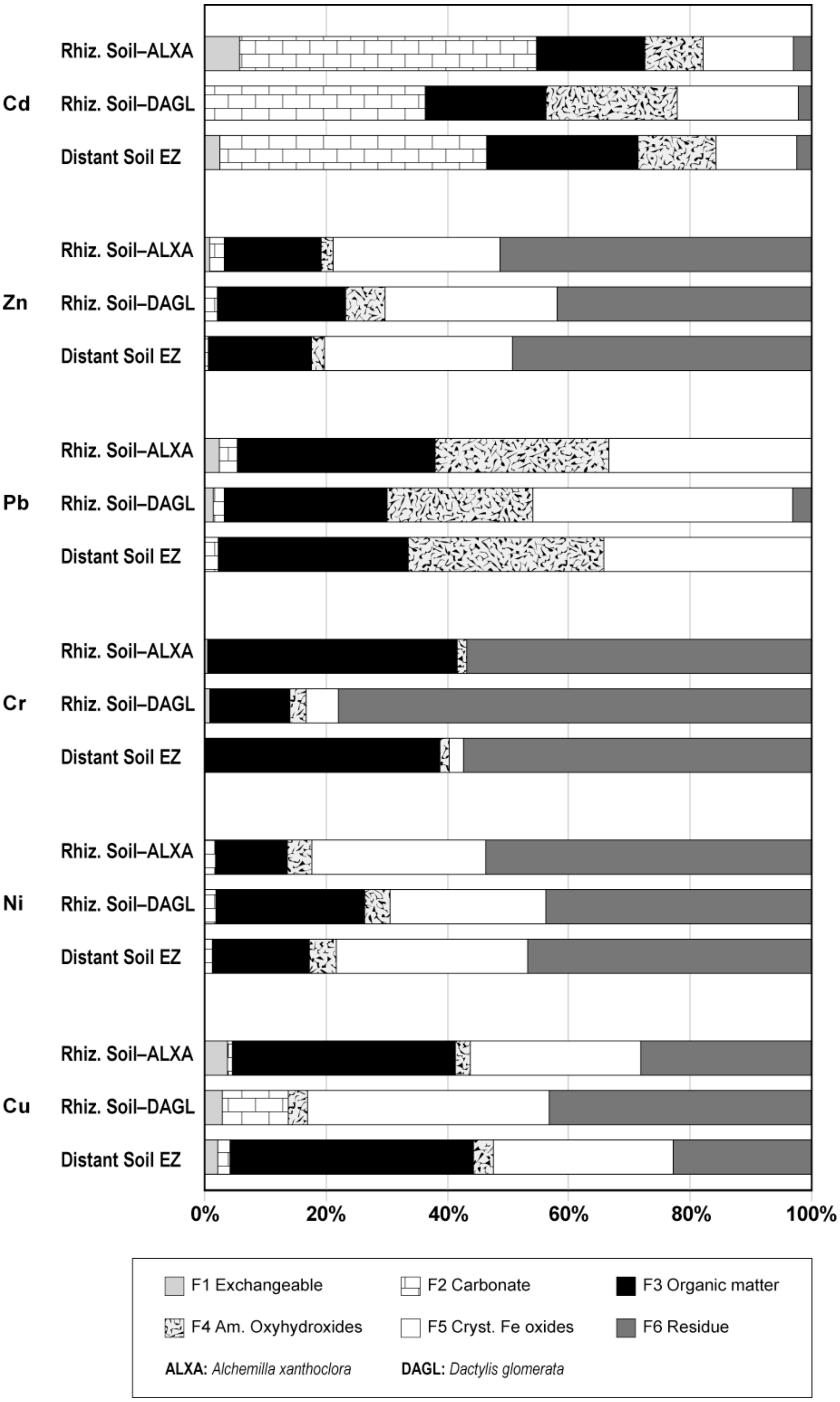

APPENDIX D

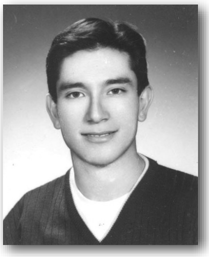

RAUL PERCY QUEZADA-HINOJOSA

Rue de l'Ecluse 38, CH-2000 Neuchâtel, Switzerland
Mobile phone: +41 79 745 46 75
raulpqh@yahoo.com
Born in Bolivia on August 12th, 1975

EDUCATION

Ph.D. in Earth Sciences
University of Neuchâtel, Switzerland
October 2006 – October 2010

Human Resources and Strategic Marketing
MBA program modules
Private University of Bolivia
May – July 2003

Licence Degree in Metallurgical Engineering
Technical University of Oruro, Bolivia
1995 – 2002

LABORATORY TECHNIQUES

- Scanning Electron Microscopy (ESEM) / Energy Dispersive x-ray Spectrometry (EDS)
- Leaching / chemical analyses of soils, rocks and plants, US-EPA Method 3051/ICP-MS
- Sequential chemical extractions of heavy metals / phosphorous in soils, sediments / rocks

LANGUAGE PROFICIENCY

- Spanish	Native
- English	Fluent: written / spoken
- French	Fluent: written / spoken
- Italian	Conversational
- Portuguese	Conversational
- German	Basic

PUBLICATIONS

Quezada-Hinojosa et al. Cadmium distribution in soils covering Jurassic oolitic limestone with high Cd contents in the Swiss Jura. Geoderma, vol.150, Issues 3-4, May 2009.

WORK EXPERIENCE

Assistant in Charge of Phosphorus Laboratory
Supervision and running of a laboratory of phosphorus analyses of rocks and sediments
Institute de Geology and Hydrogeology, University of Neuchâtel, Switzerland
September 2006 – August 2008

Technical Translator
Translation from English / French to Spanish of technical documents of hydrogeology
Geomagnetism Group, University of Neuchâtel, Switzerland
November 2005

Research Fellow
Sampling/chemical analyses of soils, rocks and plants. SEM-EDS images of thin rock slices
Institute de Geology and Hydrogeology, University of Neuchâtel, Switzerland
October 2004 – July 2007

Environmental Engineer
Mass balances of effluents/solid wastes from metallurgical plants Technical Consultancy Services (SETECO S.R.L.), Bolivia
August 2003 – June 2004

Project Engineer
Planning and design of a tin ore dressing plant
Mining Promotion Centre (CEPROMIN), Bolivia
September 2001 – February 2002

Field Assistant
Sampling and volume measuring of surface run-off / acid rock drainage from mine works
Dames & Moore Norge
December 1999 – February 2000

COMPUTER SKILLS

- Scientific software: Visual MINTEQ, MATLAB
- Graphic design software: Adobe Illustrator, Photoshop
- Office Automation: Microsoft office (Windows), iWorks (MacOS)

OTHER INTERESTS

Photography, Mineralogy, Skiing, Trips, Languages, Art History